Etude du comportement en environnement oxydant des matériaux composites 2D C/SIC

Franck Lamouroux

N° d'ordre: 860

THESE

PRESENTEE A

L'UNIVERSITE DE BORDEAUX I

POUR OBTENIR LE GRADE DE

DOCTEUR

Spécialité: SCIENCES DES MATERIAUX

PAR

Franck LAMOUROUX

ETUDE DU COMPORTEMENT EN ENVIRONNEMENT OXYDANT DES MATERIAUX COMPOSITES 2D C/SIC

Soutenue le 08 Décembre 1992, devant la Commission d'Examen:

MM.	P.	HAGENMULLER.....	*Président*
	G.	CAMUS.....	*Examinateurs*
	J.J.	CHOURY.....	
	P.	GUYOT.....	
	J.	LAHAYE.....	
	R.	NASLAIN.....	
	B.	PIERAGGI.....	

- 1992 -

N° d'ordre: 860

THESE

PRESENTEE A

L'UNIVERSITE DE BORDEAUX I

POUR OBTENIR LE GRADE DE

DOCTEUR

Spécialité: SCIENCES DES MATERIAUX

PAR

Franck LAMOUROUX

ETUDE DU COMPORTEMENT EN ENVIRONNEMENT OXYDANT DES MATERIAUX COMPOSITES 2D C/SIC

Soutenue le 08 Décembre 1992, devant la Commission d'Examen:

MM.	P.	HAGENMULLER.....	*Président*
	G.	CAMUS.....	*Examinateurs*
	J.J.	CHOURY.....	
	P.	GUYOT.....	
	J.	LAHAYE.....	
	R.	NASLAIN.....	
	B.	PIERAGGI.....	

- 1992 -

Ce travail a été réalisé au Laboratoire des Composites Thermostructuraux (Unité Mixte de Recherche du CNRS, de la Société Européenne de Propulsion et de l'Université de Bordeaux I).

Monsieur le Professeur Roger NASLAIN, Directeur du Laboratoire des Composites Thermostructuraux, m'a permis d'effectuer ce travail au sein de son groupe de recherche. Qu'il trouve ici l'expression de ma profonde gratitude.

Monsieur le Professeur Paul HAGENMULLER, m'a fait l'honneur d'accepter la Présidence de mon jury de thèse. Je lui adresse mes sincères remerciements.

Monsieur Gérald CAMUS, Chargé de Recherches au CNRS, du Laboratoire des composites Thermostructuraux, a bien voulu me guider dans mon travail de recherche. Je le remercie pour son aide et ses précieux conseils.

Monsieur Jean Jacques CHOURY, Directeur, Adjoint Recherche et Technologie à la Division Propulsion à Poudre et Composites de la Société Européenne de Propulsion, m'a fait l'honneur d'examiner ce travail. Qu'il trouve ici le témoignage de ma profonde reconnaissance.

Monsieur le Professeur Pierre GUYOT, de l'Institut National Polytechnique de Grenoble, a aimablement accepté de participer à mon jury de thèse. Je lui adresse mes sincères remerciements.

Monsieur le Professeur Jacques LAHAYE, du Centre de Recherches sur la Physico-Chimie des Surfaces Solides de Mulhouse, m'a fait l'honneur de juger ce travail. Qu'il trouve ici l'expression de mes plus vifs remerciements.

Monsieur le Professeur Bernard PIERAGGI, du Laboratoire des Matériaux de Toulouse, a aimablement accepté de juger ce travail. Je lui adresse mes remerciements les plus sincères.

Monsieur Jacques THEBAULT, Ingenieur à la Société Européenne de Propulsion, a bien voulu me conseiller durant mon travail de recherche. Qu'il soit remercié pour son aimable collaboration.

Monsieur Xavier BOURRAT, Chargé de Recherches au CNRS, du Laboratoire des Composites Thermostructuraux, a participé à ce travail de recherche. Je le remercie pour sa collaboration efficace.

Monsieur Jean SEVELY, Directeur de Recherches au CNRS, du Laboratoire d'Optique Electronique de Toulouse, a aimablement accepté de participer à ce travail. Qu'il en soit ici vivement remercié.

Je tiens à exprimer ma reconnaissance aux membres du LCTS pour leur amitié et le soutien qu'ils m'ont apporté, particulièrement Ludovic FILIPUZZI a qui je dois une grande partie de ce travail, Nathalie et Jean-Francois VILLENEUVE, Raphaël BODET, Stéphane PROUHET, Etienne SIPP, Olivier DUGNE, Philippe PLUVINAGE, Nathalie RICCA et Pascal DUPEL.

Je remercie Gérard VIGNOLES, Xavier AUBARD et Laurent GUILLAUMAT pour leur gentillesse et leur dévouement à installation du réseau informatique du LCTS.

Je remercie Bruno HUMEZ et Jean Paul SARROSTE pour leur constante disponibilité.

Je tiens à remercier Josette FORGET, Cécile DUPOUY, Florence DUCASSE et Michel COIGNARD pour toute l'aide qu'ils m'ont apporté durant mon séjour au LCTS.

Je remercie enfin le Ministère de la Recherche et de la Technologie ainsi que la Société Européenne de Propulsion qui m'ont permis de conduire cette étude en me faisant bénéficier d'une bourse de recherche.

INTRODUCTION GENERALE

INTRODUCTION GENERALE

1 - Généralités.

Les composites résultent de la combinaison de plusieurs matériaux aux caractéristiques plus ou moins complémentaires permettant d'obtenir un solide ayant des propriétés originales. Il existe de nombreux types de matériaux composites suivant la nature et la morphologie des constituants élémentaires (fibres, particules sphériques, etc...) [1]. Les matériaux composites les plus couramment rencontrés sont constitués d'un renfort fibreux (fibres courtes ou longues) noyé dans une matrice. La diversité de ces matériaux permet leur utilisation dans de nombreux domaines d'applications tels que l'industrie automobile, aéronautique et aérospatiale.

Les composites thermostructuraux sont des composites à matrice réfractaire initialement développés pour l'industrie aérospatiale. Ils présentent un ensemble de propriétés alliant légèreté, rigidité, ténacité et résistance mécanique à haute température. Comme dans l'ensemble des composites fibreux, le renfort est destiné à supporter l'essentiel des contraintes mécaniques. La matrice joue le rôle de liant et assure ainsi le transfert de la charge au sein du renfort fibreux. La réfractairité de la matrice est la principale différence entre les composites thermostructuraux et les autres composites fibreux (e.g. composites à matrice métallique et/ou polymère).

2 - Les composites à fibres longues et à matrice céramique.

2.1 - Développement

Les premiers matériaux composites développés pour les applications à hautes températures étaient constitués d'un renfort et d'une matrice tous deux en carbone. Ces matériaux possèdent une faible densité, proche de 2, qui leur confère d'excellentes propriétés spécifiques [2-4]. Les caractéristiques mécaniques des composites carbone-carbone se conservent, voire s'améliorent, lorsque la température augmente. Le faible coefficient de dilatation thermique limite les déformations à haute température. Leur résistance élevée à l'ablation permet de les utiliser comme protection thermique (e.g. des corps de rentrée). Par contre, si les composites carbone-carbone présentent une bonne inertie chimique en milieu neutre ou réducteur, ils ont malheureusement une mauvaise résistance à l'oxydation. En effet, le carbone commence à s'oxyder dès 450°C (de façon notable) en produisant les oxydes gazeux CO ou/et CO_2. La vitesse d'oxydation est d'autant plus grande que la température et la pression d'oxygène sont élevées [5-9]. Par conséquent, la matrice ne peut plus protéger les fibres du milieu oxydant et les propriétés mécaniques du matériau se dégradent rapidement [10].

Pour protéger le renfort fibreux de l'environnement, il est nécessaire d'utiliser une matrice présentant une bonne inertie chimique vis à vis de l'oxygène. Les matériaux répondant principalement à ce critère sont les oxydes, lesquels ont particulièrement conduit au développement des composites à matrice vitreuse et/ou vitrocéramique. Parmi les associations prometteuses, au plan de l'amélioration de la rigidité, de la résistance à la rupture et de la ténacité, on citera les fibres de carbone enrobées dans une matrice vitreuse (verre borosilicaté ou de silice) ou vitrocéramique (e.g. aluminosilicate de lithium: LAS) [11,12]. Pour ce type

de matériaux, l'effet composite se maintient tant que la matrice vitreuse demeure élastique, c'est à dire jusqu'au voisinage de la température de transition vitreuse (600°C pour les verres borosilicatés et 1000°C pour les verres de silices ou les vitrocéramiques).

Lorsque la température d'utilisation est supérieure à 1000°C, il est nécessaire d'utiliser des matériaux plus réfractaires, tels que les céramiques. En plus de cette importante réfractairité, ces matériaux doivent aussi posséder d'autres caractéristiques telles qu'une faible densité, un coefficient de dilatation thermique proche de celui du matériau constituant le renfort (compte tenu de la gamme de température balayée en service) et une bonne résistance mécanique. Le tableau I résume les caractéristiques de quelques réfractaires. Les matériaux potentiellement intéressants pour protéger les fibres de carbone sont: B_4C,BN, SiC et TiC. Dans un premier temps, une partie seulement de la matrice de carbone fût remplacée par une céramique. Des études ont porté sur l'élaboration et la caractérisation de composites à matrice hybride carbone/carbure et carbone/nitrure [13-15]. Malheureusement, la tenue à l'oxydation des composites à matrice hybride C/TiC, C/B_4C et C/BN s'est révélée être faible lorsque la température dépassait 1100°C. La microfissuration du film d'oxyde de titane ou la volatilisation de l'oxyde de bore sont responsables de ce comportement. Les composites à matrice hybride C/SiC ont par contre une excellente tenue à l'oxydation jusqu'à 1600°C **à condition que le revêtement de carbure de silicium ne soit pas endommagé**. L'oxyde de silicium formé durant le traitement sous oxygène est protecteur et ne se volatilise qu'à partir de 1700°C à la pression atmosphérique [16]. Néanmoins, le carbure de silicium (et nombre d'autres réfractaires) a un inconvénient majeur: la fragilité. La faible ténacité des céramiques se traduit par l'endommagement du revêtement réfractaire lors de sollicitations mécaniques. La fissuration de

Réfractaires	Tf (°C)	densité	coef. dilat. (10^{-6}/°C)	resistance compression (MPa)	module (GPa)	Toxyd. à l'air (°C) *
Graphite	3300	1,6 - 1,7	3,2	160	12	500
B_4C	2450	2,5	4,5	2860	490	1100
SiC β	2700	3,2	3,9	1100	420	1600
TiC	3067	4,9	5,5	750	400	1400
ZrC	3445	6,5	6	1640	340	1400
HfC	3928	12,6	6,6	-	340	1400
NbC	3615	7,8	6	-	340	-
TaC	3985	14,3	5,5	-	360	1400
WC	2760	15,8	4,5	3000	600	500 - 800
BN	3000	2,2	6	300	88	1100
Si_3N_4	1900	3,2	2,5	600	300	1400
TiB_2	3225	7,5	8	1200	520	1000
ZrB_2	3245	7,2	7	1560	500	1000
HfB_2	3380	11,2	5 - 7	-	-	-
$MoSi_2$	1900	3,4	2,5	-	-	1600

* températures limites d'utilisation.

Tableau I: caractéristiques de quelques réfractaires.

la matrice conduit à nouveau à l'oxydation du renfort en carbone et, par conséquent, à la chute des propriétés mécaniques. Une amélioration fût apportée avec les composites constitués d'une matrice exclusivement en céramique. Par ailleurs, le développement d'une nouvelle famille de fibres en carbure de silicium, e.g. la fibre ex-PCS (polycarbosilane Si-C-O), permit de réaliser des composites plus résistants aux environnements oxydants [17,18].

2.2 - Comportement mécanique.

De manière générale, le comportement mécanique en traction des CMC débute par un domaine élastique linéaire (fig.1). Le module d'élasticité du composite (dans le sens des fibres) est en général correctement décrit par la loi des mélanges (dans le cas d'un composite unidirectionnel) [19]:

$$Ec = Ef.Vf + Em.Vm$$

Vx étant la fraction volumique des fibres ou de la matrice au sein du composite, et Ex le module d'Young respectif du composite, de la fibre et de la matrice (les indices x=c, f,et m signifient respectivement composite, fibre et matrice).

La limite de ce domaine élastique linéaire est liée à la rupture du constituant le plus fragile: la matrice. Contrairement aux céramiques monolithiques, la rupture de ce constituant ne provoque pas nécessairement la rupture catastrophique du matériau. Quand $\varepsilon = \varepsilon m$, les premières fissures apparaissent au sein du composite. Leur direction est perpendiculaire à l'axe de la sollicitation, et la distance entre deux fissures est appelée "pas de fissuration". L'augmentation de la charge appliquée conduit à une hausse du niveau des contraintes, lesquelles sont immédiatement relaxées par la création de nouvelles fissures dans la

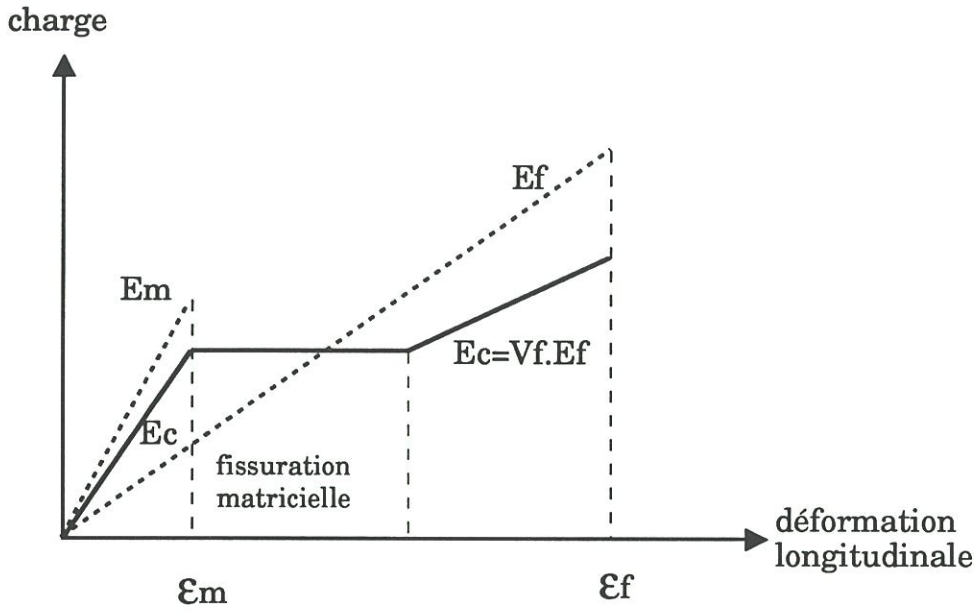

Fig. 1: schéma représentant le comportement en traction des composites unidirectionnels constitués d'une matrice rigide et de fibres dont l'allongement à rupture est supérieur à celui de la matrice [19].

matrice (fig.2). Au cours de ce domaine dit "transitoire", la microfissuration de la matrice s'intensifie. La rupture de la matrice en carbure de silicium, et des céramiques en général, est liée à la présence de défauts. La diminution du volume des blocs de matrice compris entre deux fissures voisines entraîne donc la chute de la probabilité d'une nouvelle rupture [21]. La charge appliquée n'est alors plus suffisante pour créer de nouvelles fissures dans la matrice, la fissuration atteint ainsi un niveau de saturation. La charge est alors entièrement portée par les fibres qui continuent à se déformer élastiquement jusqu'à atteindre leur limite de déformation. Dans cette troisième partie de la courbe, le module d'élasticité du composite est très voisin du produit du module des fibres par la fraction volumique de fibres portant la charge. A $\varepsilon = \varepsilon f$, la rupture des fibres entraîne automatiquement celle du composite.

L'allure de la courbe charge-déformation peut varier en modifiant la qualité du transfert de la charge entre fibres et matrice (fig.3). Si la liaison fibre-matrice est faible, le comportement du matériau se rapproche de celui décrit à la figure 1. La courbe charge-déformation comporte un plateau, correspondant au domaine transitoire, qui est d'autant plus marqué que le transfert de charge est faible. Lorsque la liaison fibre-matrice est plus importante, la matrice se fissure jusqu'à un niveau de charge plus élevé que précédemment et la courbe charge-déformations ne présente plus de plateau. Cependant, si la liaison est trop forte, la fissuration de la matrice peut créer des surcharges locales importantes au niveau des fibres, et entraîner ainsi la rupture prématurée du renfort fibreux. La rupture du composite intervient dans ce cas à un niveau de charge élevé, mais généralement à une déformation moindre du fait que les fibres n'atteignent pas la limite de leur allongement.

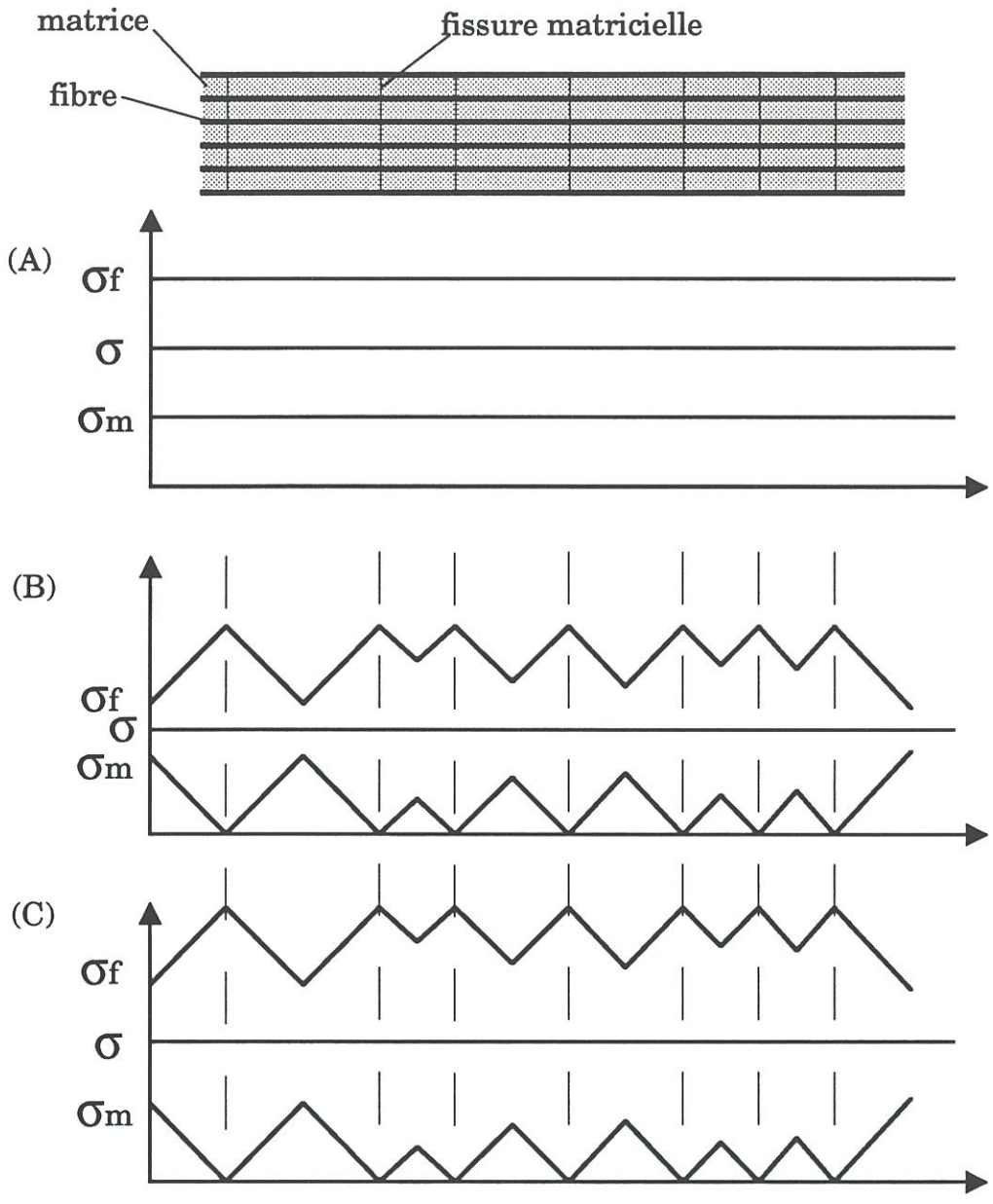

Fig.2: Schema représentant le profil des contraintes dans la matrice (σ_m) et la fibre (σ_f): (A) juste avant la fissuration matricielle, (B) juste après la fissuration matricielle et pour un niveau de contrainte σ_{mc}, (C) après fissuration et lorsque $\sigma > \sigma_{mc}$ (d'après W.A. Curtin [20]).

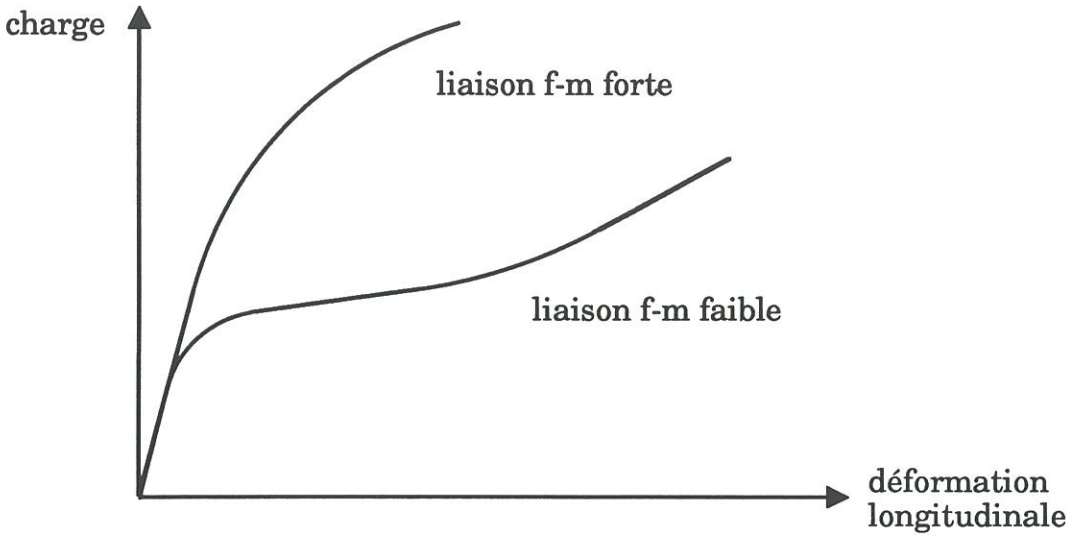

figure 3: influence de la liaison fibre-matrice
sur le comportement en traction.

Le comportement mécanique des composites peut donc être modifié en faisant varier la qualité du transfert de charge entre les fibres et la matrice. L'optimisation de cette liaison fibre-matrice peut être obtenue: (i) en jouant sur la différence des coefficients d'expansion thermique (CET) des constituants du composite [22], et/ou (ii) en interposant entre la fibre et la matrice un troisième constituant appelé "interphase". Les différences de CET entre fibres et matrice peuvent être à l'origine de contraintes résiduelles importantes par:

- effet de frettage de la matrice autour des fibres,
- effet de gonflement des fibres dans les gaines de matrice.

Le résultat de ces deux configurations est identique, les fibres étant mises en compression radiale et la matrice en tension circonférentielle, mais les causes sont différentes puisque dépendantes de la température considérée par rapport à la température d'élaboration du couple fibre-matrice (fig.4). Dans ces deux cas de figure, la liaison fibre-matrice se trouve renforcée par une composante mécanique. Le cas inverse peut se produire, lorsque les fibres se rétractent dans leur gaine de matrice, conduisant alors à une liaison fibre-matrice du type décohésive et donc faible. La modification du transfert de charge entre la matrice et les fibres peut aussi être obtenue en utilisant une interphase. Ce matériau est destiné à transmettre tout ou partie de la charge d'un constituant à l'autre tout en jouant le rôle de barrière de diffusion vis à vis des éléments chimiques. L'ajustement du transfert de charge est alors obtenu en jouant sur les propriétés thermomécaniques de cette interphase. Dans l'état actuel des connaissances, il semble que la structure requise pour ce matériau soit du type lamellaire, les plans atomiques étant au moins localement disposés parallèlement à la surface des fibres. Cette structure permet aux fissures qui se propagent dans la matrice, perpendiculairement à l'axe des fibres et donc de l'axe de sollicitation (mode I), d'être déviées au

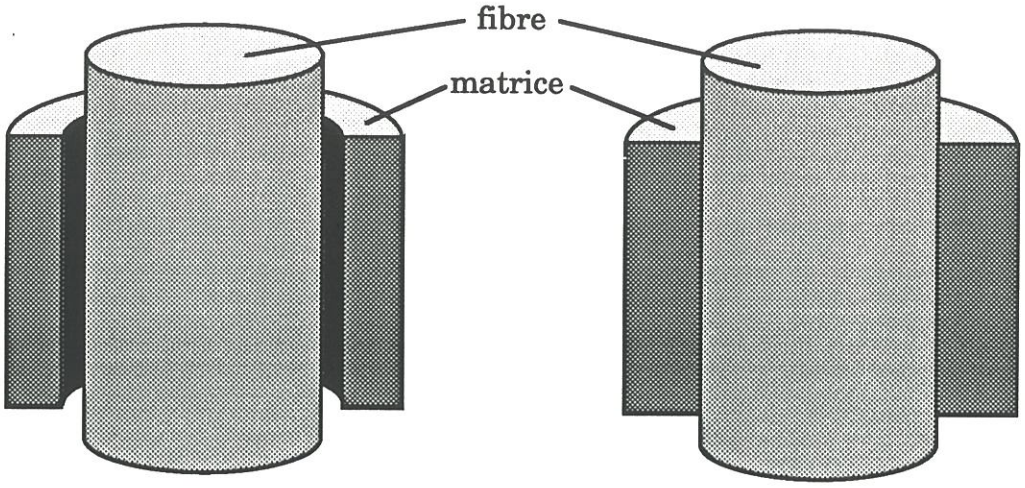

$\alpha m < \alpha fr$; $T < Telab$
$\alpha m > \alpha fr$; $T > Telab$
Liaison fibre-matrice
mécaniquement faible

$\alpha m > \alpha fr$; $T < Telab$
$\alpha m < \alpha fr$; $T > Telab$
Liaison fibre-matrice
mécaniquement forte

fig.4: effet de la différence de CET de la fibre (sens radial) et de la matrice sur la qualité de la liaison fibre-matrice.

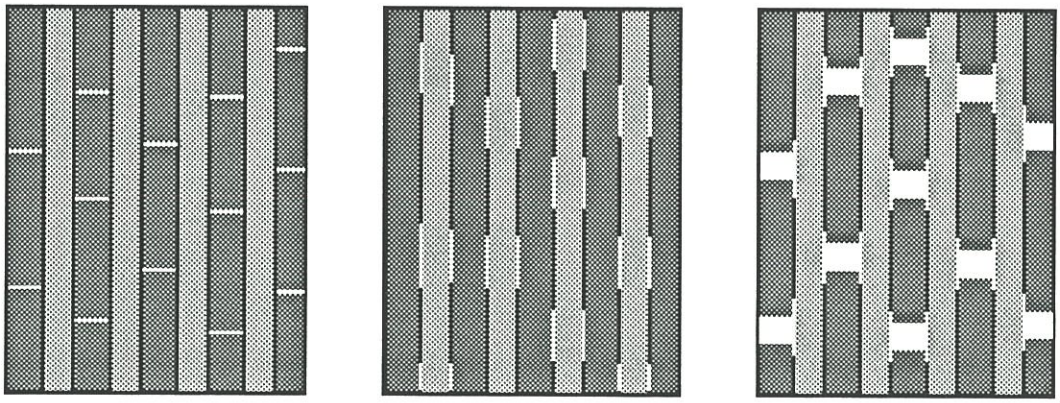

(a) (b) (c)

fig.5: mécanismes d'endommagement envisagés [27]:
(a) multifissuration de la matrice,
(b) décohésion aux interfaces,
(c) fissuration de la matrice entrainant un glissement et/ou une décohésion à l'interface.

contact de l'interphase (mode II), et de contourner les fibres sans les dégrader (d'où la fonction de "fusible" jouée par l'interphase). Les matériaux d'interphase le plus couramment utilisés sont le nitrure de bore hexagonal [23,24] et le carbone pyrolytique [25]. Tous deux présentent, en plus de leur structure feuilletée, des défauts de rotation entre les plans atomiques. Ces défauts dits "turbostratiques" affaiblissent encore les liaisons entre chaque plan et rendent l'anisotropie des propriétés de l'interphase plus marquée.

L'objectif de l'optimisation du transfert de charge fibre-matrice est de permettre au composite de subir des déformations importantes à un niveau de charge le plus élevé possible. Compte tenu de la nature fragile des constituants du composite, notamment la matrice, il est impératif que ceux-ci puissent subir les déformations sans entraîner la rupture du composite. Ce comportement recherché dit **endommageable**, résulte de la présence de plusieurs mécanismes d'endommagement qui permettent au composite d'absorber le maximum d'énergie qui lui est transmise lors des sollicitations mécaniques (fig.5) [19,26-28]. Les mécanismes d'endommagement sont identifiés comme étant:

- la multifissuration de la matrice,
- la décohésion aux interfaces fibre-matrice ou fissuration de (ou des) l'interphase(s),
- le glissement aux interfaces fibre-matrice,
- le déchaussement des fibres (pull-out).

Le transfert de charge fibre-matrice est optimisé lorsque les différents mécanismes d'endommagement ont la possibilité d'être activés au cours des sollicitations mécaniques.

3 - Les composites à matrice en carbure de silicium: C-SiC et SiC-SiC.

Les composites à matrice en carbure de silicium font partie des matériaux susceptibles de servir dans les applications thermostructurales, ce qui implique, par conséquent, la présence de sollicitations mécaniques à haute température (T≤1600°C) et dans des environnements oxydants ou corrosifs (air, à la pression atmosphérique ou à basses pressions...) [29]. Depuis quelques années, de nombreux travaux sont axés sur l'étude des procédés d'élaboration, des propriétés mécaniques et physico-chimiques de ces matériaux.

3.1 - Elaboration

Les composites à matrice céramique et à fibres longues sont élaborés principalement suivant deux techniques: la voie liquide et la voie gazeuse. Le procédé d'élaboration par voie liquide consiste en l'imprégnation d'une préforme fibreuse par un précurseur organométallique de la matrice (e.g. un polycarbosilane pour le carbure de silicium), suivie d'un traitement thermique transformant le précurseur en céramique. Le procédé relevant de la voie gazeuse consiste en un dépôt chimique en phase gazeuse (CVD: chemical vapor deposition) de la céramique autour des fibres constituant la préforme. Cette deuxième méthode connue sous le nom de procédé CVI (chemical vapor infiltration) constitue le principal procédé d'élaboration de l'interphase et de la matrice des composites C-SiC et SiC-SiC (les précurseurs gazeux étant le méthane pour l'interphase et le méthyltrichlorosilane pour la matrice) [30,31].

Ce procédé permet le traitement simultané de nombreuses préformes pouvant différer entre elles aussi bien en taille qu'en forme. Cependant les conditions favorables à l'obtention d'un dépôt homogène dans tout le

volume du substrat fibreux impliquent de faibles vitesses d'infiltration et donc des coûts de production relativement élevés.

3.2 - propriétés mécaniques en traction.

La figure 6 montre le comportement en traction des composites SiC-SiC et C-SiC à la température ambiante [32]. Les courbes contrainte-déformation enregistrées sur les deux matériaux mettent en évidence que:

- les composites SiC-SiC ont un comportement en traction qui débute par un domaine élastique linéaire (σ < 100MPa), le module d'élasticité à l'origine étant de l'ordre de 200GPa, suivi d'un domaine élastique endommageable s'étendant jusqu'à la rupture. Les cycles charge-décharge sont peu ouverts et les déformations résiduelles, après relaxation de la charge, de l'ordre de 0,05%. Les niveaux des contraintes et des déformations à rupture sont plus faibles que dans le cas des composites C-SiC puisque respectivement de l'ordre de 250MPa et de 0,5%.

- les composites C-SiC ne présentent pas de domaine linéaire initial, la courbe débute par un endommagement de la matrice. Le module d'élasticité calculé à l'origine est de l'ordre de 90GPa. Il est possible d'observer la zone transitoire liée à la saturation de la fissuration matricielle et à la reprise de la charge par les fibres de carbone. Les cycles charge-décharge sont quasiment fermés et font apparaître des déformations résiduelles non négligeables, qui évoluent avec le niveau de contrainte maximal de chaque cycle et tendent vers 0,15%. La contrainte à rupture atteint 400MPa pour une déformation longitudinale proche de 1%.

La figure 7 montre l'évolution de la contrainte à rupture en traction en fonction de la température (sous atmosphère inerte) [33]. Elle met en évidence pour $T \geq 1000°C$ une diminution de la résistance dans le cas des

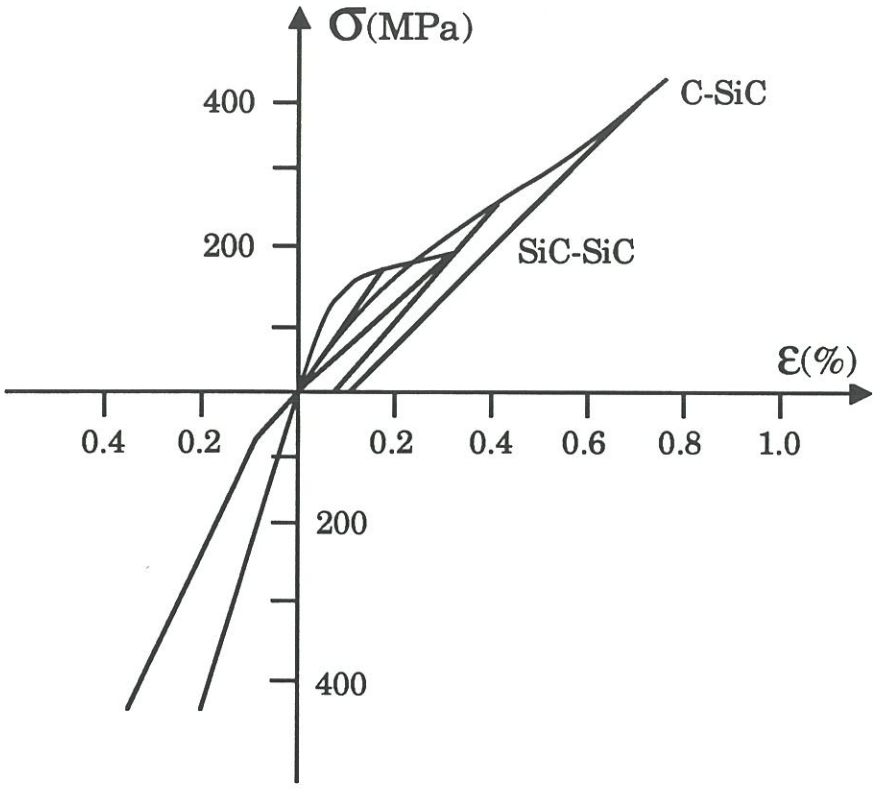

fig.6: courbes de traction / compression
des matériaux 2D SiC-SiC et C-SiC [32].

SiC-SiC et une augmentation de la résistance dans celui des C-SiC. La perte des propriétés mécaniques des SiC-SiC est principalement liée au manque de stabilité thermique de la fibre Nicalon. Cette fibre, issue de la pyrolyse d'un polycarbosilane, est en effet constituée d'une phase microcristallisée de SiC β, de clusters de carbone entourés d'hydrogène et d'une phase oxycarbure amorphe SiCxOy [34]. Au delà de 1000 - 1200°C, la fibre évolue et les propriétés mécaniques chutent d'autant plus rapidement que la température est élevée [35]. La thermostabilité limitée des fibres de carbure de silicium constitue actuellement la principale faiblesse des composites SiC-SiC à haute température. L'augmentation observée de la résistance à la traction des composites C-SiC avec la température dès 900°C pourrait être liée à l'amélioration de la qualité du transfert de charge fibre-matrice, (différence des CET de la fibre et de la matrice dans le sens radial (cf. § 2.2)). La chute de résistance des C-SiC apparaissant au-delà de 1200°C est probablement à relier à l'endommagement que subit le matériau dès lors que la température d'utilisation devient supérieure à la température d'élaboration de la matrice.

3.3 - Tenue à l'oxydation.

La résistance à l'oxydation est une propriété déterminante pour certaines applications dans le secteur aérospatial. Par exemple, les matériaux intervenant dans les structures des avions spatiaux doivent être capables de supporter des températures allant jusqu'à 1600°C dans des environnements variant de l'air ambiant au vide poussé.

Le comportement à l'oxydation des composites SiC-SiC a fait l'objet de plusieurs études [36-38]. Dans ces matériaux, l'interphase de pyrocarbone est le constituant le plus sensible à l'oxydation. Néanmoins,

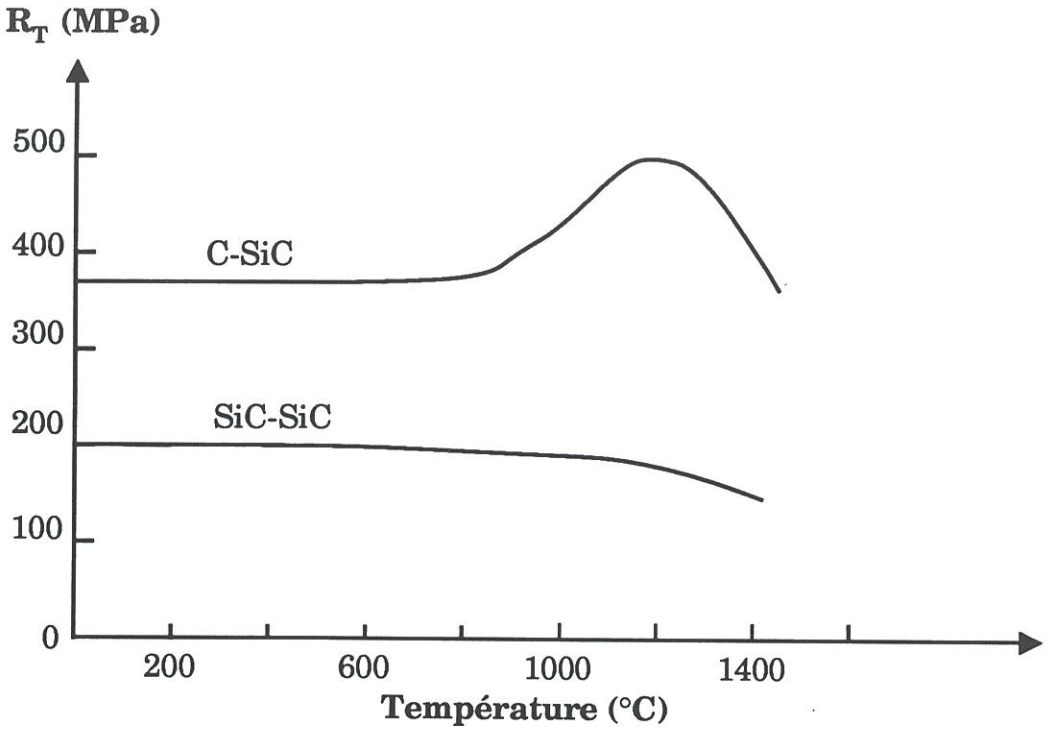

fig.7: évolution de la résistance en traction de composites à matrice SiC en fonction de la température (sous atmosphère inerte) [33].

au-dessus d'une température proche de 1000°C et lorsque l'épaisseur de pyrocarbone n'excède pas un micron, la cinétique d'oxydation est gouvernée par le transfert de masse en phase gazeuse en régime de Knudsen. En effet, l'oxydation de l'interphase laisse des pores de forme annulaire de très faible largeur qui freinent la diffusion des espèces gazeuses. La largeur de ces pores diminue au cours de l'oxydation du fait de la croissance d'une couche de silice sur les parois (fig.8). La vitesse d'oxydation de l'interphase est ainsi ralentie jusqu'à devenir nulle lorsque les pores sont totalement cicatrisés par la silice. L'importance de la dégradation des propriétés mécaniques causée par l'oxydation est alors fonction de la quantité de pyrocarbone consommé et de silice formée sur les parois des pores avant la cicatrisation.

Les composites C-SiC présentent des caractéristiques mécaniques en traction supérieures à celles des SiC-SiC. Cependant, la présence des fibres en carbone constitue un sérieux inconvénient quant à leur utilisation dans une atmosphère oxydante. La matrice en carbure de silicium n'est pas capable à elle seule d'assurer une parfaite protection contre l'oxydation du renfort en carbone du fait de la présence des fissures [39]. L'emploi des composites C-SiC en milieu oxydant, tout comme celui des composites C-C, dans un domaine de température supérieure à 500°C, nécessite donc l'utilisation d'un revêtement protecteur externe assurant une parfaite étanchéité du matériau vis à vis des gaz oxydants. La nature de ces dépôts a fait l'objet d'importants travaux [40-44]. La protection des composites à renfort en carbone n'est pas simple puisqu'elle ne peut être réalisée par un seul constituant sur un domaine de température allant de 500°C à 1600°C. Une des protection les plus efficaces est basée sur l'utilisation de l'oxyde de bore B_2O_3. Ce matériau possède une température de fusion de ≈ 500°C (i.e. proche de la température de début d'oxydation du carbone), et une température de volatilisation de ≈ 1100°C.

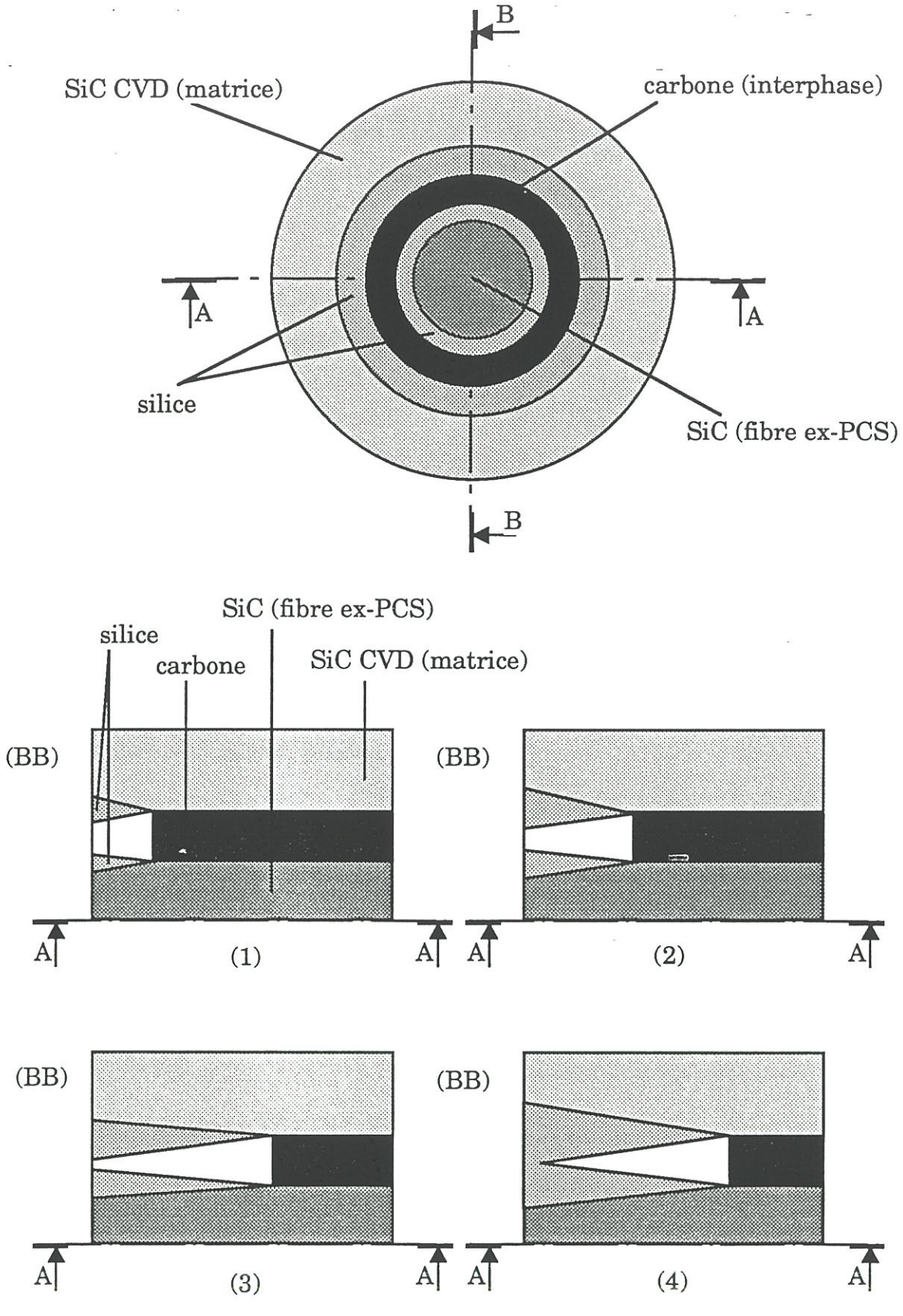

fig.8: oxydation progressive de l'interphase de carbone au sein d'un composite SiC /SiC, avec croissance de silice sur la fibre et la matrice en SiC, jusqu'à cicatrisation du pore (d'après [36]).

Le revêtement déposé sur le composite C-SiC est constitué soit d'oxyde de bore, soit d'un composé du bore (BN, B_4C, ZrB_2...) créant l'oxyde de bore en cours d'oxydation. Par exemple, la protection des C-SiC revêtus d'un oxyde de bore peut s'effectuer, suivant le domaine de température, comme suit :

- 500°C-1100°C: l'oxyde de bore liquide diffuse par capillarité dans la porosité de la matrice SiC et bloque la diffusion de l'oxygène en phase gazeuse dans les fissures conduisant aux fibres,

- 1100°C-1400°C: le carbure de silicium s'oxyde, la silice créée une solution liquide avec l'oxyde de bore. La solution B_2O_3-SiO_2 diffuse à son tour dans les fissures de la matrice,

- T>1400°C: la solution s'appauvrit en oxyde de bore, seule la silice assure la protection du matériau.

La durée de vie de ce revêtement protecteur n'est pas illimitée. L'évaporation de l'oxyde de bore au-dessus de 1100°C diminue l'efficacité de la protection à basse température. Par ailleurs, ces revêtements ne sont pas à l'abri d'un endommagement lors d'un choc mécanique en cours d'utilisation qui affaiblirait localement cette protection. Devant ce risque, il s'avère alors important de connaître le comportement à l'oxydation des composites C-SiC en absence de toute protection, autre que la matrice en carbure de silicium, et de prévoir les conséquences d'un traitement oxydant sur les propriétés mécaniques du matériau.

4 - Objectifs.

L'emploi des composites C-SiC à haute température et dans un environnement oxydant ne peut se faire sans l'utilisation d'un système de protection contre l'oxydation du renfort fibreux. Cependant, les revêtements protecteurs connus actuellement ne sont pas parfaits. Il est nécessaire de mieux connaître et de prévoir le comportement des composites C-SiC en absence de ces systèmes de protection.

L'objectif de ce travail était donc d'étudier le comportement à l'oxydation des composites C-SiC non totalement protégés.

Le premier chapitre est consacré à l'étude de la réactivité des différentes phases carbonées constituant le renfort fibreux. La relation entre la structure et la cinétique d'oxydation de ces phases y est établie.
Les deuxième et troisième chapitres sont consacrés à l'étude des mécanismes qui gouvernent la cinétique d'oxydation des composites C-SiC. Dans un premier temps, une approche expérimentale permettra d'identifier les mécanismes d'oxydation et les modes de dégradation du renfort fibreux associés à ces mécanismes. Ensuite, un modèle mathématique de la cinétique d'oxydation des composites sera développé. Ce modèle permettra: (i) de vérifier la validité des hypothèses faites pour expliquer la cinétique d'oxydation de ces matériaux et (ii) d'étudier l'influence des paramètres liés à l'environnement oxydant (T, PO_2) et au matériau (épaisseur de la couche externe fissurée de la matrice, effet des sollicitations mécaniques) sur la cinétique d'oxydation des composites C-SiC. Enfin, le dernier chapitre établira une corrélation entre les divers modes de dégradation par oxydation et l'évolution des propriétés mécaniques en traction des composites C-SiC.

REFERENCES

[1] R. NASLAIN, "Introduction aux matériaux composites fibreux à matrice inorganique", dans *Introduction aux matériaux composites* Vol.2 (édité par R. Naslain), pp 19-36, CNRS/IMC, France, Bordeaux, 1985.

[2] D.J. JOHNSON, " Carbon fibres: manufacture, properties, structure and applications", dans *Introduction to carbon science* (édité par H. Marsh), pp 197-228, Butterworths & Co, Londre, 1989.

[3] W. PATON, "Impact of carbon fibers on FRP technology" dans *Carbon fibers* (édité par The Plastics and Rubber Institute), pp 2-9, Noyes Publications, 1986.

[4] M.S. DRESSELHAUS, G. DRESSELHAUS, K. SUGIHARA, I.L. SPAIN and H.A. GOLDBERG, "Applications of graphite fibers and filaments" dans *Graphite fibers and filaments* (édité par M. Cardona), pp 304-340, Springer-Verlag, Londre, 1988.

[5] I.W. SMITH, "The intrinsic reactivity of carbon to oxygen", *Fuel*, 57, 409-414 (1978).

[6] K.S. GOTO, K.H. HAN and G.R. St. PIERRE, "A review on oxidation kinetics of carbon fiber/carbon matrix composites at high temperature", *Trans. Iron. Steel. Inst. Japan*, 26 [7] 597-603 (1986).

[7] H.W. CHANG and S.K. RHEE, "Oxidation of carbon derived from phenolic resin", *Carbon*, 16, 17-20 (1978).

[8] P. EHRBURGER and J. LAHAYE, "Characterization of carbon-carbon composites -II oxidation behavior", *Carbon*, 19, 7-10 (1981).

[9] H.W. CHANG and R.M. RUSNAK, "Oxidation behavior of carbon-carbon composites", *Carbon*, 17, 407-410 (1979).

[10] J.X. ZHAO, R.C. BRADT and P.L. WALKER, " Effect of air oxidation at 873K on the mechanical properties of carbon-carbon composite", *Carbon*, 23 [1] 9-13 (1979).

[11] D.C. PHILLIPS, "Interfacial bonding and the toughness of carbon fibre reinforced glass and glass-ceramics", *J. Mater. Sci.*, 9 (1974) 1847-1854.

[12] K.M. PREWO and J.A. BATT, "The oxidative stability of carbon fibre reinforced glass-matrix composites", *J. Mater. Sci.*, 23, 523-527 (1988).

[13] F. CHRISTIN, "Les composites carbone-carbone-carbure de silicium: une nouvelle famille de matériaux destinés à des applications à haute température", *Thèse d'Etat* n°641, Université de Bordeaux, 1979.

[14] H. HANNACHE, "CVD du nitrure et carbure de bore. Application aux matériaux composites céramique-céramique", *Thèse d'Etat* n°813, Université de Bordeaux, 1984.

[15] J.Y. ROSSIGNOL, "Sur les matériaux composites céramique-céramique à renfort bidirectionnel de fibres de carbone et à matrice hybride carbone-carbure ou carbone-nitrure élaborés par CVI", *Thèse d'Etat* n°833, Université de Bordeaux, 1985.

[16] G.H. SCHIROKY, "Oxidation behavior of chemically vapor-deposited silicon carbide", *Advanced Ceramic Materials*, 2 [2] 137-141 (1987).

[17] S. YAJIMA, K. OKAMURA, T. MATSUZAWA, Y. HASEGAWA and T. SHISHIDO, *Nature* , (Londre), 279 [5715] 706-707 (1979).

[18] G. SIMON, *Thèse*, Ecole Nationale des Mines de Paris, 1984.

[19] J.M. QUENISSET, "23ème Colloque du groupe français de Rhéologie", pp 1-41, Editeur Cermub, Bordeaux, 1988.

[20] W.A. CURTIN, "Theory of mechanical properties of ceramic-matrix composites", *J. Am. Ceram. Soc.* 74 [11] 2837-45 (1991).

[21] R. LABBENS, "Introduction à la mécanique de la rupture", Editions Pluralis, Paris 1980.

[22] M.K. BRUN and R.N. SINGH, "Effect of thermal expansion mismatch and fiber coating on the fiber/matrix interfacial shear stress in ceramic matrix composites", *Advanced Ceramic Materials*, 3 [5] 506-509 (1988).

[23] O. DUGNE, "Aspects chimiques, microstructuraux et micromécaniques des matériaux composites SiC-SiC à interphase de nitrure de bore", *Thèse* n°375, Université de Bordeaux, 1989.

[24] S. PROUHET, "Cinétique de la CVD du nitrure de bore dans le système BF_3-NH_3-Ar. Application aux matériaux composites SiC/SiC à interphase BN", *Thèse* n°662, Université de Bordeaux, 1991.

[25] J.G. THEBAULT, "Fabrication process of a composite material with a refractory reinforcement and a ceramic matrix and structure elaborated with such process", *brevet* français 2 567 874 A1, 1984.

[26] A.G. EVANS and D.B. MARSHALL, Mat. Res. Soc. Symp. Proc., Editeurs F.D. Lemkey, S.G. Fishman, A.G. Evans and J.R. Strife, 120, 213-246 (1988).

[27] R. TALREJA, "A continuum mechanics characterization of damage in composite materials", Proc. R. Soc. Lond., A 399, 195-216 (1987).

[28] D. ROUBY, "IIème Conférence Franco-Allemande sur les Céramiques Techniques", Aix-la-Chapelle, 265-286 (1987).

[29] B. BROQUERE, B. BUTTAZZONI and J.J. CHOURY, "Les composites carbone-carbone, leurs applications industrielles" dans *Introduction aux matériaux composites* (édité par R. Naslain), pp 405-438, CNRS/IMC, France, Bordeaux, 1985.

[30] R. NASLAIN, F. LANGLAIS and R. FEDOU, "The CVI-processing of ceramic matrix composites", Proc. 7th European Conf. on CVD, Journal de Physique, Colloque C5, Suppl. 5, 50, 191(1989).

[31] C. PREBENDE, "Mecanismes physico-chimiques mis en jeu dans le processus CVD d'élaboration de céramiques à base de carbure de silicium en réacteur à parois chaudes", *Thèse* n°347, Université de Bordeaux, 1989.

[32] J.M. JOUIN, "Comportement sous chargements cycliques des composites bidirectionnels à matrice carbure de silicium", dans *Matériaux composite pour applications à haute température* (Editeurs R. Naslain, J. Lamalle and J.L. Zulian), pp 169-180, Actes du colloque AMAC/CODEMAC, France, Bordeaux, 1990.

[33] J.C. CAVALIER, A. LACOMBE and J.M. ROUGES, "Composites à matrice céramique, nouveaux matériaux à trés hautes performances", dans *Developments in the science and technology of composite materials* (Editeurs A.R. Bunsell, P. Lamicq, A. Massiah), third European conference on composite materials (ECCM-3), pp 99-110, AEMC, France, Bordeaux, 1989.

[34] C. LAFFON, A.M. FLANCK, P. LAGARDE, M. LORIDJANI, R. HAGEGE, P. OLRY, J. COTTERET, J. DIXMIER, J.L. MICQUEL, H. HOMMEL and A.P. LEGRAND, *J. Mater. Sci.*, 24, 1503-1512 (1989).

[35] L. FILIPUZZI, G. CAMUS, J. THEBAULT and R. NASLAIN, "Effect of high temperature ageing treatments on the mechanical behavior of unidirectional SiC/SiC fibrous composites" dans *Structural ceramics processing, microstructure and properties* (Editeurs J.J. Bentzen, J.B. Bilde Sorensen, N. Christiansen, A. Horsewell and B. Ralph), Proc. of the 11th Risø International Symposium on Metallurgy and Materials Science, pp 283-289, Risø National Laboratory, Roskilde, Danemark, 1990.

[36] L. FILIPUZZI, "Oxydation des composites SiC/SiC et de leurs constituants: approche expérimentale, modélisation et influence sur le comportement mécanique", *Thèse* n°593, Université de Bordeaux, 1991.

[37] N. FRETTY, R. MOLINS and M. BOUSSUGE, 7ème Journée nationale sur les composites, pp 411-420, publié par G. Fantozzi and P. Fleischmann, AMAC, Paris, 1990.

[38] P. PLUVINAGE, L. FILIPUZZI and G. CAMUS, "Mechanical behavior and oxidation resistance of a unidirectional SiC/SiC fibrous composite", Proc. of the Second International Ceramic Science and Technology Congress, Symposium on Ceramic, Polymer and Metal Matrix Composites, Orlando, FL (USA), 1990.

[39] F. LAMOUROUX, G. CAMUS and R. NASLAIN, "Oxidation resistance and strength after oxidation of a 2D woven carbon fiber silicon carbide matrix composite" dans *Developments in the science and technology of composite materials* (Editeurs A.R. Bunsell, J.F. Jamet, A. Massiah), pp 409-504, ECCM-5, Bordeaux, 1992.

[40] T.D. NIXON and J.D. CAWLEY, "Oxidation inhibition mechanisms in coated carbon-carbon composites", *J. Am. Ceram. Soc.*, 75 [3] 703-708 (1992).

[41] I. JAWED and D.C. NAGLE, "oxidation protection in carbon-carbon composites", *Mater. Res. Bull.*, 21, 1391-1395 (1986).

[42] D.W. Mc KEE, "Oxidation behavior and protection of carbon/carbon composites", *Carbon*, 25 [4] 551-557 (1987).

[43] TSUNG-MING WU, WEN-CHENG WEI and SHU-EN HSU, "Sol-gel silica in the healing of microcracks in SiC-coated carbon/carbon composites", *Journal of the European Ceramic Society*, 9, 351-356 (1992).

[44] M. BONCOEUR, G. SCHNEDECKER and J.D. LULEWICZ, "HfC plasma coating of C/C composites", dans *Ceramic Engineering and Science Proceeding*, pp 348-355, Proc. of the 16th Annual Conference on Composites and Advanced Ceramic Materials, Cocoa Beach, FL (USA), 1992.

CHAPITRE 1

STRUCTURE/OXIDATION BEHAVIOR RELATIONSHIP IN THE CARBONACEOUS CONSTITUENTS OF 2D-C / PyC / SiC COMPOSITES

Les fibres de carbone T300 et l'interphase en carbone sont les deux constituants du composite C/SiC les plus sensibles aux environnements oxydants de par leur nature. L'endommagement de la matrice permet à l'oxygène de migrer vers le carbone via les fissures et les décohésions présentes dans le matériau.

Dans l'objectif de comprendre l'effet de l'environnement oxydant sur le comportement global du composite C/SiC, il s'est avéré intéressant de localiser à **l'échelle microscopique** les différentes phases de carbone préférentiellement dégradées lors d'une oxydation.

Dans cette étude, un comportement à l'oxydation original de la fibre de carbone est mis en évidence. Une corrélation est établie entre la morphologie et la cinétique d'oxydation de la fibre de carbone T300. Les effets de la température sur les paramètres morphologiques et cinétiques sont étudiés afin de prendre en considération l'évolution que peut subir le composite C/SiC lorsqu'il est porté à haute température.

Le chapitre est présenté sous la forme d'un projet de publication adressé à la revue **Carbon**.

STRUCTURE/OXIDATION BEHAVIOR RELATIONSHIP IN THE CARBONACEOUS CONSTITUENTS OF 2D-C / PyC / SiC COMPOSITES

F. LAMOUROUX, X. BOURRAT and **R. NASLAIN**
Laboratoire des Composites Thermostructuraux, UMR-47
(CNRS-SEP-UB1), Domaine Universitaire, 3 allée de la Boëtie
33600-Pessac, France.

J. SEVELY
CEMES-Laboratoire d'Optique Electronique du CNRS
(UPR), 29 rue Jeanne Marvig, BP.4347
31055 - Toulouse-cédex, France.

ABSTRACT

Oxidation tests were performed, under a flow of pure oxygen (at 500 < T < 900°C), on (i) as-received T300 fiber, (ii) PyC-infiltrated tows and (iii) C/PyC/SiC composite. The goal was to assess which carbonaceous constituent exhibits the highest reactivity with oxygen in the composites. TGA and TEM were used to establish the relationship between the behavior of the materials in oxygen and their nano/microtexture. In the as-processed state, the overall oxidation rate of the fiber is higher than that of the PyC-interphase whereas both constituents behave in a similar way after an annealing treatment at 1600°C. The oxidation rate of the uncoated fibers increases first rapidly then remains almost constant (for 20 < Δm/mo < 70%) and finally decreases smoothly. Beyond 700°C, the rate determining step in the oxidation of uncoated fibers is diffusion transport in the external stagnant boundary layer. Below 700°C, it is a mixed in-pore diffusion/surface reaction mode for the as-received fibers and mainly surface reaction for the annealed fibers. The oxidation of the fiber is selective. In cross-section, it occurs more rapidly in the outer zone, owing to the high porosity of this specific zone. Additionally, there is a ring, at mid-distance between the fiber center and surface, where carbon is better organized and which exhibits a lower reactivity. The occurrence of a high porosity zone very near the PyC-interphase plays a key role in the understanding of the effect of environment on the mechanical behavior of the composites.

Key words: Carbon fiber, pyrocarbon interphase, C/SiC composite, oxidation, TEM-analysis.

1 - INTRODUCTION

C(T300)/PyC/SiC(CVI) composites, which will be referred to more simply as C/SiC composites in the following, are fabricated from T300 carbon fiber(*) preform according to a two-step chemical vapor infiltration (CVI) process. They are designed to withstand exposures to severe environments, e.g. high temperatures (up to ≈ 1600°C) and oxidizing atmospheres, and are thus potential candidate materials for applications in the aerospace field [1-3].

One of the important advantages of the carbon fiber, with respect to the Si-C-(O) Nicalon-type fiber(**) , lies in the fact that it is stable over a much larger temperature range, the Nicalon fiber being known to undergo decomposition beyond ≈ 1100°C with a strength loss, in its present versions which contain ≈ 10 - 15 wt.% O [4-5]. A pyrocarbon (PyC) interphase (thickness : ≈ 0.5 - 1 μm) is deposited on the fiber surface (first CVI-step). This layer is acting as a mechanical fuse, i.e. deflecting the matrix microcracks along the interface and thus protecting them from an early failure. The interphase gives a non-linear mechanical behavior to the C/SiC composites [6]. The main role of the SiC-matrix (deposited on the PyC-coated carbon fibers in the second CVI-step) is in principle to protect the carbon fibers and their PyC coatings against oxidation, carbon being known to react with oxygen beyond 400-500°C. However, the situation is actually more complex.

The occurrence of residual mechanical stresses (generated in C/SiC composites by thermal expansion mismatch) and the lack of plasticity of SiC at medium temperatures are such that matrix microcracking cannot

---

(*) a high strength ex-PAN fiber from Toray, Japan.
(**) an ex-PCS ceramic fiber from Nippon Carbon, Japan.

be avoided. Therefore, additional protections against oxidation (e.g. an external coating consisting of a glass-former material) are used in order to prevent or at least to slow down the in-depth diffusion of oxygen towards the vulnerable carbon reinforcement and PyC interphase. As a matter of fact, the additional protections themselves may not behave in a perfect manner, under specific in service conditions, with the result that the risk of some oxidation of the carbonaceous constituents cannot be fully eliminated. Such an oxidation, even limited, has been reported to yield a significant weakening of the material. As an example, an oxidation treatment at medium temperatures (e.g. 900°C) corresponding to a weight loss of 2 wt.% was observed to result in a tensile failure strength decrease of almost 40 % [7]. This dramatic influence of the environment on the mechanical behavior of C/SiC composites suggests that oxygen after having diffused in-depth has reacted with a key constituent of the materials which could be the fibers or/and the PyC interphase. Since the carbon fiber and the PyC interphase are expected to exhibit different oxidation rates (owing to their different structures and impurity contents), the degradation of the mechanical properties might be related to a **preferential** oxidation process at the level of one of the carbonaceous constituents.

The carbons have been reported to exhibit different oxidation rates depending on their structures, microtextures and chemical compositions (nature and amount of impurity atoms) [8,9]. These differences are related to the nature of the organic precursor (e.g. PAN or pitch for the fibers and methane or propane for PyC) as well as to the processing technique. Specific impurities such as transition elements, oxides and salts of alkaline and alkaline earth elements, act as oxidation catalysts [10]. Poorly crystalline carbons show oxidation rates which are much

higher than those characterizing highly ordered carbons. For graphitable carbon fibers, the degree of crystallization depends on the value of the highest temperature (HTT) achieved during processing. High modulus (HM) carbon fibers, treated beyond 2000°C, exhibit a structure close to that of graphite. Their chemical reactivity with respect to oxygen is thus less than that of high strength (HS) fibers processed at much lower temperatures. Furthermore, the use of HS fibers at temperatures significantly higher than their processing temperature can result in an improvement of their crystallization state and thus in a lowering of their oxidation rate (the same effect being also observed for pyrocarbons). It is actually what may happen in C/SiC composites (processing temperature: 1000-1200°C; in service temperatures: up to 1600°C).

The aim of the present contribution, which is a continuation of an article published previously [7], was to establish whether there is a preferential oxidation of the PyC interphase or carbon fiber in C/SiC composites that could explain the dramatic effect of an oxidizing environment on their mechanical behavior. The study has been focused on: (i) the correlation between the structure/microtexture of the carbonaceous components and their behavior with respect to oxidation and (ii) the effect of an HTT on both the carbon fibers and the PyC interphases in order to take into account the influence of the thermal history of the C/SiC composites on their oxidation rates.

2 - EXPERIMENTAL

2.1 - Materials.

The oxidation tests and the physico-chemical analyses have been performed on three kinds of materials : (i) as-received C(T300) tows, (ii)

C(T300) fiber tows infiltrated with a coating of pyrocarbon and (iii) 2D-C(T300) / PyC / SiC (CVI) composites, in order to assess directly the kinetics of oxidation of the carbonaceous constituents of the actual composite materials. Additional oxidation tests were also conducted on materials previously annealed up to 1600°C in an inert atmosphere.

The pyrocarbon interphase (or coating) and the SiC-matrix were chemically deposited from a gaseous precursor (i.e. methane for carbon and a mixture of CH_3SiCl_3 (MTS) and hydrogen for SiC) according to the isothermal/isobaric chemical vapor infiltration (ICVI) process [11,12]. The experiments were performed at low temperatures (i.e. 1000-1100°C) and under reduced pressures (a few kPa or 10 kPa) in order to favor in depth deposition. For the C/SiC composite, several SiC CVI runs were necessary to achieve a low enough residual porosity, as already mentioned elsewhere [13-14].

2.2 - Oxidation tests.

The oxidation kinetics were derived from isothermal oxidation tests performed by **thermogravimetric analysis** (TGA)(*) at 550-900°C in pure oxygen(**) (P = 100kPa, gas flow Q: 1 liter per hour). The weight loss of the sample was continuously recorded versus time (sensitivity: 10^{-6} g).

2.3 - Material characterization.

The structure and microtexture of the carbon fibers, the PyC interphase, the SiC-CVI matrix and the related interfaces, were mainly studied by **transmission electron microscopy** (TEM). The thin foils were obtained from specimens (as-processed or annealed at 1600°C) cut

---

(*) TGA apparatus : 24 S 16 from SETARAM.
(**) N48 oxygen, from ALPHAGAZ, Toulouse.

perpendicular to the fibers. The specimens were thinned first mechanically and then by ion-etching(*), according to classical procedures. They were observed in bright field, dark field and lattice fringe modes (**). Chemical analyses of the T300 fibers were performed by electron energy loss spectroscopy (EELS)(***) directly on the 2D-C/PyC/SiC composites. Finally, the morphology of the specimens has been characterized by scanning electron microscopy (SEM)(****).

3 - RESULTS

3.1 - Microstructure of 2D-C/PyC/SiC composites.

An optical micrograph of a polished cross-section of an as-processed C/SiC composite (fig.1a) shows two important microstructural features of this kind of materials : (i) large **residual pores**, located between the woven plies left by an incompleted infiltration (the SiC-infiltration is usually stopped when the overall porosity is of the order of 10 to 15 %) [11, 13, 14] and (ii) **matrix microcracks** resulting from coefficient of thermal expansion (CTE) mismatching (discussed in section 4).

The three constituents, namely the carbon fiber, the PyC-interphase and the SiC-matrix are clearly apparent at higher magnification in the TEM bright field image shown in fig. 1 b.

The **T300 HS carbon fiber** exhibits an irregular elliptic cross-section, with a mean diameter of 6-8 μm and an aspect ratio (defined as the ratio between the large and small axes of the elliptic section) ranging from 1 to 1.3. Such a feature has been already reported by various authors, e.g. on

---

(*) 600-DIF , from GATAN.
(**) 2000 FX TEM, from JEOL, Japan.
(***) CM 30ST, from PHILIPS, Holland, equiped with a GATAN PEELS spectrometer.
(****) 840 A SEM, from Jeol, Japan.

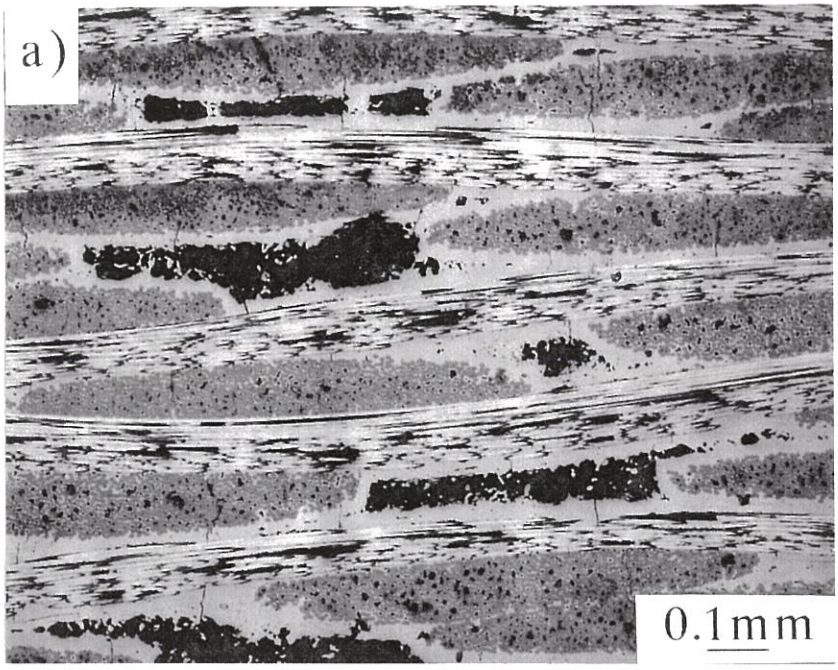

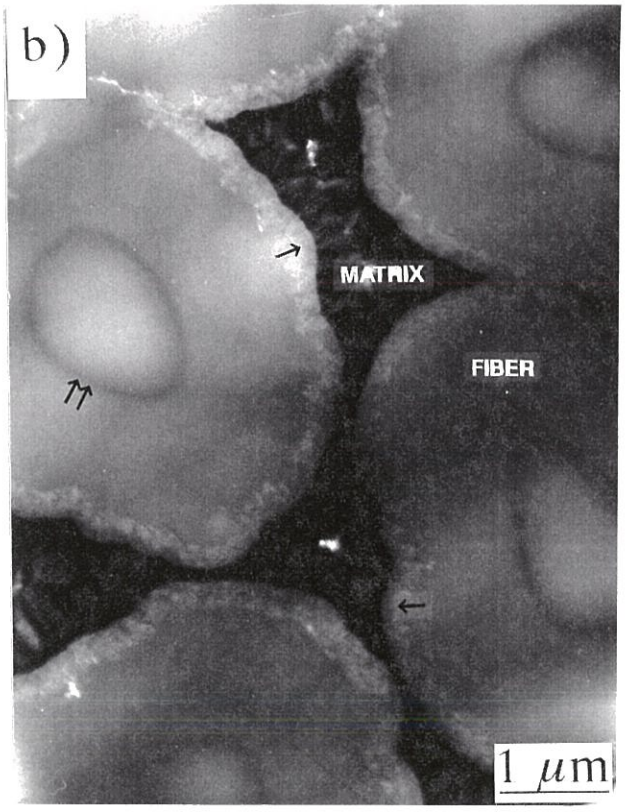

Fig.1: Cross-section micrographs of a 2D-C/PyC/SiC composites in the as-processed state: a) at low magnification: the carbon fibers and interphases appear in grey, the SiC-matrix in white and the residual pores in black (optical micrograph) and b) at high magnification (TEM bright field).

the basis of detailed laser diffraction experiments (see, for example, ref. [15] and [16]). Additionally, the surface of the T300 fiber (which is seen in cross-section, in fig. 1 b) is not smooth but appears striated, a feature which is thought to be related to the shape of the spinneret used for spinning the PAN-precursor. Finally, a ring is always observed in the fiber-cross section whatever the microscopy which is used (double arrow in fig. 1b). The nature and the origin of this ring will be discussed in the next sections.

The morphology of the **PyC-interphase** and of the related PyC/fiber and PyC/matrix interfaces is shown at low magnification in fig.1b and with more details in fig. 2. The thickness of the PyC-interphase, as measured from fig.2, is of the order of 0.4 μm but it varies within a fiber bundle (see fig. 1 b) and from one bundle to the other, a feature which is common in CVI-processed composites. Generally speaking, the interphase consists of rough laminar pyrocarbon [17] and it exhibits locally (i.e. at the 100 nm scale) significant anisotropy variations. Moreover, there is very near the interphase/fiber interface a reinforcement of the image contrast which is related to a much better organization of the carbon atomic layers (tripple arrow in fig.2). Such a feature has been already reported for 2D-SiC/PyC/SiC composites fabricated according to the same process [18,19]. There is a good cohesion betweeen the PyC-interphase and the surrounding media with however the occurrence of the opening of a network of decohesions roughly parallel to the SiC/PyC interface (double arrow in fig.2). Additionally, small pores can be noticed in the carbon fiber located near the fiber/PyC interface (single arrow in fig.2).

The microstructure of the **SiC(CVI) matrix** is shown, at low magnification, in fig. 3, for an area of a 2D-C/SiC composite located at the

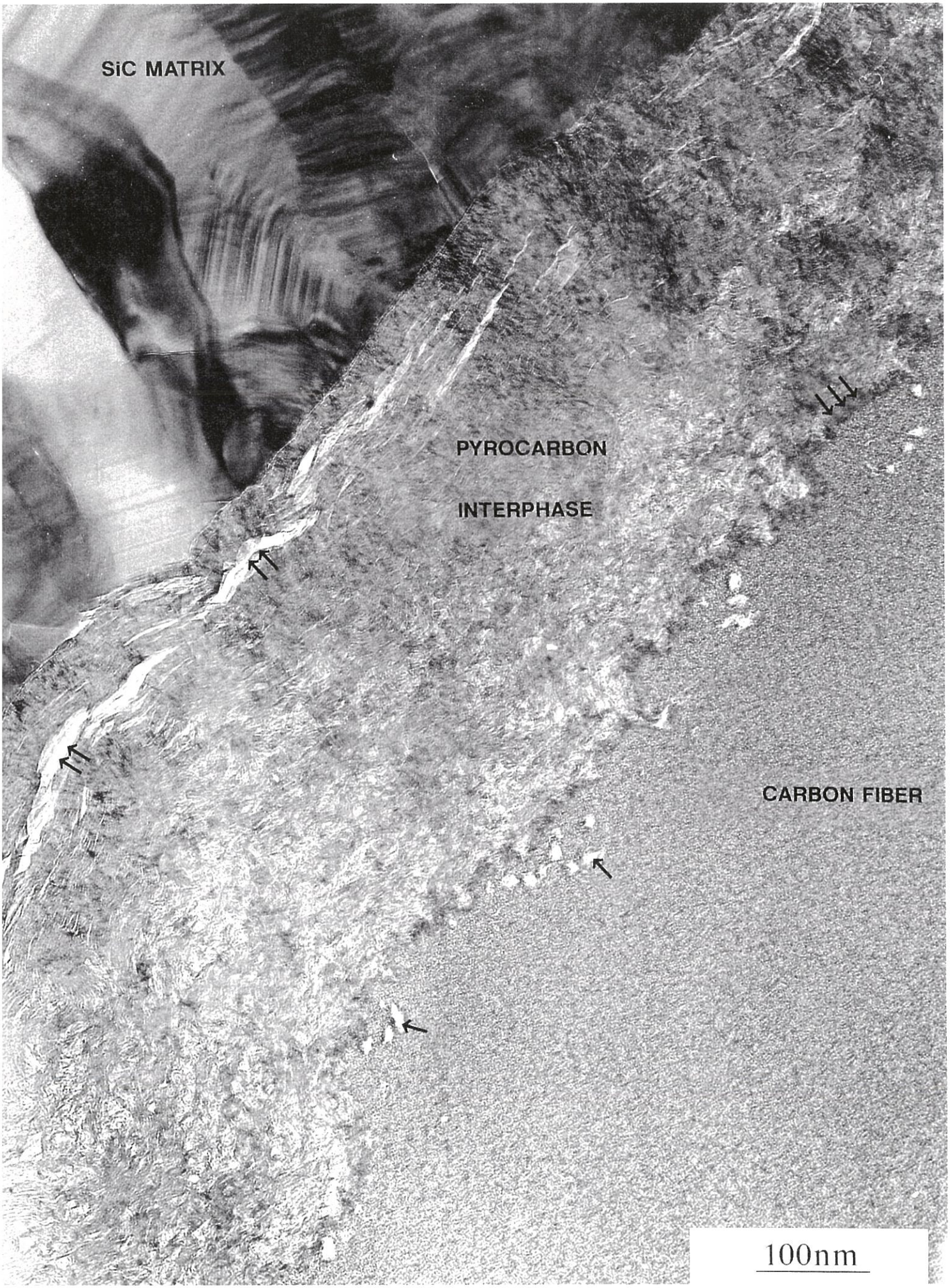

Fig.2: TEM (bright field) image of the fiber/matrix interfacial zone showing the microstructure of the PyC-interphase, the fiber/PyC and the PyC/SiC-matrix interfaces.

periphery of a fiber tow (where the matrix thickness is larger than within the tow). In such an area, all the SiC-deposits corresponding to the successive CVI-runs are clearly apparent. The first layer consists of unidirectional disordered polytypes (UDP) of SiC [20,21]. It exhibits a columnar texture with a growth direction parallel to the [111] direction of cubic β-SiC (single arrow in fig.3) and a "feather" image contrast. The next layers have more complex microstructures, as already reported by Schamm for the related 2D-SiC/SiC composites [22]. Finally, fig.3 shows a large zone of decohesion at the PyC/SiC-matrix interface (double arrow) thought to result from residual stress arising from CTE-mismatch.

The TEM-analysis shows that a network of **decohesion zones and microcracks** is present in as-processed 2D-C/SiC composites. In addition, pores of various sizes (large residual pores in the SiC-matrix and very small pores in the fiber very near the PyC/fiber interface) are also present. Part of these defects are thought to be interconnected, allowing thus oxygen to diffuse in depth and to react with the carbonaceous phases when the material is exposed to an oxidizing atmosphere. However, since carbon fibers and pyrocarbon were known to react with oxygen at different rates [23], oxidation tests on both PyC-infiltrated T300 tows and bare T300 fibers have been performed in order to assess which carbonaceous phase exhibits actually the highest reactivity with oxygen in 2D-C/SiC composites.

3.2 - Oxidation of C/C tows.

TGA-experiments were performed first on PyC-infiltrated T300 fiber tows at 600°C in pure oxygen. The variations of the relative weight loss ($\Delta m/mo$) as a function of time are shown in fig. 4a. The shape of the TGA-curve suggests the occurrence of two oxidation domains. After a transient

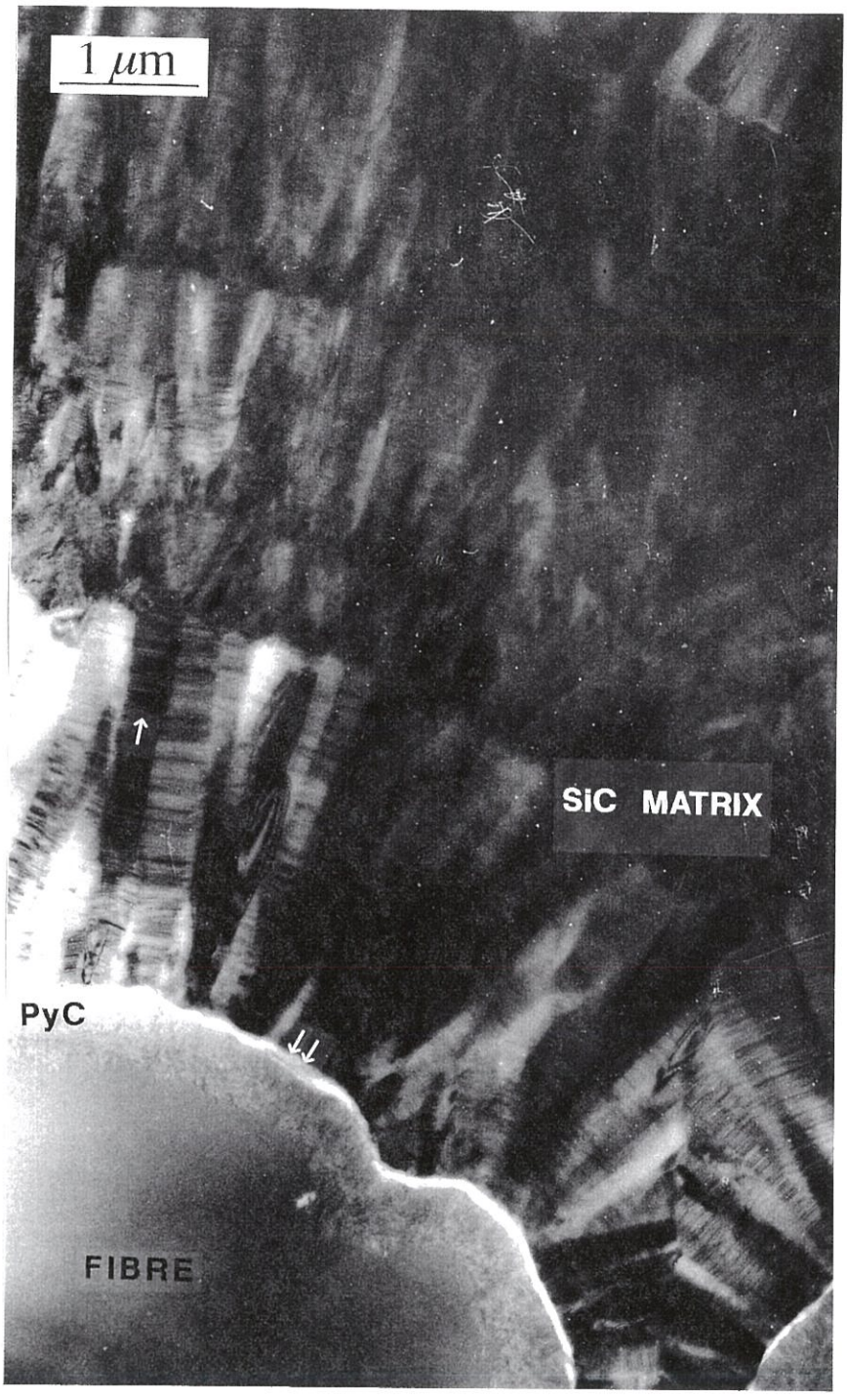

Fig.3: TEM (bright field) image of the SiC (CVI) matrix and of the fiber/matrix interfacial zone.

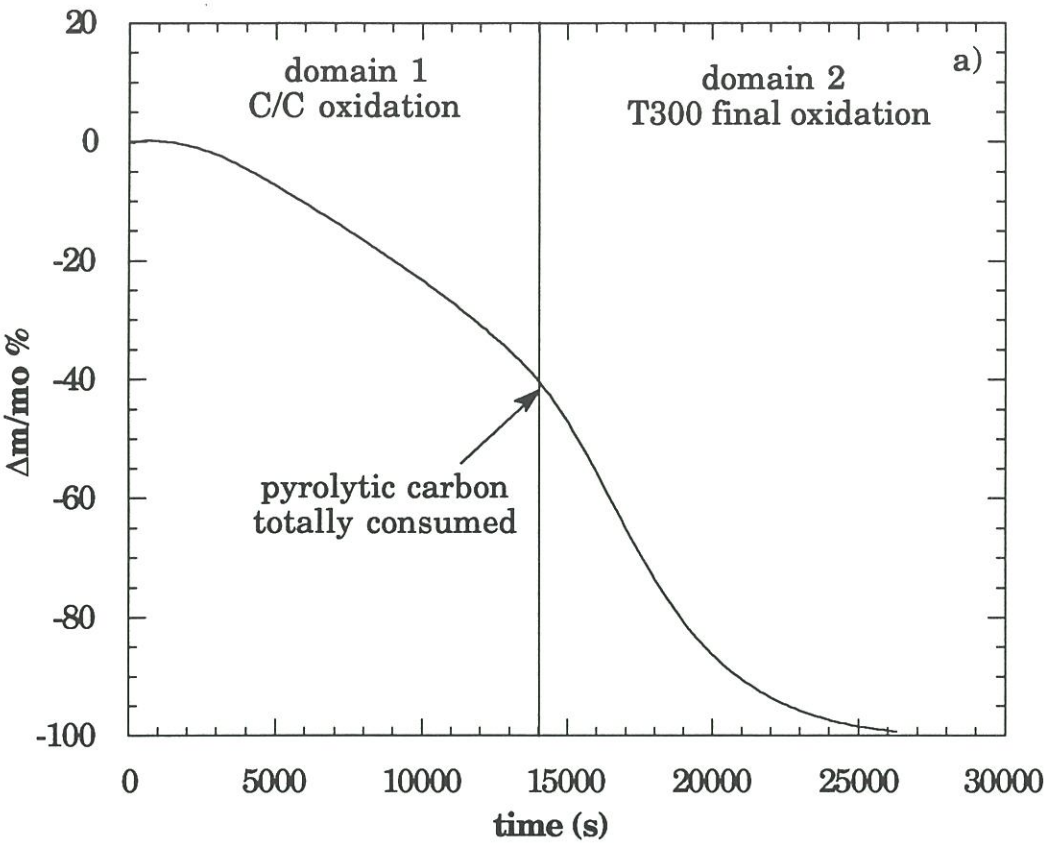

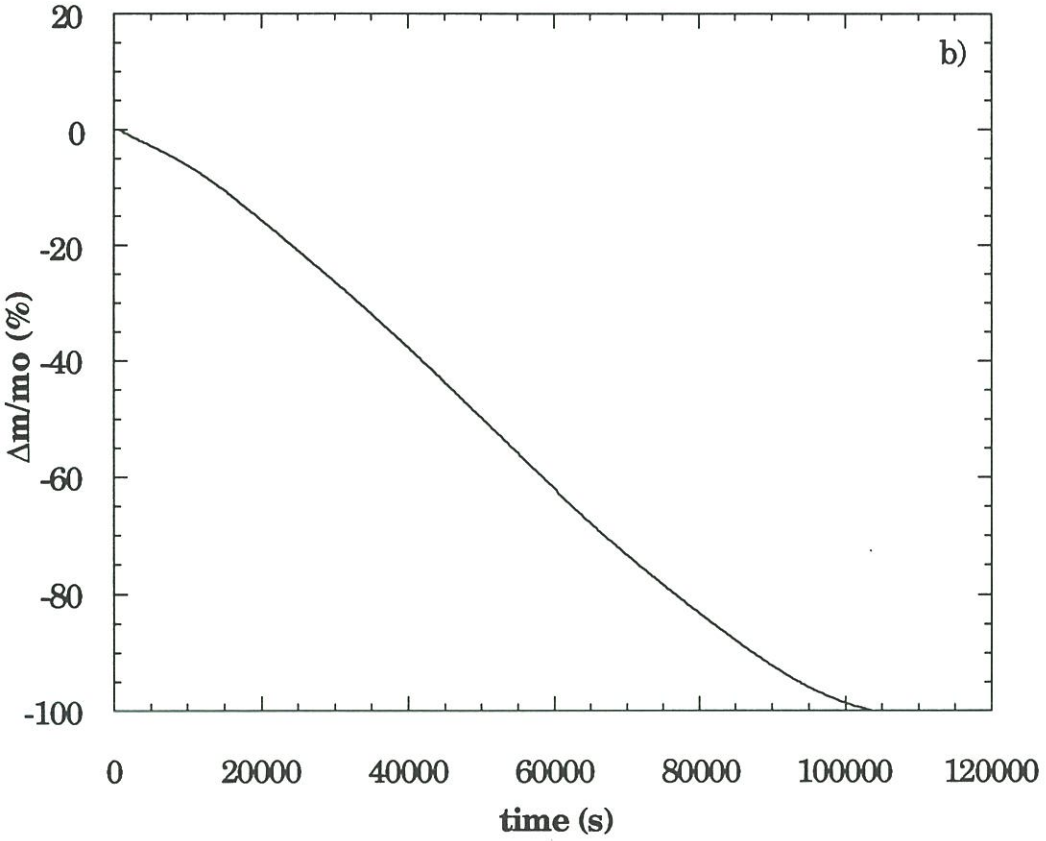

Fig.4 TGA curves for C(T300)/PyC tows treated at 600°C under an atmosphere of pure oxygen (P=100kPa):
a) as-processed tows
b) tows preannealed at 1600°C under an inert atmosphere.

period (characterized by a very limited weight loss), the oxidation rate is almost constant (domain 1 corresponding to $3000 < t < 14000$ s). Beyond about $t = 14000$s, the oxidation rate first increases rather sharply (for $14000 < t < 18000$s) and then decreases smoothly as the oxidation of the sample comes to completion (domain 2).

The SEM-micrograph of the end of a C/C tow, recorded at the beginning of an oxidation test, suggests the occurrence of **different oxidation rates** between the PyC-coating and the T300 fiber, but also within the T300 fiber itself, as seen in figure 5. Generally speaking, the overall fiber seems to be attacked by oxygen faster than the surrounding PyC-coating. Futhermore, the oxidation of the fiber occurs preferentially in specific areas of its cross-section, namely: (i) near the center of the fiber (single arrow), (ii) near the fiber surface (tripple arrow) and (iii) between the external surface and the ring (double arrow). The chemical attack at the fiber center, (i) is not systematically observed in a given fiber tow. On the other hand, the carbon of the fiber is always more significantly consumed near the fiber surface than in the remaining of the fiber cross-section. The occurrence of preferential oxidation pathways, particularly near the T300 fiber surface, is also clearly apparent in fig. 6. This figure shows the same pyrocarbon-coated tows but in a longitudinal way in the oxidized C/SiC composite. This tow belongs to the last ply just beneath the matrix and seal-coat SiC. The mark produced by the oxygen diffusion through a seal-coat crack is clearly seen on the C-coated reinforcement. First the PyC oxidizes at the level of the crack. Then the fiber is itself oxidized. The high reactivity of the very surface of the fiber is evidenced in the composite, too: channeling along the axis at the surface of the fiber (arrows). This channeling corresponds to the pre-existent porosity as seen in cross-section of figure 5.

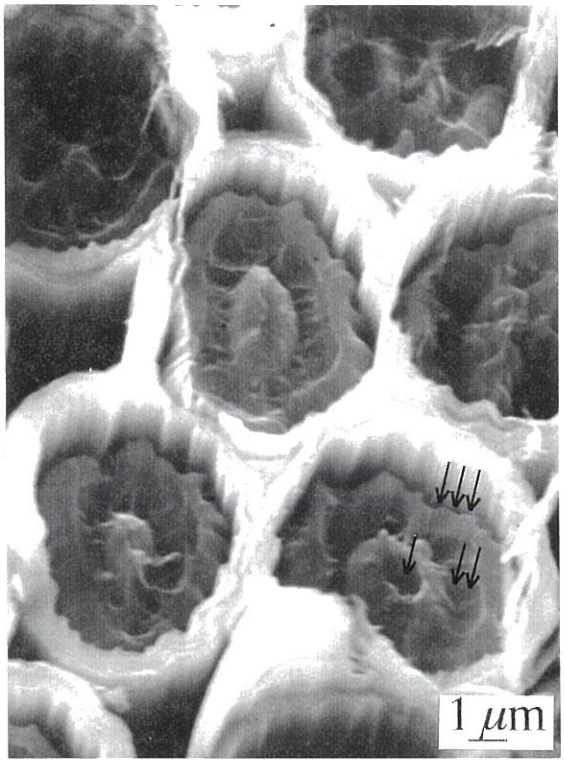

Fig.5: SEM micrograph of the end of a C/C tow after a mild oxidation treatment at 550°C under an atmosphere of pure oxygen.

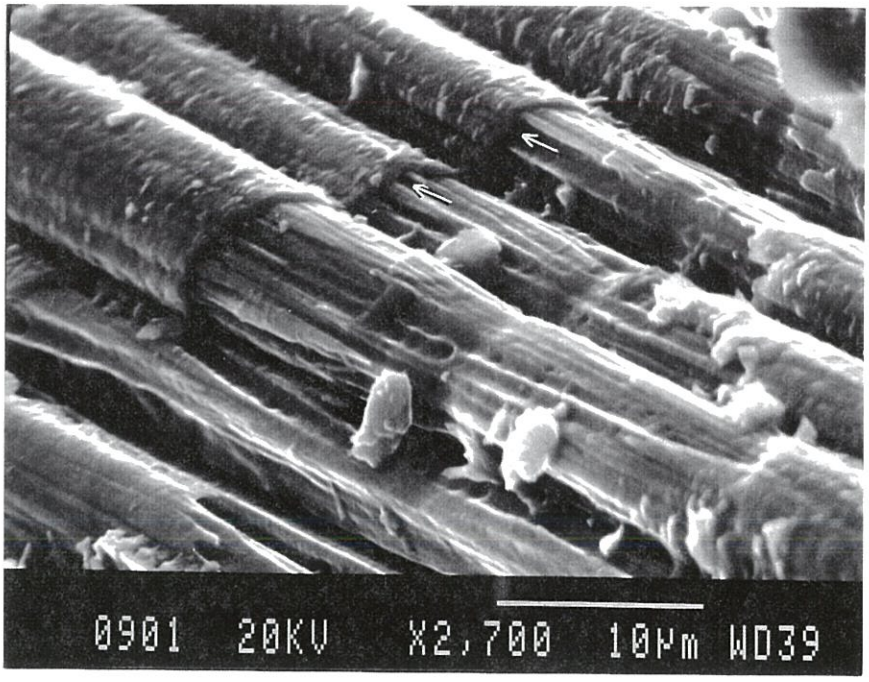

Fig.6: SEM micrograph of the external surface of a C/C tow observed in a C/PyC/SiC composite after a mild oxidation treatment (from ref. [7]).

The effect of an **annealing treatment** (1600°C; inert atmosphere) on the reactivity with oxygen of the various carbonaceous phases of C(T300)/PyC tows was then studied. As shown in fig. 4b, the TGA-curve no longer exhibits any significant variations in the oxidation rate as oxidation proceeds. This result shows that the reactivities of the PyC-coating and the overall fiber with oxygen are similar after the annealing treatment at 1600°C. However, there remains a zone of high reactivity near the fiber surface, as supported by the SEM-micrograph shown in fig.7.

3.3 - Oxidation kinetics of T300 carbon fibers.

The TGA-curves, corresponding to the oxidation of **uncoated** T300 carbon fibers, are shown in fig.8 ($\Delta m/mo$ is the relative mass variation). They exhibit a classical sigmoid shape, i.e. the oxidation rate first increases (for $\Delta m/mo < 20$ %) then it remains almost constant for $20 < \Delta m/mo < 70$ % and finally it decreases, as a function of time.

The oxidation rate being almost constant within the second domain, an apparent **kinetic constant k** (calculated in the following for $\Delta m/mo = 50$ % and expressed in s^{-1}) can be defined as :

$$k = -\frac{1}{mo} \cdot \frac{dm}{dt} \qquad (1)$$

The thermal variations of the oxidation kinetic constant were observed to obey an Arrhenius-type law (fig.9):

$$k = ko \cdot \exp\left(-\frac{Ea}{RT}\right) \qquad (2)$$

where Ea is the apparent activation energy (in $kJ.mol^{-1}$), R is the perfect gas constant (8.32 $J.mol^{-1}K^{-1}$), T is the temperature (in K) and ko a pre-exponential term. The shape of $Lnk = f(T^{-1})$ curve (curve a) suggests that

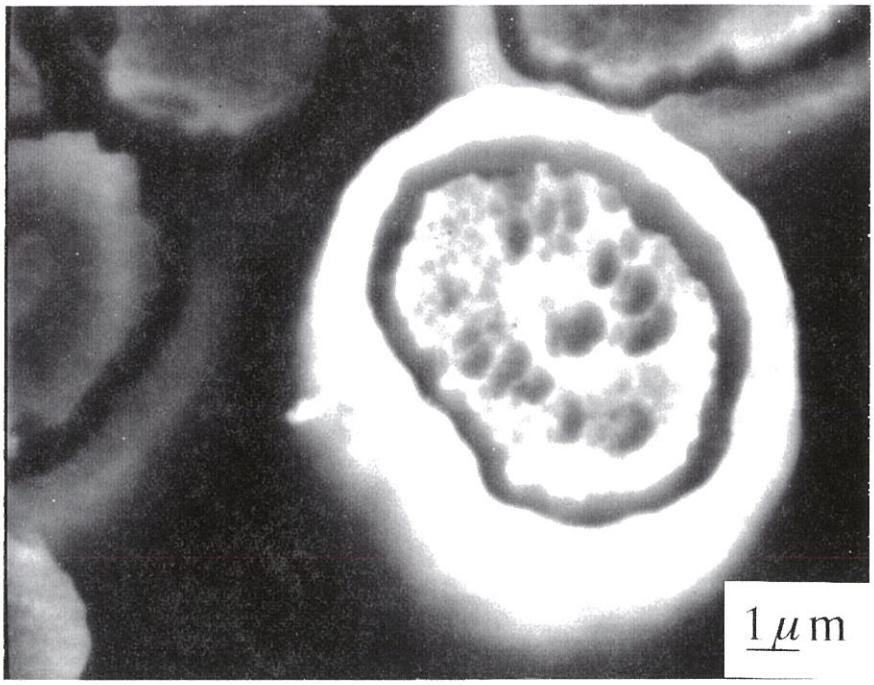

Fig.7: SEM micrograph of the cross-section of a C/C tow first annealed at 1600°C in an inert atmosphere and then submitted to a mild oxidation treatment.

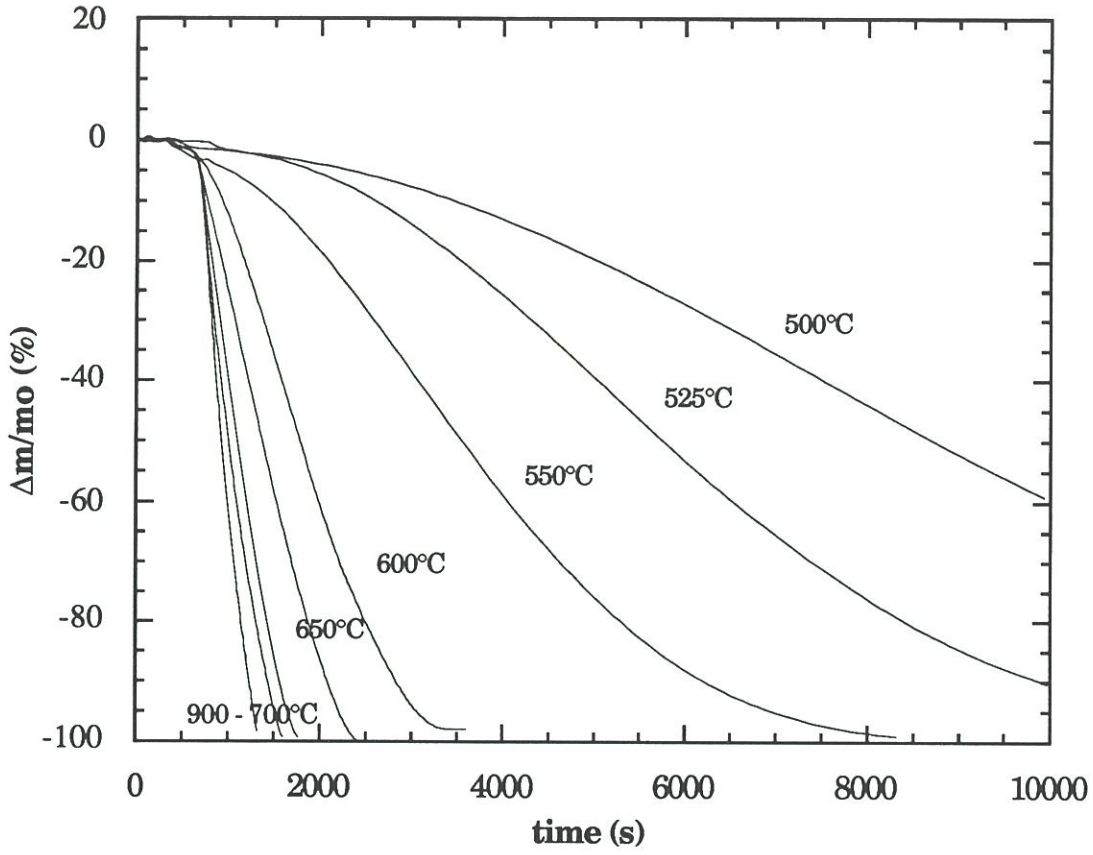

Fig.8: TGA oxidation curves for uncoated T300-carbon fibers (pure oxygen; P=100kPa).

the oxidation of the fibers proceeds according to two different mechanisms depending on the temperature of the oxidation test. At low temperatures, i.e. for 500 < T < 700°C, the apparent activation energy is rather high (80 $kJ.mol^{-1}$) whereas beyond 700°C it is much lower (15 $kJ.mol^{-1}$). Fig.9 also shows the $Lnk = f(T^{-1})$ curve corresponding to uncoated T300 fibers annealed at 1600°C in inert atmosphere prior to the oxidation test (curve b). It appears that at high temperatures (T > 750°C), the oxidation constant k and the apparent activation energy Ea are very similar to those observed for as-received fibers whereas, at low temperatures (500 < T < 750°C) they are significantly different (Ea = 150 $kJ.mol^{-1}$).

3.4 - Structure of the T300-carbon fiber.

The results of the oxidation test performed on C/C tows and uncoated fibers have shown that: (i) the T300 carbon fiber is the carbonaceous phase exhibiting the highest oxidation rate among the constituents of the C/PyC/SiC composites, (ii) its oxidation rate is not uniform (there is near the external surface of the fiber an area of high reactivity) and (iii) its oxidation rate is significantly lowered within the temperature range 500-700°C after an annealing at high temperatures (HTT: 1600°C) in an inert atmosphere. In order to assess whether these features are related to local heterogeneities (in terms of chemical composition and microtexture), a TEM-analysis has been performed on thin foils cut perpendicular to the fiber axis.

The microtexture of T300-type fibers has been already studied either by optical microscopy or TEM and the occurrence of a duplex core/skin structure previously reported [25,26]. However, the results of our oxidation tests (section 3.3) suggest that the structural model proposed by Bennett

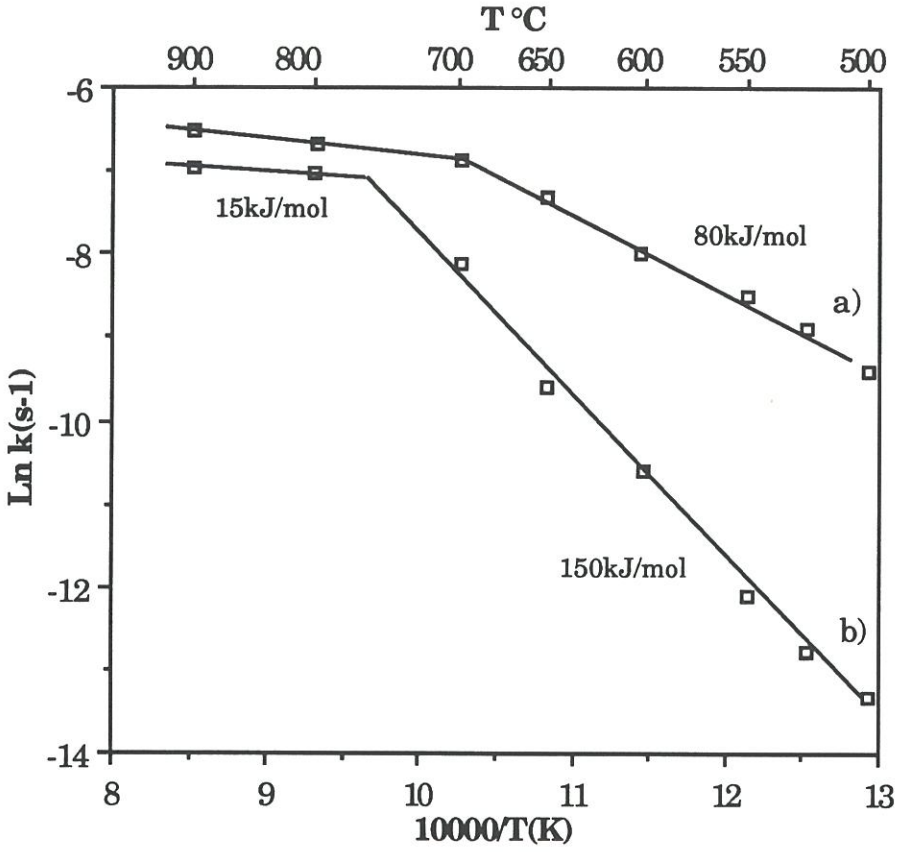

Fig.9: Thermal variations (Arrhenius plot) of the apparent oxidation constant k (calculed from fig.8 for $\Delta m/mo=50\%$) for uncoated T300 carbon fibers.

and Johnson might no longer corresponds exactly to the fibers presently available on the market and which have been used in our study.

As already mentioned in section 3.1 (see fig. 1b and 2), a T300 carbon fiber, when observed in cross-section, exhibits four concentric zones: (i) a porous thin outer zone, (ii) the bulk, (iii) a narrow ring and (iv) the core.

3.4.1 - The porous outer zone

Fig. 10 shows the TEM image (bright field) of the outer zones of two adjacent fibers observed in the cross section of a PyC-infiltrated tow. It clearly appears that there is a **high concentration of pores** extending over a thickness of about 500 nm immediately beneath the external surface of the fiber. No pore accumulation is observed in the fiber cross-section out of this specific zone. Within this thin outer zone, the pores are randomly distributed, their size ranging from 10 to 100 nm with exceptionally few pores as large as 200 nm.

The high magnification lattice fringe TEM-image (fig.11) shows that the carbon in the outer zone is, generally speaking, poorly organized. Additionally, the pores (P) are obvioulsy intrinsic part of the nano/micro-texture, as supported by the fact that the adjacent carbon atomic layers lie parallel to the internal surface of the pores (simple arrow in fig.11). These two specific features are probably related to an overstabilization of the porous texture occurring during fiber processing [25].

It is noteworthy that the T300-fibers studied here do not exhibit a so-called "skin", i.e. a thin outer shell in which there is an increase of the size of the carbon atomic layers (La), the thickness of the carbon layer stacks (Lc) and the radius of curvature of the layers (r). This is a noticeable difference with respect to the results reported previously by Bennett and Johnson for T300-type fibers [25].

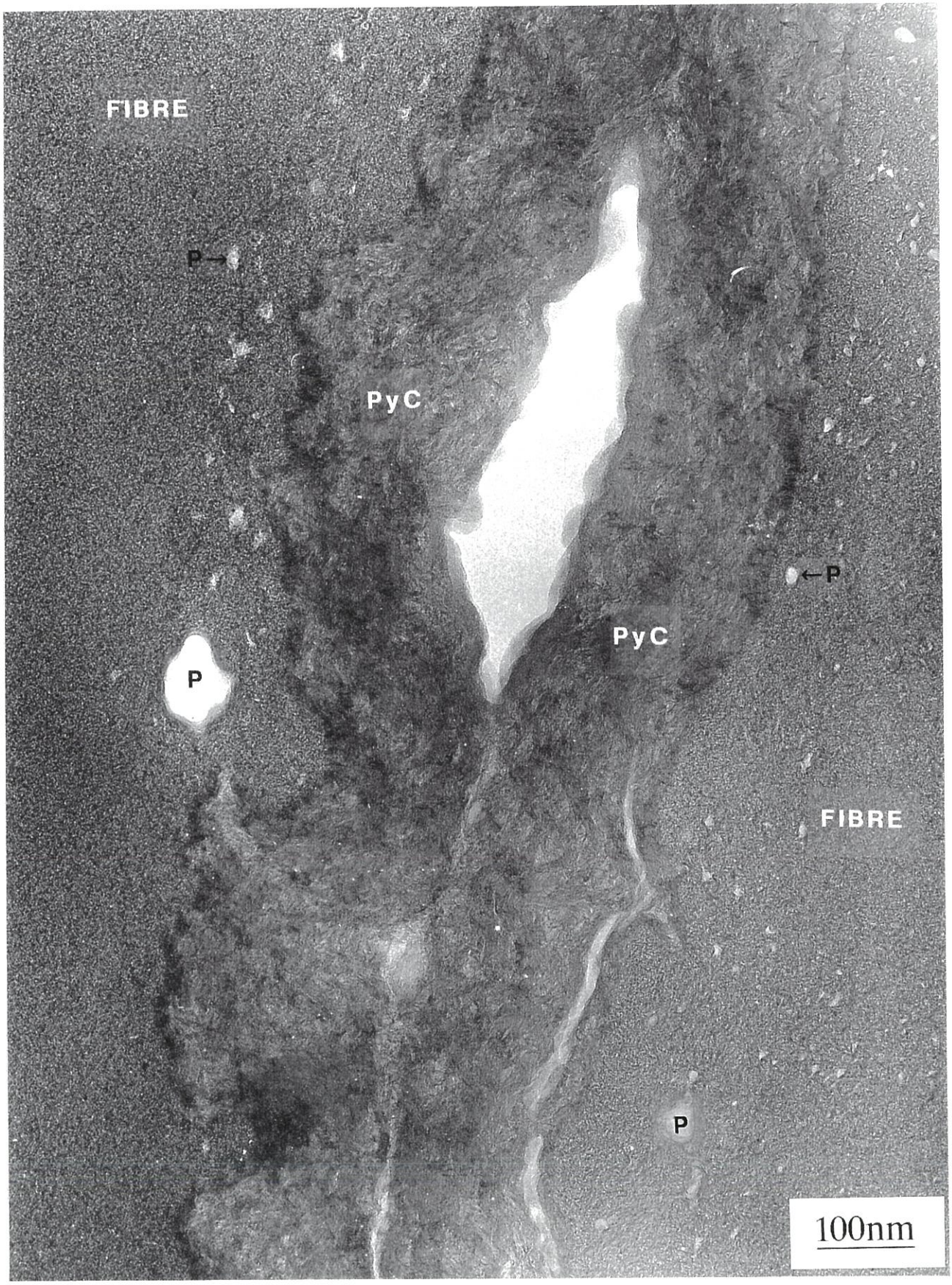

Fig.10: TEM (bright field) image of the outer zones of two adjacent fibers in a PyC-infiltrated T300 fiber tow: the pores (P) are concentrated in a thin zone near the fiber surfaces.

Fig.11: Lattice fringe TEM image of the porous outer zone in a T300-fiber showing the nanotexture of the carbon.

3.4.2 - The bulk and the core

The concentric zones located on each side of the ring, referred to as the bulk and the core, exhibit, generally speaking the same kind of textural organization of the carbon layers, the core appearing most of the time more "crystalline".

Within both the bulk and the core of the fiber (see fig. 12), the nano/microtexture of the carbon shows **common specific features**, when observed in the fiber cross-section. First, there is a significant continuity in the carbon atomic layers. Second the mean values of the radius of curvature of the layers are low and rather similar. They have been assessed indirectly through the measurement of the size of the local molecular orientation (LMO) domain (*) from 002 dark field images, with LMO values of about 10 nm for both the bulk and the core, a result suggesting that the corresponding textures are close to one another. Third, there is a rather good layer stacking (i.e. Lc is rather large). Such a nano/micro texture is known to be the result of an optimization of two antagonistic parameters, i.e. the interlinking of the carbon layers and their stacking in the C-direction. This optimization is known to control the strength of the ex-PAN HS carbon fibers like T300 [25-27].

Meanwhile some **differences** are noticeable at the level of the carbon structure between the two concentric zones. First the size of the carbon atomic layers, La, does not exceed 5 nm in the bulk whereas it is of the order of 10 nm (and sometimes even more locally) in the core. Moreover, the layers are more regular in the core. Second, the layer stack which is in coherence does not exceed 4 to 5 layers in the bulk whereas it consists of

---

(*) the LMO domain is defined as a volume where all basic structural units are approximately parallel.

Fig.12: Lattice fringe TEM-image showing the nanotexture of the carbon in the core of a T300 fiber.

5 to 6 layers in the core (and even locally 10 layers). In short, both textures are very close but the carbon ordering is slightly much ordered in the core than in the bulk.

3.4.3 - The ring

The occurrence of a ring in the cross-section of T300 carbon fibers has been already reported [27-28]. However and as far as we know, no model has been proposed yet to explain the high optical reflectivity of the ring, the high secondary electron re-emission which is observed in SEM for this particular zone, the various contrasts observed in TEM and, finally, the enhanced resistance of the ring to oxidation and abrasion.

The ring results from both an effect of statistical orientation (concentric and radial) of the porous nano/microtexture in the fiber cross-section and a strong improvement of "crystallinity".

(i) The ring exhibits roughly the same shape as the fiber external surface, as shown by the diffraction contrast of the bright field TEM image of the fiber cross-section at low magnification (fig. 13a). Dark field images have been recorded with an objective aperture of 2.95 nm^{-1} for three positions at 45° from one another corresponding to an azimuthal aperture of ± 30° on the carbon 002 diffraction ring (only two of these images corresponding to positions at 90° are shown in fig. 14a and b). In each of the three dark field positions, the full ring remains in contrast: **the ring is continuous but it is oval** along that direction of the carbon layers selected for the dark field image (double dash in fig. 14a and b insets). Such a contrast, observed for a finely porous nano/microstructure (assumed to be isotropic *a priori*) is likely to be due to some "preferential statistical" orientation of the carbon layers occurring along a given direction, i.e. to a **flattened-pore nano/microtexture**. The contrasts observed in the dark field

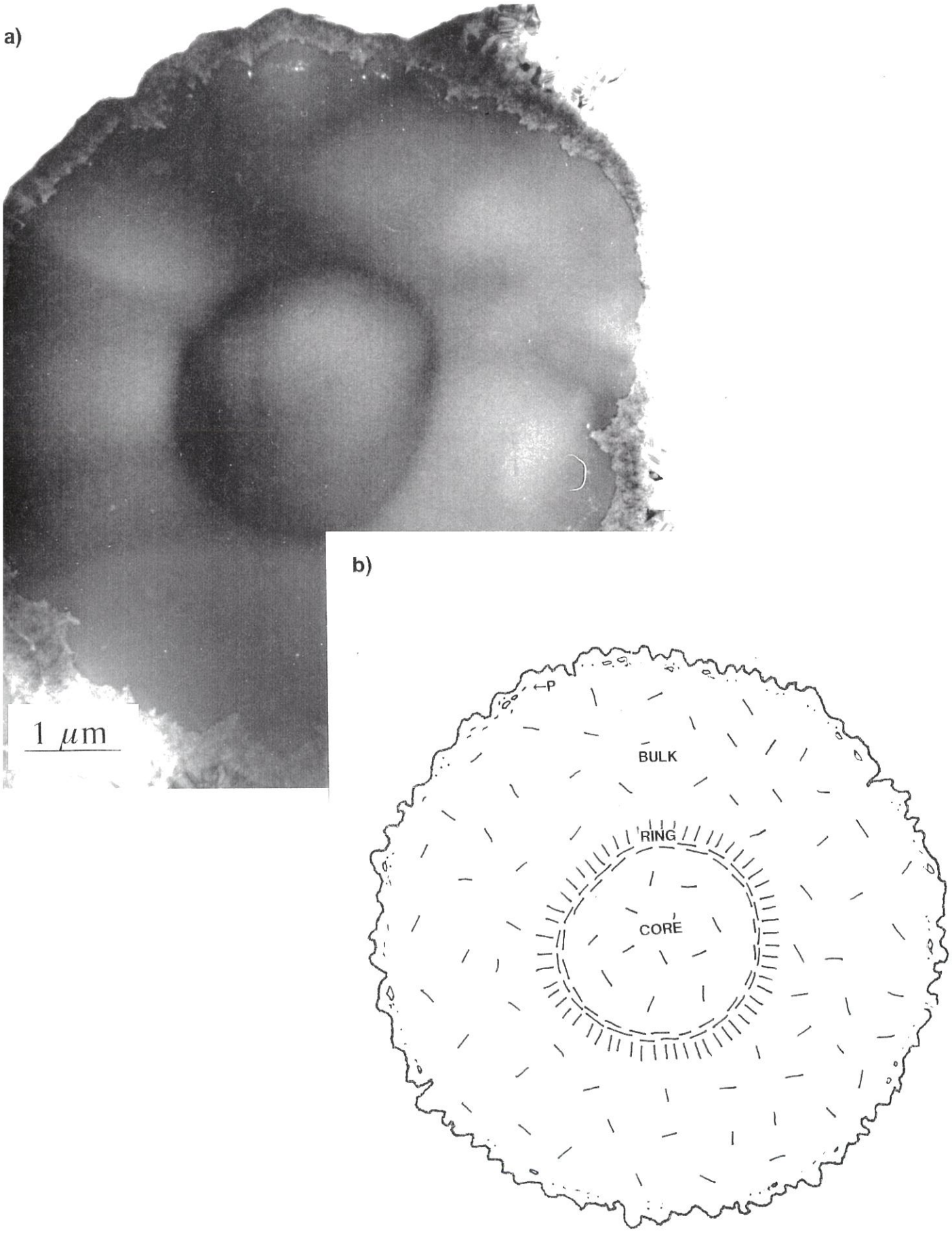

Fig.13 TEM-analysis of the cross-section of a T300-carbon fiber at a low magnification, as observed within a C/PyC/SiC composite: a) bright field image; b) schematic of the various nano/microtextures: (P) porous outer zone; bulk: isotropic nanoporous structure; ring: flattened-pore nano/microtexture with a concentric/radial preferred orientation; core: isotropic nanoporous structure.

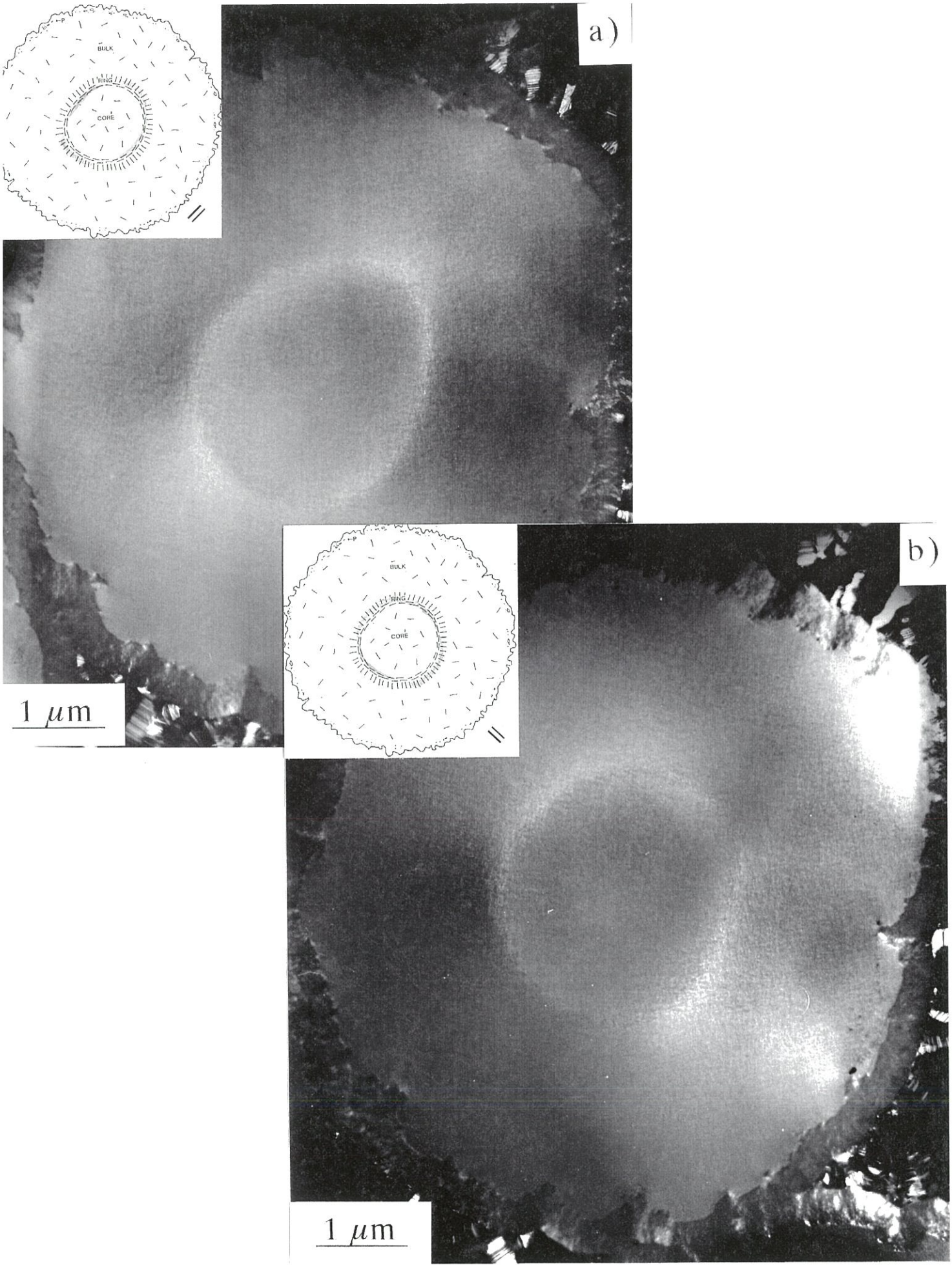

Fig.14: Dark field (carbon 002) TEM analysis of a T300 carbon fiber within a C/PyC/SiC composite for two positions at 90° (the orientations of the carbon layers are shown by the double dash in insets).

images (continuity of the ring and direction of the ovalization) show that this preferred orientation of the carbon layers is double: it is **concentric** within the fiber ring and **radial** outside (one moves from one orientation to the other by progressive rotation). The relations existing between the dark field image contrast features (continuity/ovalization) and the preferred double orientation (concentric/radial) of the carbon layers, are shown schematically in the insets of fig. 14a and b.

(ii) Furthermore, the ring is that part of the fiber which exhibits the **highest degree of crystallization**: the carbon layers are more extended and contain less defects, on the one hand, and the coherent pile (thickness of the layer stack, L_c) is larger, on the other hand as shown in the HR-lattice fringe image (fig. 15). The occurrence of a flattened-nanoporous texture within the ring is readily observed in fig. 15. Conversely, that of a "preferential statistical" orientation of the carbon layers, which is not observed in fig. 15 (owing to the analysis conditions), becomes rather clearly apparent in the complementary dark field image shown in fig. 16 (double dash: selected carbon layer orientation). Each bright spot represents one coherent domain, i.e. the carbon layer stack which is diffracting. It appears in the ring that the bright spot clusters, i.e. local molecular orientation (LMO) domains, are more extended and elongated showing that the nano/microtexture is no longer isotropic. Futhermore, the local molecular orientation of the carbon is seen to be different in the ring from what it is in both the core and the bulk. Finally, the contrast in the ring is, generally speaking, higher than in the other parts of the fiber cross-section, a feature which supports a **better crystallinity** (note that for this particular cross-section, the core itself shows a rather good crystallinity). With the ring, the proportion of coherent domains which

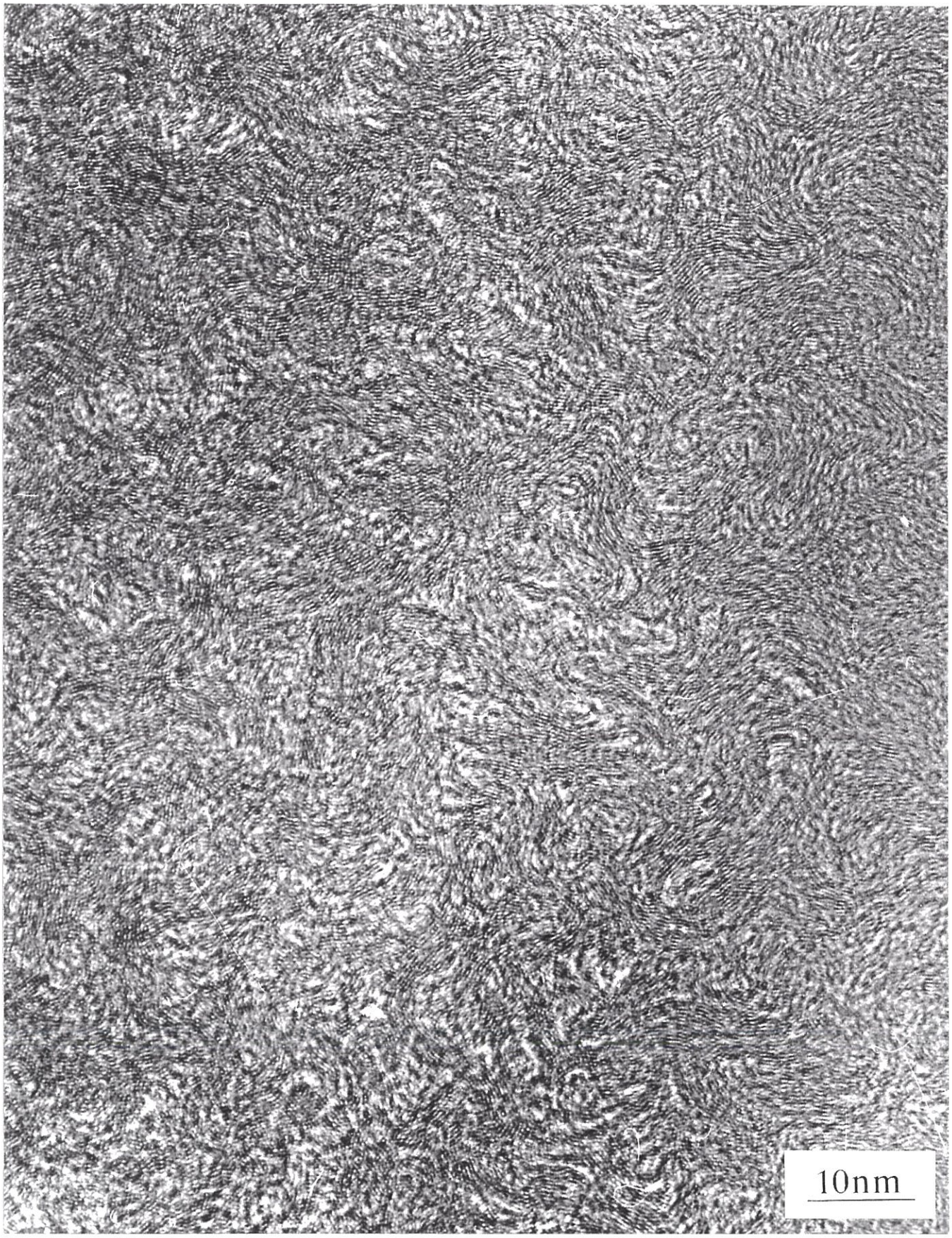

Fig.15: Lattice fringe HR-TEM image of the ring in a T300 carbon fiber cross-section.

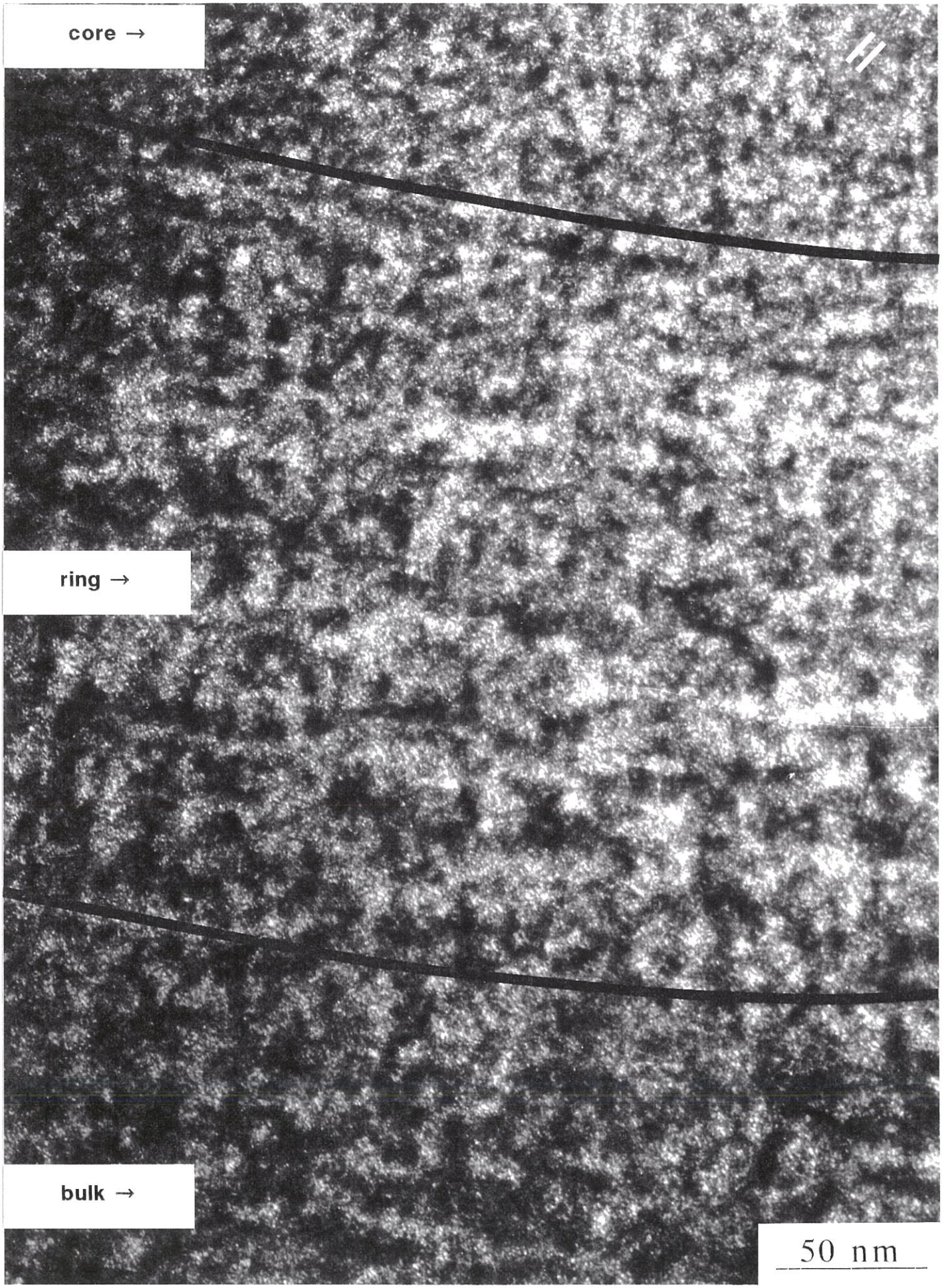

Fig.16: High resolution dark field image (carbon 002) of the ring in a T300 carbon fiber cross section.

are elongated along the carbon c-axis increases (with Lc up to 1.5 nm corresponding to stacks of about 6 layers).

(iii) An analysis of the plasmon energy loss has shown that the ring is also that part of the fiber which exhibits the **highest density**, a feature which is in agreement with its better crystallinity. The energy loss of the plasmon peak maximum is proportional to the square root of the density of the free electron gas in the material. By this way it is representative of the number of atoms per unit volume in the solid [29]. The plasmon energy loss is higher for the ring, where it is observed at 23.9eV, spectrum c, than in the other parts of the fiber cross section where it is observed at 23.4eV, spectra a,b et d (fig.17). The conclusion is reinforced by the relative intensity of the peak, proportional to this excitation probability, which is also higher in the ring than in the other parts of the fiber section.

3.4.4 - Effect of an annealing treatment at 1600°C on the fiber structure

As could be expected from the relatively low value of HTT (i.e. 1600°C), the annealing treatment performed on the fibers did not result in a dramatic change in the carbon ordering of the fiber [30-34]. All the TEM analyses support the assumption that the arrangement of the carbon layers is limited to that corresponding to **stage 2** in the scenario depicted by Oberlin and Guigon [32]. First, the annealing treatment has removed part of the interlayer defects, as supported by some increase in the value of L_c. Second, the degree of organization of the carbon is increased, mainly in the bulk of the fiber. Third, some opening of the porosity is observed in the outer zone of the fiber cross-section. Conversely, the main features of the nano/microtexture (e.g. the curvature radius, the size (La) and the orientation of the carbon layers), as observed in fiber cross-section, remain basically the same (the removal of the in-plane defects occurring at higher temperatures, i.e. in stage 3).

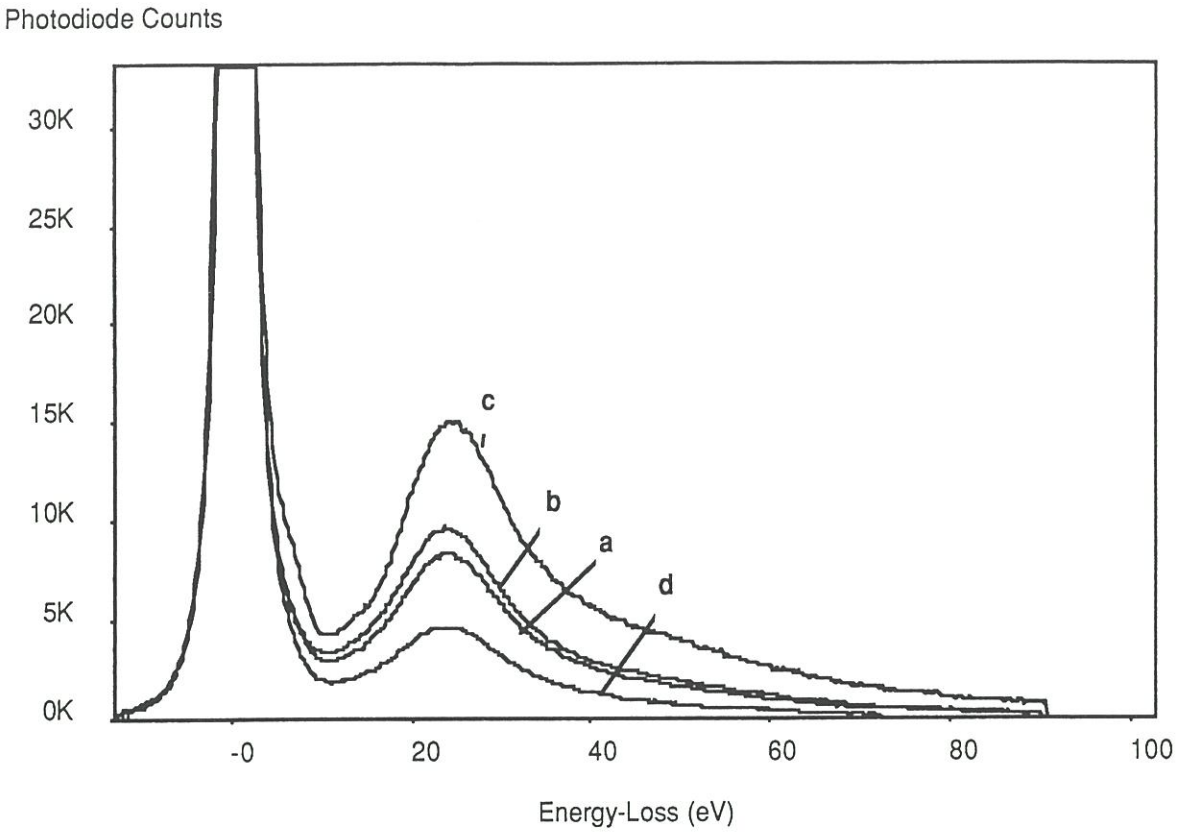

Fig.17: Plasmon energy loss TEM-analysis performed for various zones in a T300 carbon fiber, namely: (a) the porous outer zone, (b) the bulk, (c) the ring and (d) the core.

Finally, EELS analyses of the fibers have been performed on both the as-received and annealed composites in order to assess whether **heteroelements** (which might act as oxidation catalysts) were present or not in significant amounts. Nitrogen was the only elements (apart from carbon) detected (fig.18). It was present in the as-received composite (its concentration being assumed to be of the order of 4 % in the T300 fiber before the composite processing) but no longer observed in the annealed material. Thus and as previously known, there is no heteroatoms in the as-received T300-fiber in significant amounts other than the nitrogen coming from the PAN-precursor and this nitrogen is likely to have been removed during the annealing treatment at 1600°C.

4 - DISCUSSION

4.1 - Origin of the matrix damaging phenomena.

The analyses performed both by optical microscopy (fig. 1a) and TEM (fig. 2), have shown that the SiC-matrix and the PyC/SiC matrix interface exhibit **microcracks** and **decohesions** which are thought to favor the in-depth diffusion of oxygen during an oxidation test. Since these defects are already present in the material in the as-processed state, their origin must be related to processing considerations.

The T300 fibers and SiC (CVI) matrix are known to exhibit coefficients of **thermal expansion** (CTE) which are significantly different. The T300 fiber is an anisotropic material. It is characterized by two CTEs: a radial CTE, α_f^r , and a longitudinal CTE, α_f^l. The longitudinal CTE of the T300 fibers has been measured by various authors. It is considered usually as slightly negative, with α_f^l ranging from - 0.1 x 10^{-6} to - 1.1 x $10^{-6}°C^{-1}$ [39, 40]. Conversely, their radial CTE is positive and high. Although

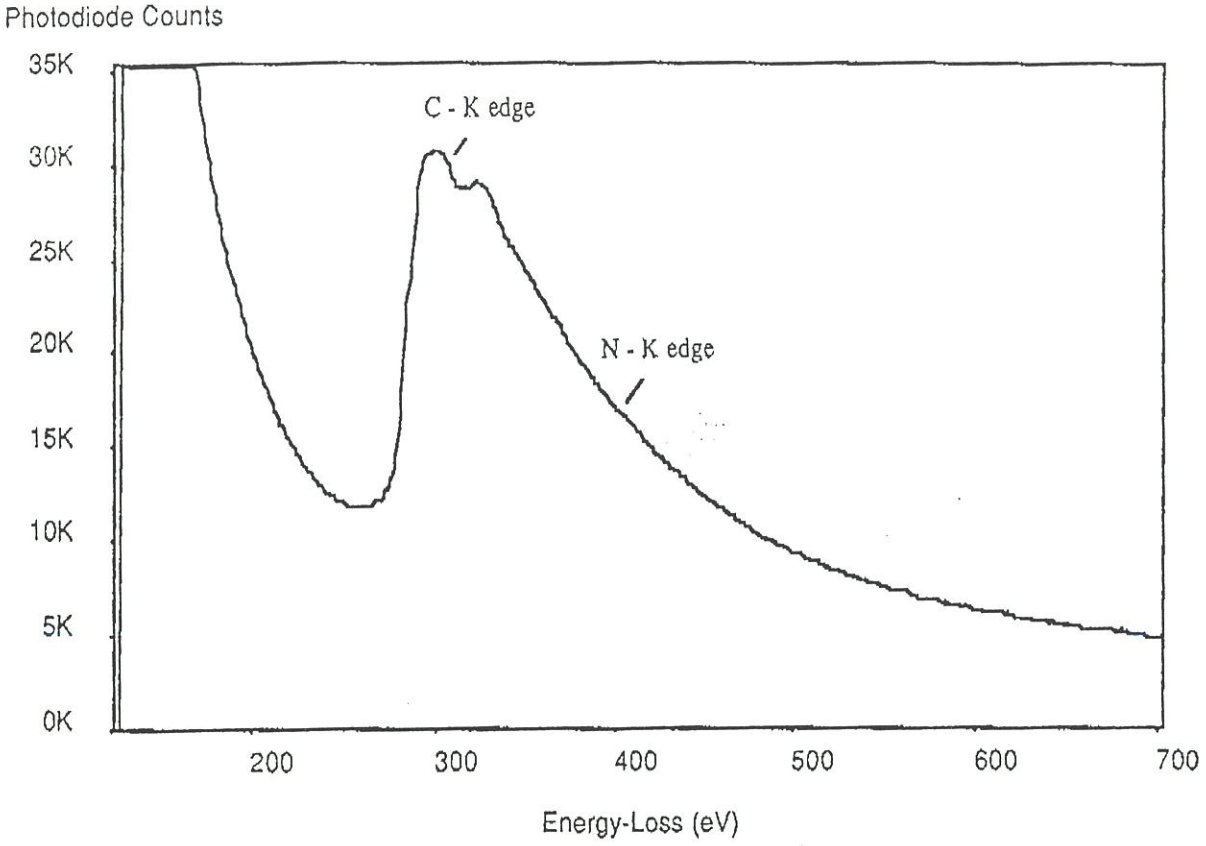

Fig.18: EELS-spectrum recorded for the bulk of a T300-fiber in the as-received state.

difficult, the direct measurement of α_f^r has been performed recently according to a TEM-technique for different carbon fibers, the value of α_f^r reported for the T300 fibers being $\alpha_f^r \approx 7 \times 10^{-6}°C^{-1}$ [41]. Finally, the CTE of the SiC (CVI) matrix, assumed to be isotropic, is often taken as $\alpha_m = 4.8 \times 10^{-6}°C^{-1}$ [42].

During the CVI-processing of the C/SiC composites (at 1000-1100°C), **mechanical stresses** are generated in the material when cooling to room temperature (ΔT = 1000 - 1100°C) as the result of differential thermal expansion. These stresses are relaxed by microcracking of the most brittle constituent, i.e. the SiC matrix. Since $\alpha_f^l < \alpha_m$, the matrix experiences a tensile stress state upon cooling with microcracks formed perpendicular to the fiber axis. As a result, a 2D-microcrack array is generated in the material (fig. 1a). Moreover, since $\alpha_f^r > \alpha_m$, the carbon fiber has a tendency to shrink radially within the SiC-matrix upon cooling. The partial relaxation of the radial stresses might be responsible for the decohesion observed in the PyC-interphase, near the PyC/SiC-matrix interface (double arrows in fig. 2 and 3).

A similar effect occurs as well during the annealing treatment at 1600°C but according to a more complex pattern since the material is first heated above the CVI-processing temperature, i.e. from 1000-1100 to 1600°C, and then cooled to room temperature. As a result, the microcracks in the SiC-matrix are expected to be more numerous and more open, on the one hand, and the decohesion phenomena in the PyC-interphase more important, on the other hand, in the annealed material than in the as-processed composite.

4.2 - Oxidation kinetics of the C/C tow.

During an oxidation test performed on a C/PyC/SiC composite, the oxygen which has diffused in-depth via the open porosity left by the CVI-process and the array of microcracks resulting from the CTE-mismatch, finally reacts with the PyC-infiltrated T300 fiber tow in a **selective manner**, as shown in section 3.2 (see fig. 4 to 7).

The oxidation kinetic curve for a T300/PyC infiltrated tow exhibits, for a test temperature of 600°C, two domains (fig. 4a). On the basis of the SEM-analysis, these domains can be assigned to two different oxidation phenomena. The **first domain** seems to correspond to a mixed oxidation mode, namely : (i) the oxidation of pyrocarbon in a direction perpendicular to the tow axis and (ii) both the oxidation of the fiber (when oxygen has reached the fiber surface) and the remaining pyrocarbon in a direction parallel to the tow axis. Within this domain, the oxidation rate remains rather low since the process involves mainly pyrocarbon. When the PyC-interphase has been totally consumed (i.e. for about $t = 15 \times 10^3$s in fig. 4), the oxidation process involves only the fibers with a much higher overall oxidation rate (**domain 2**). The sharp increase in the oxidation rate, occurring between domains 1 and 2, shows that the fibers exhibit an overall reactivity vs oxygen which is much higher than that of the pyrocarbon. This result is in agreement with those reported by Louys in an independent study performed on materials of same origin [24].

The assignment of domains 1 and 2 to different oxidation modes is further supported by the features of the oxidation kinetic curve performed on T300/PyC infiltrated tows annealed at 1600°C prior to the oxidation test (fig. 4b). The main effect of the annealing treatment has been a change in the structure (and possibly composition) of the T300 fiber (which will be

discussed in the following sections) whereas the pyrocarbon has remained almost unchanged. As a result, the overall chemical reactivity of the fiber is now of the same order as that of the PyC (fig. 7) and the oxidation rate remains almost constant during the oxidation test up to the total consumption of the sample.

4.3 - Oxidation kinetics of T300 carbon fibers.

The thermal variations of the oxidation kinetic constant k, shown in fig. 9 for both as-received and annealed T300 fibers support the occurrence of different rate-limiting phenomena, as temperature is raised from 500 to 900°C.

Generally speaking, the oxidation of a carbon involves the following steps : (i) diffusion of oxygen in the boundary stagnant gas layer surrounding the solid, (ii) surface diffusion of adsorbed oxygen towards the **active sites**(*) , (iii) chemical surface reaction between oxygen and carbon with formation of carbon oxides (CO/CO_2) and finally (iv) diffusion of the reaction products in the boundary layer. Furthermore, when the carbon is **porous**, both the reactant (oxygen) and reaction products (CO/CO_2) have to diffuse additionally in the open porosity of the solid (such a diffusion being much more difficult than that in the boundary layer when the pores are of very small size).

As already discussed by previous authors, the nature of the **rate determining step** (RDS) in the oxidation of a porous carbon varies when temperature is raised (Arrhenius plots) [9, 35, 36]. At **low temperatures** (domain I), the RDS is assumed to be the surface chemical reaction with, consequently, an apparent activation energy Ea(I) which is high

(*) the active sites are located mainly at the edges of carbon layers and at defects in the basal plane.

(typically, Ea(I) = 160-200 kJ.mol^{-1}). Within this temperature range, the oxidation rate depends on the number of active sites and is sensitive to catalytic effects (related to the occurrence of specific impurity atoms, such as Na, K, Ca, Fe...). At **high temperatures** (domain III), the RDS is assumed to be the transport of the reactant or/and products in the boundary layer to the carbon external surface. It is thus expected not to depend on the carbon nano/micro structure and characterized by a low apparent activation energy, Ea(III). For intermediate temperatures (domain II), the rate is partially controlled by diffusion in the carbon pores, i.e. the oxidation occurs according to a diffusion/reaction mixed mode, with an apparent activation energy Ea(II) which is depending on the nature of the carbon porosity and of the order of 0.5 Ea(I).

Our results (see fig. 9) corroborate the above assumptions. The low value of Ea, i.e. 15 kJ.mol^{-1}, observed for **750 < T < 950°C**, strongly suggests that within this "high temperature" range, the RDS is an **almost pure diffusion phenomenon**, presumably the diffusion of the reactant (or products) in the boundary stagnant gas layer (domain III of the Arrhenius plot schematically shown in fig. 4(a) of ref. [9]).

The value of Ea, i.e. Ea = 80 kJ.mol^{-1}, derived from the oxidation tests performed at **500 < T < 700°C** for the as-received fibers, is obviously too low to be assigned to a pure rate control by the oxygen-carbon surface reaction (since Ea(I) = 160-200 kJ.mol^{-1}). Furthermore, it is unlikely that it could be related to some catalytic effect due to impurity atoms. As a matter of fact, T300 fibers (which may be however of different origin) have been reported [36] to contain only very small amounts (typically ≈ 10 ppm) of those elements (i.e. Na, K) known to catalyse the reaction. These amounts are far below the detection limits of the present EELS analysis and cannot be observed by this technique.

Conversely, an Ea-value of 80 $kJ.mol^{-1}$ is indeed of the order of that assigned above to a RDS of type-II suggesting that oxidation rate is controlled, for $20 < \Delta m/mo < 70$ %, by a **mixed in-pore diffusion/surface reaction mode**. A similar conclusion has been previously drawn by Ismail who reported an Ea-value of same order (i.e. Ea = 94 $kJ.mol^{-1}$) for oxidation tests performed (in air and within the 600-950°C temperature range) also on T300 fiber [36]. Such a conclusion could seem in contradiction with the fact that T300 fibers exhibit a very low open porosity in the as-received state as supported by their low total surface area TSA(*) and active surface area (ASA)(*), i.e. 0.56 and $0.075 m^2 g^{-1}$, respectively [36]. However, it is worthy of note that the k-values, used to draw the Arrhenius plots shown in fig. 9, have been derived from oxidation rates measured for **$\Delta m/mo = 50$ %** and it is generally admitted that the pores (the T300 fiber is instrinsically a nanoporous material) are almost instantaneously opened once oxidation commences [36].

As shown in fig. 8, the oxidation rate increases rapidly versus time at the beginning of an oxidation test, i.e. for $0 < \Delta m/mo < 20$ %, then it remains almost constant within the 20-70 % range. These variations are similar to those reported by Louys for the active surface area [24] and consistent with the assumption of the opening and developement of porosity at the beginning of the test. These features might be explained by the fact that the outer zone of the fiber cross-section, which reacts with oxygen first, is much more porous than the bulk and the core, as shown in section 3.4 (see fig. 10 and 11). Additionally, the occurrence of a radial nitrogen concentration gradient in T300 fibers has been reported by Serin et al. [37]: the N/C at. ratio varying from 2 to 7 % when moving from the

(*) TSA is determined by krypton adsorption at 77 K and ASA by oxygen chemisorption techniques at 573 K.

core to the fiber surface. Although nitrogen is not considered as a catalytic element by itself, its evolution as gaseous molecules, particularly during the oxidation of the outer zone of the fiber cross-section at the beginning of the oxidation test, might well generate active sites which in turn favor the oxidation process.

The **annealing treatment** (HTT = 1600°C) performed on the fiber prior to the oxidation tests has two effects on the Arrhenius plot (fig.9): it slightly extends (by about 50°C) the low temperature domain towards the high temperature side and more importantly its increases, in a significant manner, the related apparent activation energy (from 80 to 150 $kJ.mol^{-1}$). Conversely it does not change the value of Ea(III) which remains of the order of 15 $kJ.mol^{-1}$ (since in an oxidation regime rate controlled by pure diffusion in the boundary layer, the kinetics are not sensitive to change occurring in the solid). The increase in the Ea-value corresponding to the low temperature range might be related to two factors : (i) the increase of the pore mean size during the annealing treatment and (ii) the lowering of the carbon reactivity related to a better organization of the carbon. As a result, in-pore diffusion might no be any longer a slow step with respect to surface reaction and the activation energy, i.e. 150 $kJ.\ mol^{-1}$, is now close to that of the pure reaction RDS. However, it is still lower than those reported by Ismail for a graphitized petroleum pitch-based fiber, i.e. ≈ 185 kJ.mol-1 [36] and by Vix for a M40 (ex-PAN) fiber(*) which has seen a HTT higher than 2000°C, i.e. 195 $kJ.mol^{-1}$ [38]. All these data are consistent with the fact that the effect of the annealing treatment at 1600°C on the structure of the carbon fiber has been limited, i.e. to stage-2, according to the scenario depicted by Oberlin

(*) M40 is a fiber produced by Toray, Japan.

and Guigon in ref. [32], but noticeable enough to change the oxidation behavior of the material at low temperatures.

4.4 - Selectivity of the oxidation reaction.

As shown in fig. 5-7, the oxidation of the T300/PyC infiltrated tow occurs in a selective manner. For the unannealed infiltrated tow, the overall oxidation rate of the fiber is higher than that of the PyC-coating as supported by the SEM-image of the fiber end shown in fig. 5 and the different slopes of the TGA-curve shown in fig. 4a. This difference in the oxidation rates is assumed to be mainly related to the poor organization of the carbon in the fiber with respect to pyrocarbon. Conversely, when the tow has been annealed (HTT = 1600°C), the **overall** oxidation rate of the fiber is now similar to that of the PyC-coating, as supported by fig. 4 b and 7 (the decrease in the oxidation rate of the fiber being related presumably to the structural changes that have taken place in the fiber, as depicted in section 3.4.4).

Two nano/microstructural features could explain the selective reaction of oxygen with the fiber shown in fig.5-7 : (i) the high porosity of the outer zone of the fiber and (ii) the anisotropy and better crystallinity of the ring. First and as clearly apparent in fig.2 and 10, the number and the size of the pores are much larger in the outer zone. As a result, at the beginning of an oxidation test, there is an **opening of porosity** which increases both the TSA and ASA with, consequently, a rapid increase of the oxidation rate (for $0 < \Delta m/mo < 20$ % in fig.8). In cross-section, this selective oxidation is responsible for the **annular hole** observed between the PyC-coating and the fiber (fig. 5 and 7). The fact that this effect is present for both the as-received and annealed tows suggests that the porosity factor in the outer zone of the fiber is dominant, with respect to

the change occurring in the chemical composition (some heteroatoms are removed) and the carbon organization during the HTT. Second, the low chemical attack observed in fiber cross-section at the **level of the ring** is likely to be related to the higher density of the carbon in this specific area (fig.17) and to its anisotropy and better cristallinity (fig. 14-16).

4.5 - Origin of the fiber ring.

The origin of the fiber ring, although still a matter of speculation is likely to be related to fiber processing considerations and more specifically to the internal stresses experienced by the material. The mechanical stretching which is applied to the PAN-green fiber is responsible for Poisson effect (i.e. a striction of the fiber cross-section) which might induce a state of compressive stress in the core and a state of tensile stress in the skin. The formation of the ring might be related to the frontier between these two **different stress state domains**. The difference between the core and the bulk, in terms of both density (curves b and d in fig. 17) and chemical reactivity (fig. 5), might be related to the occurrence of a **radial oxygen gradient** during the curing and pyrolysis steps, i.e. the carbon yield is expected to be higher in the bulk than in the core (respectively 50 and 30 %, according to [27]). The specific nano/microtexture of the ring, characterized by flattened pores and a preferential statistical orientation of the carbon layers (concentric on the core side and radial on the bulk-side) (fig. 13 and 14), could be explained by the fact that this narrow portion of the fiber cross section has been pyrolysed in a discontinuous state of compressive / tensile stresses.

5 - CONCLUSIONS

On the basis of the results presented and discussed in sections 3 and 4, the following main conclusions can be drawn :

(i) - During an oxidation test performed on T300/PyC/SiC (CVI) composites, the in-depth transport by diffusion of the gaseous species (oxygen and carbon oxides) to the PyC-infiltrated carbon fiber tows, is favored by the **open porosity** of the material (i.e. the residual pores related to the CVI-process, matrix microcracks resulting from CTE-mismatch and decohesion in the PyC interphase),

(ii) - For as CVI-processed composites, the overall reactivity of the fiber is higher than the reactivity of the PyC-interphase whereas both constituents exhibit similar reactivity with respect to oxygen after annealing at 1600°C,

(iii) - At a given temperature, the rate of oxidation of the T300 fiber first increases rapidly vs time (for $0 < \Delta m/mo < 20$ %), this effect being related to the occurrence of a high concentration of pores (both numerous and of large sizes) in the outer portion of the fiber. Then, the oxidation rate remains almost constant for $20 < \Delta m/mo < 70$ %. Under this latter condition, **two different steps control the rate** depending on temperature. For $700 < T < 900$°C, the oxidation rate is controlled by the diffusion transport of the reactant/products across the stagnant boundary layer to the external surface of the fibers. Conversely, for $500 < T < 700$°C it is determined mainly by surface reaction for the 1600°C-annealed material and by a combination of surface reaction and in-pore diffusion for the as-recieved fibers. The high oxidation rate observed for the as-recieved T300-fiber is assigned to the poor overall organization of the carbon layers. The effect of the annealing treatment at 1600°C, on the oxidation rate at low temperatures, is related to nanostructural change.

(iv) - The oxidation of the fiber occurs in a **selective manner** : it is much faster for the outer portion (owing to its high porosity) than for the ring (where density and crystallinity are higher). The selective oxidation of the outer portion of the fiber, which occurs first, might be responsible for the strength decrease reported at low weight loss (since it takes place in a key area, i.e. the interface between the PyC-interphase and the fiber, of the composite). This conclusion remains valid whether or not an annealing treatment at 1600°C has been applied to the material.

ACKNOWLEDGEMENTS

This work has been supported by MRT and SEP through a grant given to F.L. The authors acknowledge the assistance that they received from SEP for the CVI-processing of the materials and through valuable discussions.

REFERENCES

[1] - P. LAMICQ, C. BONNET and S. CHATEIGNER, "Ceramic-composite development", in *Designing with structural Ceramics* (R.W. Davidge and M.H.J. Van de Voorde, eds.), pp. 251-257, Elsevier Applied Science, London and New York, 1991.

[2] - J. C. CAVALIER, A. LACOMBE and J.M. ROUGES, " Ceramic matrix composites, new high performance materials " (in French),pp 99-110 in *Developments in the science and technology of composite material.* Edited by A. R. Bunsell, P. Lamicq AND A. Massiah. Elsevier, London, U.K., 1989.

[3] - T.P. HERBELL and A.J. ECKEL, "Ceramic for rocket engine components", *Aerospace Eng.*, 11 [12], 21-23 (1991).

[4] - E. BOUILLON, D. MOCAER, J.F. VILLENEUVE, R. PAILLER, R. NASLAIN, M. MONTHIOUX, A. OBERLIN, C. GUIMON and G. FISTER, "Composition - microstructure - property relationships in ceramic-monofilaments resulting from the pyrolysis of a polycarbosilane precursor at 800-1400°C", *J. Mater. Sci.*, 26, 1517-1530 (1991).

[5] - S.M. JOHNSON, R.D. BRITTAIN, R.H. LAMOREAUX and D.J. RAWCLIFFE, " Degradation mechanisms of silicon carbide fibers", *J. Amer. Ceram. Soc.*, 71 [3] C132-C135 (1988).

[6] - D. ROUBY, "2nd-French-German Conf. on Technical Ceramics", pp 265-286, France, Aix-la-Chapelle, 1987.

[7] F. LAMOUROUX, G. CAMUS AND J. THEBAULT, "Oxidation resistance and strength after oxidation of a 2D woven carbon fiber silicon carbide matrix composite"; pp 499-504 in *Developments in the science and technology of composite materials.* Edited by A. R. Bunsell, J.F. Jamet AND A. Massiah. Elsevier, London, U.K., 1992.

[8] - J.W. SMITH, "The intrinsic reactivity of carbon to oxygen", *Fuel*, 57, 409-414 (1978).

[9] - H. MARSH and K. KUO, "Kinetics and Catalysis of carbon gasification" in *Introduction to carbon science* (H. Marsh, ed.), pp 107-151, Butterworths, London, 1989.

[10] - D.W. Mc KEE and D. CHATTERJI, " The catalysis behaviour of alkali metal carbonates and oxides in graphite oxidation reactions", *Carbon*, 13, p381, 1975.

[11] - R. NASLAIN, J.Y. ROSSIGNOL, P. HAGENMULLER, F. CHRISTIN, L. HERAUD and J.J. CHOURY, "Synthesis and properties of new composite materials for high temperature applications based on carbon fibers and C-SiC or C-TiC hybrid matrices", *Rev. Chimie Minérale*, 18, 544 - 564, (1981).

[12] - W.J. LACKEY and T.L. STARR "Fabrication of fiber-reinforced ceramic composites by chemical vapor infiltration: processing, structure and properties", in *Fiber reinforced ceramic composites* (K.S. Mazdiyasni, ed.), pp. 397-450, Noyes Publications, Park Ridge (NJ), USA, 1990.

[13] - R. NASLAIN and F. LANGLAIS, "CVD-processing of ceramic-ceramic composite material", in *Tailoring multiphase and composite ceramics* (R.E. Tressler, G.L. Messing, C.G. Pantano and R.E. Newnham, eds.), Mater. Sci. Res., 20, 145-164, Plenum Press, New York and London, 1986.

[14] - R. NASLAIN, "CVI-composites" in *Ceramic matrix composites* (R. Warren, ed.), pp. 199-244, Blackie, Glasgow and London, 1992.

[15] - J.F. VILLENEUVE and R. NASLAIN, "Shear moduli of carbon, Si-C-O, Si-C-Ti-O and alumina single ceramic fibers as assessed through pendulum torsion tests", *Composite Science and Technology*, in press.

[16] - P. GAGNAIRE, P. DELHAES and A. PACAULT, "Analysis of the optical images observed by diffraction of a laser beam with carbon fibers", *J. Chimie Phys.* 84 [11/12], 1407-1417 (1987).

[17] - J.G. THEBAULT, "Fabrication process of a composite material with a refractory reinforcement and a ceramic matrix and structure elaborated with such process", French Patent 2 567 874 A1, July 20, 1984.

[18] - D. COJEAN, M. MONTHIOUX and A. OBERLIN, "Interfacial phenomena in 2D-SiC composites with various mechanical behavious", Proc. JNC-7 (G. Fantozzi and P. Fleischmann, eds.), Lyon, Nov.6-8, 1990, pp.381-390, AMAC Publ., Paris 1990.

[19] - R. NASLAIN, "Fiber-matrix interphases and interfaces in ceramic matrix composites processed by CVI", *Composite Interfaces*, in-press.

[20] - G. VIGNOLES, "Atomic relaxation and dynamical generation of ordered and disordered chemical vapor infiltration (CVI) SiC polytipes ", *J. Crystal Growth*, 118, 430-438 (1992).

[21] - S. SCHAMM, A. MAZEL, D. DORIGNAC and J. SEVELY, "Analysis by high resolution transmission microscopy of the SiC-polytypism in the matrix of SiC/SiC composites", in *Composite materials for applications at high temperatures* (R. Naslain, J. Lamalle and J.L. Zullian, eds.), pp. 207-219, AMAC, Bordeaux, 1990.

[22] - S. SCHAMM, private communication, 1992.

[23] - P. EHRBURGER, J. LAHAYE and C. BOURGEOIS, "Characterization of carbon-carbon composites - II: oxidation behaviour ", *Carbon*, 19, 7-10 (1981).

[24] - F. LOUYS, "Role of interfaces in the oxidation mechanism of carbon-carbon composites" (in French), Thesis, University of Mulhouse, (1987).

[25] - S.C. BENNET and D.J. JOHNSON, " Electron-microscope studies of structural heterogeneity in PAN-based carbon fibres", *Carbon*, 17, 25-39 (1990).

[26] - M. GUIGON, A. OBERLIN and G. DESARMOT, "Microtexture and structure of some high tensile strength, PAN-base carbon fibres", *Fibre Science and Technology*, 20, 55-72, (1984).

[27] - W. JOHNSON, " PAN-based carbon fibers", in *handbook of Composites* (W. Watt and B.V. Perov, eds.), 1, 389-444 (1985).

[28] - L.E. JONES and P.A. THROWER, " Influence of boron on carbon fiber microstructure, physical properties, and oxidation behavior", *Carbon*, 29 [2], 251-269 (1991).

[29] - H. RAETHER, "Excitation of plasmons and interband transitions by electron", in *Springer Tracts in Modern Physics*, 88 Berlin, Heidelberg New York, 1980.

[30] - A. OBERLIN, "High resolution TEM studies of carbonization and graphitization", *Chem and Phys. of Carbon*, 22,1-143 (1989).

[31] - B.P. RICHARD, "Relationship between interlayer spacing, stacking order and crystallinity in carbon materials", *J. Appl. Cryst.*, 1, 35-48 (1968).

[32] - A. OBERLIN and M. GUIGON, "The structure of carbon fibres" in *Composite Materials Series* (R.B. Pipes, ed.), Vol. 2 *Fibre reinforcements for composite materials (*A.R. Bunsell, ed.), pp. 149-210, Elsevier, Amsterdam and New York, 1988.

[33] - A. FOURDEUX, R. PERRET and W. RULAND, in Proc. Int. Conf. on Carbon Fibers, London, p 57 (1971).

[34] - X. BOURRAT and A. OBERLIN, " The role of disclination in the structure of the mesophase pitch-based carbon fibers", in Proc. Int. Symp. Carbon, Tsukuba, Japan, 1990.

[35] - P.L.WALKER, F. RUSINKO and L.G. AUSTIN, " Gas reaction of carbon ", *Adv. Catalysis*, 11, p133, (1959).

[36] - M.K. ISMAIL, "On the reactivity, structure and porosity of carbon fibers and fabrics", *Carbon*, 29 [6], 777-792 (1991).

[37] - V. SERIN, R. FOURMEAUX, J. SEVELY and M. GUIGON, "Nitrogen distribution in high tensile strength carbon fibres ", *Carbon*, 28 [4], 573-578 (1990).

[38] - C. VIX, private communication

[39] - E. MENESSIER, J.P. DUMONT, A. GUETTE, R. PAILLER, L. RABARDEL and R. NASLAIN "Axial and radial coefficients of thermal expansion of carbon fibers in the 20-430°C temperature range as derived from the thermal expansion of 1D-C-$SiO_2(B_2O_3)$ composites", *Ceram. Eng. Sci. Proc.*, [10] n°9-10, 1426-1439 (1989).

[40] - E. YASUDA, T. TANABE, H. MACHINO and A. TAKAKU, "Thermal expansion behaviour of various types of carbon fibers up to 1000°C", Extended Abstract, 18 th Biennal Conf. Carbon, Worester (MA), *Amer. Carbon Soc.*, ed., University Park (PA), pp. 30-31, .

[41] - J.F. VILLENEUVE, R. NASLAIN, R. FOURMEAUX and J. SEVELY, "Longitudinal/radial thermal expansion and Poisson ratio of some ceramic fibers as measured by TEM", *Composite Sci. Technology* (in press).

[42] - R.A. LOWDEN, "Characterization and control of the fiber-matrix interface in ceramic matrix composites", ORNL/TM-11039, march 1989, Available NTIS, US Dept. Commerce, Springfield (VA), pp. 26-32.

CHAPITRE 2

KINETICS AND MECHANISMS OF OXIDATION OF 2D WOVEN C/SiC COMPOSITES : 1- EXPERIMENTAL APPROACH

Si la structure de la fibre de carbone HR T300 conditionne son comportement à l'oxydation, il n'en reste pas moins que la texture du composite, plus particulièrement l'état d'endommagement de la matrice, contrôle la localisation de l'oxydation à **l'échelle macroscopique**. L'oxydation peut ainsi concerner tout ou partie du renfort fibreux selon la vitesse de diffusion de l'oxygène à travers la texture du composite.

L'objectif de ce chapitre est de mettre en évidence les différents mécanismes responsables de la cinétique d'oxydation du composite C/SiC, d'une part, et de l'évolution morphologique de la texture du composite en cours d'oxydation, d'autre part. Les effets de la température et de la teneur en oxygène sont analysés. Les variations morphologiques du matériau, induites par un traitement thermique à haute température, sont à nouveau prises en considération.

Le chapitre est présenté sous la forme d'un projet de publication adressé au **Journal of the American Ceramic Society**.

KINETICS AND MECHANISMS OF OXIDATION OF 2D WOVEN C/SiC COMPOSITES : 1- EXPERIMENTAL APPROACH

F. LAMOUROUX and **G. CAMUS**
Laboratoire des Composites Thermostructuraux
UMR 47 (CNRS-SEP-UB1)
3, Allée de La Boëtie, 33600 Pessac, France.

J. THEBAULT
Société Européenne de Propulsion
BP 37, 33165 Saint Médard-en-Jalles, France

ABSTRACT

The oxidation behavior of a 2D woven C/SiC composite partly protected with a SiC seal-coating and heat-treated (stabilized) at 1600°C in inert gas has been investigated through an experimental approach based on thermogravimetric analyses and optical/electron microscopy. Results of the tests, performed under flowing oxygen, have shown that the oxidation behavior of the composite material in terms of oxidation kinetics and morphological evolutions, may be summarized in three different temperature domains. At low temperatures (i.e. < 800°C), the mechanisms of reaction between carbon and oxygen control the oxidation kinetics and are associated to a uniform degradation of the carbon reinforcement. At intermediate temperatures, (i.e. between 800°C and 1100°C), the oxidation kinetics are controlled by the gas phase diffusion through the SiC seal-coating microcracks network which results in a non uniform degradation of the carbon phases. At high temperatures (i.e. > 1100°C), such diffusion mechanisms are limited by the sealing of the microcracks by silica and the degradation of the composite remains superficial. The study of the oxidation behavior (i) of the heat-treated composite in a lower oxygen content environment (dry air) and (ii) of the as-processed unstabilized composite in dry oxygen, confirms the different mechanisms proposed to explain the oxidation behavior of the composite material.

Key words: Oxidation, kinetics, SiC, Carbon, C/SiC composites, ex-Pan carbon fibers.

1- INTRODUCTION

C/SiC fibrous composites have been designed and developed for high temperature structural applications such as engines and re-entry thermal protection for spacecrafts, due to their combination of both high strength carbon fibers and high modulus, oxidation resistant, CVI-processed SiC matrix [1,2]. The SiC matrix, used also in the present study as an external sealing, thus theoretically protects the carbon fibers and their carbon coating towards oxidation. Such a coating, referred to as an interphase, is classically interposed between the fibers and the matrix in order to promote the desired non linear/non-brittle tensile behavior of most of the ceramic matrix composites (CMCs), through an optimisation of the fiber/matrix load-transfer conditions [3]. However, the main energy dissipating mechanisms which contribute to avoid catastrophic failure, i.e. matrix microcracking and fiber/matrix partial debonding, also unfortunately render the highly reactive carbon substrates (i.e. fibers and interphase) more easily accessible to oxygen during thermomechanical loading in oxidizing environments. Besides, the high value of the fiber/matrix thermal expansion coefficient mismatch in the carbon fiber/SiC matrix system already induces matrix and seal-coating microcracking upon cooling from the processing temperature [4]. Therefore, above temperatures as low as 500°C, the oxidation of a part of the composite fiber and interphase content is susceptible to occur [5]. This oxidation of the carbon phases should in turn give rise to a severe degradation of the mechanical properties, as previously established on other CMCs based on ceramic or glass ceramic matrices reinforced with carbon or SiC fibers [6-9].

The protection of C/SiC composites against oxidizing environments requires therefore the use of external seal-coatings impeding the diffusion of oxygen towards the fibrous reinforcement. Such coatings have been already extensively studied in the case of C/C composites [10-12]. However none of these external protections have proved to be totally efficient under the all range of time/temperature conditions required for thermostructural applications. In the eventuality of a severe weakening of the external protection, it may be interesting to have a precise knowledge of the intrinsic oxidation behavior of the material.

The present investigation is the first of two papers dealing with the study of the oxidation behavior of unprotected C/SiC composites (or more exactly only partly protected with a SiC-CVD processed external seal-coating). In this first part, mass loss kinetics and oxidation induced microstructural changes were investigated in order to evidence the main oxidation mechanisms. The influence of several parameters such as temperature, time, gaseous environment and pre-existing matrix microcracks array was more specifically analysed. The modelling of the different mechanisms involved in the oxidation of 2D woven C/SiC composites is treated in the second article [13].

2- EXPERIMENTAL PROCEDURE

The composite material used in the present investigation has been processed* according to the so-called isothermal-isobaric CVI process from a fibrous preform consisting of a 0° stack of ex-PAN carbon fiber** two dimensional (plain-weave) fabrics. In a first step, the fibers were in-

---

* by SEP (Societe Europeenne de Propulsion).

** High strength carbon fiber HR T300 from Toray.

situ coated with a pyrocarbon layer (the interphase) formed from cracking of CH_4, and whose mean thickness was in the range 0.5 to 1 μm. In a second step, the carbon coated preform was infiltrated by the SiC matrix formed in-situ from a CH_3SiCl_3/H_2 mixture, at about 1000°C, according to the ICVI process which has been described elsewhere [14]. These processing steps resulted in a material having a density close to 2, a fiber content of approximately 40 Vol%, a carbon mass content (fibers and interphase) near 40% and a residual porosity in the range 10-15%. Machining of the various samples used in this study left uncoated fibers on both sides. Consequently, once cut at their final dimensions and prior to testing, these samples were coated with a CVD-processed SiC layer of the order of 100 μm in mean thickness.

In order to avoid possible interacting effects resulting from changes in the microstructure and/or the composition of the constituents when aged at temperatures exceeding the processing temperature (e.g. especially regarding the ex-PAN fiber [15]), these samples were then thermally stabilized by a heat treatment performed at 1600°C under an inert atmosphere. This material thus processed and heat treated (stabilized) constitued the reference material used in the major part of the study. Nevertheless, for purpose of comparison and in order to fully understand the possible effects of the stabilizing heat treatment on the oxidation behavior of the material, some samples were also tested in the as-processed (unstabilized) state.

The oxidation kinetics of the composites, were examined by means of thermogravimetric isothermal analysis (TGA) between 600°C and 1400°C using 3 x 3 x 10 mm^3 rectangular coupons. Two different oxidizing atmospheres, namely dry oxygen and a nitrogen/oxygen 80/20 mixture

(equivalent to dry air) were successively used, at a constant total pressure of 100 kPa and a flow rate of 1 l/h. In any case, weight changes were only recorded once the test temperature was reached (at a constant heating rate of 60°C/min).

Microstructures and morphologies of the composites were studied by means of optical microscopy, Scanning Electron Microscopy (SEM) and Transmission Electron Microscopy (TEM) in the as-processed condition, and only by optical microscopy once variously oxidized. In the former case, an heating stage was added to the SEM (maximum temperature: 800°C) in order to follow thermally induced changes in the microcracks opening. In the latter case, samples aged at 700°C, 900°C and 1400°C, for duration corresponding to 2% and 6% of relative mass loss were selected, respectively.

3- RESULTS

3.1- Characterization of the as-processed materials.

3.1.1- Microstructural observations.

The observation by optical microscopy of a polished cross-section of the as-processed material (i.e. before the stabilizing treatment), in a plane perpendicular to the fibers direction, reveals an **array of matrix microcracks** present inside and outside the fiber tows, in conjunction with fiber/matrix partial debondings located at the crack tips (figure 1). TEM allows to precisely localize these debondings inside the carbon interphase, in the vicinity of the pyrocarbon-matrix interface (double arrow in fig.2). These microcracks, whose maximum opening is of the order of 1 to 2 μm (determined through SEM measurements), have to be related to the large difference between the coefficients of thermal expansion (CTEs) of the

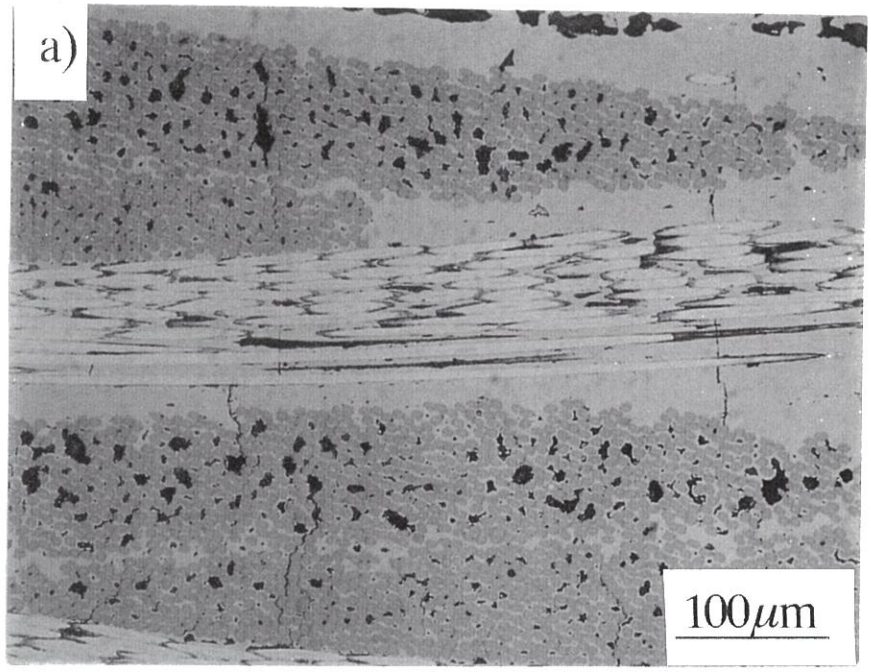

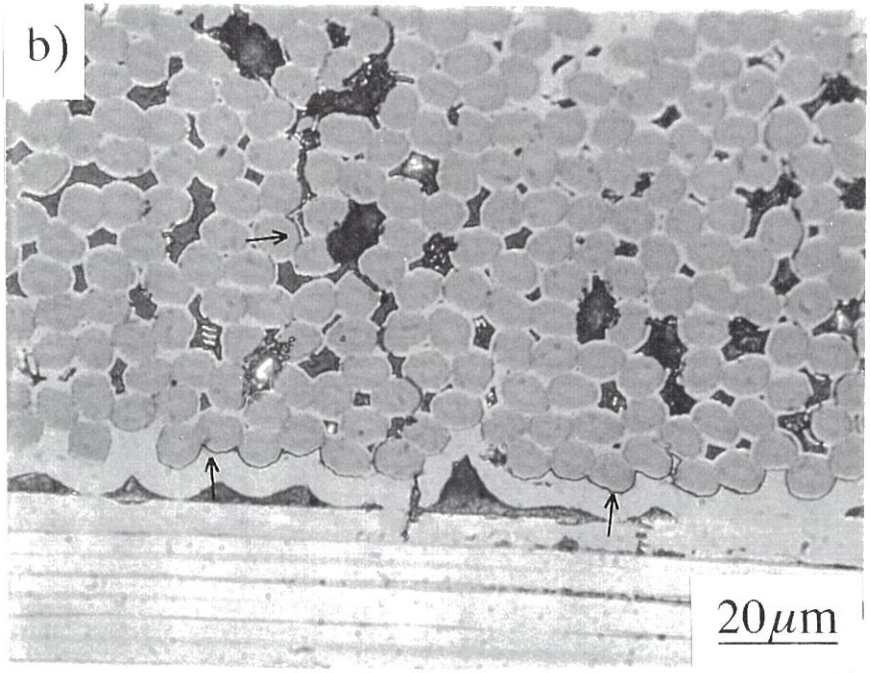

Fig.1: Optical micrographs of a polished section of a 2D C/SiC composite (as-processed) revealing a) matrix microcracks and b) fiber/matrix partial debondings (arrows).

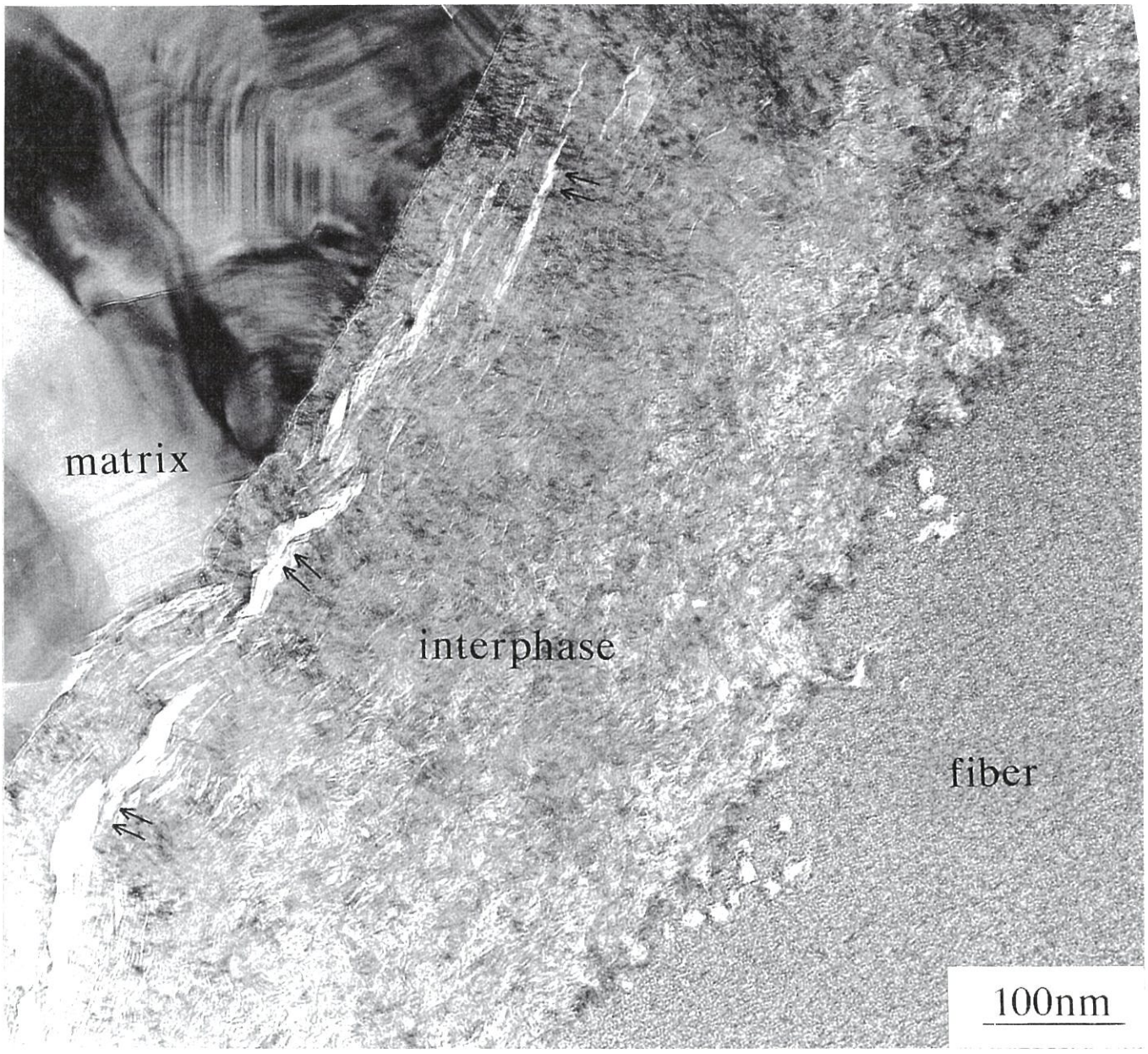

Fig.2: Bright field TEM micrograph of the fiber/matrix interfacial zone of the as-processed C/SiC composite. Debondings are indicated by arrows.

fibers and the matrix. Upon cooling from the processing temperature, the matrix thus encounters both axial and radial tensile residual stresses resulting in the occurrence of microcracking and partial debonding. Damage encountered by the material during processing thus results in the presence of an important free surface within the SiC matrix as well as within both the fiber surface and the carbon interphase.

The stabilizing heat-treatment performed at 1600°C (under inert atmosphere) results in a significantly **higher degree of damage** (figure 3, to be compared with figure 1). The average crack spacing has decreased while the crack opening has nearly doubled. As these microcracks propagate perpendicular to the fiber axis, a bidirectional cracking pattern, reflecting the 2D texture of the reinforcement is thus generated in the matrix as well as in the seal-coating (fig.4). The degree of the fiber/matrix partial debonding has also noticeably increased. The total surface directly exposed to the gaseous environment has thus globally increased subsequently to the stabilizing heat treatment.

3.1.2- Thermally induced changes.

Matrix microcracking results in an easier diffusion of oxygen towards the carbon phases. The oxidation behavior of the composites is thus partly related to the morphology of these matrix microcracks, which should change with temperature since their onset was related to a CTE mismatch effect. In order to understand the oxidation behavior of C/SiC composites, it is therefore necessary to get a good knowledge of the intrinsic variations of the cracks opening with temperature (i.e. in the absence of any oxidation process). Figure 5 displays the results obtained from the observation of the evolution of the microcracks opening as a function of temperature, for both the as-processed and stabilized

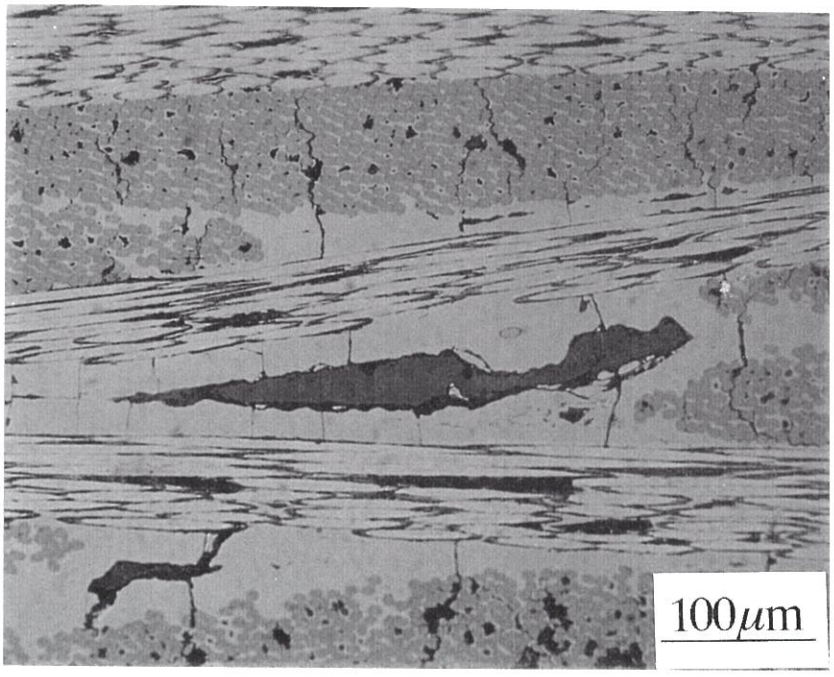

Fig.3: Optical micrograph of a polished section of a 2D C/SiC composite heat-treated at 1600°C under inert atmosphere.

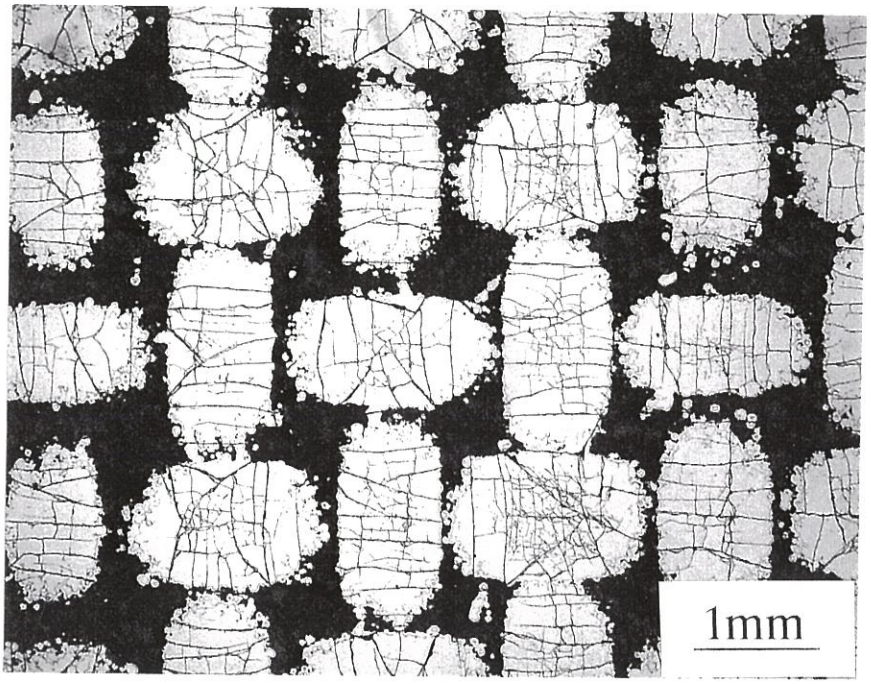

Fig.4: Optical micrograph of the polished surface of a sample (stabilized) revealing the cracking pattern of the SiC seal-coating.

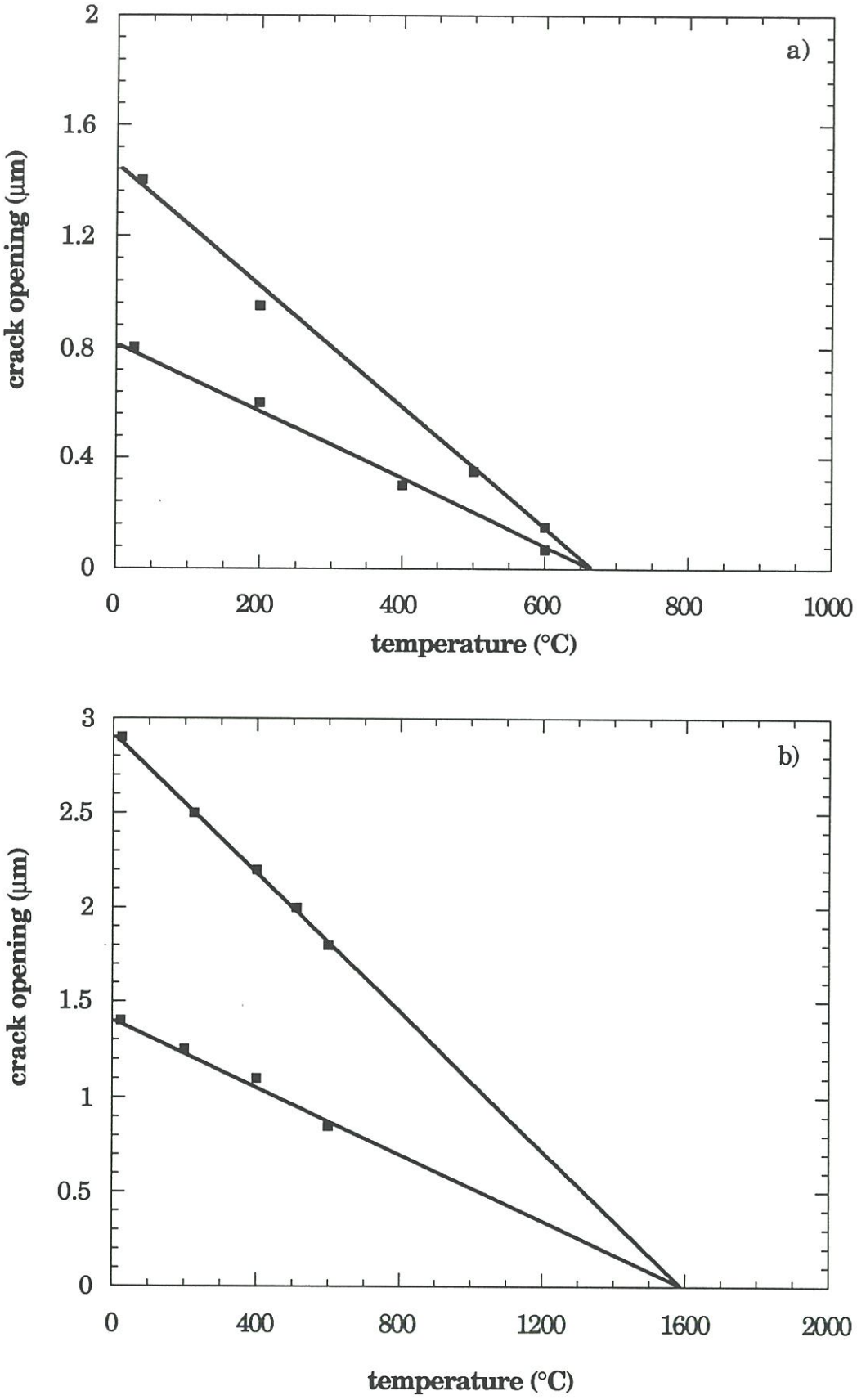

Fig.5: Variations of the SiC seal-coating cracks of a 2D C/SiC composite as a function of the temperature for two different families of initial crack opening (as determined by SEM equipped with an heating stage):
a) as-processed b) stabilized at 1600°C under inert atmosphere.

materials (by SEM fitted with an heating stage). In both cases, the crack opening appears to decrease as the temperature increases, in a quasi-linear manner. Straight lines associated with the variations of two different families of cracks are, for each material, concurrent at **single temperature.** For the as-processed (unstabilized) material, this temperature approximately corresponds to the temperature beyond which the onset of damage took place in the material when cooled down from the processing temperature. The mismatch between the processing temperature (≈1000°C) and this damage temperature (≈650°C) characterizes the thermomechanical resistance of the SiC seal-coating. For the heat-treated (stabilized) material, the converging temperature is nearly identical to the heat-treatment temperature (i.e. 1600°C). Evolution of the crack opening, e, as a function of temperature may therefore be represented by a linear relation of the form:

$$e(T) = e_0 \cdot (1 - \frac{T}{T_0}) \qquad (1)$$

with : e_0, crack width at room temperature,

T, test temperature,

T_0, converging temperature.

3.2 - Thermogravimetric analyses and morphological changes induced by oxidizing treatments.

3.2.1- Influence of the ageing temperature.

TGA plots of stabilized C/SiC composites oxidized in dry oxygen (P=100kPa) between 600°C and 1400°C are displayed in figure 6. These results first indicate that the simultaneous oxidation of the different constituents of the composites (i.e. fiber, interphase and matrix) always leads to overall mass losses.

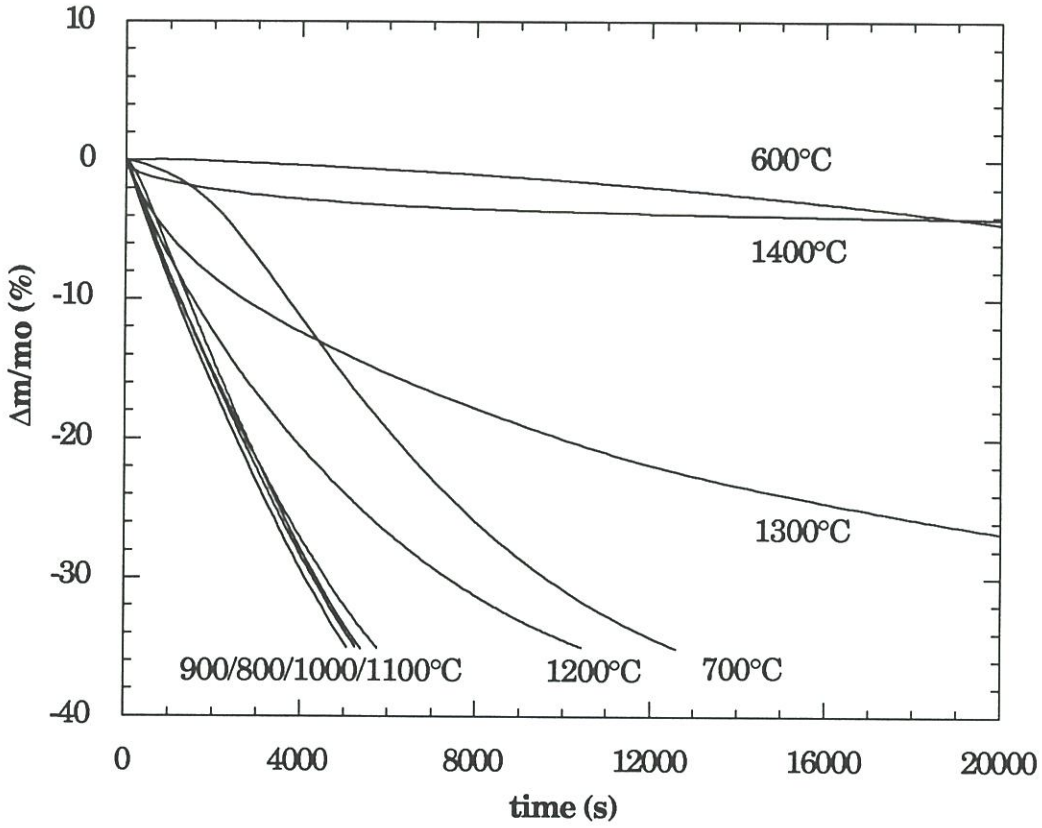

Fig.6: Relative mass variations as a function of time for the stabilized 2D C/SiC composite under flowing oxygen (P=100kPa).

The oxidation kinetics of the composite may be further divided into three main temperature domains :

(i) 600°C to 800°C : the rate of the mass loss strongly increases with temperature. Morphological observations made on samples tested at 700°C reveal a rapid degradation of the first carbon plies (i.e. adjacent to the seal-coating). At an early stage of oxidation corresponding to relative mass loss of 2%, the major part of the fibers localized in the external tows appear to be more or less partly oxidized. At later stages of oxidation, for a relative mass loss of 6%, micrographs show that all the carbon tows are partly oxidized (fig.7a). A closer look, at the scale of the fibers, reveals that the pyrocarbon interphase was totally consumed while the carbon fibers were degraded mainly at their periphery (fig.7b).

(ii) 800°C to 1100°C : the rate of mass loss remains nearly constant. Besides, the quasi-linear aspect of the mass loss curves show that oxidation rates may be assumed as time-independent. Morphological observations made on sample oxidized at 900°C, reveal a preferential oxidation of the outer part of the fiber tows, as well as of the fibers located nearly the seal-coating microcrack tip (fig.8a). This degradation remains localized at the periphery of the fibers leading to a decrease of their section. At a later stage of oxidation, the oxidizing attack appears to have propagated in the bulk of the sample. However, this attack is not uniform and the external plies are more degraded than the internal plies.

(iii) 1100°C to 1400°C : the rate of mass loss decreases as the temperature increases. Moreover, beyond 1100°C, this rate also decreases with the ageing treatment duration and even sets aside at 1400°C. From a sample oxidized at 1400°C, it may be seen that the degradation of the reinforcement remains localized in the vicinity of the seal-coating microcracks tips while the bulk of the samples is unaffected. Clusters of

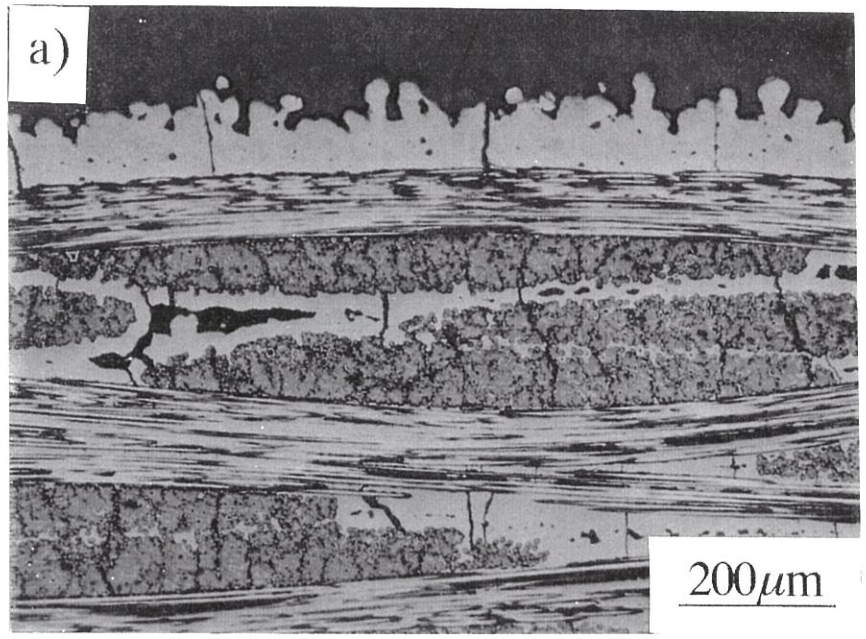

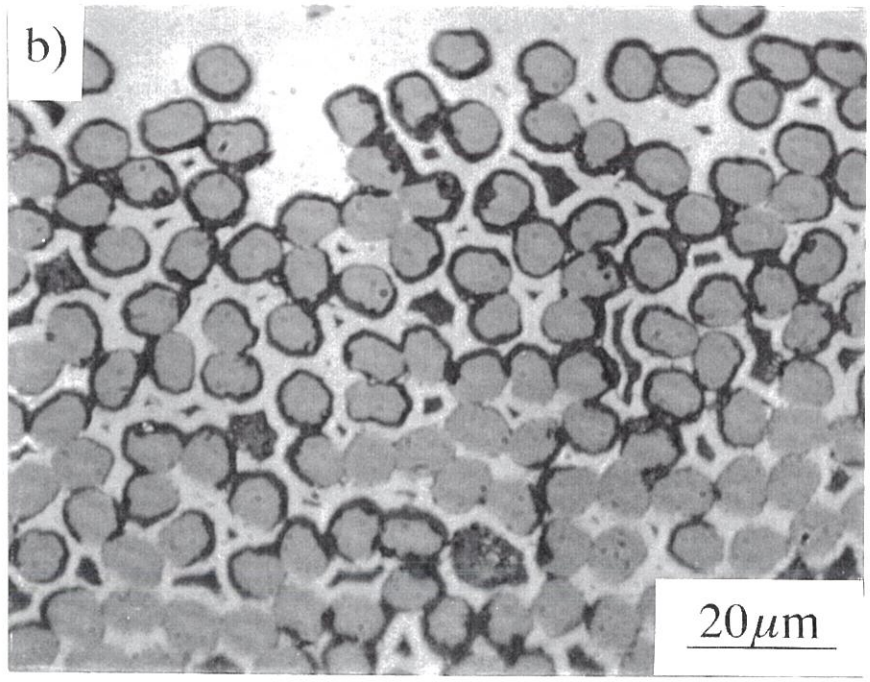

Fig.7: Optical micrographs of polished section of stabilized 2D C/SiC composites aged at 700°C under flowing oxygen (P=100kPa), for a relative mass loss of 6%, showing the partial oxidation of:
a) the fiber tows , b) the fibers and interphase.

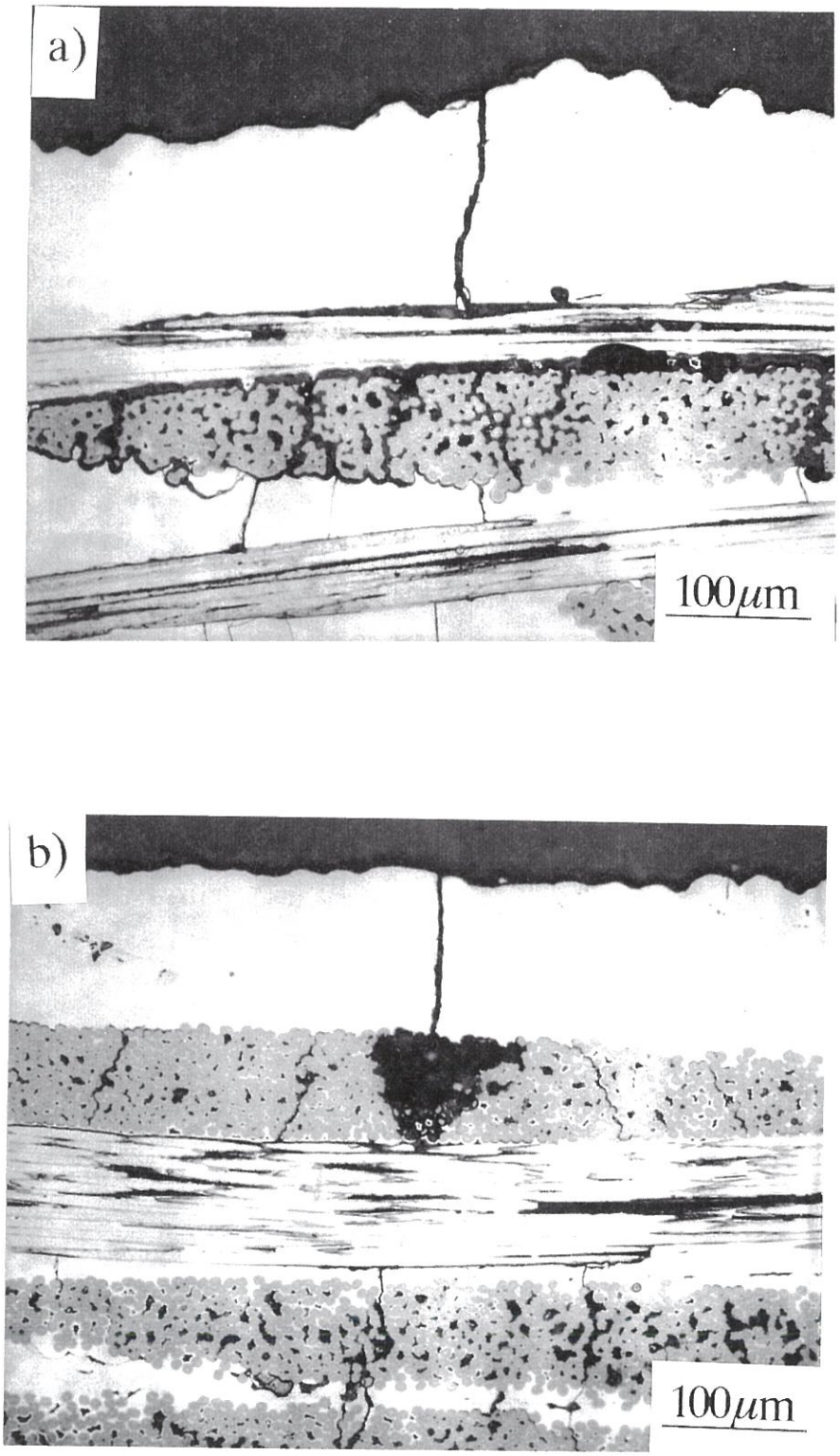

Fig.8: Optical micrographs of polished section of stabilized 2D C/SiC composites aged under flowing oxygen (P=100kPa) at a relative mass loss of 2%, a) at 900°C , b) at 1400°C.

oxidized carbon phases thus take place under the seal-coating at the microcracks tips (fig.8b). Contrary to the oxidation treatments performed at low temperatures, oxidation no longer takes place selectively and both the fibers and the interphase are similarly consumed.

3.2.2- Influence of the atmosphere composition.

Figure 9 displays the results of TGA experiments performed on stabilized C/SiC composites under flowing dry air (more exactly a mixture of N_2/O_2 - 80/20) between 600°C and 1400°C. The aspect of the mass loss curves remains seemingly unchanged while the oxidation rates are substantially changed.

The decrease of oxygen content associated with the change of atmosphere composition allows to determine a global dependence of the oxidation kinetics of the composite material to the oxygen partial pressure. This dependence may be related in the present case to the ratio of the rate of oxidation in oxygen to the rate of oxidation in air. Calculation of this ratio for each temperature allows to further distinguish the same temperature domains, corresponding to different oxidation regimes, than established in the preceding section:

(i) $T < 800°C$: the oxidation rates ratio is inferior to 5,

(ii) $800°C < T < 1100°C$: the oxidation rates ratio is equal to 5,

(iii) $T > 1100°C$: the oxidation rates ratio is superior to 5.

The signification of these differences in the oxidation kinetics ratio and their connection to the different mechanisms governing these oxidation kinetics will be discussed lately.

Examinations of selected samples oxidized at 700°C, 900°C and 1400°C brings up the following results regarding the localization of the oxidizing attacks.

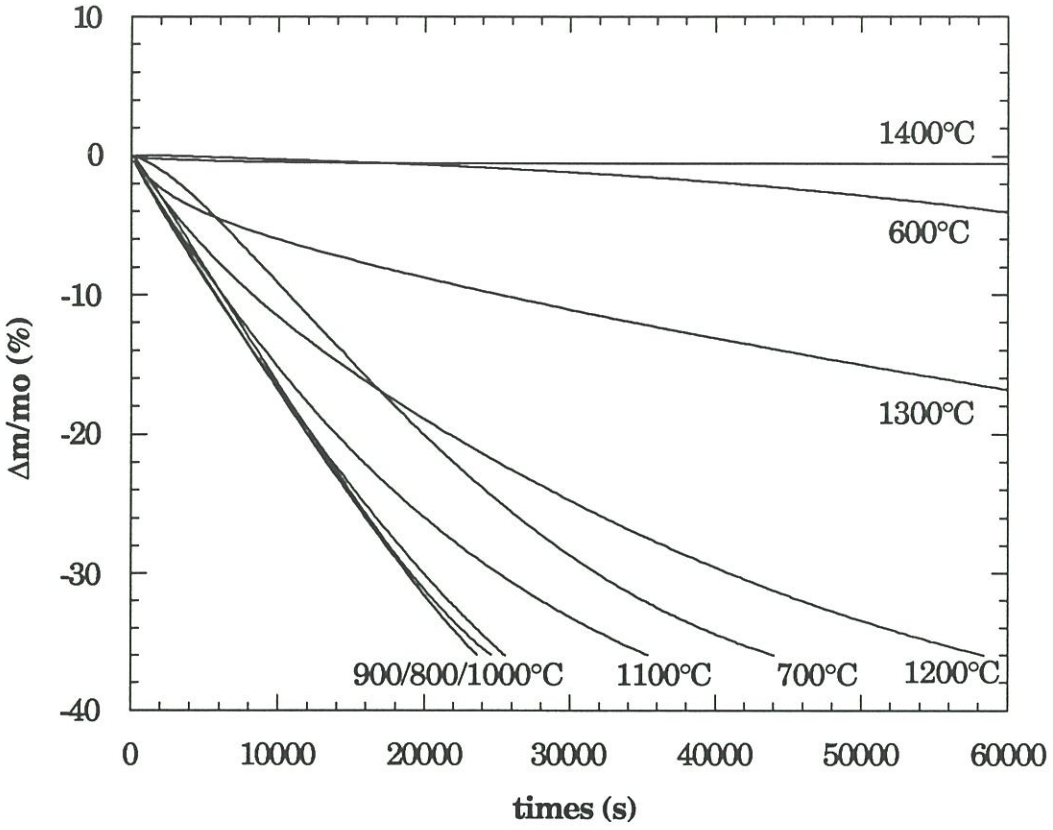

Fig.9: Relative mass variations as a function of time for the stabilized 2D C/SiC composite under an N2/O2 gas mixture (80/20) (P=100kPa).

In the case of the ageing treatments at 700°C and 900°C, apart from a more homogeneous degradation of the material, no really significant change were noticed between tests performed under both environments. At 1400°C, for an ageing treatment corresponding to a relative mass loss of 2%, clusters of oxidized fibers and interphase have also formed under the SiC seal-coating. However, contrary to the treatments performed under dry oxygen, degradation does not take place immediately under the cracks tips, but propagates at the entire periphery of the fiber tows (fig.10).

3.2.3- Thermally unstabilized material.

For purpose of comparison and in order to understand the possible effects of the stabilizing heat-treatment on the oxidation behavior of the material, oxidation kinetics of the unstabilized (as-processed) composite were also studied by mean of TGA, under flowing oxygen only (P=100kPa). Initial oxidation rates calculated for both materials (i.e. as-processed and stabilized composites) from the TGA experiments are plotted as a function of temperature in figure 11. These plots evidence some significant changes in the oxidation kinetics caused by the stabilizing treatment. Thus, it may be noticed that: (i) the temperature corresponding to a transition in the oxidation regime is lower for the unstabilized composite (see dash line in fig.11), (ii) the composite does not encounter any mass variation in the temperature range 1000°C - 1200°C and (iii) the oxidation rate of the stabilized composite seriously increases beyond 1300°C.

Morphological observations performed on as-processed (unstabilized) composites variously aged at 700°C, 900°C and 1400°C also reveal some noticeable differences as compared to the stabilized composites:

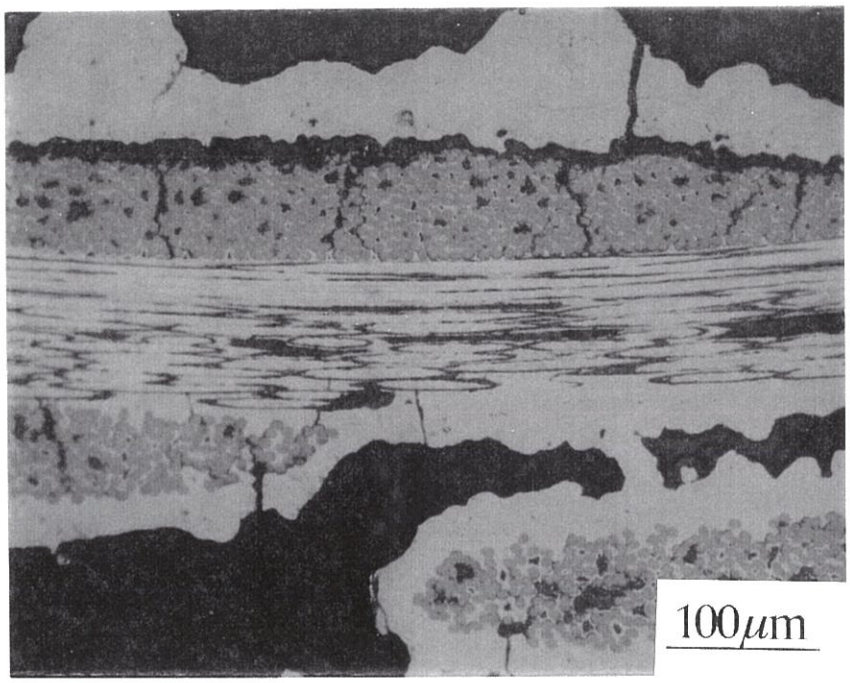

Fig.10: Optical micrograph of a polished section of a stabilised 2D C/SiC composite aged at 1400°C under a N_2/O_2 (80/20) gas mixture (P=100kPa), for a relative mass loss of 2%.

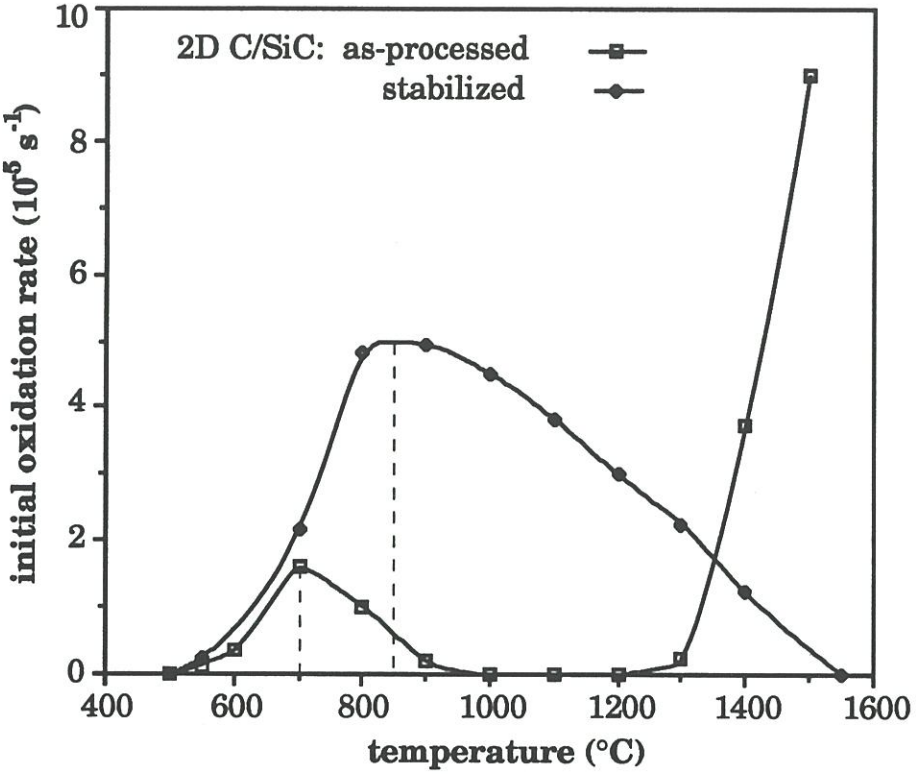

Fig.11: Dependence of the initial oxidation rate of the as-processed and heat-treated (stabilized) C/SiC composites to the temperature of the ageing treatments under flowing oxygen (P=100kPa).

- at 700°C a preferential attack occurring at the two interfaces fiber/pyrocarbon and pyrocarbon/matrix is strongly apparant (see fig. 12). For a relative mass loss of 6%, oxidation reaches all the carbon plies present in the material while remaining localized near the free-surfaces (i.e. matrix/tow debonds and intratow microcracks), similarly to the stabilized composite aged at 900°C,

- at 900°C, a front of oxidation starts to appear under the SiC seal-coating whereas this phenomenom was only observed at 1400°C for the stabilized materials (fig.13a).

- At 1400°C, the front of oxidation is more pronounced. However, oxidation only takes place along the lateral sides of the specimens (fig.13b).

4- DISCUSSION

4.1 - Oxidation phenomena.

The general oxidation behavior of 2D C/SiC composites may be depicted by considering the various mechanisms, both diffusional and reactional, which are thought to control the oxidation kinetics of the composite:

(i) gas phase diffusion of oxygen and product species through the SiC seal-coating microcracks,

(ii) diffusion of oxygen and gaseous product species through the porosity developed inside the material by the oxidation of the carbon phases (i.e. fibers and interphase),

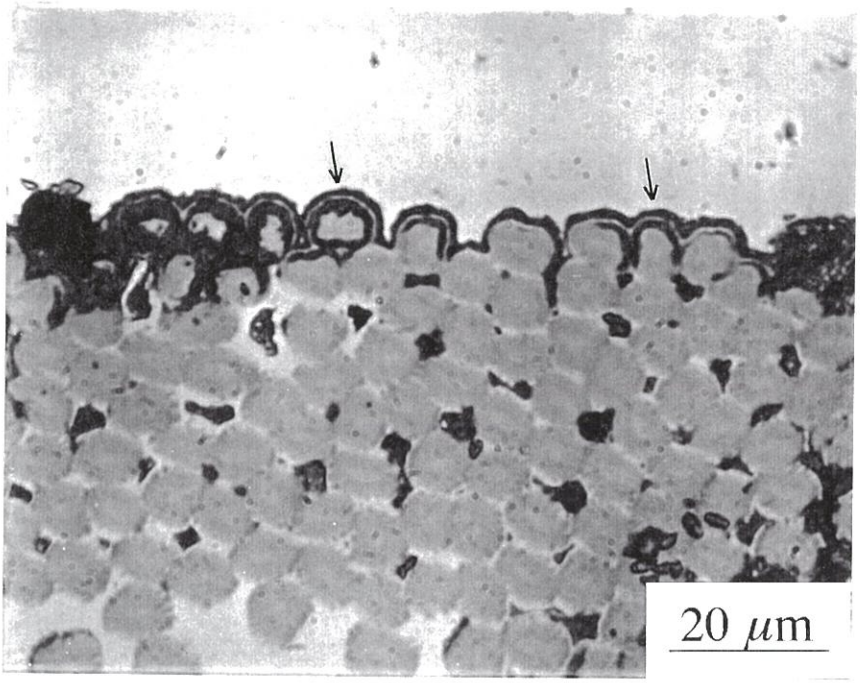

Fig.12: Optical micrograph of a polished section of the as-processed C/SiC composites aged at 700°C under flowing oxygen (P=100kPa), for a relative mass loss of 6%. Evidence of the partial oxidation of the carbon fibers (arrows).

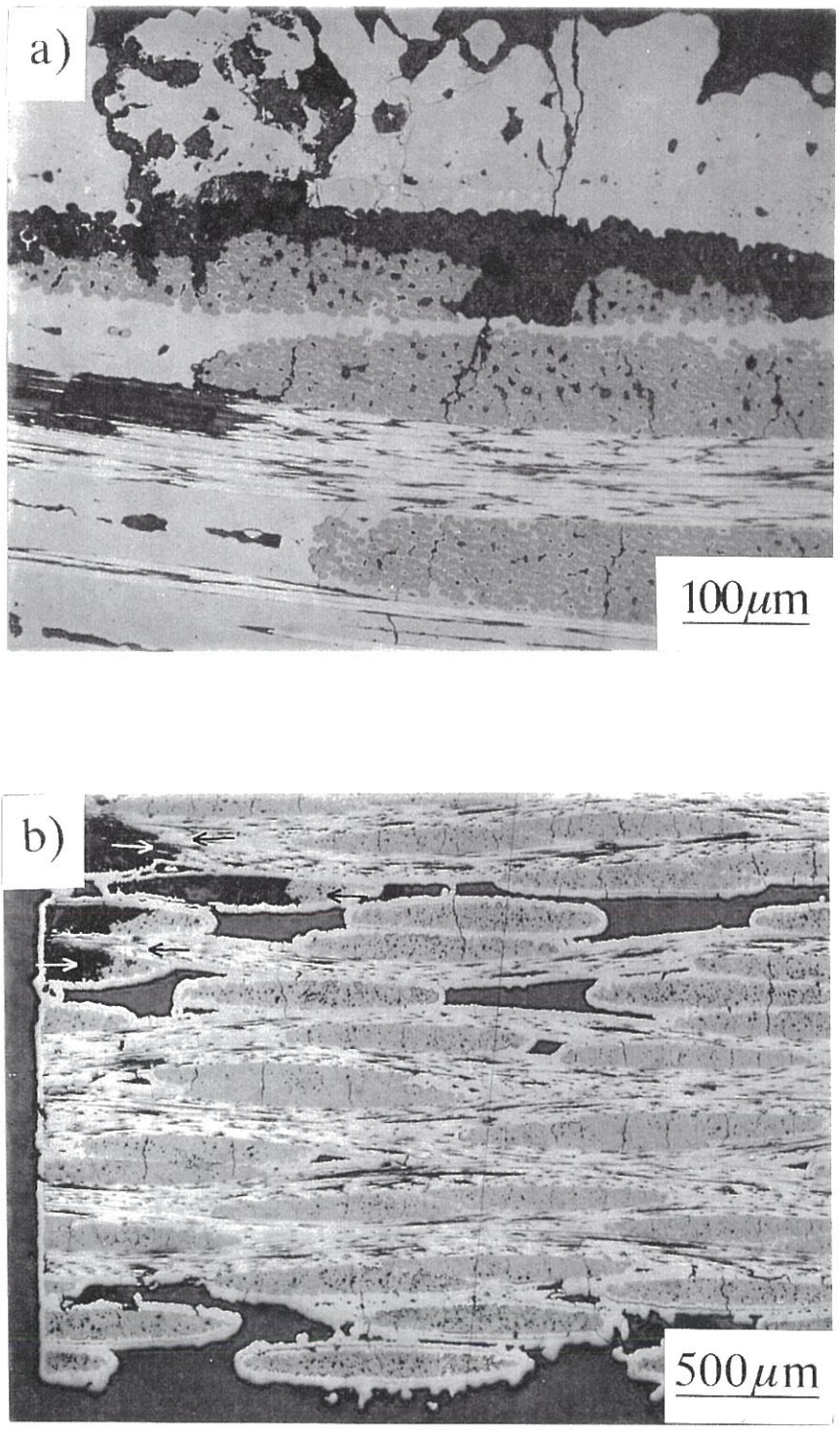

Fig.13: Optical micrographs of polished section of the as-processed C/SiC composites aged under flowing oxygen (P=100kPa), for a relative mass loss of 6%, a) at 900°C , b) at 1400°C.

(iii) diffusion of oxygen at the carbon surface towards reaction sites.

(iv) reactions between oxygen and carbon according to the following equations :

$$C_{(s)} + O_{2(g)} \longrightarrow CO_{2(g)} \qquad (2)$$

$$2C_{(s)} + O_{2(g)} \longrightarrow 2CO_{(g)} \qquad (3)$$

(v) growth of silica layers from the oxidation of silicon carbide according to the following equations :

$$SiC_{(s)} + 2O_{2(g)} \longrightarrow SiO_{2(s)} + CO_{2(g)} \qquad (4)$$

$$SiC_{(s)} + \frac{3}{2}O_{2(g)} \longrightarrow SiO_{2(s)} + CO_{(g)} \qquad (5)$$

The equivalent area corresponding to the total surface of SiC seal-coating microcracks is low compared to the surface of the sample. Consequently, diffusion of gaseous species through the gas layer present over the material (i.e. boundary layer) should not be considered as a mechanism susceptible to control the oxidation kinetics of the composite under the conditions of the present study.

In the oxidation process of the 2D C/SiC composites, a **competition** will obviously take place between the oxidation of carbon and silicon carbide phases according to mechanisms (iv) and (v), on one hand, and oxygen diffusion from the external environment to the carbon active surfaces, implying mechanisms (i), (ii) and (iii), on the other hand.

From the TGA experiments and the microstructural observations performed on the reference 2D C/SiC composite (i.e. stabilized at 1600°C under inert atmosphere), it appears that **three main temperature domains** associated to different oxidation rate controlling mechanisms may be considered for this material. These various temperature domains/oxidation phenomena are graphically depicted in figure 14 and discussed below.

At low temperatures (i.e., ≤ 800°C), the rate of oxygen diffusion inside the material is elevated compared to the rate over which the oxidation takes place at the surface of both the carbon phases and silicon carbide. Figure 15 reveals that, for an ageing temperature of 700°C, the general features of the TGA plot of the C/SiC composite are largely similar to those of the TGA plot obtained from a previous study of C/C bundles of the same carbon phases and similarly stabilized at 1600°C under inert gas [15]. Consequently, there is a strong evidence for that, at temperatures inferior to 800°C, the mechanisms which controlling the oxidation rates of the C/SiC composite and the C/C bundles should be identical, that is to say, the **chemical reactions** between carbon and oxygen.

Because of the rapid diffusion of oxygen, on one hand, and the low reactivity of both the carbon phases and silicon carbide, on the other hand, the oxidative attack rapidly reaches the bulk of the samples which gets thus **homogeneously** oxidized (fig.14a). As previously established, fiber/matrix debonding takes place inside the carbon interphase, while the ex-PAN fibers are selectively oxidized at their surface (see double and triple arrows in figure 2 and reference [15]). Consequently, when the fibers are locally uncoated, oxidation preferentially propagates on both sides of the carbon interphase, which gets therefore rapidly consumed.

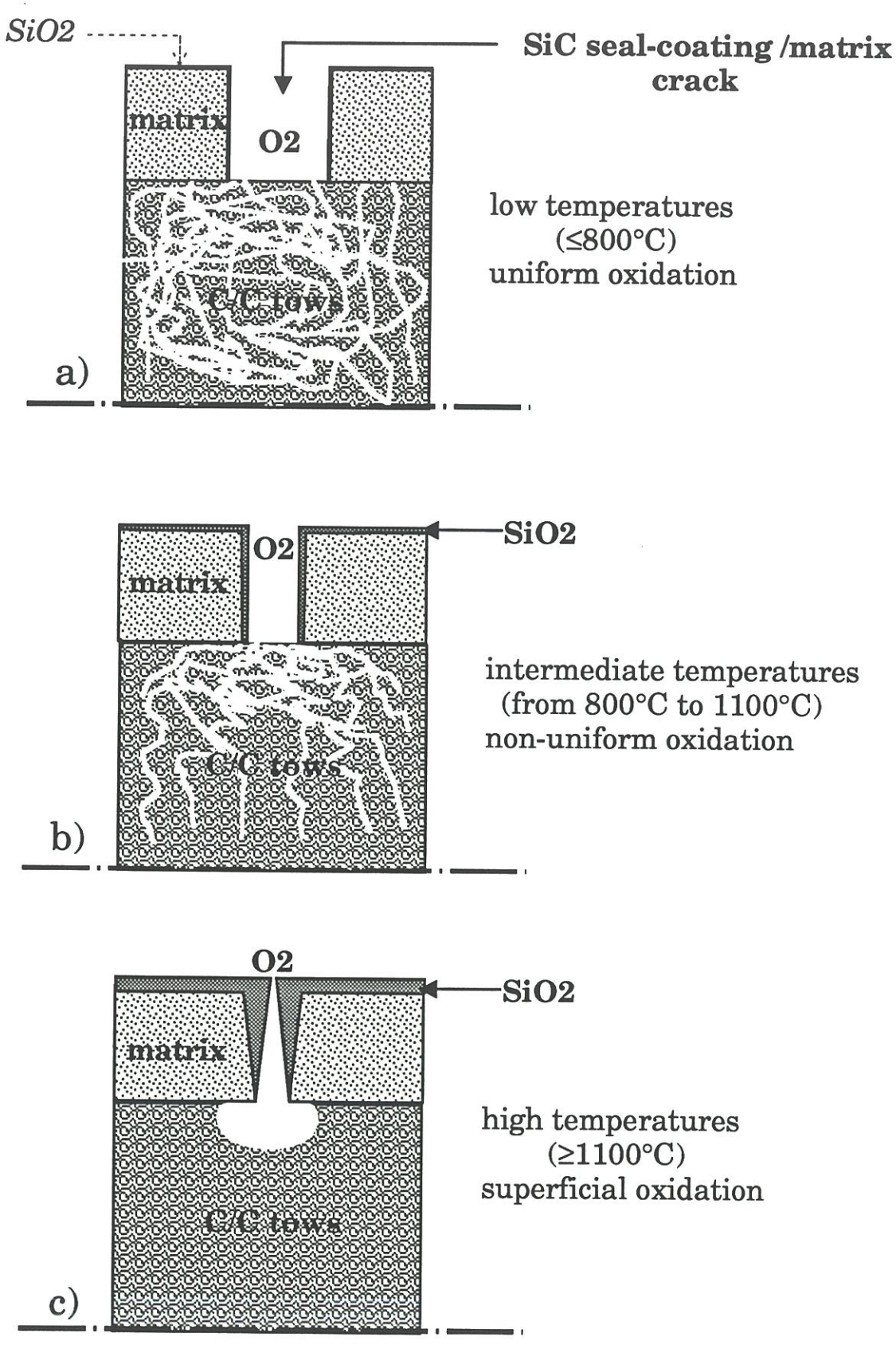

fig.14: Schematic representation of heat treated (stabilized) 2D C/SiC oxidation phenomena.

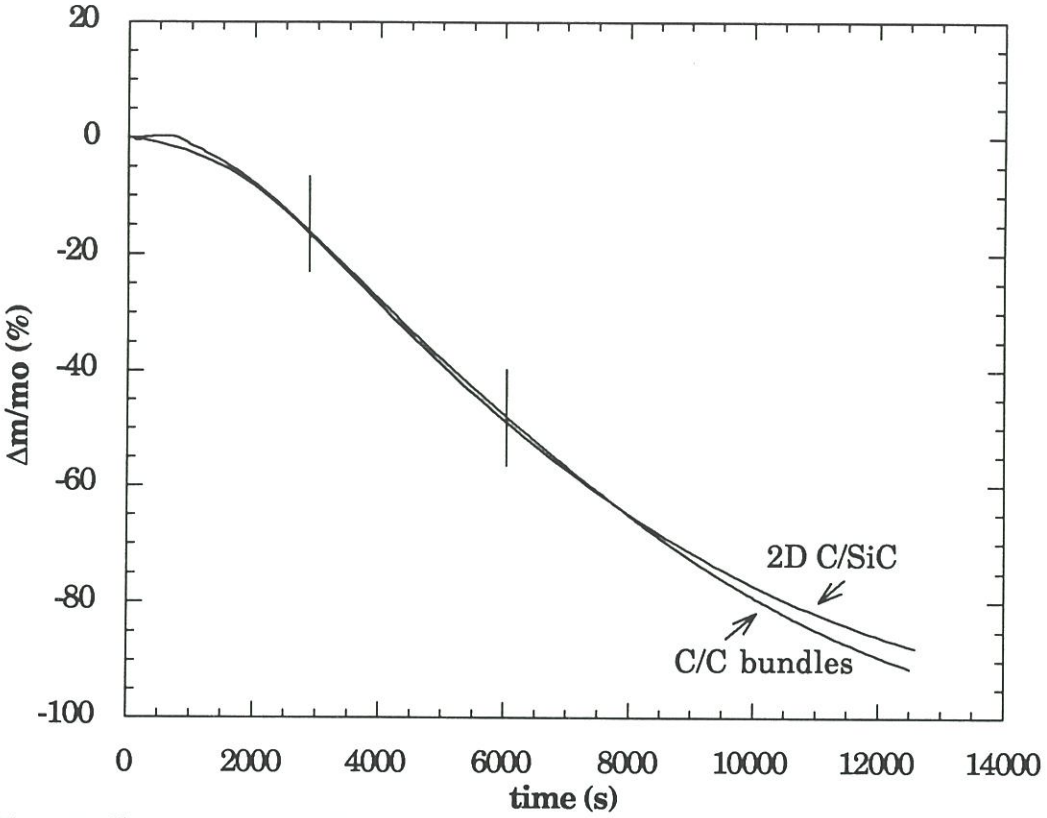

Fig.15: Comparison of the relative mass variations as a function of time at 700°C under flowing oxygen (P=100kPa) between the heat treated C/SiC composite (normalized to the total carbon content inside the material) and the heat treated C/C bundles.

When oxidation is further prolongated, fibers become in turn partly degraded.

At intermediate temperatures (800°C ≤ T ≤ 1100°C), the oxygen **diffusion regime** takes over. The rate of oxygen transport is limited by collisions between molecules (Fick regime), as expressed by the following equation:

$$\frac{dn_{O_2}}{dt} = l \cdot e \cdot Df \cdot \frac{dC}{dx} \qquad (6)$$

with n_{O_2}, number of moles of oxygen diffusing,

t, time

e, crack width at a given temperature,

l, the crack length (in m),

Df, oxygen diffusion coefficient in a Fick regime,

$\frac{dC}{dx}$, oxygen concentration gradient inside a crack.

As the ageing temperature is increased, the Fick diffusion coefficient of oxygen also increases according to the following equation [16]:

$$D_f = a \,.\, T^{1.75} \,.\, P^{-1} \qquad (7)$$

Where a , T and P represent a proportionality factor, the temperature and the total pressure, respectively.

However, when diffusion is the rate controlling step, oxidation kinetics of the material also strongly depend on the surface of diffusion (i.e. the size of the microcracks). As the ageing temperature is increased, the thermal expansion of silicon carbide becomes significant which leads

to a decrease of the thickness of the microcracks (see equation (1)). As expressed in equation (6), the rate of oxygen transport is proportional to the product $D_f.e$. The variations of this product with temperature reveal a **transition zone** associated to a **constant rate** of oxygen transport for the whole intermediate temperatures range (fig.16a). As a result of this competition between the respective variations of the Fick diffusion coefficient and the surface of oxygen diffusion, the oxidation kinetics of the C/SiC composite remain thus independent from the temperature in the domain considered.

This transition may also be assigned to an alteration of the diffusion regime. As a matter of fact, when the width of the cracks gets significantly reduced, the diffusion mechanism may switch from a Fick regime to a Knudsen regime. In this latter case, diffusion of oxygen is controlled by collisions of molecules with the crack walls. The Knudsen coefficient of diffusion obeys the following equation [17]:

$$D_k = b \,.\, e \,.\, T^{0,5} \qquad (8)$$

where b is a proportionality factor.

The Bosanquet equation defines an effective coefficient $\bar{D}$ taking into account the two diffusion regimes [18], as follows:

$$\bar{D}^{-1} = D_f^{-1} + D_k^{-1} \qquad (9)$$

The rate of oxygen transport may still be expressed by equation (6), replacing the Fick diffusion coefficient by this effective coefficient.
At low temperatures, the largelly opened microcracks result in the Knudsen coefficient being higher than the Fick coefficient and thus,

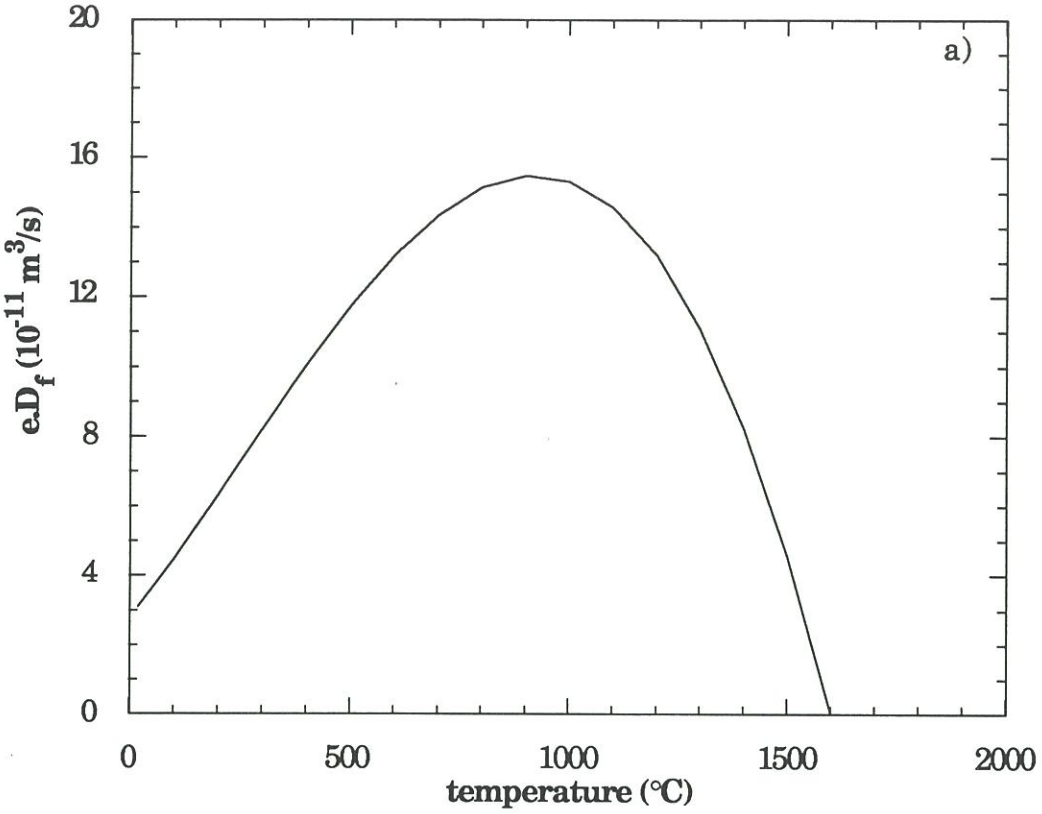

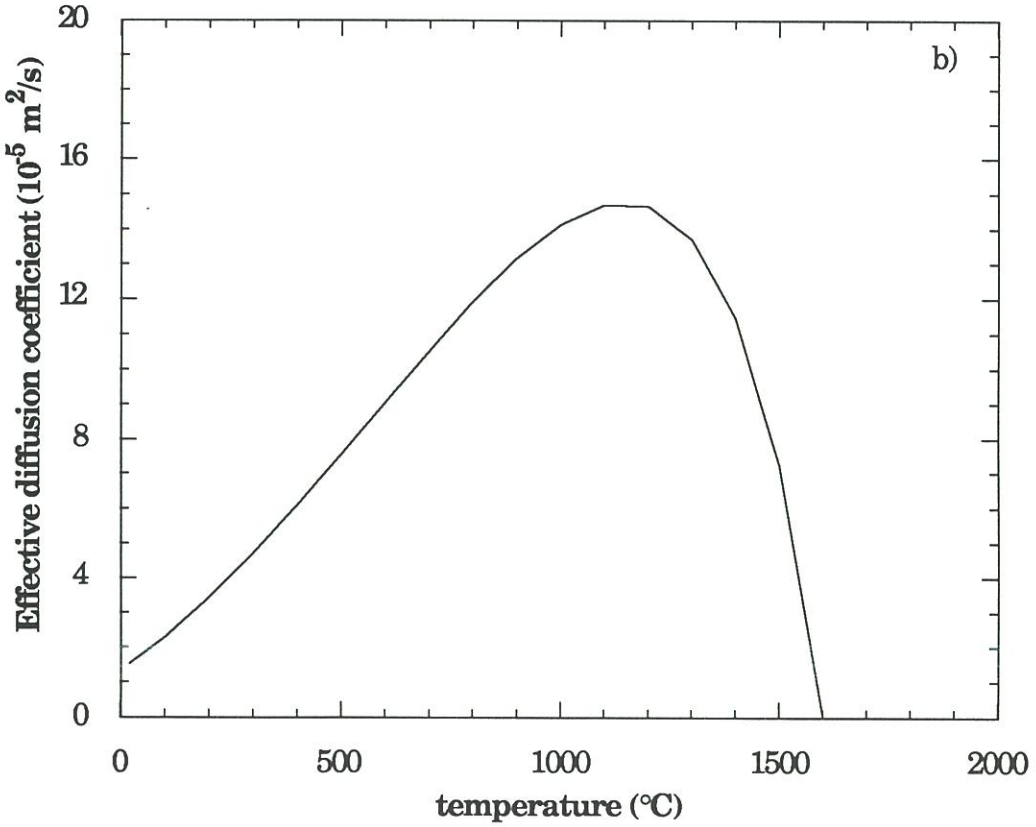

Fig.16: Effect of an increase in temperature on a) the product of a crack width (e=2μm) by the Fick diffusion coefficient according to equation (6), b) the effective diffusion coefficient according to equation (9).

according to equation (9), in the preponderance of the Fick regime. However, at intermediate temperatures, the values taken by these two coefficients become comparable and a competition between the two diffusion regimes occurs. A transition in the composite oxidation kinetics may thus also be observed when the Knudsen diffusion regime takes over (Fig.16b).

In this intermediate temperature domain, the global reactivity of carbon towards oxygen is known to increase noticeably. Thus, if the cracks width has decreased, the amount of oxygen diffusing through these cracks is still high enough to reach the carbon plies up to the bulk of the sample. However, since the outer carbon plies consumed more oxygen than at lower temperatures, an oxygen gradient and consequently a carbon consumption gradient takes place between the bulk and the surface of the material (fig.14b). The appearance of the oxidizing attack in the composite is thus **non-homogeneous**.

At high temperatures (≥ 1100°C), the initial opening of the thermal microcracks is strongly reduced. Besides, the rate of oxidation of silicon carbide (which is classicaly thermally activated) starts to increase significantly [19]. The **growth of silica layers along the cracks walls** induces a gradual closure of these cracks and, consequently, a decrease of the kinetics of oxidation of the composite as the duration and the temperature of the oxidizing treatment are increased. At 1400°C, the silica layers growing from the cracks walls connect and the oxidation kinetics rapidly set aside. In this temperature range, gas phase **diffusion of oxygen** through the seal-coating microcracks is thus **strongly modified** by oxidation of the silicon carbide.

The proportion of oxygen which reaches the first carbon plies is limited in amount and immediately consumed. The rate of reaction of carbon with oxygen is so high that oxidation takes place indifferently on the fibers and the interphase. When the cracks are sealed by silica, the bulk of the sample remains thus unoxidized while only the vicinity of the microcrack tips are consumed. The oxidation is then **superficial** (fig.14c).

4.2 - Effect of a decrease in the oxygen content.

As it may be observed from the tests performed under flowing dry air (or more exactly N_2/O_2 - 80/20), decreasing the oxygen content leads to modifications in the oxidation rates of the C/SiC composites. Such modifications were previously assessed in a work performed on heat treated C/C bundles (ex-PAN carbon fiber tows coated with pyrocarbon and similarly heat treated at 1600°C under inert gas) [20], on the basis of the values taken by the ratio K of the oxidation rates in oxygen to the rates in air :

$$K = \frac{k_r(O_2)}{k_r(air)} = \left[\frac{C(O_2)}{C(air)}\right]^n = 5^n \qquad (9)$$

with: k_r, global oxidation rate

C, oxygen content of the gaseous environment

n, the apparent reaction order with respect to oxygen.

- for T < 800°C, kinetics were found to be controlled by carbon/oxygen reactions, and n took the value 0.75.

- for T > 800°C, kinetics were found to be controlled by gas phase diffusion of the gaseous species through the boundary layer, and n was equal to 1.

These results may then be compared to those obtained in the present study with C/SiC composites:

- for T < 800°C : K is equal to 3.6, which leads to a value n equal to 0.79. This value is in good agreement with the hypothesis of an oxidation kinetics being controlled by the carbon/oxygen reactions.

- for 800 < T < 1100°C : K is equal to 5, which leads to an exponent n equal to 1. Comparison with the oxidation of C/C tows confirms that oxidation kinetics are controlled by gas phase diffusion phenomena.

- for T > 1100°C : K is superior to 5. The decrease of the composite oxidation rate appears therefore to be proportionally more important than the decrease of the oxygen content induced by the case of air instead of oxygen as gaseous environment. As it has been reported elsewhere, in the considered temperature range, the oxidation rates of SiC are less affected by a decrease in the oxygen partial pressure than the carbon phases [21,22]. It may be concluded, thus, that the oxidation kinetics of the C/SiC composites are effectively slowed down by the growth of silica layers on the cracks walls.

The above results obtained from tests performed in dry air thus further **confirm** the oxidation rate controlling mechanisms discussed in the preceeding section.

From a microstructural point view, a **more homogeneous degradation** of the carbon phases due to the decrease in oxygen content was noticed. The global reactivity of the carbon phases is lowered by the decrease of the oxygen partial pressure, and oxygen may thus more easily diffuse inside the sample. At intermediate temperatures, a reduction in the gradient of oxidation between the bulk and the surface of the samples is thus observed. At high temperatures, the decrease of both the oxygen

molar flux and the global carbon reactivity results in an attenuation of the concentration of the oxidized zones at the crack tips. The oxidation front gets spread at the periphery of the outer tows, at the level of the free surfaces constituted by matrix-tow debondings.

4.3 - Thermally unstabilized material.

Oxidation kinetics and morphological changes induced by oxidizing treatments proved to be different for the as-processed (unstabilized) material. These differences were essentially related to the temperature domains associated to the oxidation mechanisms previously discussed. Comparisons between the oxidation behavior of the as-processed and stabilized C/SiC composites also further evidence the possibility of **associating** an **oxidation mechanisms** with a **degradation mode** induced by oxidation, as represented in figure 17 and discussed below.

For T<700°C, the mechanisms controlling the composite oxidation rates are similar to those involved in the oxidation of as-processed C/C bundles (as established in [15]) and correspond to a mixed reaction/diffusion mode at the carbon surface.

As the C/SiC composite in the as-processed state has an overall array of microcracks thinner than that after the stabilizing treatment, the onset of the first variation in the oxidation kinetics consequently takes place at a lower temperature, i.e. 700°C instead of 900°C. The morphological changes occurring during the oxidizing treatments are in good agreement with diffusional mechanisms. Degradation is localized near the free surfaces of the carbon phase, and an oxidation gradient appears in the fiber tows. The figure 5 indicates a closure of thermal cracks taking place at about 700°C, which is in contradiction with the TGA data

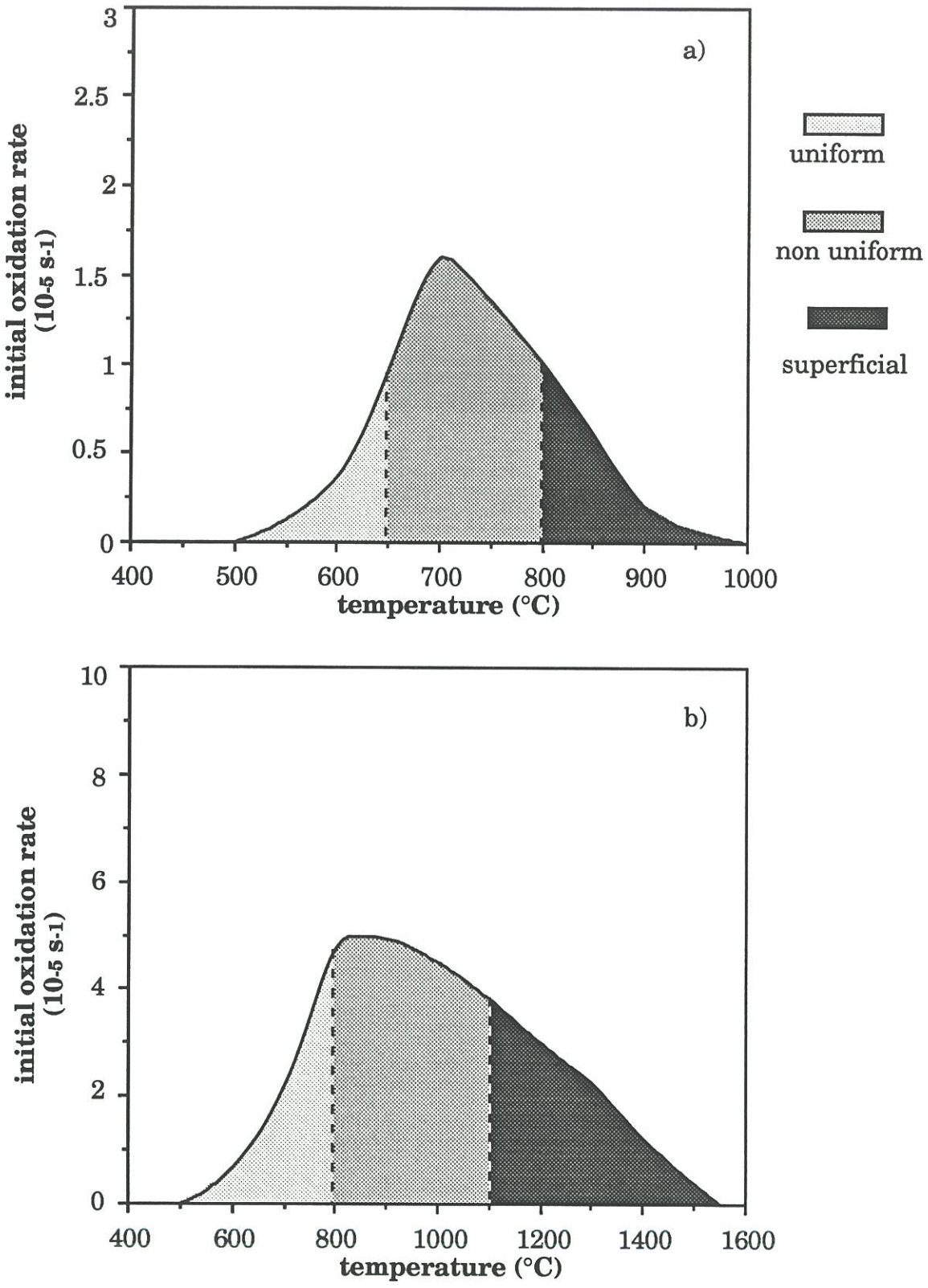

Fig.17: Temperature domains of the oxidation kinetics associated to a particular degradation mode of the 2D C/SiC composite materials a) as-processed (unstabilized) b) heat treated (stabilized).

showing that the oxidation of the composite continues up to 900°C. This discrepancy between SEM analyses and TGA data is very likely related to (i) some larger microcracks not taken into account which would be thermally close only at 900°C and/or (ii) presence of fragments into the microcracks preventing from a perfect thermal closure at 700°C. At 900°C, i.e. close to the closure temperature of the microcracks, the oxygen flux inside the microcracks is limited. Beside, as the reactivity of carbon phases towards oxygen is more elevated in the absence of any post-processing heat treatment [15], the degradation of the as-processed composite at 900°C remains superficial and similar to that observed for the stabilized composite at 1400°C (see fig.8b and fig.13a respectively).

At 1000°C, cracks are thermally closed and the oxidation kinetics have consequently set aside. When the crack closure temperature is exceeded, thermomechanical stresses are again generated inside the composite resulting in a new onset of matrix microcracking over 1200°C.

At 1400°C, as oxidation was found to proceed preferentially by the lateral sides of the samples, it is then possible to assign the oxidizing attacks detected on the TGA plots between 1200°C and 1500°C to a preferential microcracking at these **lateral sides**.

5 - CONCLUSIONS

(i) - The oxidation behavior of a 2D woven C/SiC composite partly protected with a SiC seal-coating and **thermally stabilized at 1600°C** in inert gas, has been investigated under both pure oxygen and dry air, on the basis of relative mass variations kinetics (assessed by thermogravimetric analyses) and microstructural changes induced by the oxidizing attacks. This behavior proved to be caused by the diffusion of oxygen through the seal-coating/matrix thermal microcracks (i.e.

generated by a CTE mismatch between the fibers and the matrix). The observed changes in the rate of oxidation with temperature and/or duration of ageing treatments, as well as the depth of penetration of the oxidative attacks were thus both related to: (i) the opening of the thermal microcracks which decreases with an increase in temperature and (ii) the reactivity towards oxygen of both SiC and the carbon constituents which, conversely, increases with an increase in temperature. The existence of several temperature domains corresponding to different oxidation kinetics regimes associated to different degradation modes were consequently evidenced as follows:

- At low temperatures (i.e. T<800°C), oxidation kinetics are controlled by the **carbon/oxygen reactions**. Since the reactivity of the carbon phases (i.e. fibers and interphase) is low as compared to the rate of diffusion of the gaseous species, the carbon reinforcement is **uniformaly** degraded all over the samples.

- At intermediate temperatures (i.e. 800°C<T<1100°C), **diffusion of the gaseous species** through the SiC seal-coating microcracks under a Fick and/or a Knudsen regimes becomes the oxidation rate controlling step. The degradation of the carbon phases is **non-uniform** and gradually decreases from the surface to the bulk of the samples.

- At high temperatures (i.e. T>1100°C), the high reactivity of the carbon phases coupled to the **limited flux of oxygen** diffusing through the narrow SiC seal-coating microcracks, rapidly sealed by silica, leads to a degradation strictly **localized at the surface** of the material.

(ii) - A decrease in oxygen content of the gaseous atmosphere (when switching from pure oxygen to simulated dry air) results in modifications of the global oxidation rate of both carbon and silicon carbide in different proportions, and also in a decrease of the oxygen diffusional flux in the

material. Consequently, with respect to the oxidation rate, the oxidation behavior is **proportionally improved**. Similarly, the degradation of the superficial tows taking place at high temperatures is also decreased.

(iii) - The oxidation behavior of the **as-processed (unstabilized) C/SiC** composite confirms the presence of three temperature domains related to the evolution of both the oxidation kinetics and the oxidizing attacks induced degradations. However, modifications of the global reactivity of the carbon phases and the morphology of the microcrack network, results in **changes in the temperature bordering**. At high temperatures (i.e. T>1100°C), the onset of a supplementary thermally induced damage inside the material leads to an important increase in the oxidation rate. Such an oxidation behavior would be idendical for the heat treated composite if the ageing treatments were performed at temperature overpassing the stabilizing temperature (i.e. 1600°C).
The quantitative description of the oxidation kinetics of stabilized C/SiC composites is addressed in the second part of this study [13].

ACKNOWLEDGEMENTS:

This work has been supported jointly by the French Ministry of Research and Space and by the Société Européenne de Propulsion through a grant given to F.L. The authors acknowledge the contribution of Mr. GARRI and Mr. DANG from CEMES-LOE-CNRS-Toulouse to the HT-SEM analyses. The authors also gratefully acknowledge helpful discussions with Dr L. FILIPUZZI.

REFERENCES

[1] B.BERTON, M.P. BACOS, D. DEMANGE and J. LAHAYE, "High temperature behaviour of the hot structural materials of Hermes space shuttle" (in French); pp 315-325 in *Composite Materials for High Temperature Applications.* Edited by R. Naslain, J. Lamalle and J.L. Zulian. AMAC, Paris, France, 1990.

[2] J.C. CAVALIER, A.LACOMBE and J.M. ROUGES, "Ceramic matrix composites, new high performance materials" (in French); pp 99-110 in *Developments in the science and technology of composite materials.* Edited by A. R. Bunsell, P. Lamicq and A. Massiah. Elsevier, London, 1989.

[3] - J. THEBAULT, "Fabrication process of a composite material with a refractory reinforcement and a ceramic matrix and structure elaborated with such process", French Patent 2 567 874 A1, July 20, 1984.

[4] F. LAMOUROUX, G. CAMUS and J. THEBAULT, "Oxidation resistance and strength after oxidation of a 2D woven carbon fiber silicon carbide matrix composite"; pp 499-504 in *Developments in the science and technology of composite materials.* Edited by A. R. Bunsell, J.F. Jamet and A. Massiah. Elsevier, London, 1992.

[5] B. DACIC and S. MARINKOVIC, "Kinetics of air oxidation of unidirectional carbon fibers/CVD carbon composites", *Carbon*, 25 [3] 409-415 (1987).

[6] N. FRETTY and M. BOUSSUGE, " Relationship between high-temperature development of fibre-matrix interfaces and the mechanical behaviour of SiC-SiC composites", *Composites Science and Technology*, 37, 177-189 (1990).

[7] K. PREWO and J. BATT, " The oxidative stability of carbon fibre reinforced glass-matrix composites", *J. Mater. Sci.*, 23, 523-527 (1988).

[8] R.T. BHATT, " Oxidation effects on mechanical properties of a SiC-fiber-reinforced reaction-bonded Si_3N_4 matrix composite", *J. Am. Ceram. Soc.*, 75 [2] 406-412 (1992).

[9] L. FILIPUZZI, G. CAMUS, J. THEBAULT and R.NASLAIN, "Effect of high temperature ageing treatments on the mechanical behaviour of unidirectional SiC/SiC fribrous composites"; pp 283-289 in *Structural Ceramics Processing, Microstructure and Properties*. Edited by J.J. Bentzen, J.B. Bilde-Sorensen, N. Christiansen, A. Horsewell, B. Ralph. RISØ National Laboratory, Roskilde, Denmark, (1990).

[10] J. R. STRIFE and J. E. SHEEHAN, "Ceramic coatings for carbon-carbon composites", *Ceram. Bull.*, 67 [2] 369-374 (1988).

[11] K. L. LUTHRA, "Oxidation of carbon/carbon composites–A: Theoretical analysis", *Carbon*, 26 [2] 217-224 (1988).

[12] D. W. McKEE, "Oxidation behavior and protection of carbon/carbon composites", *Carbon*, 25 [4] 551-557 (1987).

[13] F. LAMOUROUX, R. NASLAIN and J.M. JOUIN, "Kinetics and mechanisms of oxidation of 2D woven C/SiC composites–2: Theoretical approach", (submitted to *J. Am. Ceram. Soc.*).

[14] - R. NASLAIN, J.Y. ROSSIGNOL, P. HAGENMULLER, F. CHRISTIN, L. HERAUD and J.J. CHOURY, "Synthesis properties of new composite materials for high temperature application based on carbon fibers and C-SiC or C-TiC hybrid matrices", Rev. Chimie Minerale, 18, 544-564 (1981).

[15] F. LAMOUROUX, X. BOURRAT, J. SEVELY and R. NASLAIN, "Structure/oxidation behavior relations in the carboneous constituents of 2D - C (T300) / PyC / SiC (CVI) composites", submitted to *Carbon*.

[16] E.N. FULLER and G.C. GIDDINGS, " A new method for prediction of binary gas-phase diffusion coefficients", *Ind. Eng. Chem.* 58 [5] p18 (1966).

[17] M. KNUDSEN," Moleburlarströmung und innere reibungströmung der gase", *Ann. Physik*, 28, 75-130 (1909).

[18] G.F. HEWITT, "Gaseous mass transport within graphite", *Chemistry and Physics of Carbon*, 1, 73-120 (1965).

[19] L. FILIPUZZI, R. NASLAIN and C. JAUSSAUD, "Oxidation kinetics of SiC deposited from CH_3SiCl_3/H_2 under CVI-conditions", *J. of Mater. Sci.*, 27, (1992) 3330-3334.

[20] F. LAMOUROUX, unpublished work.

[21] Z. ZHENG, R. E. TRESSLER and K. E. SPEAR, "Oxidation of single-crystal silicon carbide", *J. Electrochem. Soc.*, 137 [9] 2812-16 (1990).

[22] E. FITZER and R. EBI, "Kinetics studies on the oxidation of silicon carbide"; pp 320-328 in *Silicon Carbide 1973*. Edited by R. C. Marshall, J. W. Faust and C. E. Ryan. Univ. of South Carolina Press, Columbia SC, 1973.

CHAPITRE 3

KINETICS AND MECHANISMS OF OXIDATION OF 2D WOVEN C/SIC COMPOSITES: 2 - THEORETICAL APPROACH

Les mécanismes gouvernant le comportement à l'oxydation des composites C/SiC ayant été identifiés, l'étape suivante a consisté à modéliser la cinétique d'oxydation de ces matériaux.

Les résultats expérimentaux et ceux issus de la modélisation étant en assez bon accord, il était alors tentant d'utiliser le modèle pour simuler l'influence de quelques paramètres importants tels que: (i) l'influence d'environnements oxydants à basses pressions, (ii) l'effet de l'épaisseur du revêtement externe en carbure de silicium et enfin (iii) l'influence du degré d'endommagement du seal-coat SiC en présence d'une sollicitation mécanique.

Les résultats de ces simulations restent qualitatifs. Ils permettent toutefois de donner des tendances et par là même de mieux prévoir l'évolution du comportement à l'oxydation des composites C/SiC.

Le présent article est présenté sous la forme d'un projet de publication soumis au **Journal of the American Ceramic Society**.

KINETICS AND MECHANISMS OF OXIDATION OF 2D WOVEN C/SIC COMPOSITES: 2 - THEORETICAL APPROACH

F. LAMOUROUX and **R. NASLAIN**
Laboratoire des Composites Thermostructuraux, UMR-47
(CNRS-SEP-UB1), 3 allée La Boëtie
33600, Pessac - France.

J.M. JOUIN
Société Européenne de Propulsion
BP 37, 33 165, Saint Médard en Jalles - France.

ABSTRACT

A model for the oxidation kinetics of SiC-coated 2D-C/SiC composites is developed on the basis of mechanisms derived from TGA data (temperature range 700°C - 1500°C; dry oxygen or air P=100kPa). Carbon/oxygen reaction, gas phase diffusion through microcracks present in the external SiC-coating and silica growth are the main phenomena taken into account in the modelling. A morphological characterization of the microcracks network based on a compression test and SEM observations, has been developed. The differential equations of the model are solved according to an iterative procedure. The mass variations of the composite during an oxidation test, as derived from the model, are in good agreement with the experimental data. The model is then used to predict the oxidation rate variations when: (i) the oxygen partial pressure is decreased, (ii) the thickness of the external SiC-coating is changed and (iii) the state of damage of the external SiC-coating is increased by mechanical loading.

Key words: Oxidation, kinetics, modelling, carbon, SiC, C/SiC composites, seal-coating.

1 - INTRODUCTION.

Carbon/carbon composites (C/C) are attractive materials for use in aerospace applications owing to their excellent high temperature mechanical properties in inert atmosphere or vacuum. However, the main drawback of C/C is their low oxidation resistance at temperatures as low as 500°C. Therefore, another generation of composite materials has been specifically developed for use in oxidizing environments. Ceramic matrix composites (CMC) such as C/SiC combine the good oxidation resistance of a silicon carbide matrix with the high temperature strength of carbon fibers [1]. C/SiC materials represent thus potential candidates for use in applications requiring lightness as well as strength and toughness at high temperatures in oxidizing environments.

The non-catastrophic failure observed in C/SiC composites during thermomecanical loading is generally related to the onset of damage [2]. This damage consists mainly in matrix microcracking and fiber/matrix partial debonding. Such flaws present in the composite are responsible for a decrease in its oxidation resistance, oxygen diffusing through the matrix cracks and oxidizing the carbon fibers and interphase. The degradation of the composite in oxidizing environments results in a severe decrease in mechanical properties [3].

In part 1 [4], the relations between the kinetics of oxidation of the C/SiC materials and environmental parameters (such as temperature, oxygen partial pressure...), on the one hand and the degree of SiC-coating damage (i.e. morphology of the microcrack network), on the other hand, were more specifically addressed. It has been shown that different modes

of morphological degradations of the carbon phases may occur during the oxidation treatments (i.e. homogeneous, non-homogeneous and superficial attacks). Temperature and oxygen partial pressure have been found to strongly influence oxidation kinetics and morphological change (at both the microscopic and macroscopic scales). The localization of the oxygen attack is an important factor in the understanding of the effect of oxidation on the mechanical properties of the materials [3]. The knowledge of the oxidation rates is also important since it determines (i) the lifetime of the materials and (ii) the rate of decrease of their mechanical properties.

In order to predict the consequences of oxidation treatments on C/SiC materials, it is necessary to understand the effect of the main parameters which control the oxidation kinetics. However, some of these parameters are strongly interrelated and it may be thus difficult to study their effect separately according to an experimental approach. It is the case for **morphological parameters** such as the length, width and/or depth of microcracks. The study of the effect of **oxygen partial pressure** on the oxidation kinetics is another example. For these reasons, this second part is aimed to develop a model which can be used to study the effect of environmental parameters (T, P) as well as morphological parameters (i.e. the thickness of the external coating and its state of damage under mechanical loading) on the oxidation kinetics of SiC-coated 2D-C/SiC composites with a pyrocarbon interphase.

Among the different studies which have been devoted to the modelling of the oxidation kinetics of carbon phases, the work recently performed by J.E. Medford on silicon carbide coated carbon/carbon composites [5] has to be mentioned. The CTE mismatch between the

carbon phases and the silicon carbide coating results in microcracking of the coating upon cooling from the processing temperature. This study has proposed a model taking into account the main steps which control the oxidation of SiC-coated C/C composites in large temperature and oxygen pressure ranges. At low temperatures (T<1000°C), the oxidation kinetics are controlled by carbon/oxygen reactions, the carbon oxidation rate being then proportional to the area of the coating microcracks. At high temperatures (T>1000°C), the diffusion mass transport through microcracks controls the oxidation kinetics. For these temperatures, time dependent change in the crack width induced by the growth of the silica layer is also taken into account. The main difficulty which is encountered in these oxidation models deals with the morphological characterization of the coating microcracks and thus the area of carbon phase exposed to oxygen. In some studies, the material texture allowed the authors an easy characterization of this carbon area. For example, Bernstein and Koger [6] studied a model of oxidation kinetics for a carbon-silicon multilayered structure, the area of carbon exposed to oxygen being defined by the thickness and the width of each carbon layer. In the same way, Filipuzzi [7] studied the oxidation behavior of an unidirectional-SiC/SiC composite with a carbon interphase. The area of carbon exposed to oxygen was also defined by the thickness of the carbon interphase and the fiber volume content of the composite. For coated C/C composites and/or carbon fiber/ceramic matrix composites, the oxygen diffusion area is determined by the microcrack network induced by the processing conditions and/or various thermomechanical loadings. Medford proposed an analytical calculation of this area based on CTE data [5]. Conversely, Luthra [8] suggested the use of a cracked area fraction being proportional to the ratio between the average width of microcracks and the average crack spacing.

In the present study, the SiC coating microcracks network, taken into account in the modelling, is accurately defined by means of morphological (scanning electron microscopy) and mechanical compression test analyses. The model is applied to the study of the oxidation kinetics of C/SiC HT (heat treated) under several environmental conditions, and is then extended to the prediction of the effects of various material parameters such as the thickness of the SiC coating and its state of damage under mechanical loading.

2 - MODELLING

2.1 - Materials.

The materials studied are heat treated C/SiC composites referred to as C/SiC HT, precisely described in part 1 [4]. They consist of a 2D plain weave architecture of ex-PAN carbon fibers* with a carbon interphase and a SiC matrix infiltrated according to the isothermal-isobaric chemical vapor infiltration (ICVI) process. In addition, once cut at their final dimensions, the specimens were coated with a CVD SiC layer (referred to as the seal-coating). Finally, they received an additional heat treatment (1600°C under inert gas) for structural stabilization. After these processing steps, an extended array of matrix and coating microcracks, of several microns in width, are present (related to the large difference between the thermal expansion coefficients of carbon and silicon carbide) [4].

---

* T300, high strength carbon fiber from Toray.

2.2 - Mechanisms.

The experimental study [4] has shown that several phenomena may control the oxidation kinetics of C/SiC HT composites :

- (i) diffusion of gaseous species through the SiC-coating microcracks, in a Fick and/or Knudsen regimes,
- (ii) diffusion of the gaseous species through the pores created by oxidation of the carbon fibrous substrate,
- (iii) diffusion of oxygen at the carbon surface towards active sites [10],
- (iv) surface reactions between oxygen and carbon according to the following equations:

$$C + O_2 \rightarrow CO_2 \qquad (1)$$

$$2C + O_2 \rightarrow 2CO \qquad (2)$$

- (v) growth of silica layer occurring during the oxidation of the SiC matrix and coating according to the following equations:

$$SiC + 2O_2 \rightarrow SiO_2 + CO_2 \qquad (3)$$

$$SiC + \frac{3}{2}O_2 \rightarrow SiO_2 + CO \qquad (4)$$

Previous studies performed on the oxidation of carbon fibers and pyrolytic carbon [10] have shown that carbon monoxide is the main gaseous oxidation product present beyond 700°C. Therefore, considering the temperature range used in the present study (700°C - 1500°C), only

equation (2) will be taken into account. For the oxidation of silicon carbide, reaction according to (4) is more likely to occur than reaction according to (3) at high temperatures whereas reaction according to (3) may also occur at intermediate temperatures. However, calculations performed with the model did not show any noticeable difference in the use of equations (3) and (4). As a matter of fact, the number of moles of oxygen consumed (per time unit) by silicon carbide is insignificant as compared to that consumed by the carbon substrate.

The various phenomena occurring during the oxidation of the composite are schematically shown in fig. 1. In a first step, oxygen diffuses through the seal-coating microcracks (i) and reacts with the silicon carbide on the crack wall surface (v). Once at the bottom of microcracks, oxygen then diffuses through the composite internal porosity to the carbon surfaces (ii), and on the carbon fiber or interphase surfaces towards active sites (iii). The reaction between carbon and oxygen (iv) produces gaseous carbon oxides which diffuse in the opposite direction towards the external environment (ii, i). The silica layers which are formed inside the microcracks result in changes of the microcrack width e (along the y axis). These variations occur faster at high temperatures, and lead to the sealing of the microcracks. Oxygen has then to diffuse through a condensed phase (SiO_2) in order to oxidize the carbon substrate, which results in a strong decrease of the C/SiC HT oxidation rate [11].

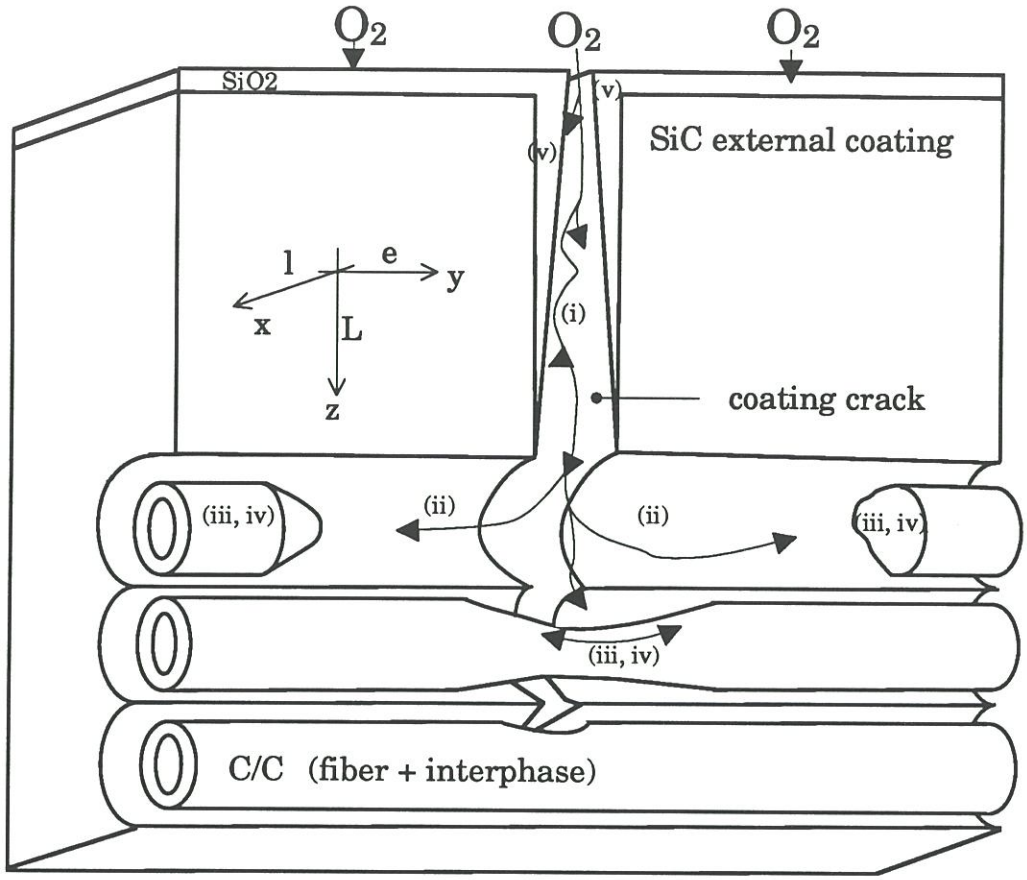

e: crack width; l: crack length; L: crack depth.

Fig.1: Phenomena occurring during the C/SiC HT composite oxidation.

2.3 - Model.

2.3.1 - Hypotheses.

The rate of the different diffusion and reaction phenomena vary with the experimental conditions. However, some of the oxidation steps always occur rapidly. This is the case for the diffusion of the gaseous species through the boundary layer surrounding the composite surface. In neglecting this step it is assumed that the boundary layer is thin and the oxygen concentration at the top of microcracks is equal to that in the external gas phase.

The mass variations observed during the oxidation of the C/SiC HT specimens come from the combined reaction of silicon carbide and carbon with oxygen. However, the rate of oxidation of carbon is much faster than that of silicon carbide. For this reason, the model only considers the mass variations of the carbon substrate.

When oxygen diffuses through the microcracks towards the carbon substrate, part of the reactant is consumed by the crack walls resulting in the growth of silica layers. The oxidation rate of the crack walls is controlled by the oxygen diffusion through the silica layer, perpendicular to the crack plane (y axis in fig.1). The silica growth rate is thus a function of the oxygen concentration at any given depth in the microcrack (z-axis).

Finally, it is assumed that the oxidation steady state is rapidly reached with respect to the pore geometry change [7].

2.3.2 - Theoretical analysis.

The first part of the modelling consists in determining the oxygen concentration profile in a crack (along the z-axis) and the oxygen flux at

the bottom of the seal-coating crack. In a second step, the carbon oxidation rate and the composite mass variations are calculated.

The use of the equation of mass conservation, for the diffusion of oxygen through the seal-coating crack assuming steady state, allows one to determine the change in oxygen concentration along the crack (z-axis).

On an elementary depth of crack dz, the difference between the mole number of oxygen diffusing at (z+dz) and at z is related to the oxygen consumed by the crack wall:

$$\frac{d(No(z).S(z))}{dz} + Ro = 0 \qquad (5)$$

with: - No(z) (in $mol.m^{-2}.s^{-1}$) the absolute molar flux of oxygen at the abscissa z,

- S(z) (in m^2), the crack cross-section at the abscissa z,

- Ro (in $mol.m^{-1}.s^{-1}$), the number of moles of oxygen consumed by the crack wall, per unit of time dt and unit of depth dz.

The absolute molar flux is given by the following equation [12]:

$$No = Jo + Xo.\sum_i Ni \qquad (6)$$

The first term Jo is the diffusion flux, given by the first Fick law:

$$Jo = -\overline{D} \cdot \frac{d(C(z))}{dz} \qquad (7)$$

where C(z) (in mol.m-3) is the concentration of oxygen at the abscissa z and $\overline{D}$ an effective diffusion coefficient of oxygen taking into account both

the Fick and Knudsen diffusion regimes according to the following equation:

$$\overline{D}^{-1} = D_F^{-1} + D_K^{-1} \qquad (8)$$

Expressions of D_F and D_K, respectively the Fick and Knudsen diffusion coefficients, are explicited in Appendix 1.

The second term of equation (6) is the Stefan flux, which represents the non-conservation of the total mole number after reaction between carbon and oxygen (2). Xo is the molar fraction of oxygen and Ni is the molar flux of each species present in the gaseous phase. The quantities of gaseous oxides related to equations (3) and (4) being smaller than those related to equations (1) and (2), the associate molar flux were therefore neglected. For equation (2), the Stefan flux is:

$$Xo.\sum_i Ni = \frac{C(z)}{C_T} \cdot [No + Nco] \qquad (9)$$

with: C_T (in $mol.m^{-3}$), the total concentration of gaseous species, No and Nco, the molar flux of oxygen and carbon monoxide respectively.

According to equation (2), Nco may be written as :

$$Nco = -2 \, . \, No \qquad (10)$$

Taking into account equations (7), (9) and (10), equation (6) can be rewritten as:

$$No = \frac{-\overline{D}}{1 + Xo} \cdot \frac{dC(z)}{dz} \qquad (11)$$

The surface, S(z) in equation (5), is given by the crack length l(x) (along the x axis) and crack width e(z,T) at an abscissa z and a given temperature T (the crack width varying owing to the thermal expansion of the matrix):

$$S(z) = e(z,T) \cdot l(x) \qquad (12)$$

The number of moles of oxygen, Ro in equation (5), consumed by the crack walls results from the oxidation of silicon carbide according to equations (3) and (4). The oxidation kinetics of CVI-processed SiC have been reported by Filipuzzi et al. [13]. The equation giving the thickness of the silica layer growing as the result of the oxidation of silicon carbide is :

$$\frac{d\delta(z)}{dt} = \frac{kp_o \cdot \left(\frac{C(z)}{C_o}\right)^p}{2 \cdot \delta(z)} \qquad (13)$$

With: - kpo (in $m^2.s^{-1}$), the parabolic kinetic constant for the oxygen concentration Co (in $mol.m^{-3}$),

- $\delta(z)$ (in m), the silica layer thickness at the abscissa z,
- p, the apparent reaction order with respect to oxygen.

The number of moles of oxygen consumed is proportional to the number of moles of silica formed according to equations (3) or (4):

$$\frac{dn_{O_2}}{dt} = \gamma \cdot \frac{dn_{SiO_2}}{dt} \qquad (14)$$

with $\gamma = \frac{3}{2}$ for equation (3) or $\gamma = 2$ for equation (4).

The number of moles of silica formed on the crack wall at the abscissa z, along an elementary depth of crack dz, can be written as:

$$\frac{dn_{SiO_2}}{dt} = \frac{\rho_{SiO_2} \cdot S_{SiO_2}(x,z)}{M_{SiO_2}} \cdot \frac{d\delta(z)}{dt} \qquad (15)$$

with: $S_{SiO_2}(x,z)$ (in m^2), the silica surface in the crack plane, that is to say the product (l(x) . dz),

ρ_{SiO_2} (in $g.m^{-3}$), the density of silica,

M_{SiO_2} (in $g.mol^{-1}$), the molar mass of silica.

Combining equations (13), (14) and (15) leads to:

$$\frac{dn_{O_2}}{dt} = \frac{\gamma}{2} \cdot \frac{\rho_{SiO_2} \cdot S_{SiO_2}(x,z)}{M_{SiO_2}} \cdot \frac{kp_o \cdot \left(\frac{C(z)}{C_o}\right)^p}{\delta(z)} \qquad (16)$$

The number of moles of oxygen consumed by the two walls of a crack per unit of depth (dz) and unit of time (dt) can be written as:

$$Ro = \gamma \cdot \frac{\rho_{SiO_2} \cdot l(x)}{M_{SiO_2}} \cdot \frac{kp_o \cdot \left(\frac{C(z)}{C_o}\right)^p}{\delta(z)} \qquad (17)$$

Finally, combining (11), (12) and (17) into (5) leads to:

$$\frac{d}{dz}\left[\frac{-\overline{D}(z) \cdot e(z,T)}{1 + Xo(z)} \cdot \frac{dC(z)}{dz}\right] + \frac{\gamma \cdot \rho_{SiO_2}}{M_{SiO_2}} \cdot \frac{kp_o \cdot \left(\frac{C(z)}{C_o}\right)^p}{\delta(z)} = 0 \qquad (18)$$

The equation (18) allows one to calculate the oxygen concentration profile C(z) along the crack z axis (see fig. 1).

2.3.3 - Boundary conditions.

The boundary conditions used to solve the differential equation (18) are as follows:

(i) - The oxygen concentration at the entrance of the cracks is the same as that in the external gaseous atmosphere Ce (in $mol.m^{-3}$):

$$\text{at } z = 0, \qquad C(z) = Ce.$$

The carbon massic oxidation rate in the composite, Ko (in $g.s^{-1}$), depends on the global carbon oxidation rate of fibers and interphase kro (in s^{-1}):

$$Ko = kr_o \,.\, m_c = kr_o \,.\, \nu_c \,.\, m_o \qquad (19)$$

with: m_c (in g), the total mass of carbon in the composite,

m_o (in g), the mass of the composite,

ν_c , the mass fraction of carbon in the composite ($\approx 40\%$).

(ii) - At steady state, the oxygen diffusing at the bottom of the cracks is consumed by the carbon fibers and interphases. Then, at z=L, (L (in m) being the depth of the cracks, that is to say the thickness of the SiC coating), the diffusion flux of oxygen from the microcracks equal the consumption flux of oxygen by the carbon phases (equation (2)) :

$$\text{at } z = L, \qquad \frac{-\overline{D}(z) \cdot S(z)}{(1 + Xo(z))} \cdot \frac{dC(z)}{dz} = \frac{Ko}{2 \cdot M_c} \cdot \left(\frac{C(z)}{Co}\right)^n \qquad (20)$$

with n, apparent reaction order with respect to oxygen of the carbon oxidation kinetic law,

Mc, the molar mass of carbon.

The differential equation (18) could not be solved analytically. Therefore, it has been solved using a numerical integration based on a classical Runge and Kutta algorithm [14] and an iterative procedure.
The oxygen flux thus determined along the crack z axis (fig. 1), is then used to calculate the composite mass loss as a function of the duration of the oxidation treatment.

2.3.4 - Composite mass variations.

The carbon mass oxidized during the time dt, is determined in writing that the calculated diffusion flux of oxygen at the bottom of the crack No(L) is proportional to the consumption flux of carbon Nc (equation (2)).

$$No(L) = \frac{-\overline{D}}{1 + Xo} \cdot \left(\frac{dC(z)}{dz}\right)_{z=L} \qquad (21)$$

and

$$Nc = \frac{-1}{S_c \cdot M_c} \cdot \frac{dm_c}{dt} \qquad (22)$$

where Sc is the carbon surface exposed to oxygen at the bottom of the crack, that is to say the cross-section of the cracks or the cross-section area through which oxygen diffuses at z=L.

The relation between oxygen and carbon flux, Nc = 2.No(L), leads to:

$$\frac{dm_c}{dt} = \frac{2 \cdot \overline{D} \cdot S_c \cdot Mc}{1 + Xo} \cdot \left(\frac{dC(z)}{dz}\right)_{z=L} \qquad (23)$$

If $\alpha(t)$ is the relative mass change of the composite as a function of time (in fact $\Delta m(t)/mo$), then:

$$\alpha(t) = \frac{2.Mc}{mo} \cdot \int_0^t \frac{\bar{D} \cdot S_c}{1 + Xo} \cdot \left(\frac{dC(z)}{dz}\right)_{z=L} dt \qquad (24)$$

The cross-section area through which oxygen diffuses is defined by the dimension parameters of the microcrack population. If a family of cracks is characterized by its dimensions e_i in width, along the y-axis, and l_i in length (the summation in length of all the cracks having the same width e_i), along the x-axis, then the total open surface may be estimated as follows:

$$S_c = \sum_{i=1}^{n} e_i(T) \, . \, l_i \qquad (25)$$

The partial mass loss assigned to a family of cracks (e_i, l_i) is calculated with equation (24), knowing that :

$$(S_c)_i = e_i(T) \, . \, l_i \qquad (26)$$

Then the **total mass loss of the composite** is the summation of the partial mass losses caused by each family of cracks:

$$\alpha_T(t) = \sum_{i=1}^{n} \alpha i(t) = \sum_{i=1}^{n} \frac{2.Mc}{mo} \cdot \int_0^t \frac{\bar{D}.ei(T).li}{1 + Xo} \cdot \left(\frac{dC(z)}{dz}\right)_{z=L} dt \qquad (27)$$

2.4 - Kinetic constants and morphological parameters.

Several parameters concerning the oxidation kinetics of the silicon carbide matrix and the carbon substrates are used in equations (13), (19) and (20). The values taken for these parameters are listed in table 1. Most of them are known from the literature. The global oxidation rate of the carbon substrate (fiber and interphase), kr_o, and the related apparent reaction order with respect to oxygen, n, were determined by thermogravimetric analyses. The use of the global oxidation rate, kr_o, allows one to take into account the different phenomena which control the oxidation kinetics of the carbon substrate into the composite (reaction between carbon and oxygen, diffusion of oxygen towards the active sites, diffusion of oxygen through the composite porosity...) [15].

Calculations of $\alpha(t)$ with equation (27), require a good characterization of the cracks population (depth L, width e_i and length l_i) of the damaged SiC-coating. The depth of microcracks is defined by the SiC-coating thickness. The width and length of the cracks must be assessed experimentally. Two experimental methods have been used to **classify cracks population**. The first consists in Scanning Electron Microscopy (SEM) detailed observations of the whole SiC-coating surface, and measurements of the microcracks width and spacing. The number of the microcracks being too high, another experimental method has been used to obtain more rapidly the crack morphological parameters. This method, developed in Appendix 2 is based on compression tests and limited SEM observation. The stress-strain curve of the C/SiC HT composites loading compression generally shows a transition strain range (see fig. 13 in appendix 2) related to the closure of the microcracks. This transition range corresponds to a population of cracks which is

	Fibers + interphase + HT		CVD processed SiC	
T°C	kro (s^{-1})	n	kp (m^2s^{-1}) [7]	p [16,17]
700	9.10^{-5}	0,75	$1,9.10^{-22}$	0,5
800	26.10^{-5}	1	$5,2.10^{-21}$	0,5
900	30.10^{-5}	1	$8,6.10^{-20}$	0,5
1000	33.10^{-5}	1	$8,2.10^{-19}$	0,5
1100	37.10^{-5}	1	$3,12.10^{-18}$	0,5
1200	41.10^{-5}	1	$6,73.10^{-18}$	0,5
1300	45.10^{-5}	1	$12,5.10^{-18}$	0,5
1400	50.10^{-5}	1	25.10^{-18}	0,45
1500	55.10^{-5}	1	52.10^{-18}	0,4

HT: heat-treatment (1600°C, inert gas)

Table 1: kinetics parameters of C/SiC HT components

characterized by a minimal and a maximal widths which are determined by SEM observation. The mathematical exploitation of the transition range leads to the determination of the width $e_i(T)$ and the length l_i of each family of cracks:

$$\nu_i = \frac{l_i . e_i}{S_c} \qquad (28)$$

with ν_i, the fraction of cross-section area of each family of cracks,

S_c, the total cracks cross-section area, also determined with the compression test.

The values of crack width are determined at room temperature. In fact, when the composite is used at high temperatures, the thermal expansion of SiC causes the partial closure of the cracks. The crack width change has been studied in the companion article [4], and obeys the following law :

$$e_i(T) = e_{io} . (1 - \frac{Te}{To}) \qquad (29)$$

with e_{io}, the room temperature width of the crack,

T_e, the temperature,

T_o, the temperature achieved during the HT treatment.

3 - RESULTS & DISCUSSION

3.1 - Effects of environmental parameters.

3.1.1 - Temperature effects.

Calculation of the oxygen profile along a crack.

The oxygen profiles along the SiC-coating microcracks, have been calculated from the present model in the temperature range 500°C - 1400°C for a pure oxygen external environment (P=100kPa). The different

curves corresponding to the beginning of an oxidation treatment (i.e. for t=500s) are displayed in figure 2.

At low temperatures, owing to the low reactivity of the silicon carbide towards oxygen, the morphology of the cracks remains unchanged and the oxygen profiles along the crack are **quasi-linear** and almost **time-independent**. At 500°C, the oxygen concentration along the crack is constant because of a rapid diffusion of the gas species and low oxidation rate of carbon. The slope of the profiles increases as the rate of the carbon consumption at the bottom of the crack increases (i.e. as T is raised). The increase of the silicon carbide reactivity with temperature induces a morphological change in the microcracks and causes the **non-linearity** of the oxygen profiles. However, at about 900°C, the cracks are still large and the oxygen profiles remain **time-independent**. Beyond 1200°C, SiC thermal expansion causes the partial closure of the cracks. Besides, the important growth of silica layers on the crack wall also induces an important morphological change of the cracks. Consequently, oxygen profiles are no longer linear and their **sharpness increases with the oxidation duration** (fig.3). Moreover, the oxygen concentration at the bottom of the microcracks decreases sharply because of the high reactivity of the carbon phases.

Kinetics of the composite mass loss.

Isothermal mass variations have been derived (equations (20) and (27)) from the oxygen profiles previously described. The results of the simulation are displayed in figure 4, along with the experimental mass variations, taken from the companion article [4]. The comparison of the experimental and numerical results leads to the conclusion that the model is in fair agreement with the actual composite oxidation kinetics.

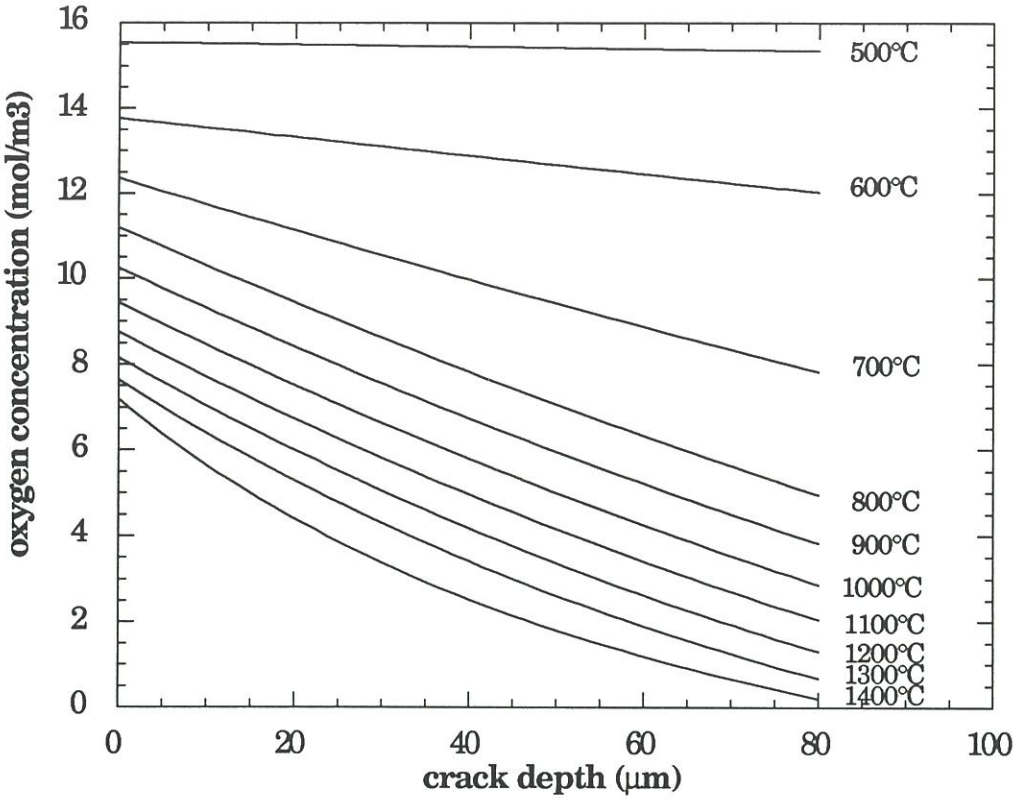

Fig.2 : simulation of the oxygen profile along a microcrack at the beginning of oxidation treatments for different temperatures.

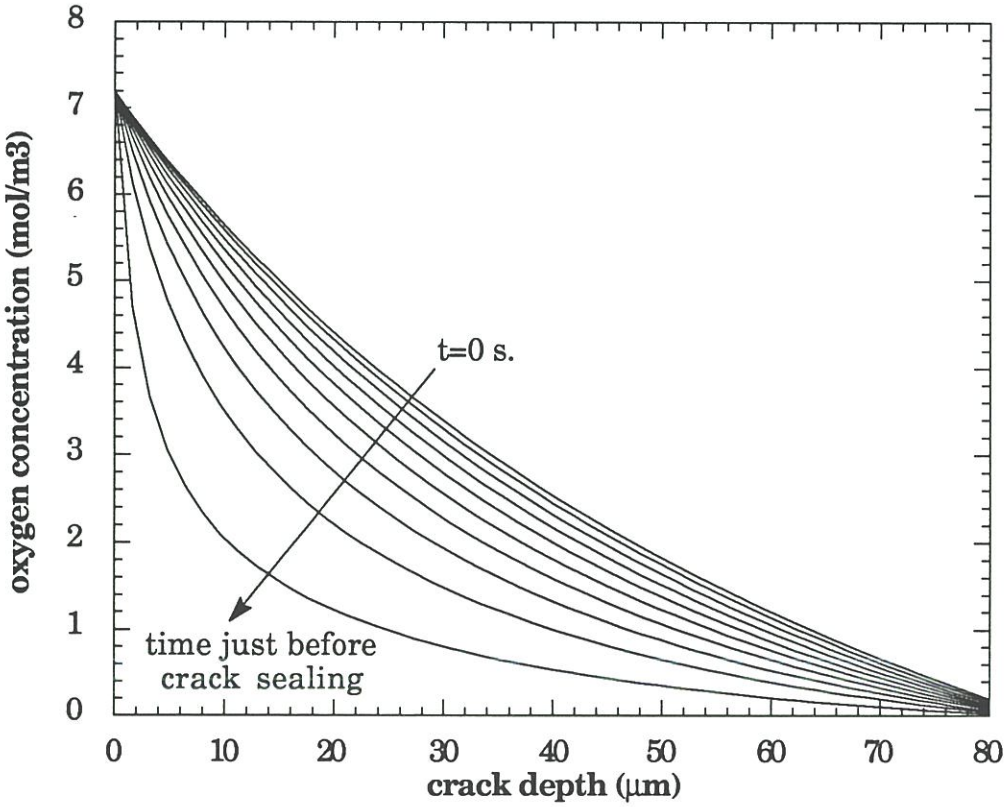

Fig.3: oxygen profile change as a function of the duration of the oxidation treatments calculated along a microcrack at 1400°C.

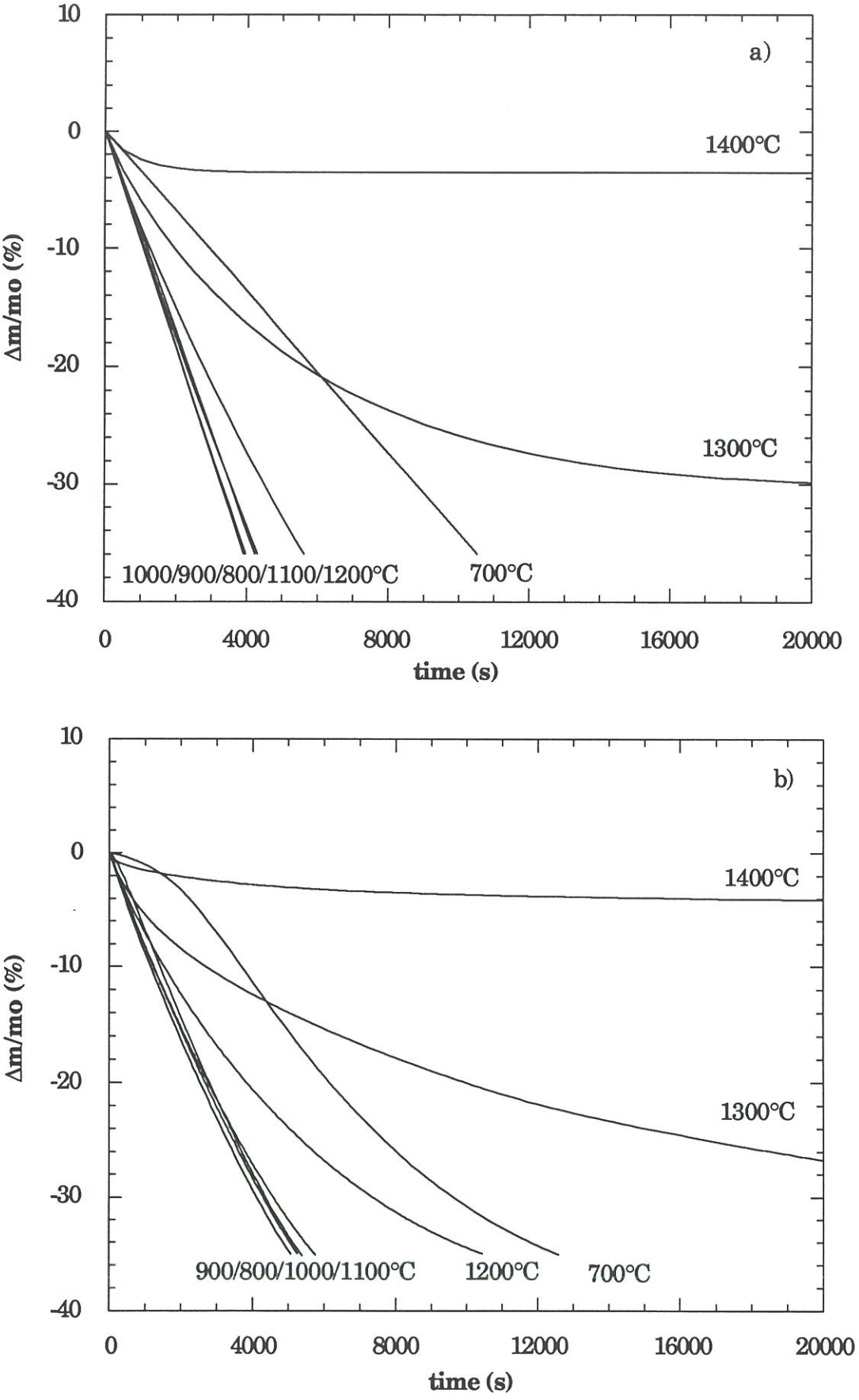

Fig.4: mass variations of C/SiC HT in oxygen (P=100kPa) as a function of time and temperature a) from modelling, b) from TGA [4].

The different hypotheses used to build up the model appear therefore to be validated.

The different steps taking place in the oxidation of the composite may be depicted as follows :

- at low temperatures (i.e. T<800°C), kinetics are controlled by **carbon/oxygen surface reaction** (iv). The oxidation rates are therefore function of the surface of the carbon substrate accessible to oxygen [10, 15]. Changes in the active surface area (ASA) of the carbon fibers and interphase during the oxidation treatment are responsible for the non-linear aspect of the experimental mass loss curve recorded for 700°C. Conversely, the model taking into account an average global reactivity of the carbon substrate (see table 1 and [15]), the calculated mass variations at 700°C as a function of duration are thus linear.

- at intermediate temperatures (i.e. 800°C<T<1100°C), the oxidation kinetics are controlled by **the diffusion of oxygen through the microcracks**. The mass loss rate is consequently independent of the change occurring in the ASA of the carbon substrate. The oxygen profiles being time-independent, the oxidation rate of the composite remains therefore constant which results in a linear mass loss curve. In the temperature range 800°C - 900°C, the oxidation rate increases in relation with the increase of the oxygen diffusion coefficient ($\bar{D}$ in (27) and appendix 1). Beyond 900°C, the thermal contraction of the microcracks is responsible for the decrease of both the cross-section of oxygen diffusion and the rate of the composite mass loss with temperature [4].

- at high temperatures, (i.e. T>1100°C), the **growth of silica on the cracks walls** causes a noticeable decrease of the oxidation rate with the temperature and the duration of the treatments. The increase of the sharpness of the oxygen profile (fig.3) causes the decrease vs time of the

oxygen flux in the microcracks and is responsible for the non-linear aspect of the mass loss curves. When the microcracks are entirely sealed by silica, the oxidation of the carbon substrate is no longer possible.

3.1.2 - Effect of oxygen partial pressure.

The study of the oxidation behavior of C/SiC HT materials in a low oxygen content atmosphere allows one to assess the mechanisms controlling the composite oxidation kinetics, because of their dependence with the oxygen partial pressure.

The C/SiC HT oxidation kinetics are controlled by several phenomena which are differently influenced by changes in oxygen partial pressure.

For carbon phases, the global oxidation rate k_r obeys the following relation:

$$k_r = k_{ro} \cdot \left(\frac{C}{Co}\right)^n \qquad (30)$$

- At low temperatures (i.e. T<800°C) the carbon/oxygen surface reaction controls the composite oxidation kinetics. Thus, the oxygen partial pressure dependence is the same for both the carbon and composite oxidation kinetics and n is lower than 1 (0,75 in table 1).

- At intermediate temperatures (i.e. 800°C<T<1100°C), gas phase diffusion is the step controlling both the carbon and composite oxidation kinetics. Thus, n = 1.

- At high temperatures (i.e. T>1100°C), the growth of the silica layer changes the gas phase diffusion process.

The variations of the silicon carbide oxidation rate k_p with the oxygen partial pressure is expressed by a similar equation:

$$k_p = k_{po} \cdot \left(\frac{C}{Co}\right)^p \qquad (31)$$

In this temperature range, p is close to 0.5 (see table 1). The silica growth is then less affected by a decrease in oxygen partial pressure than gas phase diffusion. Consequently, n is higher than 1.

These different variation modes of the composite oxidation rate with the oxygen partial pressure have been verified experimentally in the companion paper [4], by comparing the oxidation rates in pure oxygen and in dry air at 100kPa.
A simulation of the composite oxidation in dry air conditions shows the same variations (fig.5).

To emphasize the effect of **low oxygen pressures** on the oxidation kinetics of C/SiC HT composites, the model has been used to simulate their oxidation in air within the pressure range 100kPa to 1kPa. For these calculations, the active oxidation of silicon carbide has been neglected, the passive to active transition being below 100Pa at 1400°C [18].

Figures 6 shows the isothermal mass loss curves calculated at 100kPa, 10kPa and 1kPa for the temperature range 700°C - 1400°C. It may be noticed that:

- the critical temperature Tc, corresponding to the highest oxidation rate, decreases with the oxygen partial pressure is lowered. At 100kPa, the maximum oxidation rate is observed at Tc = 900°C, whereas at 1kPa

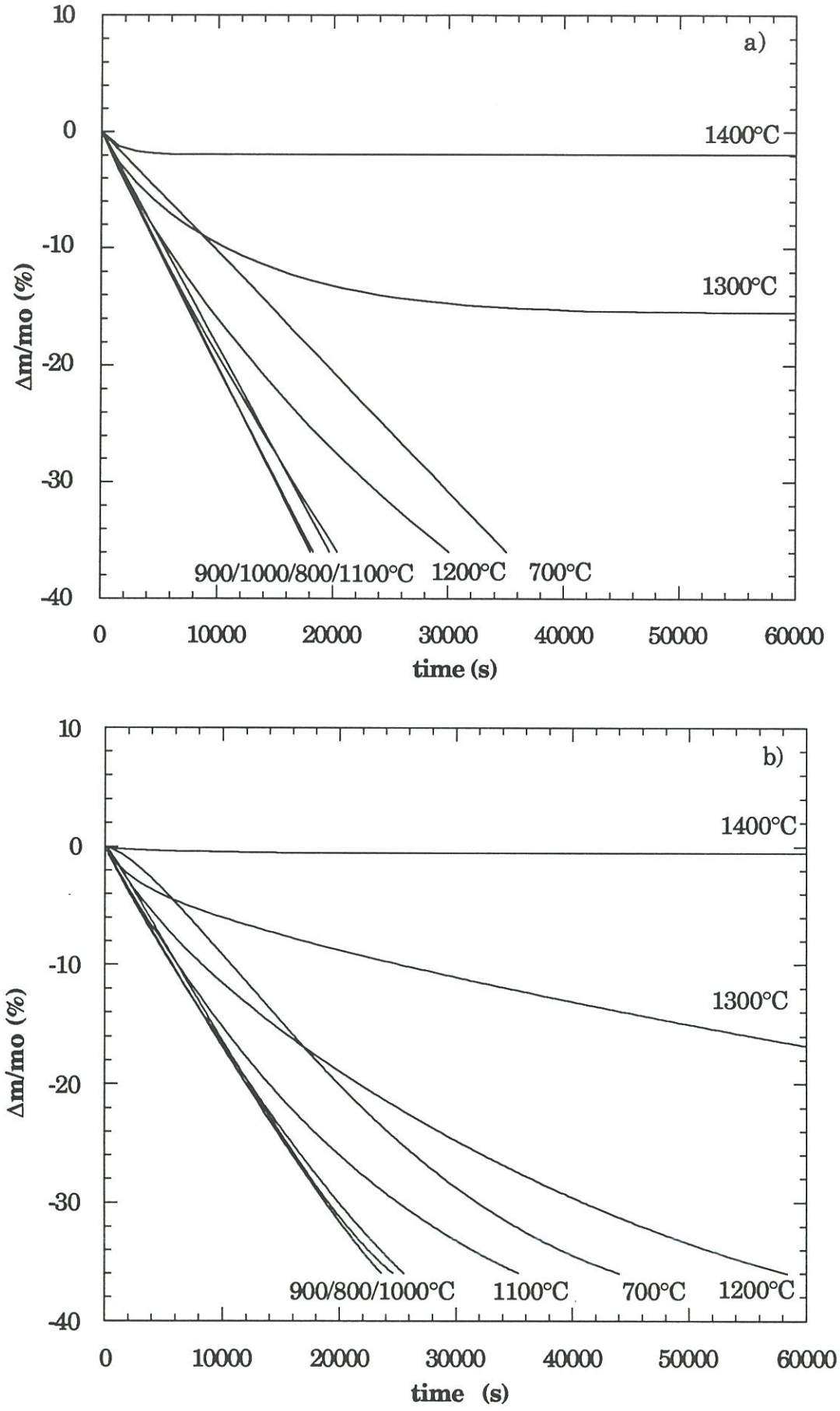

Fig.5: mass variations of C/SiC HT in air environments (P=100kPa) as a function of time and temperature a) from modelling, b) from TGA.

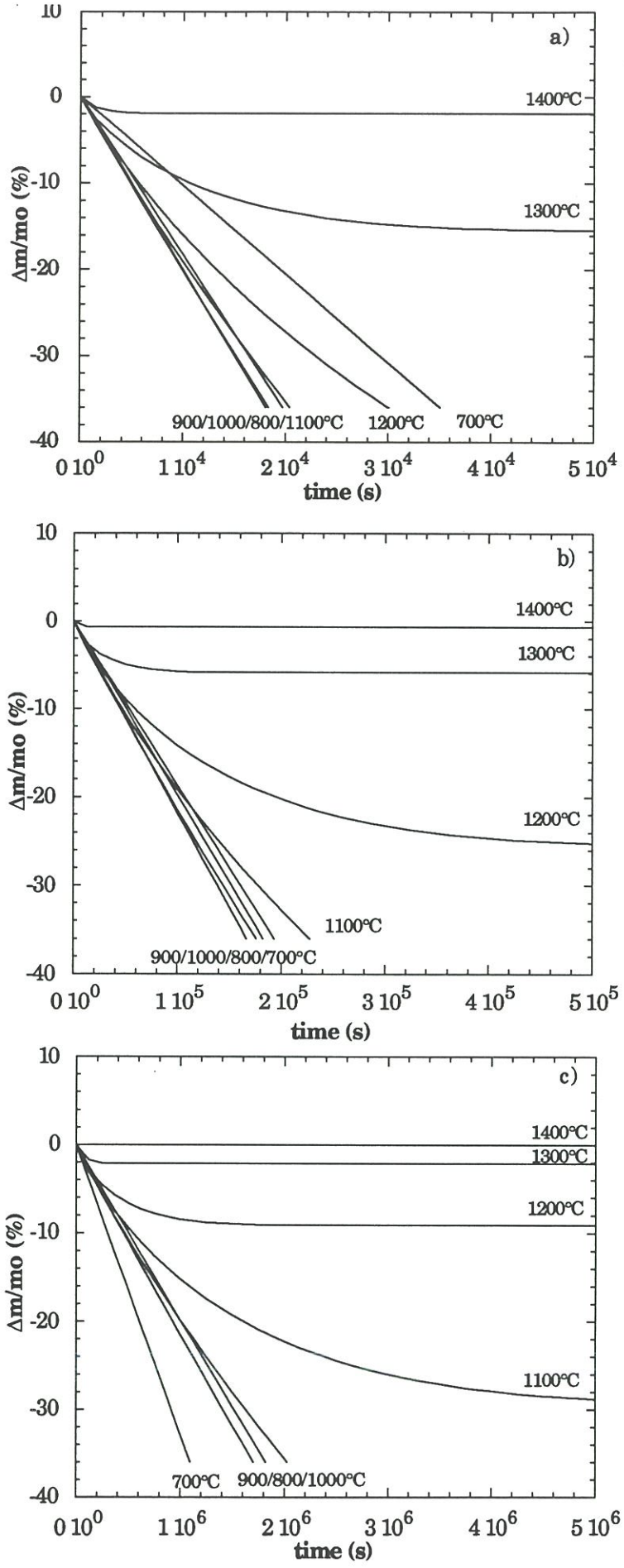

Fig.6: mass variations of C/SiC HT (calculated) corresponding to oxidation tests in air at a) P=100kPa; b) P=10kPa; c) P=1kPa.

Tc = 700°C. The fact that the apparent reaction order n is lower for the kinetics rate-controlled by the carbon/oxygen surface reaction (n<1) than for the kinetics rate-controlled by diffusion (n=1) is responsible for this phenomena.

- the sealing effects of the SiC coating may be observed at intermediate temperatures when the oxygen partial pressure decreases. At 100kPa, these effects are apparent at 1200°C/1300°C whereas at 1kPa they are observed as early as 1100°C. The carbon phases (40 wt. % in C/SiC HT) are completly oxidized for P=100kPa and T=1200°C (fig. 6a) whereas the cracks are sealed after $\approx 2.10^6$ seconds for the same temperature at P=1kPa with only 10% of mass loss (fig. 6c). In this case, it is the low dependence of the silica growth with the oxygen partial pressure which induces **a better protection of the C/SiC HT composite**.

The lifetime of C/SiC HT composites is dependent upon the time necessary to seal the coating microcracks and the mass loss occurring during this period. The decrease in the oxygen partial pressure (or external pressure) induces an increase in the crack sealing rate with respect to the carbon oxidation rate. Thereby, it results in an increase of the composite lifetime.

3.2 - Effect of variations in the seal-coat thickness.

The importance of the seal-coating microcracking pattern on the C/SiC HT oxidation kinetics clearly appears from the present model (see equation(27)). Thus, changing the seal-coating thickness should result in important variations of the oxidation rates of the material. However, because the seal-coating cracks result from a thermomechanical accomodation of the residual stresses appearing in the material during

processing, the width and interspacing of the microcracks, on the one hand, and the seal-coating thickness, on the other hand (i.e. the crack depth) should be interrelated. C/SiC HT composites of various seal-coating thicknesses (in the range 10μm to 300μm) were analysed according to the procedure developed in Appendix 2. Figure 7 shows the variations of the maximal crack width with the thickness of the SiC seal-coating. Coatings with thicknesses less than 100μm exhibit cracks whose width are dependent upon the SiC-coating thickness whereas for thicker coating, no global change is observed. Furthermore, it was observed from compression tests that the maximal strain of the transition range (fig.13) always lies at the same strain level. It may be concluded that the total crack cross-section area does not depend upon the coating thickness. These results suggest that the crack width is proportional to the crack reciprocal length which has been verified by SEM observations.

The morphological changes in the cracking pattern related to coatings of different thicknesses have several consequences on the C/SiC HT oxidation kinetics:

- when the thickness of the coating is small, the microcracks width is low and contributes to a decrease of the oxidation rate. Conversely, the oxygen gradients are high and lead to an increase of the oxidation rate.

- when the thickness of the coating is important, the microcracks are large and results in the opposite effects on the oxidation rate.

Consequently, when the coating thickness is varied, there is a competition between the crack width and depth effects. The model has been used to study the consequences of these morphological changes on the composite oxidation rate.

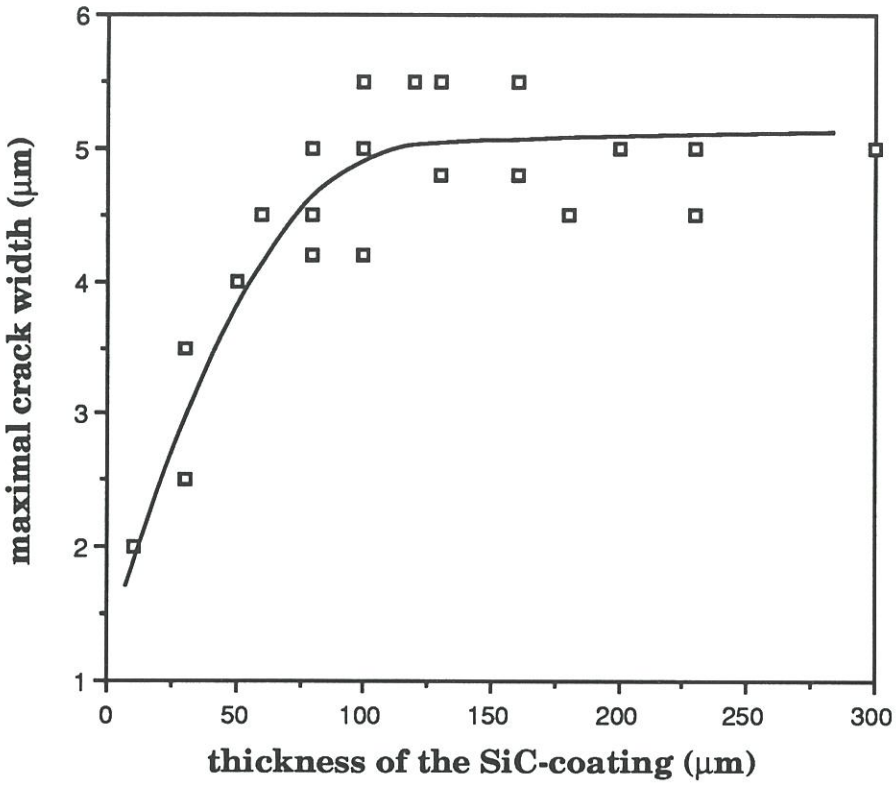

Fig.7: variations of the width of the cracks as a function of the thickness of the SiC-coating.

Isothermal mass loss has been calculated (air environment; P_{tot}=100kPa) for C/SiC HT composites having different SiC seal-coating thicknesses.

The initial oxidation rates of the composite calculated for each temperature (at t=500s) are plotted in figure 8.

At 700°C, an increase of the coating thickness does not cause any significant change in the oxidation rate. This phenomenon results from the nature of the step controlling the oxidation kinetics, i.e. the carbon/oxygen surface reaction. If one assumes that the oxidation rate of the composite is proportionnal to the fraction of carbon surface exposed to oxygen, the absence of any variation in the total crack cross-section area when the SiC seal-coating thickness is increased leads to the quasi-absence of oxidation rate variations.

For temperatures higher than 700°C, the oxidation kinetics are controlled by diffusion. Thus, both the crack depth and width have an influence on the oxidation rates and a decrease of the initial mass loss rate with an increase in the coating thickness may be observed. Moreover, the effect of the coating thickness on the decrease of the oxidation rate is more important when the temperature is high (fig.9). At intermediate temperatures (800°C - 1100°C), the growth of silica is limited and consequently does not change the oxidation rate as oxidation proceeds, due to the presence of large cracks. The oxidation rate remains thus constant vs time and the composite mass loss, occurring at a given time, decreases as the coating thickness increases (fig.10a)

At high temperatures (T>1100°C), the growth of silica on the crack walls causes a progressive closure of the cracks as previously established. The time necessary for the total crack closure is lower when the crack width is small, i.e. for thin coatings (see fig.7). Therefore, for coatings less than 100μm in thickness, the total mass loss occurring prior to the sealing of

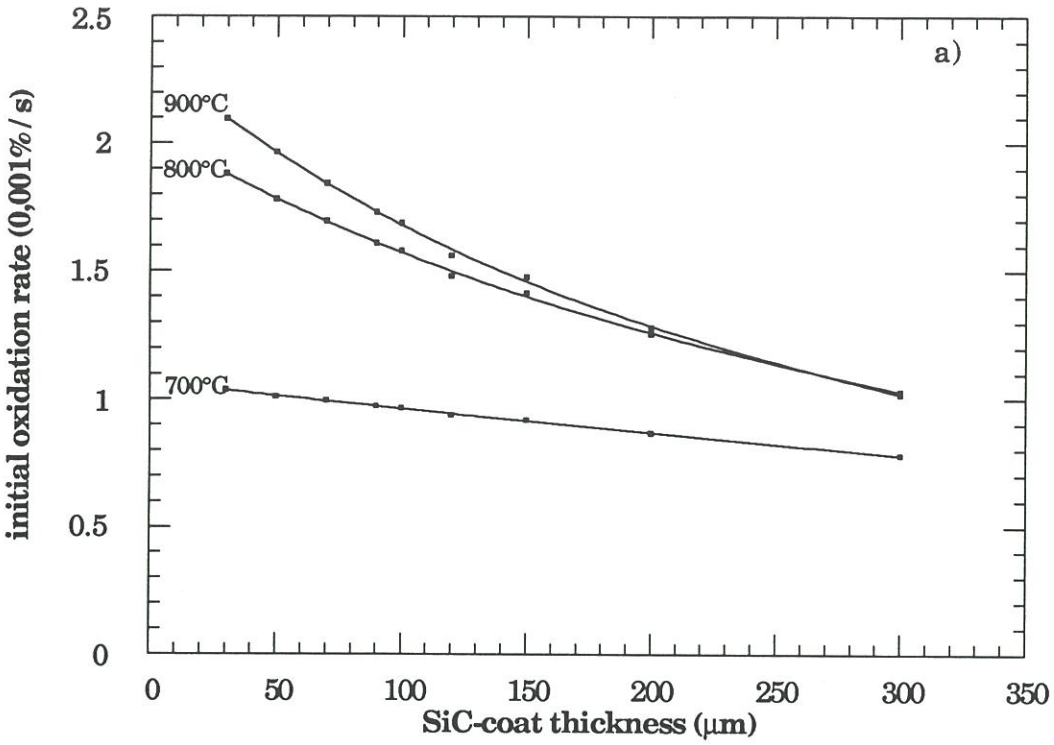

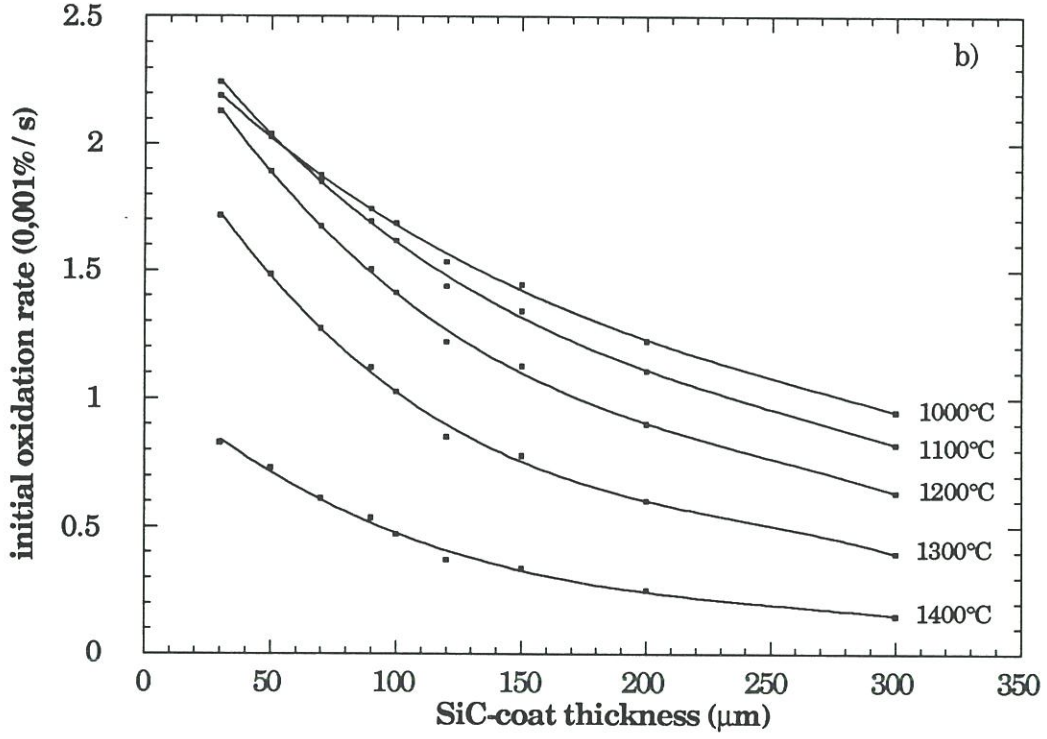

Fig. 8a,b: variations of the initial oxidation rate of C/SiC HT composites in air (P=100kPa) as a function of the thickness of the SiC-coating for several temperatures.

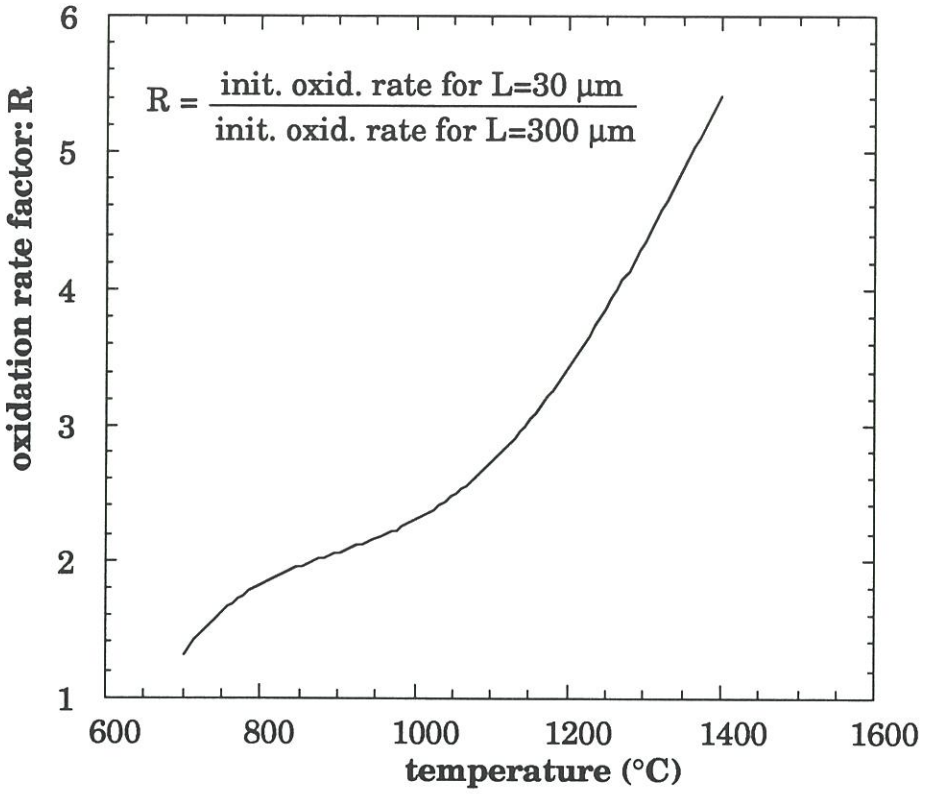

Fig.9: effect of a change in the SiC-coating thickness (30μm to 300μm) on the C/SiC HT initial oxidation rate in air (P=100kPa).

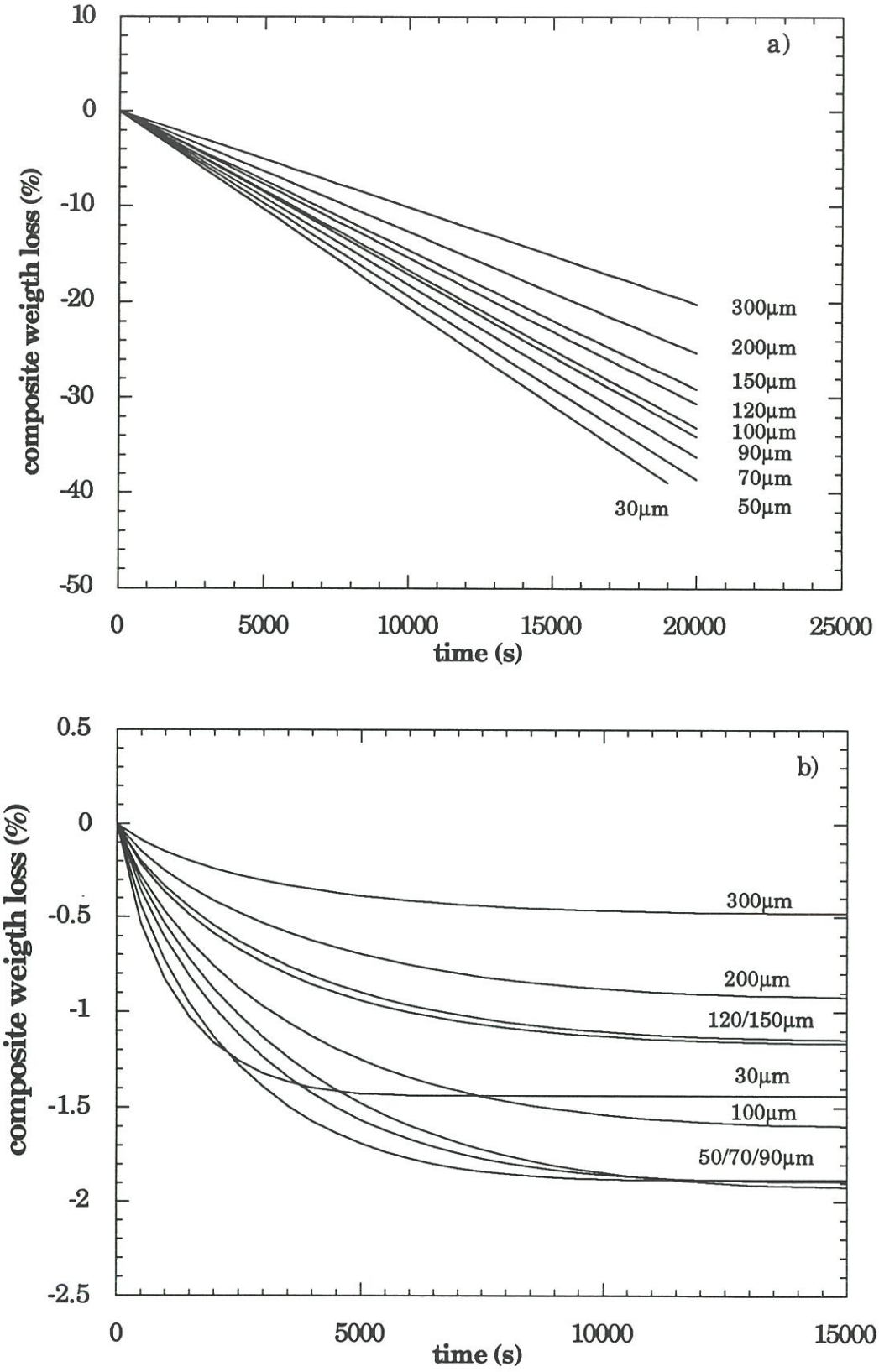

Fig.10: C/SiC HT oxidation weight loss calculated in air (P=100kPa) for several SiC-coat thicknesses a) at 900°C and b) at 1400°C.

the SiC-coating is much lower in spite of higher initial oxidation rate (fig.10b). However, for coating thicknesses higher than 100μm, the maximal crack width and then the time for sealing remain nearly constant (fig.7). Consequently, the initial oxidation rate and the total composite mass loss decrease when the coating thickness increases (fig.10b).

Considering the morphological changes of the coating crack pattern shown in figure 7, it may be concluded that the coating thickness is a parameter more important than the width of the cracks present in the coating, for the control of the oxidation kinetics of C/SiC HT composites. This result shows that **better protection** based on silicon carbide is obtained with **thick coatings** (despite the fact that they exhibit large cracks).

3.3 - Simulation of the effect of an applied loading in an oxidative environment.

C/SiC HT composites are materials intended to be used in high temperature structural applications. Thereby, the actual conditions of use of these materials correspond to oxidation under applied loading or strain. The study of the oxidation behavior under such conditions presents some difficulty because of interactions of mechanical damage with oxidation ageing. An applied tensile stress causes the SiC-coating multicracking and probably some increase of the intrinsic carbon and silicon carbide oxidation rates. Moreover, the oxidation of the composite is likely to change the stress distribution in the material. The experimental study (e.g. by TGA under load) of the oxidation kinetics under applied loading or strain is difficult. Thereby, the model has been used to predict

the main effects of applied loading on the oxidation rates, with the following assumptions (for purpose of simplification) :

- subcritical crack growth during the oxidation duration is not taken into account,

- the reactivity of the differents phases is not modified by the applied stress.

To simulate the composite oxidation rate under applied loading, it is necessary in a first step to characterize the coating damage occurring under such conditions.

The method used for the characterization of the state of damage of the SiC-coating under stress is developed in Appendix 3. It is based on a morphological analysis after loading combining (i) a characterization of the new microcrack network after mechanical loading, as described in Appendix 2, and (ii) a change of the microcrack width which takes into account the mechanical opening of the microcracks under loading.

In a second step, the kinetics of the composite mass loss are simulated (in air (P=100kPa) and under 0, 100, 200 MPa of applied loading) (fig.11). At low temperatures (T< 800°C), the carbon/oxygen surface reaction controls the oxidation kinetics. Therefore, the increase of the crack width under stress leads to an increase of the composite oxidation rate through the variations of S_c (see equations (24) and (25)).

At high temperatures (T>1200°C), the growth of silica on the walls of the cracks causes a decrease of the oxidation rate as oxidation proceeds. Under applied tensile load, the cracks are large and diffusion is less affected by the growth of silica. Thereby, the isothermal mass loss are linear within a large temperature range: [T<1000°C] for the unstressed

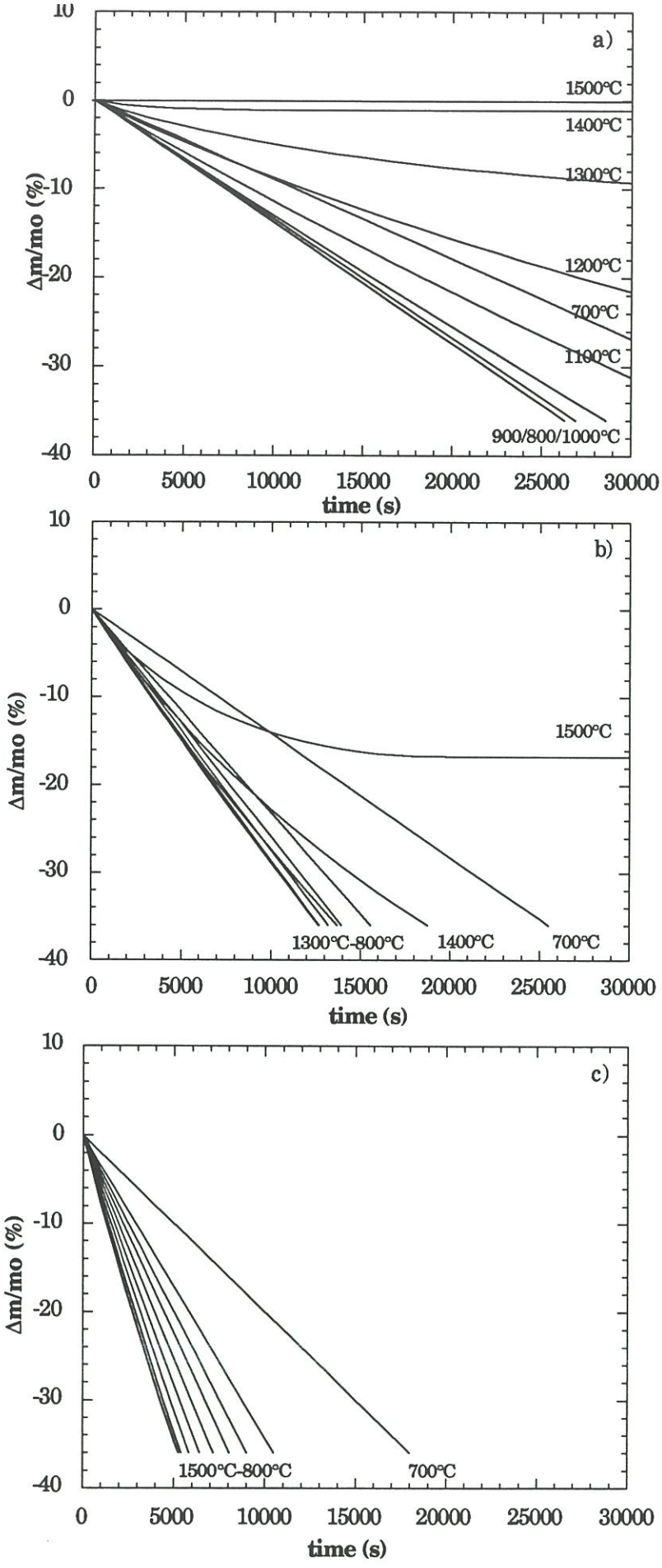

Fig.11: simulation of the C/SiC HT composite oxidation in air (P=100kPa) : without any loading (a), and under 100 MPa (b) and 200 MPa (c) tensile loading.

material versus [T<1200°C] and [T<1500°C] respectively for the 100MPa and 200MPa applied tensile loading.

The fact that the material is maintained under load causes a shift in the temperature range which depends on the nature of the rate determining step of the oxidation kinetics. As an example, the transition temperature corresponding to the **maximal oxidation rate is shifted to the high temperature** side when the load increases (fig.12). The oxidation resistance of the C/SiC HT decreases when that temperature is increased. The transition is the results of a competition between the variations of the diffusion surface S_c, which decreases when temperature increases, and those of the diffusion coefficient $\bar{D}$ which increases with temperature (see equation (23)). The mechanical loading causes the opening of the cracks and then the increase of the surface of diffusion S_c. For the unstressed material, the maximun oxidation rate is achieved at a temperature of 850°C, whereas it is achieved at 1300°C under 100MPa and beyond 1500°C under 200MPa loading.

These results show that, for a 200MPa loading, no decrease in the C/SiC HT oxidation rate with temperature (no transition zone) and with time (no sealing effect) is possible in the temperature range 0-1500°C in air (P=100kPa).

4 - CONCLUSIONS.

(i) - A model has been proposed which permits the calculations of the oxygen concentration profiles along the cracks of the SiC-coating in 2D-C/SiC composites with a pyrocarbon interphase, as well as the mass loss during an oxidation test.

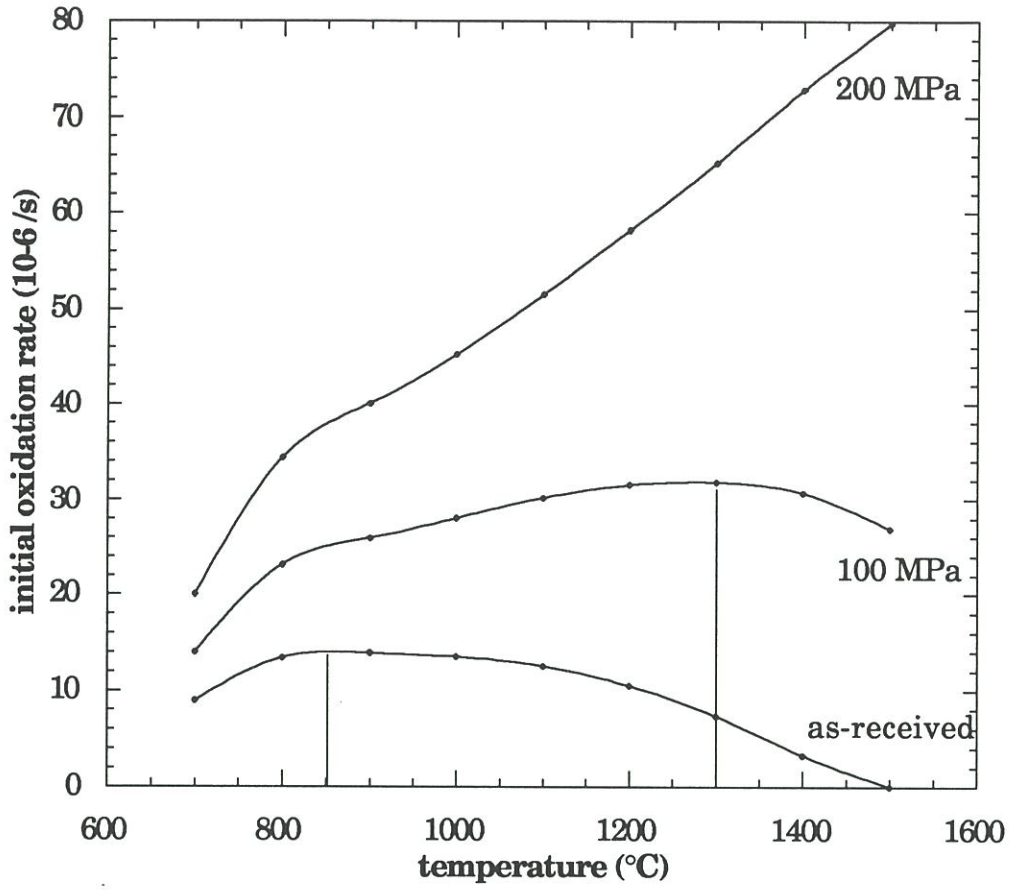

Fig.12: variations of the initial oxidation rate of the C/SiC HT composite with temperature in air (P=100kPa) and under several conditions of tensile loading (computer simulation).

(ii) - At low temperatures (i.e. < 800°C), the **carbon/oxygen surface reaction** controls the oxidation kinetics. At intermediate temperatures (i.e. 800°C - 1100°C), **gas phase diffusion through microcracks** is the rate limiting step. To have a better oxidation resistance, a C/SiC composite, must receive a thick SiC-coating in order to minimize the oxygen flux in the microcracks. Finally, at high temperatures (T>1100°C), **the growth of silica layer on crack wall changes the diffusion features**. Thus, it is important to have both a **thick seal-coating** and thin microcracks in order to rapidly seal the SiC-coating and to limit the mass loss before sealing.

(iii) - Under low pressure air environments, C/SiC composites exhibit a **better oxidation resistance** at high temperatures due to an increase in the amount of the silica produced by the oxidation of SiC with respect to carbon consumption.

(iv) - When the composite is mechanically loaded, the oxidation kinetic changes are essentially due to: (i) an **increase of the temperature of the transition zone** corresponding to the maximun composite oxidation rate and (ii) a **decrease of the sealing effect** due to the presence of largely opened microcracks. Consequently, for a 200MPa applied loading, the composite oxidation rate is time-independent and increase with temperature up to 1500°C.

ACKNOWLEDGEMENTS:

This work has been supported jointly by the French Ministry of Research and Space and the Société Européenne de Propulsion (SEP) through a grant given to F.L.

The authors like to thank L.FILIPUZZI, J. THEBAULT (from SEP), and G.CAMUS (from LCTS) for fruitful discussions.

APPENDIX 1

$\bar{D}$ is an effective diffusion coefficient of oxygen taking into account both the Fick and Knudsen diffusion regimes according to the following equation:

$$\bar{D}^{-1} = D_F^{-1} + D_K^{-1} \qquad (A1)$$

In this equation, the binary diffusion coefficient D_F, has been calculated according to the following equation [19]:

$$D_F = \frac{0{,}00143 \cdot T^{1,75}}{P \cdot M^{0,5} \cdot \left[(\Sigma_v)_o^{1/3} + (\Sigma_v)_{co}^{1/3}\right]^2} \qquad (A2)$$

with T, temperature (K),

P, total pressure (Pa),

M, molar mass of the gaseous species (g. mol^{-1}),

Σ_v, constant given by [19].

and

$$M = \frac{2}{M_o^{-1} + M_{co}^{-1}} \qquad (A3)$$

The Knudsen diffusion coefficient in the microcracks has been calculated according to the following equation [20]:

$$Dk = \frac{2}{3} \cdot \left(\frac{8.R.T}{\pi.M_o}\right)^{0,5} \cdot d \qquad (A4)$$

with d, width of the microcracks (in m).

APPENDIX 2

The compression curve for a C/SiC HT material presents several domains (fig.13a). The first part (looking the curve from the right to the left) corresponds to the compression of the damaged material, characterized by the initial stiffness (approximatively 70 GPa). Then, a transition range is observed. This transition range is due to the closure of the microcracks which results in a change of the composite stiffness. The third domain corresponds to the undamaged-like composite compression with a final stiffness of about 120 GPa before failure. Between -0,22% and -0,46% (in this case), a continuous stiffness change is observed (fig.13b) which is assigned to the progressive closure of the population of microcracks. At the beginning of the transition range, the thinnest cracks are closed whereas the end corresponds to the closure of the largest cracks. The first derivative of the strain-stress curve determines the variations of stiffness with strain during the compression test (fig.13b). The second derivative of the curve allows one to quantify the stiffness variations (fig.13c). Between -0,22% and -0,46%, it is possible to define a crack population limited by minimal and maximal witdhs which are determined by SEM. Each family of cracks, in the coating, is quantified with a parameter ν_i corresponding to the stiffness variation degree (fig.13c). ν_i is also the surface fraction of the cracks family according to its definition:

$$\nu_i = \frac{\left(\frac{d^2\sigma}{d\varepsilon^2}\right)_i}{\Sigma_i\left(\frac{d^2\sigma}{d\varepsilon^2}\right)_i} = \frac{n_i.e_i}{\Sigma_i(n_i.e_i)} = \frac{l_i.e_i}{S_c} \qquad (A5)$$

with ni, the number of cracks of same width e_i.

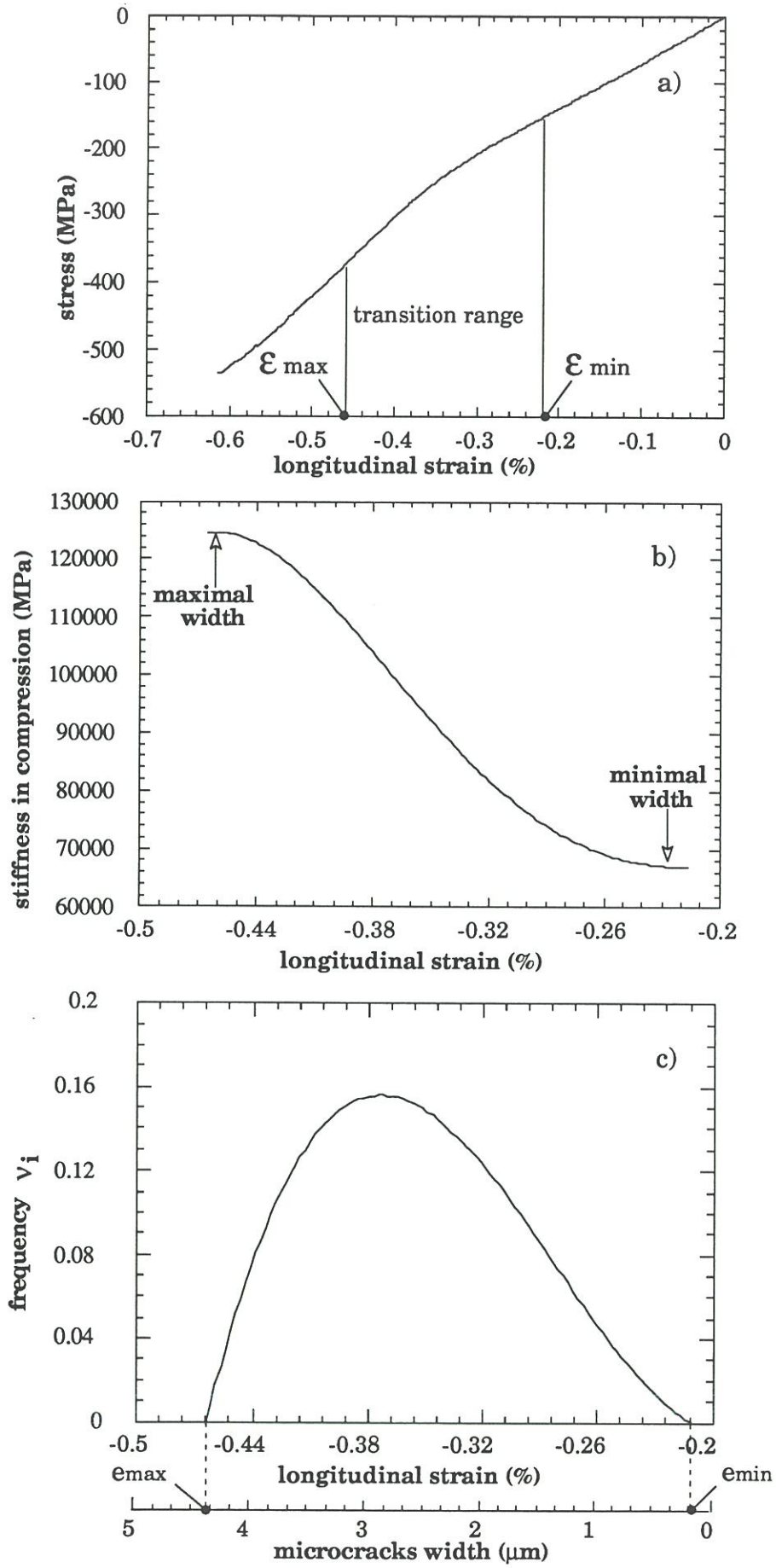

Fig.13:determination of the crack width distribution using the compression test stress-train curve.

The total area of the cracks in the external coating is determined by the use of the maximal strain recorded in the compression test:

$$Sc = F \cdot \varepsilon_{max} \qquad (A6)$$

with F: the surface of the cracked C/SiC HT face.

The morphological studies performed on C/SiC HT materials in ref.[4] show microcracks in seal coat SiC with a direction of propagation perpendicular to the fiber axis. For (2D C/SiC) with a plain weave carbon fabric reinforcement, the faces (1,2) which are parallel to the plies present a bidirectional pattern of cracks. The faces (1,3) and (2,3) perpendicular to the plies are cracked only in one direction. If the external dimensions of the composite are (a, b, c), with the faces (a,b) parallel to the plies, F can be calculated with the following equation:

$$F = 2 \cdot (2.a.b + a.c + b.c) \qquad (A7)$$

Then, in equation (27), the crack area for each family will be:

$$l_i \cdot e_i = S_c \cdot \nu_i = F \cdot \nu_i \cdot \varepsilon_{max} \qquad (A8)$$

The compression test associated with SEM observation allows one to characterize the crack population in the SiC coating more rapidly than a complete SEM observation of the coating surface. The results obtained by the two methods are in relatively good agreement, as shown in figure 14.

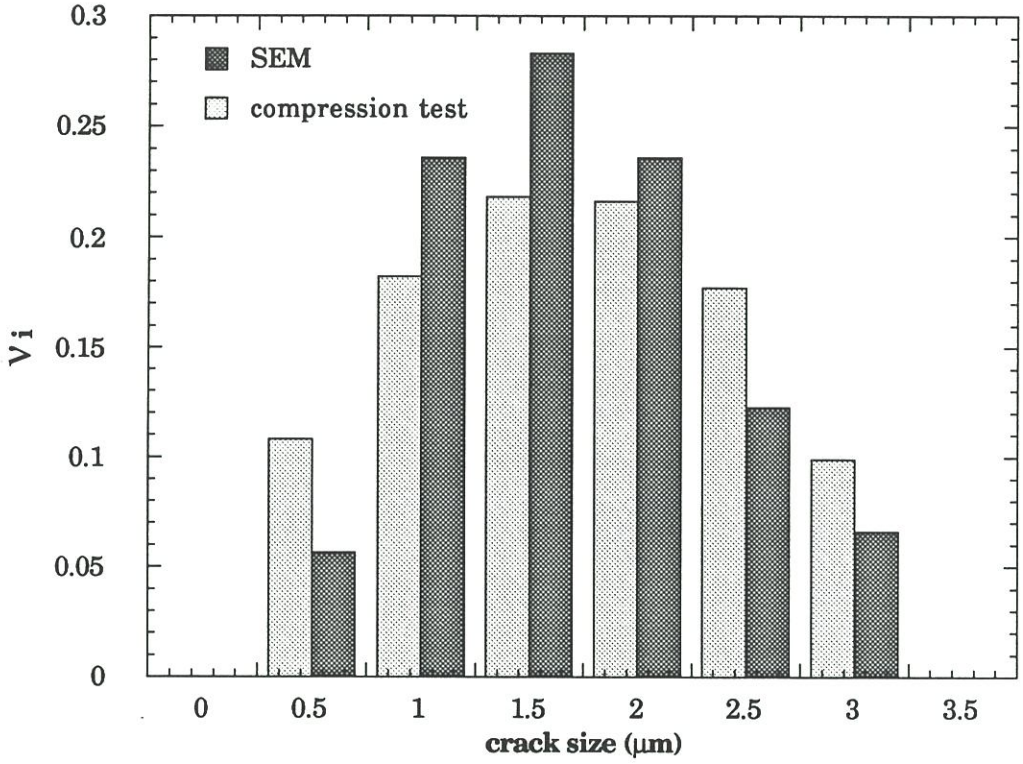

Fig.14: distribution of the crack width obtained with two different methods: SEM and compression test.

APPENDIX 3

When a 2D-C/SiC composite is submitted to tensile loading, three domains appear in the strain-stress curve [3] (fig.15):

- I: SiC matrix microcracking and fiber-matrix partial debonding,
- II: saturation of the matrix damage, transition zone,
- III: fibers carry the entire load.

During loading in the first domain, cracks are created in the SiC coating/matrix which are added to those resulting from processing.

During the unloading, a quasi-elastic strain-stress behavior is observed between Ej and Ei (fig.15) with a residual strain ε_i. The coating crack features after unloading are determined by the damaged state Ei, according to the experimental procedure described in appendix 2. Due to the quasi-elastic deformation of the composite between Ei and Ej, it is possible to define the coating crack distribution under stress, at Ej, by translation of the damaged state Ei by ε_{ij}. In fact, that translation is a mechanical crack opening, of Δe in width, which is calculated according to equation (A9). To simplify the calculations, it is assumed that the global deformation of the surface coating is entirely related to crack opening, which means a complete debonding between the composite and the SiC-coating :

$$\varepsilon_{ij} = \frac{\Delta L}{Lo} = \frac{\Delta e}{p} = \frac{\Delta e \cdot \sum_{i=1}^{n} l_i}{F} \qquad (A9)$$

with ΔL: the mechanical strain, measured by extensometry for a gage length Lo,

p: the average of crack spacing,

F and l_i are calculated from (34) and (35).

ε_{ij} is the difference (ε_j - ε_i) derived from the tensile test curve.

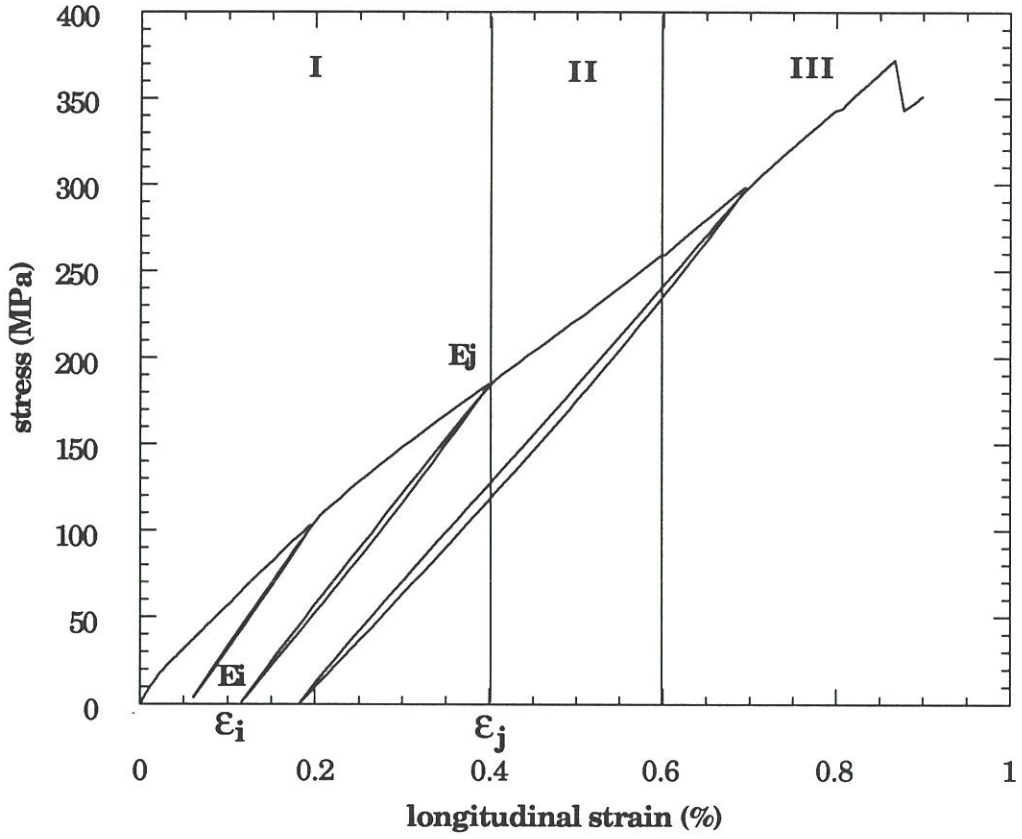

Fig.15: Tensile stress-strain curve for a C/SiC HT composite.

The equation (29), related to the thermal change of the crack width is thus modified as :

$$e(T) = e_o \cdot (1 - \frac{Te}{To}) + \Delta e \qquad \text{(A10)}$$

REFERENCES

[1] E. FITZER and R. GADOW, "Fiber-reinforced silicon carbide", *Am. Ceram. Soc. Bull*, 65 [2] 326-335 (1986).

[2] R. TALREJA, "A continuum mechanics characterization of damage in composite materials", Proc. R. Soc. Lond., A 399, 195-216 (1985).

[3] F. LAMOUROUX, G. CAMUS and J. THEBAULT, "Oxidation resistance and strength after oxidation of a 2D woven carbon fiber silicon carbide matrix composite"; pp 499-504 in *Developments in the science and technology of composite materials.* Edited by A. R. Bunsell, J.F. Jamet and A. Massiah. Elsevier, London, U.K., 1992.

[4] F. LAMOUROUX, G. CAMUS, R. NASLAIN and J. THEBAULT, "Kinetics and mechanisms of oxidation of 2D woven C/SiC composites: 1 - experimental approach", (submitted to *J. of Am. Ceram. Soc.*)

[5] J.E. MEDFORD, "Prediction of oxidation performance of reinforced carbon-carbon material for space shuttle leading edges", A.I.A.A. 10^{th} Thermophysics Conference, Denver, Colorado, May 1975.

[6] J. BERNSTEIN and T.C. KOGER, "Carbon film oxidation-undercut kinetics", *J. Electrochem. Soc.*, 135 [8], 2086-2090 (1988).

[7] L. FILIPUZZI, "Oxidation of both the SiC/SiC composites and their components", Thesis n°593, University of Bordeaux, (1991).

[8] K. L. LUTHRA,"Oxidation of carbon/carbon composites–A: Theoretical analysis", *Carbon*, 26 [2], 217-224 (1988).

[9] J.C. CAVALIER, A.LACOMBE and J.M. ROUGES, "Ceramic matrix composites, new high performance materials" (in French); pp 99-110 in *Developments in the science and technology of composite materials.* Edited by A. R. Bunsell, P. Lamicq and A. Massiah. Elsevier, London, U.K., 1989.

[10] F. LOUYS "Role of interface in the oxidation mechanism of carbon-carbon composites" (in French), Thesis, University of Mulhouse, (1987).

[11] L.FILIPUZZI and R. NASLAIN, " Oxidation mechanisms and kinetics of 1D-SiC/C/SiC composite materials: 2 - modelling", *J. Am. Ceram. Soc.* (in press).

[12] R.B. BIRD, W.E. STEWART and E.N. LIGHTFOOT, "Transport phenomena", Edited by J. WILEY, New York (1960).

[13] L. FILIPUZZI, R. NASLAIN and C. JAUSSAUD, "Oxidation kinetics of SiC deposited from CH_3SiCl_3/H_2 under CVI-conditions", *J. of Mater. Sci.*, 27, (1992) 3330-3334.

[14] M. CROUZEIX and A.L. MAGNOT, "Numerical analysis of differential equations" (in French); pp 95-119, Edited by Masson, Paris (1989).

[15] F. LAMOUROUX, X. BOURRAT, J. SEVELY and R. NASLAIN, "Structure/oxidation behavior relations in the carboneous constituents of 2D - C (T300) / PyC / SiC (CVI) composites", submitted to *Carbon*.

[16] Z. ZHENG, R.E. TRESSLER and K.E. SPEAR, "Oxidation of single-crystal silicon carbide", *J. Electrochem Soc.*, 137 [9] 2812-2816 (1990).

[17] E. FITZER and R. EBI, "Kinetics studies on the oxidation of silicon carbide"; pp 320-328 in *Silicon Carbide 1973*. Edited by R. C. Marshall, J. W. Faust and C. E. Ryan. Univ. of South Carolina Press, Columbia SC, 1973.

[18] T. NARUSHIMA, T. GOTO, Y. IGUCHI and T. HIRAI, "High-temperature active oxidation of chemically vapor-deposited silicon carbide in an Ar-O_2 atmosphere", *J. of Am. Ceram. Soc.*, 74 [10] (1991) 2583-2586.

[19] E.N. FULLER and G.C. GIDDINGS, " A new method for prediction of binary gas-phase diffusion coefficients", *Ind. Eng. Chem.*, 58 [5] 18 (1966).

[20] M. KNUDSEN," Moleburlarströmung und innere reibungströmung der gase", *Ann. Physik*, 28, 75-130 (1909).

CHAPITRE 4

OXIDATION EFFECTS ON THE MECHANICAL PROPERTIES OF 2D WOVEN C/SIC COMPOSITES.

Le comportement en environnement oxydant des composites C/SiC étant déterminé du point de vue de la cinétique d'oxydation et de l'évolution morphologique en cours d'oxydation, le chapitre suivant traite l'effet de l'oxydation sur les propriétés mécaniques.

Ce travail a pour objectif d'établir une relation entre l'évolution morphologique en cours d'oxydation et le comportement résiduel en traction du composite. La finalité de cette étude est de pouvoir corréler les mécanismes gouvernant la cinétique d'oxydation (lesquels ont été modélisés) avec l'évolution des propriétés mécaniques.

Suivant la même démarche que lors de l'étude phénoménologique de l'oxydation des composites C/SiC, le chapitre 4 étudie l'effet de la température et de la composition gazeuse de l'environnement oxydant sur le comportement résiduels en traction des composites 2D C/SiC.

Le chapitre est présenté sous la forme d'un projet de publication adressé au **Journal of the European Ceramic Society.**

OXIDATION EFFECTS ON THE MECHANICAL PROPERTIES OF 2D WOVEN C/SIC COMPOSITES.

F. LAMOUROUX and **G. CAMUS**
Laboratoire des Composites Thermostructuraux
UMR 47 (CNRS-SEP-UB1)
3, Allée de La Boëtie, 33600 Pessac, France.

J. THEBAULT
Société Européenne de Propulsion
BP 37, 33165 Saint Médard-en-Jalles, France

ABSTRACT

The oxidation effects on the tensile properties of a 2D woven C/SiC composite partly protected with a SiC seal-coating and heat-treated (stabilized) at 1600°C in an inert gas have been investigated. Results of the room temperature tensile tests performed on specimens variously aged in flowing oxygen between 700°C and 1400°C, have evidenced three main mechanisms of composite property degradation corresponding to three well differenced morphological changes. Oxidation at low temperatures (i.e. < 800°C) induces a dramatical decrease of the composite tensile properties in relation with a notch effect arrising from the partial degradation of the carbon fibers located near the matrix microcrack tips. The intermediate temperature ageing treatments (i.e. 800 < T < 1100°C) result in less important decrease of the tensile properties in connection with a composite rupture arrising through overloading of the superficial carbon plies (which were more intensively degraded than in the bulk of the samples). At high temperatures (i.e. > 1100°C), the ageing treatments lead to a limited decrease of the tensile properpies owing to a notch/overloading effect taking place only at high stress levels from the superficial degradation of the composite reinforcement. For ageing treaments performed in a lower oxygen content environment (i.e. dry air), a decrease of both overloading and notch effects is observed. Tensile properties are consequently better preserved. The study of the tensile properties degradation of the as-processed (unstabilized) materials confirms these relations established between the morphological oxidation mode and the mechanisms responsible for the loss of tensile strength.

Key words: Mechanical properties, oxidation, C/SiC composites, carbon fibers, silicon carbide.

1 - INTRODUCTION

The increasing use of carbon-base materials is related to major attractive properties such as lightness, elevated mechanical strength and thermal stability. Carbon fibers are thus extensively used in aerospace industries which require structural materials intended for high temperatures and aggressive environments. Composite materials made of carbon fibers and silicon carbide matrix are excellent potential candidates for such applications, since they combine both the elevated specific properties of the carbon fibers with the high oxidation resistance of the SiC matrix. However, the various thermomechanical cycles which may be encountered by these materials in service and/or when processed result in the onset of matrix microcracking [1,2]. If this matrix multiple-microcracking phenomena is an important advantage from a mechanical point of view, since it primarily contributes to the **non-linear/non catastrophic tensile behavior** and high impact resistance of this class of material (in conjunction with fiber/matrix debonding), such is not the case when the oxidation resistance is considered. As a matter of fact, each of these microcracks represents an easy path for the diffusion of oxygen towards the carbon reinforcement, which significantly reduces the protective role played by the SiC matrix. Consequently, for high temperature applications, an additional external protection (i.e. a seal coating) should be used. In most cases, these external protections are based on oxide coatings, whose nature depends on the service temperature [3,4]. However, none of the existing protective systems have proved to be entierely reliable for long time exposures up to 1600°C (and P $\leq$ 100 kPa). Consequently, it is of great importance to get a good knowledge of the changes which may be induced by oxidation in the microstructure

and mechanical properties of the material when the external protections are no longer efficient.

Previous works devoted to other Ceramic Matrix Composites (CMCs) have established some correlations between the loss of strength and the microstructural changes induced by oxidation [5-7]. For carbon fiber reinforced glass matrix composites, the loss of strength was essentially related to the degradation of the reinforcement. Conversely, for SiC/SiC or SiC/Glass composites [6,7], changes in the mechanical behavior proved to be related to modifications of the fiber/matrix load transfer conditions induced by a degradation of the carbon interphase (whose function is to optimize these load-transfer conditions [8]).

The aim of the present investigation was to study experimentally the **oxidation effects on the tensile behavior** of 2D woven C/SiC composites having no other complementary protections than a simple SiC seal-coating.

This work follows a previous study aimed at establishing the kinetics and mechanisms of oxidation of the same 2D C/SiC composites materials [9]. Results of this study showed that the oxidation was related to the diffusion of oxygen through the seal coating/matrix thermal microcracks generated upon cooling from the processing temperature (by a fiber/matrix CTE mismatch (see fig.1)). The observed changes in the rate of oxidation with temperature and/or duration of ageing treatments, as well as the depth of penetration of the oxidizing attacks were thus both related to: (i) the opening of the thermal microcracks which decreases with an increase in temperature and (ii) the reactivity towards oxygen of both SiC and the carbon constituents which, conversely, increases with an

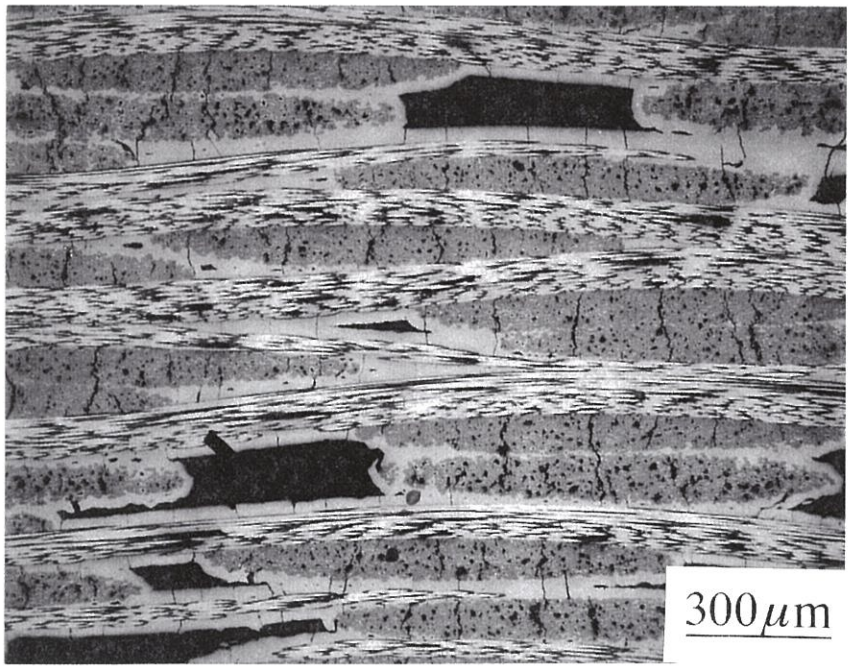

Fig.1: Optical micrograph of a polished section of a 2D C/SiC composite stabilized at 1600°C under inert gas.

increase in temperature. The existence of several temperature domains corresponding to different oxidation kinetics regimes/degradaion modes was evidenced as follows :

- At low temperatures, oxidation kinetics are controlled by carbon/oxygen reaction. Since the reactivity of the carbon phases (i.e. fiber and interphase) is low as compared to the rate of diffusion of the gaseous species, the carbon reinforcement was uniformely degraded all over the samples.

- At intermediate temperatures, diffusion of the gaseous species through the SiC seal-coating microcracks becomes the oxidation rate controlling step. The degradation of the carbon phase was non-uniform, decreasing gradually from the surface to the bulk of the samples. Besides, inside each fiber tow, the surface was also systematically more degraded.

- At high temperatures, the high reactivity of the carbon phase coupled to the limited oxygen flux diffusing through the narrower SiC seal-coating microcracks rapidly sealed by silica led to a degradation strictly localized at the surface of the material (i.e. at the seal-coating microcrack tips).

The relationships which were evidenced between oxidation kinetics, ageing temperature and degradation modes are schematically represented in figure 2, for two different states of the 2D C/SiC material. As a matter of fact, the "reference" composite received a post-processing heat treatment performed at 1600°C under an argon inert atmosphere (referred to as a stabilizing heat treatment). This treatment is aimed at avoiding possible interacting effects resulting from changes in the microstructure and/or the composition of the constituents when aged at temperatures exceeding the processing temperature. It results in (i) changes in the physico-chemical characteristics of the composite

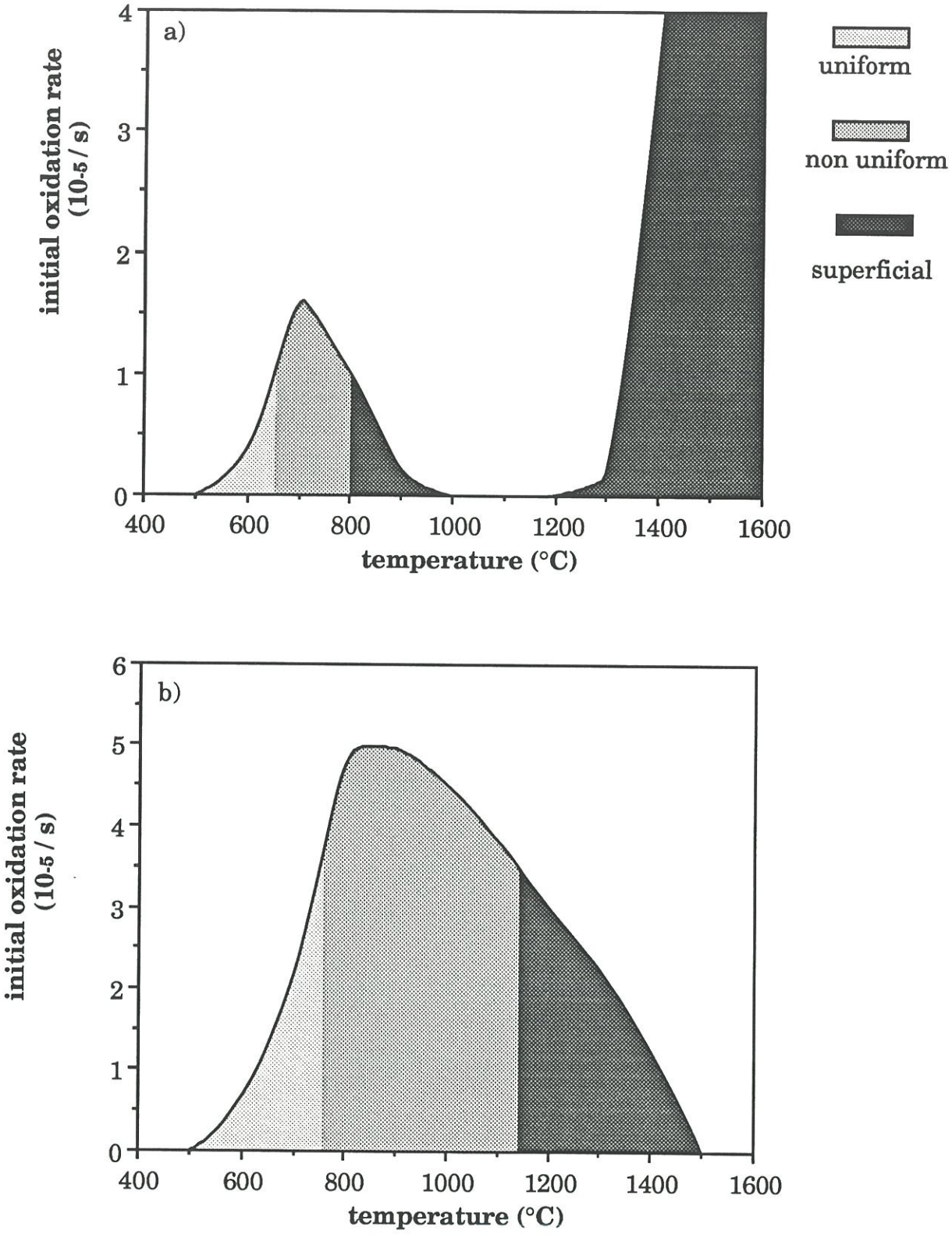

Fig.2: Dependence of the initial oxidation rate, in association with the different oxidation modes , to the ageing temperature (under flowing oxygen) for 2D C/SiC composites a) as-processed b) stabilized at 1600°C under inert gas.

constituents (especially the ex-PAN fiber [10]) and (ii) the onset of an increase in the thermomechanical damage since the processing temperature (i.e. 1000°C) was largely exceeded. Consequently, in the absence of this stabilizing treatment, lower average crack opening, crack closing temperature and a higher reactivity towards oxygen of the carbon phases led to systematically narrower temperature domains. Besides, over 1200°C, thermomechanical damage induced by the CTE mismatch resulted in an important increase of the oxidation kinetics.

The repartition of the oxidized zones inside the composite is a preponderant factor governing the mechanical resistance of the material in an oxidizing environment. These different degradation modes being observed for both as-processed and stabilized 2D C/SiC composites, it is therefore of great interest to determine their consequence from a mechanical point of view. Besides, since these materials might be used in environments with different oxygen contents, it is also interesting to determine changes in the tensile behavior when the composition of the gaseous phase is modified.

2 - EXPERIMENTAL PROCEDURE

The composite material used in the present investigation has been processed(*) according to the so-called isothermal-isobaric CVI process from a fibrous preform consisting of a 0° stack of ex-PAN carbon fiber (**) two dimensional (plain-weave) fabrics. In a first step, the fibers were in-situ coated with a pyrocarbon layer (the interphase) formed from cracking of CH_4 and whose mean thickness was in the range 0.5 to 1 μm. In a

(*) by SEP (Société Européenne de Propulsion)
(**) High strength carbon fiber HR T300 from Toray

second step, the carbon coated preform was infiltrated by the SiC matrix formed in-situ from a CH_3SiCl_3/H_2 mixture, at about 1000°C, according to the ICVI process which has been described elsewhere [11,12]. These processing steps resulted in a material having a density close to 2 $g.cm^{-3}$, a fiber content of approximately 40 vol.% and a residual porosity in the range 10-15%. Once cut at their final dimensions and prior to testing, tensile samples were coated with a CVD-processed SiC layer of the order of 100 μm in mean thickness. Finally, the samples were thermally stabilized by a heat treatment performed at 1600°C under an inert atmosphere. This material thus processed and heat treated (stabilized) constituted the reference material used in the major part of the study. Nevertheless, for purpose of comparison and in order to understand the possible effects of the stabilizing heat treatment on the oxidation behavior of the material, some samples were also tested in the as-processed (unstabilized) state. The average room-temperature physical and mechanical properties of the 2D C/SiC composites are listed in table 1.

Tensile tests were performed at room temperature, at a constant strain rate of 0.1 %. min^{-1} (monitored by a clip-on extensometer), using flat dog bone shape specimens of 200 mm total length and 40 x 8 x 3 mm^3 gage section. Specimens were tested in the as-processed states (stabilized and unstabilized) and/or after various oxidizing treatments performed between 700°C and 1400°C. Two different oxidizing atmospheres, namely dry oxygen and a nitrogen/oxygen 80/20 mixture (equivalent to dry air) were successively used, at a constant total pressure of 100 kPa. In order to minimize a degradation of the sample ends induced by the ageing treatments as well as to concentrate the oxidizing attacks in the gage section, these ends were coated with a phosphorous oxide based film. However, because its composition varies during the ageing treatments,

Table 1: Room-temperature physical and mechanical property data for 2D woven C/SiC composites.

	as-processed	stabilized
Fiber fraction (%)	40	40
Density ($g.cm^{-3}$)	2	2
Seal coating microcracks: average width (μm)	1.2	2.5
Elastic modulus (GPa)	90 ± 5	70 ± 5
Ultimate tensile strength (MPa)	390 ± 20	390 ± 20
Strain to rupture (%)	0.85 ± 0.05	0.90 ± 0.05
Stress at matrix microcracking saturation (MPa)	250 ± 20	180 ± 20

the presence of such a coating rendered impossible any direct mass variation measurement. Therefore, duration of the ageing treatments were selected from TGA data [9], and corresponded to 2 and 6% of equivalent relative mass loss, respectively. Ageing treatments performed on the materials will be thus further referred to as 2 and 6 % mass loss treatments (the corresponding durations being listed in table 2).

Loading/unloading cycles and acoustic emission monitoring were used in order to follow the occurrence and the propagation of damage into the material during the tests. Since the values directly obtained, in terms of cumulative hits, from the AE signals were not quantitavely representative, the rate of AE variation was systematically calculated from each test (by deriving the plots of cumulative hits as a function of elongation normalized by the total number of hits).

For each ageing treatment condition, 2 specimens were tested.

The fractured specimens were examined using optical microscopy and scanning electron microscopy (SEM) to determine morphological changes and composite failure behavior.

3 - RESULTS

3.1 - Tensile behavior prior to oxidizing treatments.

The room temperature tensile properties of both the as-processed and stabilized materials are summarized in table 1, in terms of Young's modulus, tensil rupture stress and rupture strain, and stress at matrix microcracking saturation (determined by acoustic emission recording).

Table 2: Influence of thermal oxidizing treatments on the tensile properties of 2D C/SiC composites.

Material and Environment	Ageing treatment T (°C)	time (s)	$\Delta m/m_o$ (%)	Tensile properties σ_R (MPa)	ε_R (%)
stabilized		None		390 ±20	0.85 ±0.05
flowing oxygen	700	1500	2	280 ±10	0.6 ±0.05
	700	2700	6	190 ±5	0.38 ±0.01
	900	200	2	270 ±10	0.55 ±0.03
	900	600	6	200 ±3	0.45 ±0.05
	1200	300	2	285 ±10	0.68 ±0.05
	1200	800	6	260 ±5	0.58 ±0.04
	1400	800	<2	335 ±10	0.79 ±0.05
	1400	1850	2	285 ±10	0.65 ±0.05
stabilized		None		390 ±20	0.85 ±0.05
flowing air	700	3200	2	310 ±10	0.65 ±0.05
	700	7200	6	280 ±10	0.6 ±0.05
	900	1050	2	310 ±15	0.67 ±0.08
	900	3200	6	290 ±5	0.63 ±0.02
	1200	1300	2	330 ±10	0,75 ±0.05
	1200	4300	6	300 ±5	0.65 ±0.02
	1400	1850	<2	360 ±5	0.78 ±0.01
as-processed		None		390 ±20	0.90 ±0.05
flowing oxygen	700	1500	<2	320 ±20	0.75 ±0.05
	700	2700	2	290 ±20	0.68 ±0.05
	700	5900	6	215 ±5	0.5 ±0.03
	900	8600	2	280 ±20	0.65 ±0.05
	900	32000	6	260 ±5	0.58 ±0.05
	1400	800	2	335 ±10	0.8 ±0.03
	1400	1850	6	310 ±10	0.77 ±0.05

The tensile stress-strain curves obtained for both materials are plotted in figure 3. The general phenomena associated with these tensile behaviors may be more easily assessed from the typical stress-strain curve shown as an example in figure 3b (for the stabilized composite). The two composites behave as typical damageable materials exhibiting an extended non-linear stress-strain domain up to rupture. Besides, as a consequence of the onset of damage upon processing (i.e. matrix microcracking and fiber/matrix debonding), **no linear/elastic part** is evidenced at the beginning of the curves [1, 13]. Three distinct domains corresponding to three different steps in the onset/extension of the damage phenomena may be further noticed from the curves. The first domain exhibits a knee along with a nearly constant increase in the rate of accumulation of AE events and corresponds to the multiplication of **matrix microcracking** and **fiber/matrix partial debonding** until saturation is reached. The second domain represents a transition involving **crack opening** and **fiber sliding**, marked by a change of curvature in the stress-strain curve and a noticeable decrease in the rate of accumulation of AE events. The last part of the curves is linear and corresponds to the elongation of the fibers which **carry entirely the load** until rupture occurs. The rate of accumulation of AE events remains seemingly constant. Loading/unloading cycles point out the damage consequences, i.e. a progressive decrease in the material longitudinal stiffness along an extension of residual strains.

Comparison of the tensile behavior of the as-processed and stabilized composites shows that the Young's modulus and the stress at matrix microcracking saturation were decreased by the stabilizing treatment while the ultimate tensile stress and tensile strain remained

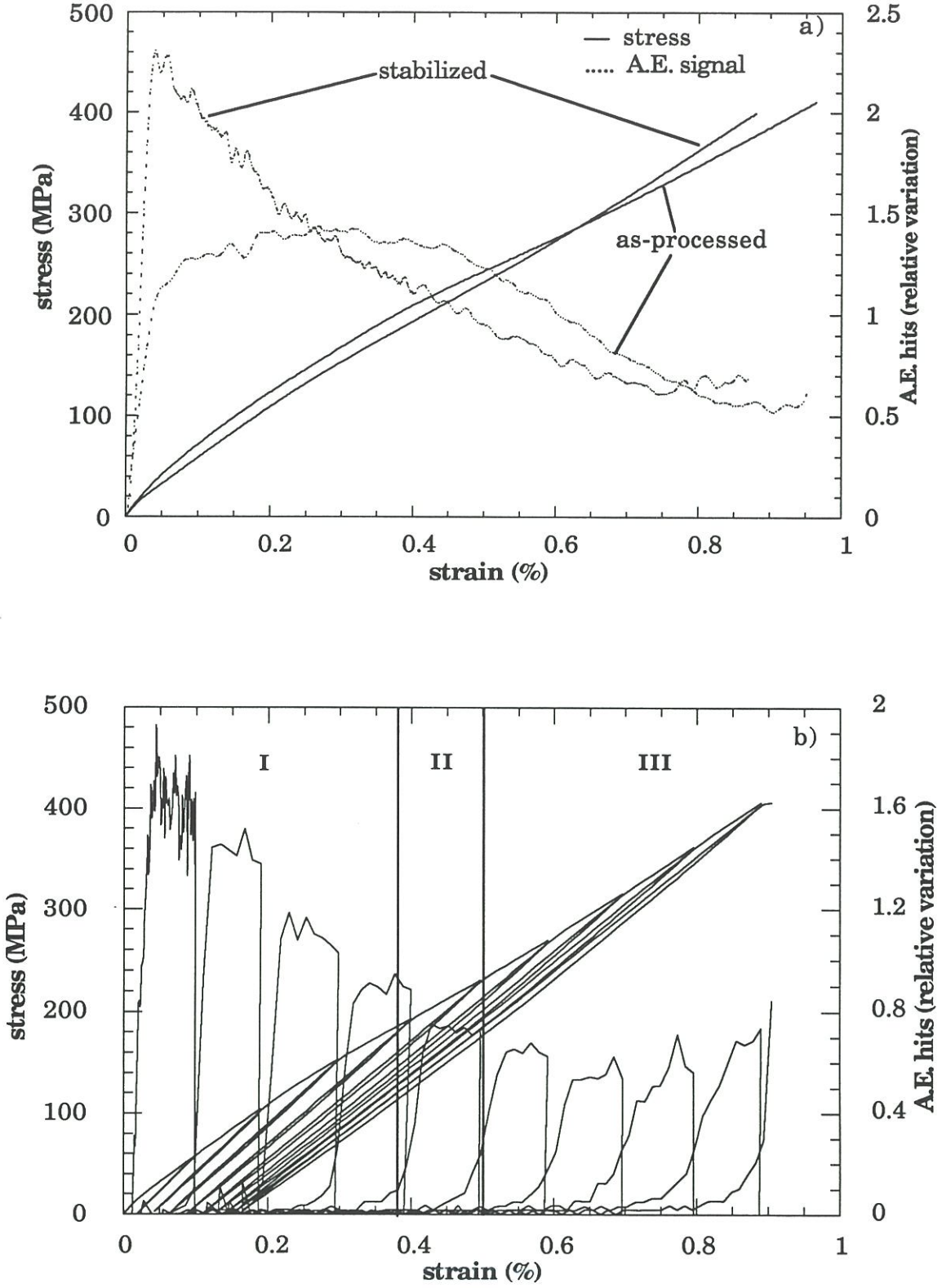

Fig.3: Room temperature tensile stress-strain curves and relative variations of cumulative A.E. hits for 2D C/SiC composites:
a) comparison between the as-processed and the stabilized materials,
b) stress-strain curve with cycling for the stabilized material.

highly comparable (see table 1). Morever, consecutively to this stabilizing treatment, the transition domain (i.e. domain II) appeared to be less extended while exhibiting more markedly the appearance of a plateau followed by a more subtantial stiffening in the third domain.

The fracture surface of the two material, as shown in figure 4, displays extensive pull out of both individual tows and, inside each tow, of the carbon fibers. This phenomena is more pronounced for the stabilized material. The fracture surface of the carbon fibers evidences the presence of striations concurrent at a single point located near the surface of the fiber (figure 5). This feature is likely related to the existence of micropores near the fiber surface, as evidenced from a previous study [10].

3.2 - Environmental effects on the tensile properties.

Results from all the tensile tests performed on the 2D C/SiC composites under various ageing conditions are summarized in table 2. Owing to the weak level of mass losses encountered by the materials during the ageing treatments, no significant changes in Young's modulus were noticed under any ageing conditions for both as-processed and stabilized materials.

3.2.1 - Influence of the ageing temperature.

Stress-strain curves for the 2D C/SiC composites stabilized at 1600°C in inert gas and aged in flowing oxygen between 700°C and 1400°C, for equivalent relative mass losses of 2 and 6% are reported in figure 6. All the oxidizing treatments leading to an equivalent relative mass loss of 2% result in a reduction in strength of approximately 30%, while the general aspect of the stress-strain curve is always preserved. Rupture occurs at

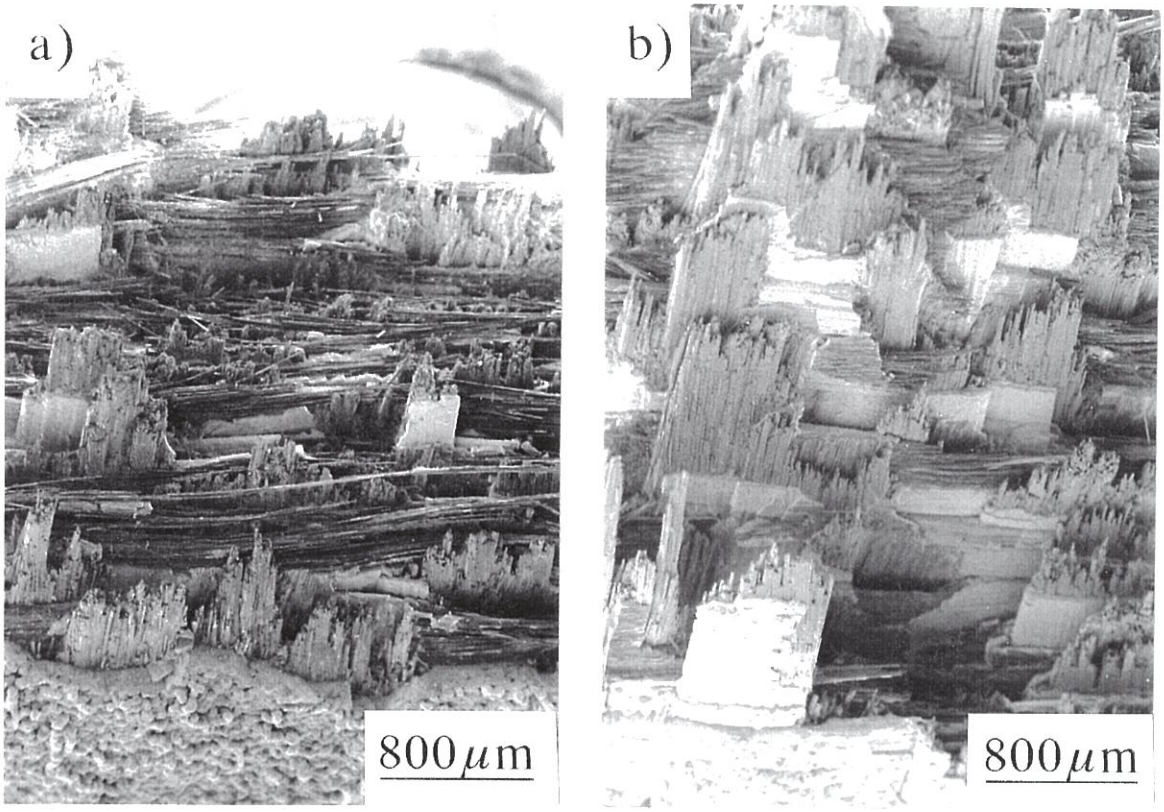

Fig.4: SEM micrographs showing the fracture surfaces of 2D C/SiC tensile specimens a) as-processed, b) stabilized at 1600°C under inert gas.

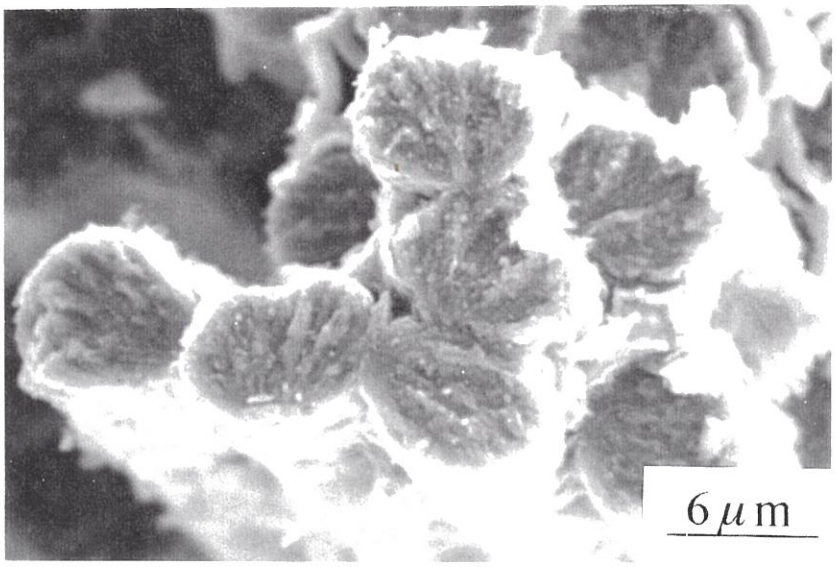

Fig.5: SEM micrograph of the fracture surface of ex-PAN carbon fibers from a tensile specimen of stabilized material.

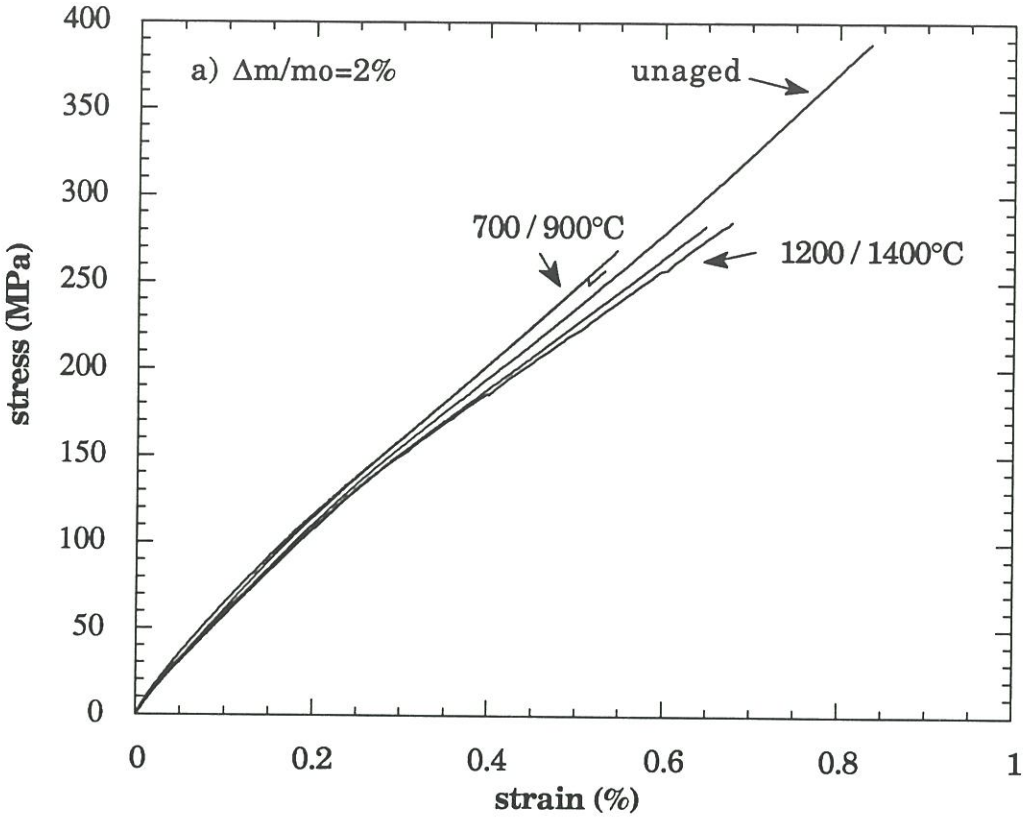

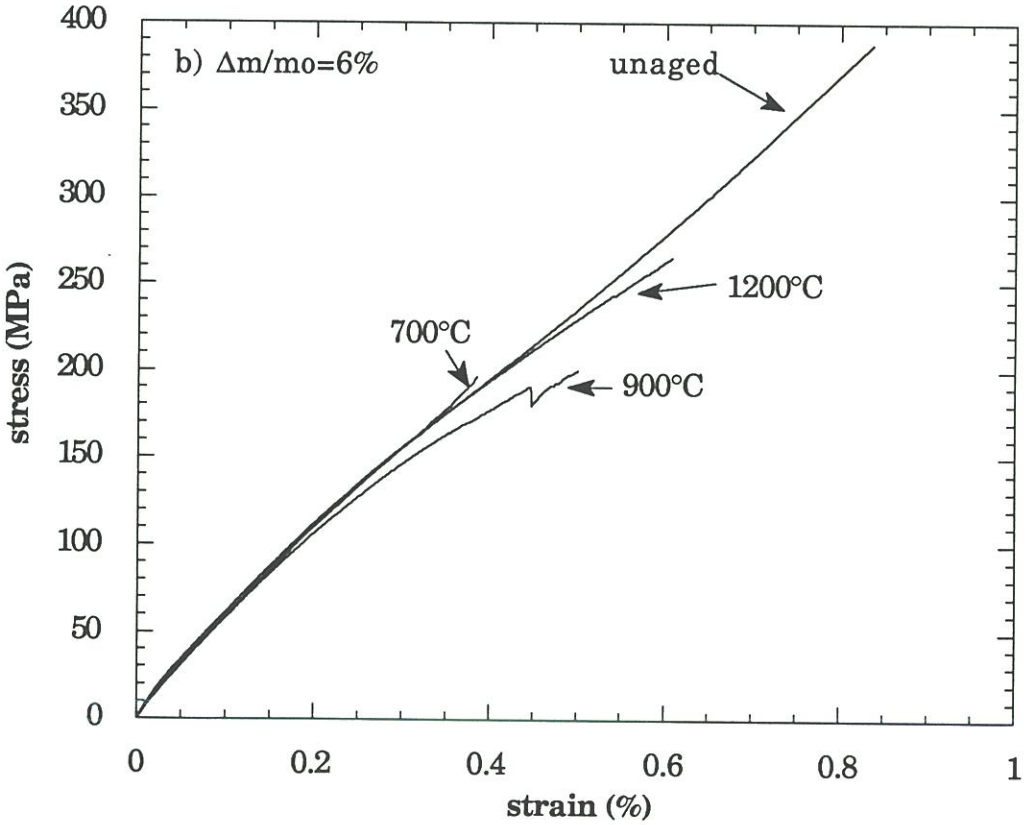

Fig.6: R. T. Tensile stress-train curves for stabilized (heat treated) 2D C/SiC composites variously aged under flowing oxygen (P=100kPa) for durations corresponding to a) 2% and b) 6% of relative mass loss.

the beginning of the third domain of curves. For treatments corresponding to a relative mass loss of 6%, variations in the tensile behavior induced by changes in the ageing temperature become noticeable:

- At 700°C: the aspect of the stress-strain curve remains nearly unchanged (as compared to the unaged composite). However, the decrease of the ultimate tensile strength reaches about 50% of the value of the unaged material. The SEM micrograph of a fiber tow (fig.7a) evidences a notch-like local degradation of the carbon fibers and interphases. Rupture of the carbon fiber appears to be located near this notch (fig.7b).

- At 900°C: the ageing treatment also results in a loss of strength of approximately 50%. The strain to rupture has also noticeably decreased and, besides, the appearance of the stress-strain curve is no longer preserved: the third domain is barely observable and the apparent "damage strengthening rate" is reduced. Observation of the fracture surface reveals a more important level of pull out of the tows located near the surface of the sample (fig.8a). Inside these outer tows, the carbon fibers appear to be more intensively degraded and debonded from the SiC matrix (fig.8b).

-At 1200°C, the aspect of the stress-strain curves remains unchanged, and rupture takes place at the end of the second domain. The decrease in the ultimate strength reaches about 35% of the initial value.

Because of the sealing of the SiC seal-coating microcracks by silica, a relative mass loss of 6% could not be reached by the ageing treatments performed at 1400°C [9]. For a relative mass loss of 2%, the oxidizing attack of the carbon fibers and interphase remains superficial and located

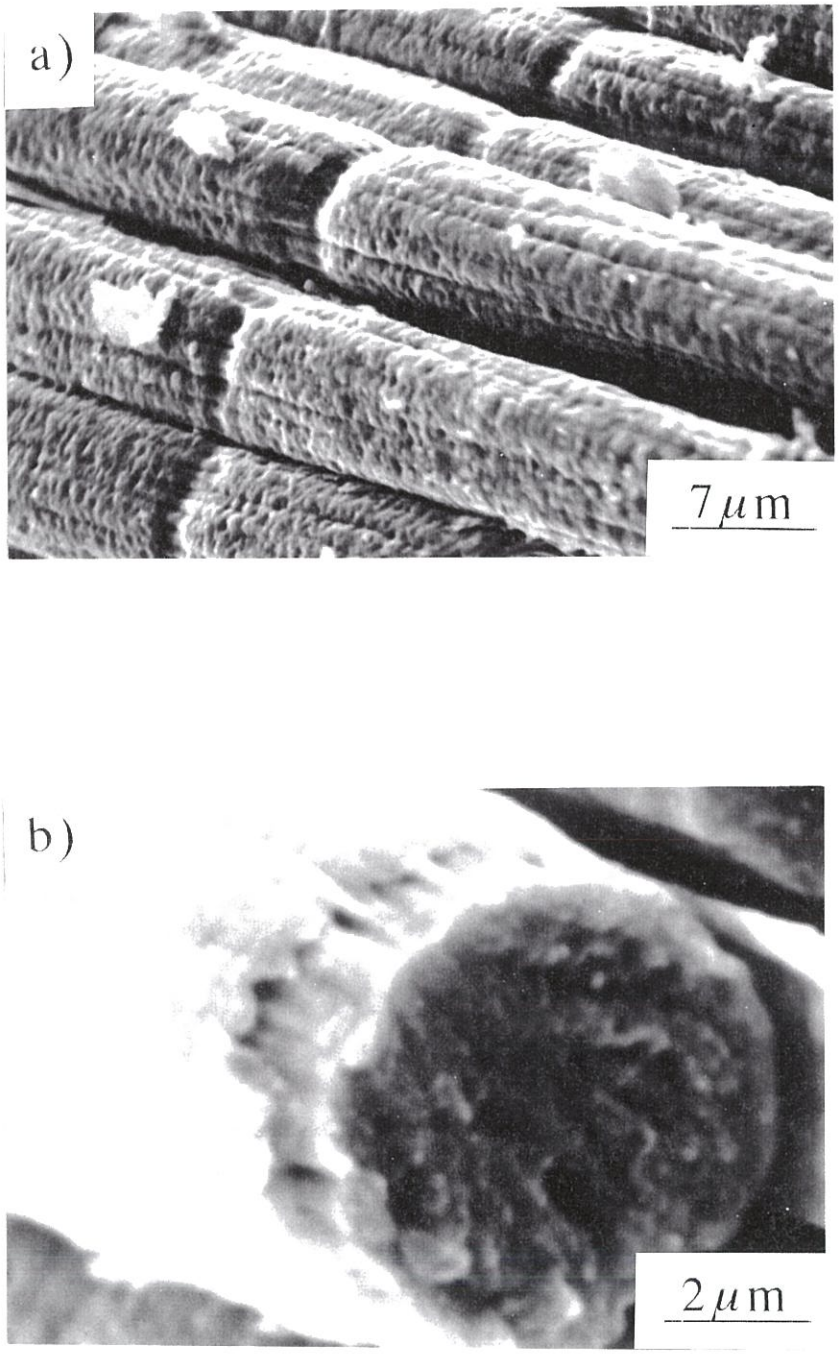

Fig.7: SEM micrographs revealing a) the periphery and b) the fracture surface of the carbon fibers of a composite aged at 700°C under flowing oxygen (P=100kPa) for a duration corresponding to a relative mass loss of 6%.

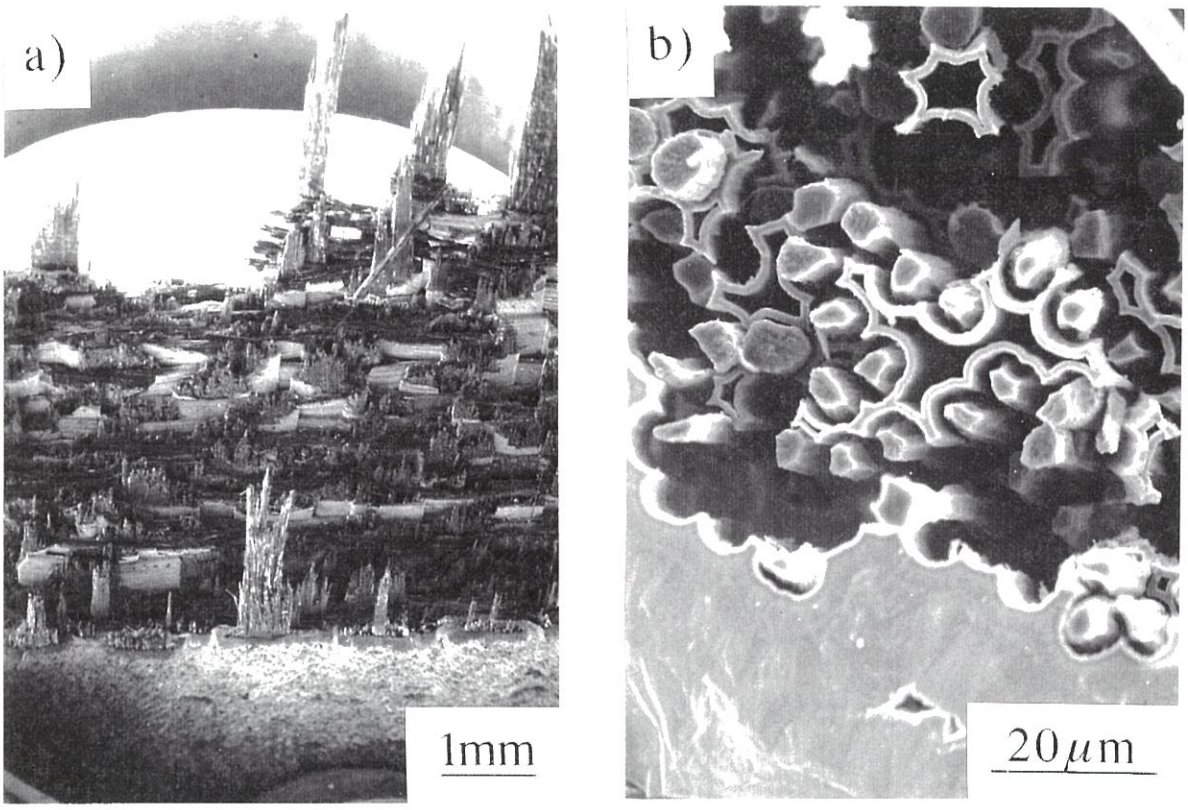

Fig.8: SEM micrographs showing a) the fracture surface of a stabilized 2D C/SiC composite aged at 900°C under flowing oxygen (P=100kPa) for a duration corresponding to a relative mass loss of 6%, b) an outer carbon tow at a higher magnification.

near the seal-coating microcrack tips. Notch-like superficial pores are thus generated (fig.9).

3.2.2 - Influence of the atmosphere composition.

Ageing treatments performed on the stabilized 2D C/SiC composites in dry air (P=100kPa) result in noticeable differences in the tensile behavior as compared to the same oxidizing treatments performed in flowing oxygen. The stress-strain curves are more longer preserved and the strengths to rupture are almost similar whatever the ageing treatment (fig.10). The variations of stress and strain to rupture as a function of temperature for oxidizing treatments performed in air or pure oxygen are shown in fig.11. For an equivalent relative mass loss of 2%, differences between the tests performed in air and in oxygen are more important for the high temperature ageing treatments. For 6% of relative mass loss, these differences are conversely more important at low temperatures. SEM observation of the composite aged in air at 700°C evidences a local degradation of the carbon fiber. However, the notch-like appearance of this degradation is less important as-compared to that developed in pure oxygen (compare fig. 12 and 7a). For an ageing at 1400°C, the superficial attack of the carbon fibers and interphases remains, but contrary to ageing treatments performed in pure oxygen, no notch-like clusters of oxidized carbon constituents appear at the microcrack tips (fig.13).

3.2.3 - Thermally unstabilized material.

When the as-processed (unstabilized) 2D C/SiC composites are tested after ageing in flowing oxygen (P=100kPa) between 700°C and 1400°C, noticeable differences may be observed with the stabilized composites. After 2% of mass loss, the aspect of the stress- strain curves is

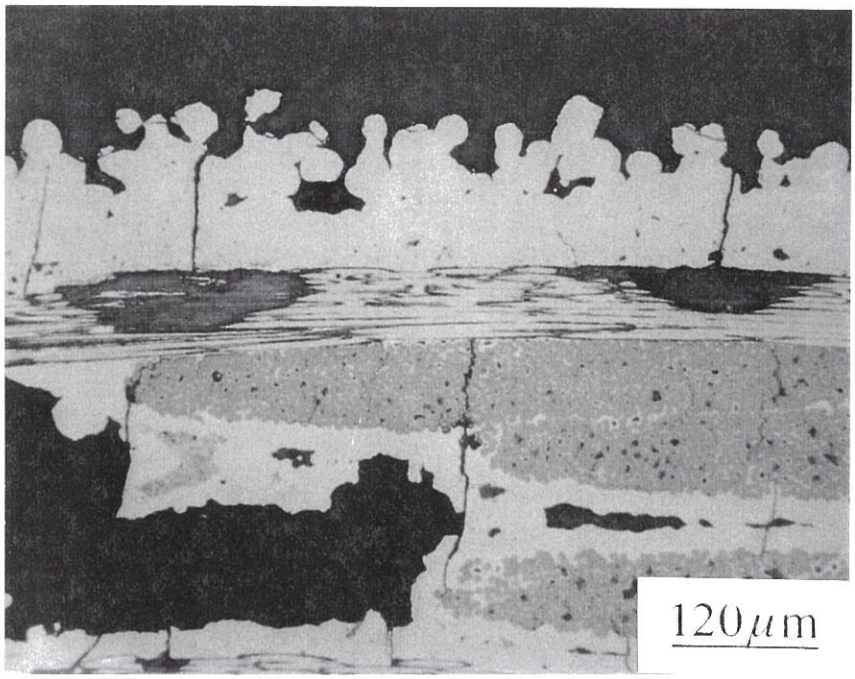

Fig.9: Optical micrograph of a polished section of a stabilized 2D C/SiC composite aged under flowing oxygen (P=100kPa) at 1400°C for a relative mass loss of 2%.

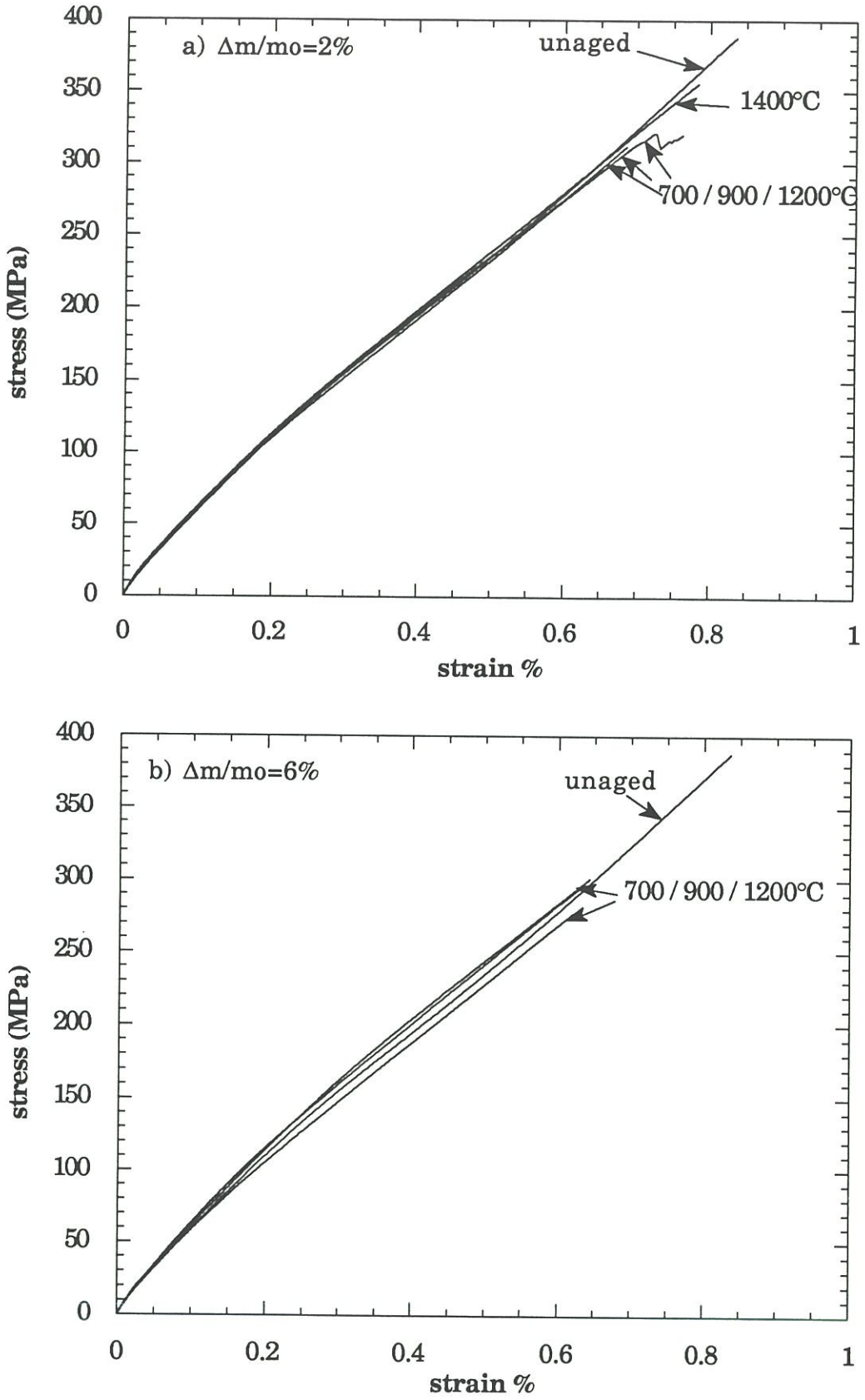

Fig.10: R. T. Tensile stress-strain curves for stabilized (heat treated) 2D C/SiC composites variaously aged under dry air (P=100kPa) coressponding to a) 2% and b) 6% of relative mass loss.

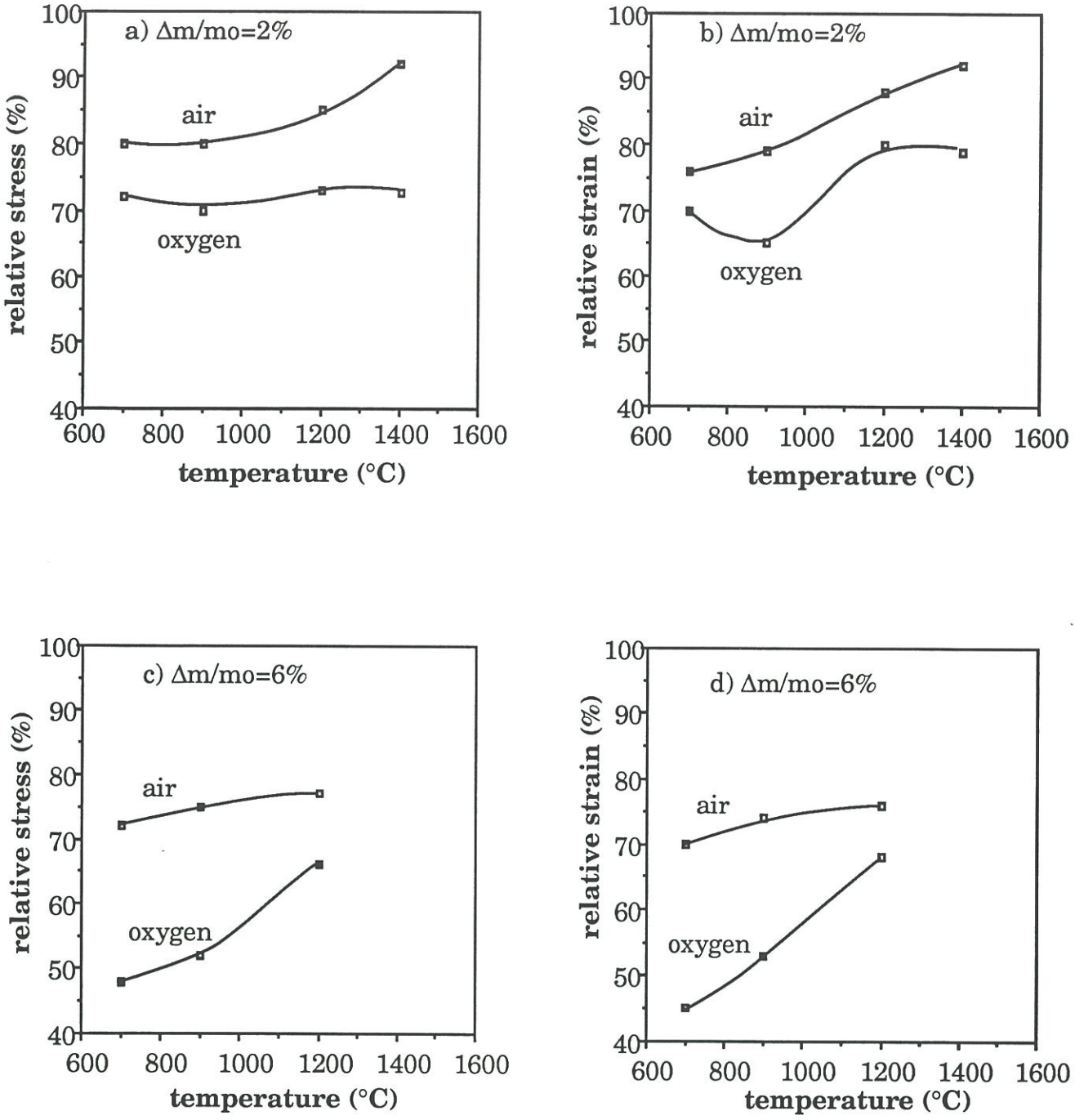

Fig.11: Comparison of the room temperature ultimate tensile properties of stabilized 2D C/SiC composites aged under flowing air and oxygen.

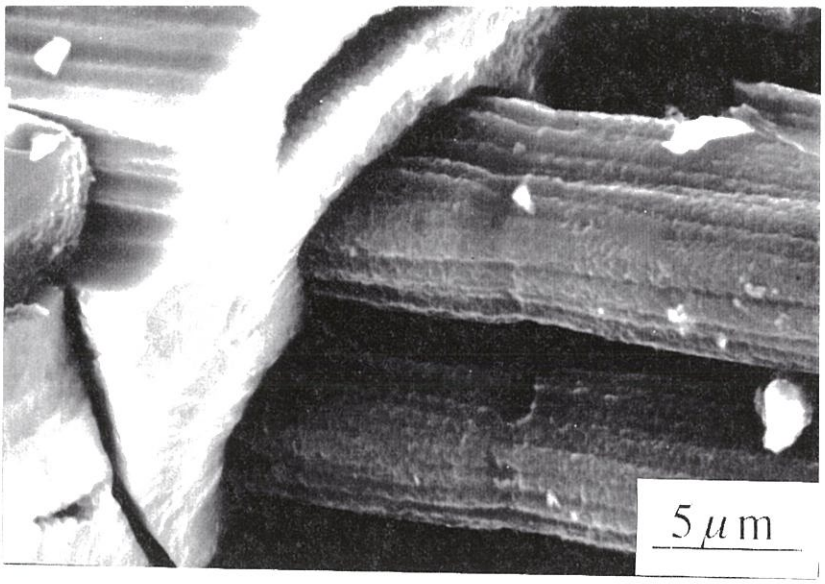

Fig.12: SEM micrograph revealing the periphery of carbon fibers from the fracture surface of a stabilized 2D C/SiC composite aged at 700°C under dry air (P=100kPa), at a relative mass loss of 6%.

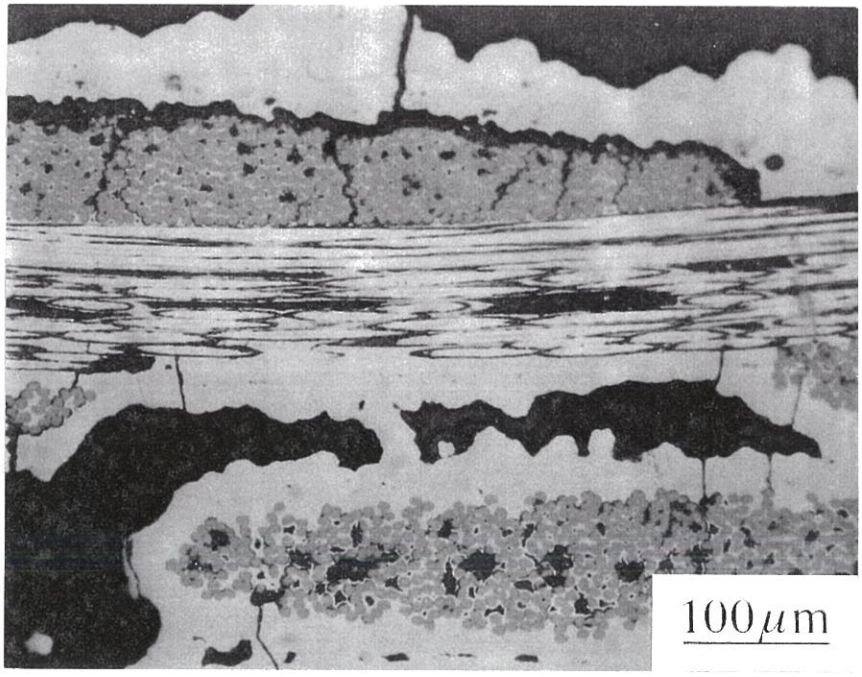

Fig.13: Optical micrograph of a polished section of a stabilized 2D C/SiC composite aged under dry air (P=100kPa) at 1400°C for a relative mass loss of 2%.

preserved for ageing temperatures less than 1000°C (fig. 14). At high temperatures, the ageing treatment results in a decrease of the damage strengthening rate, similarly to the 1600°C stabilizing treatment in inert gas (compare fig.14 curve 1400°C and fig.3a). After 6% of relative mass loss, the ageing treatments at 700°C and 900°C also results in a decrease of the damage strengthening rate while reductions in the strength to rupture are noticeably temperature dependant. Figure 15 displays a comparison between the variations of the stress and strain to rupture as a function of temperature for both as-processed and stabilized materials. Results at 1200°C do not appear since the as-processed composite is nearly unoxidized because of the thermal microcrack closure [9]. For a relative mass loss of 2%, the difference between the ultimate tensile stresses of the two composites is more important at high temperatures (i.e.1400°C) than at low temperatures (i.e. 700°C and 900°C). This difference grows in importance as the relative mass loss is increased to 6%.

Morphological analyses performed after oxidation on the as-processed (unstabilized) 2D C/SiC composites showed the same forms of degradation than for the stabilized material, but at different temperatures [9]. At 700°C, the non uniform degradation already takes place and the fracture surface consequently reveals the pull out of the outer tows. At 900 and 1400°C, the oxidation of the as-processed composites remains superficial. However, at 1400°C oxidation takes place preferentially near the lateral sides of the specimens (fig.16) [9], while at 900°C notch-like clusters of oxidized carbon constituents are present at the vicinity of all the seal-coating microcrack tips.

The composite oxidation rate is an important factor since it is responsible for the lifetime of the material. Figure 17 shows the mass

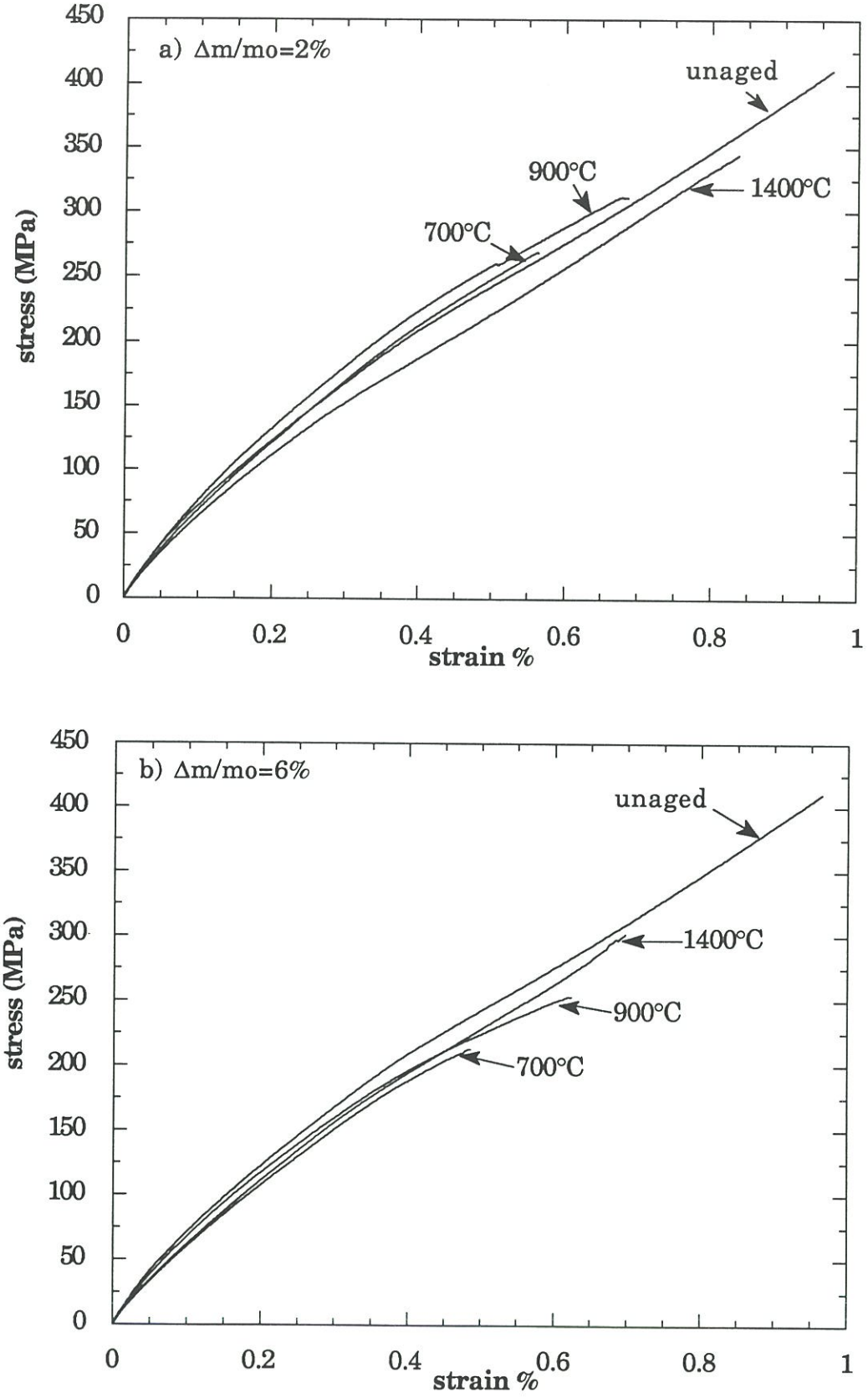

Fig.14: R. T. Tensile stress-strain curves for as-processed (unstabilized) 2D C/SiC composites variously aged under flowing oxygen (P=100kPa) corresponding to a) 2% and b) 6% of relative mass loss.

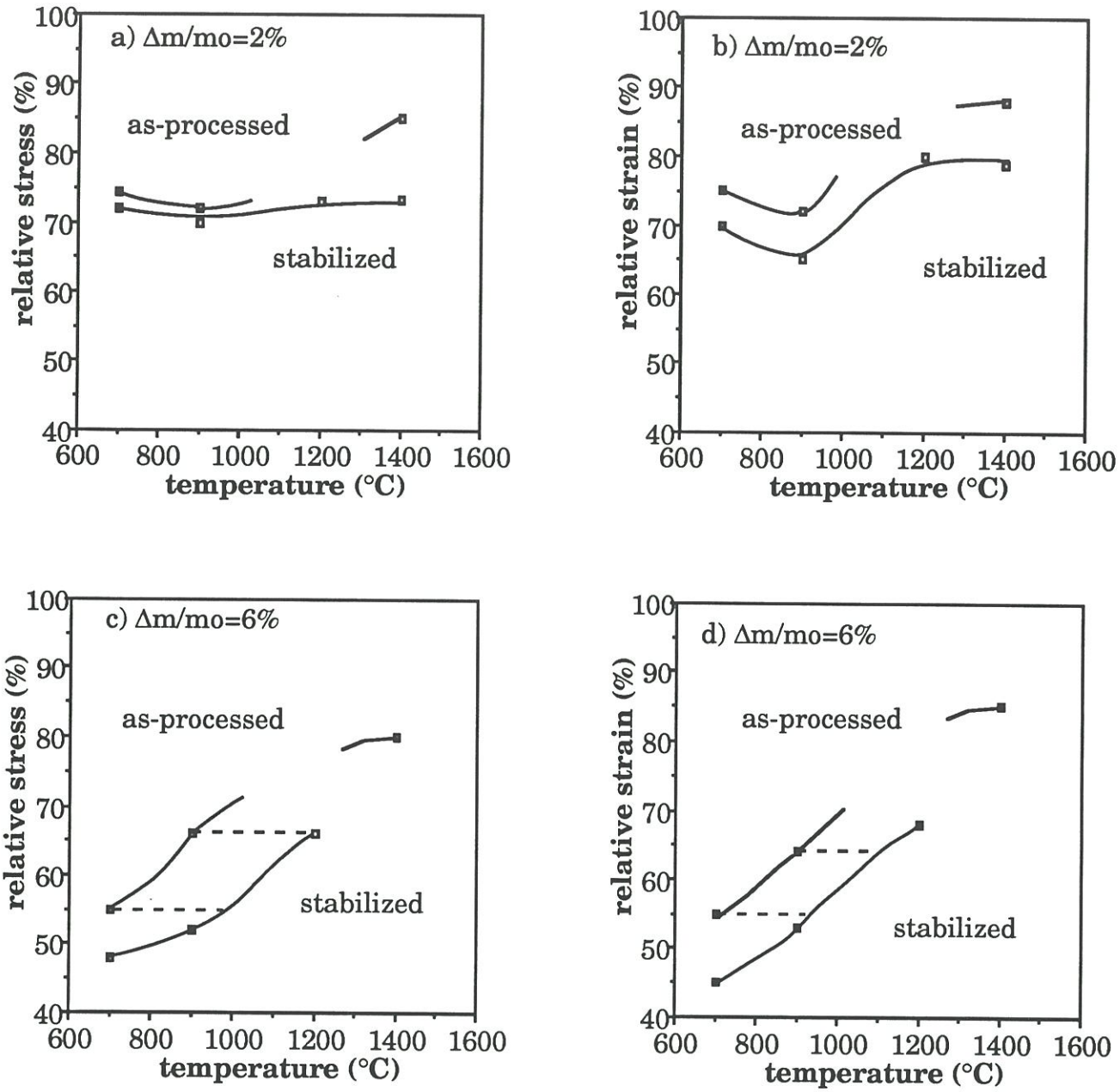

Fig.15: Comparison of the room temperature ultimate tensile properties of as-processed and stabilized 2D C/SiC composites variously aged under flowing oxygen (P=100kPa).

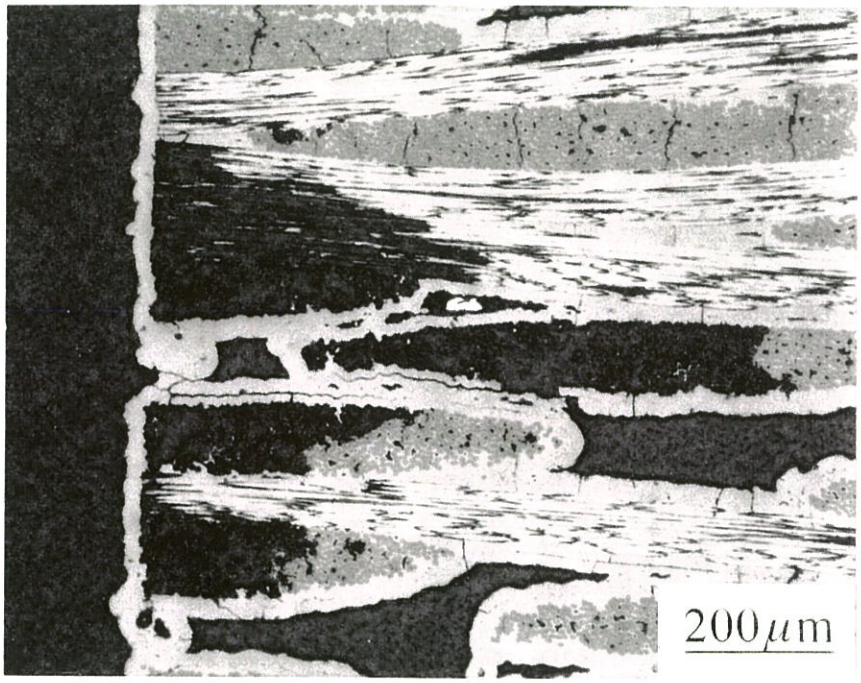

Fig.16: Optical micrograph of a polished section of an as-processed (unstabilized) 2D C/SiC composite aged at 1400°C under flowing oxygen (P=100kPa), for a relative mass loss of 6%.

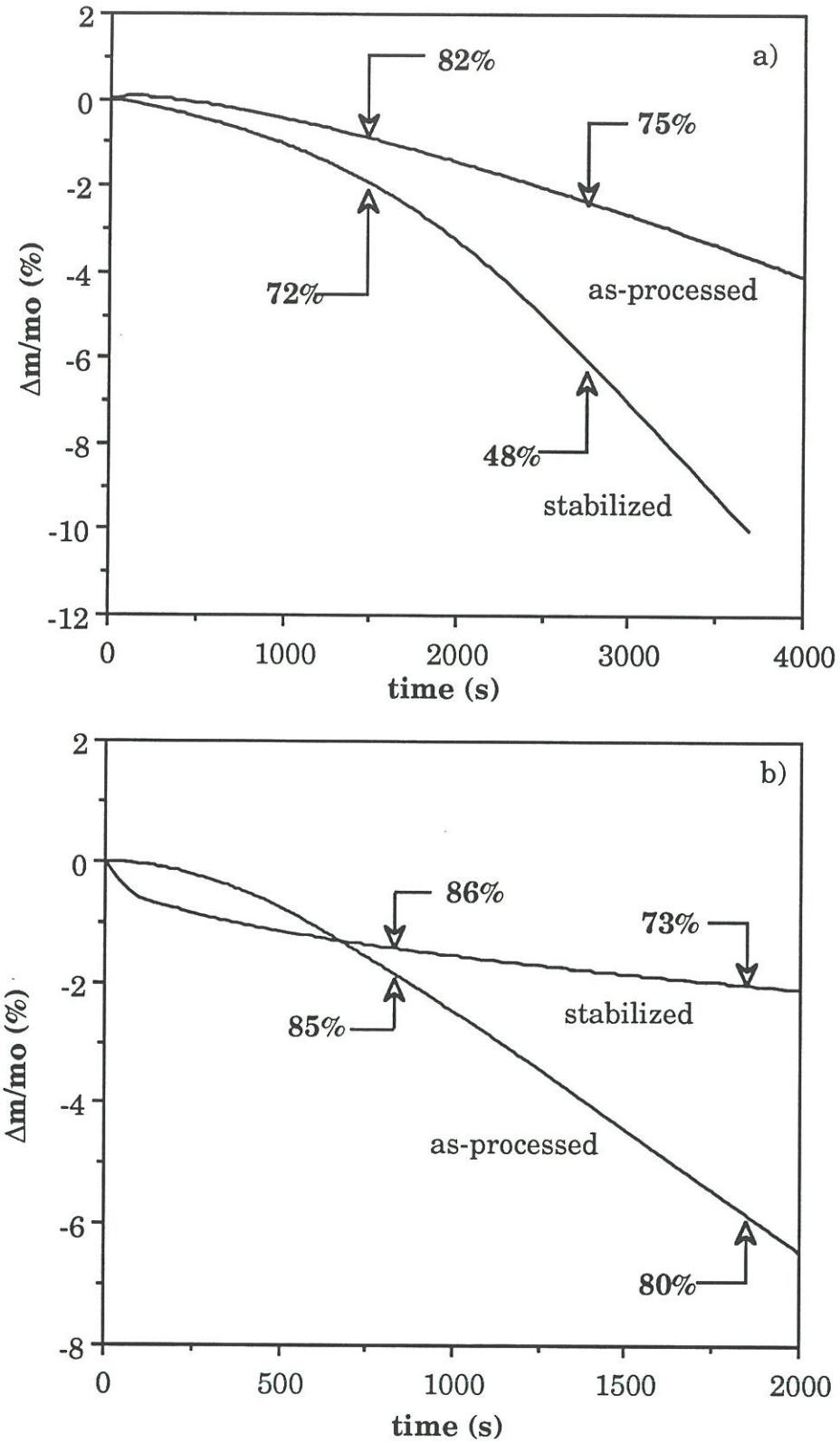

Fig.17: Correlation between relative mass loss curves (from TGA data taken from ref. [9]) and relative tensile strength of specimens aged under flowing oxygen for both as-processed and stabilized 2D C/SiC composites a) at 700°C and b) at 1400°C.

variations of the as-processed and stabilized 2D C/SiC composites as a function of time (from TGA data taken in ref. [9]). On these curves, the tensile strength of the composites variously aged in oxygen are also plotted. At 700°C, the difference in rupture strength of the two materials follows the same trend that the difference in the mass variations. At 1400°C, the difference in the rupture strength does not any longer follow the difference of mass variations. For example, the rupture strengths after 1850 seconds of ageing treatment at 1400°C were at 80% and 73% of the values of unaged materials for the as-processed and the stabilized composites, respectively, whereas the mass variations were 6% and 2%, respectively. This later result evidences the importance of the localization of the degradation occurring during the ageing treatments.

4 - DISCUSSION

4.1 - Mechanisms of composite property degradation.

The previous study on oxidation kinetics of the 2D C/SiC composites has evidenced three temperature domains corresponding to different mechanisms controlling the oxidation behavior. Each of these mechanisms has proved to be associated to a particular mode of morphological changes induced by oxidation and concerning the degradation of the carbon reinforcement: uniform (at low temperatures), non uniform (at intermediate temperatures) and superficial (at high temperatures).

4.1.1 - uniform degradation.

For oxidizing treatments performed at T<700°C, the rate of oxygen diffusion inside the composite, through the microcracks, is higher than

the rate of carbon consumption. Carbon fibers and interphases are thus simultaneously degraded inside the composite, which causes a **uniform** oxidation of the material. Since oxygen first degrades the carbon free surfaces, the carbon interphase is consequently preferentially consumed near the microcrack tips. When the fibers are locally uncoated, oxidation then takes place near their surfaces, where the reactivity is particularly high [10]. Such a degradation may be observed on figure 7a with **notches** being located near the microcrack tips. Then, for relative mass losses less than 6%, the appearance of the stress-strain curve remains unchanged as compared to the unaged composite since fibers and pyrocarbon are only degraded near the microcracks. When entering the second domain of the stress-strain curve, the part of the tensile load applied to these degraded fibers is sufficient to cause their premature rupture, which results in the composite sudden rupture. The tensile rupture strength therefore also decreases with an increase in the depth of the fiber notch, that is to say with an increase in the mass loss.

4.1.2 - non uniform degradation.

The increase of the carbon reactivity at intermediate temperatures (i.e. 900°C), results in a higher consumption of oxygen by the first carbon plies. A **difference in oxidizing attacks** may thus be observed between the surface and the bulk of the samples. Such a degradation mode leads to the premature rupture of the first plies during loading. The sudden rupture of these first plies induces an **overloading effect** on the inner plies which then also break. The fracture surface of the composite reveals these different behaviors between the surface and the bulk of the sample. As a matter of fact, the pull out length of the fiber tows is more important near the surface than in the center of the specimens.

4.1.3 - superficial degradation.

This mechanism occurs at T>1200°C, when the carbon reactivity is important as compared to the rate of oxygen diffusion through the narrow microcracks of the SiC seal-coating. Oxygen is thus immediately consumed at the microcrack tips, resulting in the **development of pores** under the SiC seal-coating. These pores very likely induce a **notch effect** in the composite, and lead to a sudden rupture when the load bearing capacity of the outer tows is exceeded. Before rupture, the aspect of the stress-strain curve is preserved owing to the important part of the composite which remains unoxidized. Since silica layers developed on the microcrack walls, the oxidation rate is thus progressively reduced until closure of the microcracks. Consequently, the rupture strength after oxidation is only related to the quantity of carbon consumed before sealing.

Figure 6 clearly shows that an oxididizing treament performed at low temperatures leads to a more **severe degradation of the tensile properties** than at higher temperatures. This phenomenon is related to the high sensitivity of the carbon fibers towards oxidation [10] on one hand, and to the uniform degradation of the composite reinforcement, on the other hand. Such a degradation mode is also related to the presence of the oxidation-resistant SiC matrix. As a matter of fact, the macrocracks in the matrix allow an easy oxygen diffusion in the bulk of the specimen.

4.2 - Effect of a decrease in the oxygen content.

The degradation mode of the composite controls its tensile behavior in an oxidizing environment. The decrease of the oxygen content modifies the distribution of the degraded zones mainly through a decrease in the carbon reactivity. The difference between the behavior in dry air and in

dry oxygen at low temperatures (i.e. 700°C), can be explained by considering the extent of the notch-like attack of each carbon fiber occurring during ageing treatments. The decrease of oxygen content lowers the oxygen gradient and consequently the oxygen diffusional flux through the microcracks. Carbon fibers thus appear to be not so intensively degraded in air than in pure oxygen (fig.18). As oxidation acts preferentially near the debonded areas in the carbon interphase, the fiber degradation near the microcrack tips is therefore limited.

The mechanisms responsible for the sudden rupture of the composite aged in air at 900°C is also induced by the overloading process of the inner fiber tows, similarly to the test performed in oxygen. However, the decrease of the carbon reactivity with the oxygen partial pressure attenuates the difference of degradation between the surface and the center of the composite reinforcement. Thus, the overloading effect is limited.

The oxidizing attacks at high temperatures in dry air are also superficial (as in dry oxygen). However, these attacks do not only occur at the microcrack tips but also propagate around the fibers tows. This feature was explained by the reduction of the carbon reactivity towards oxygen which may therefore diffuse along the debonded tow/matrix zones. The notch/overloading effect leading to the composite sudden rupture is thus reduced.

Therefore, the decrease in the oxygen content limits the mechanisms which are responsible for the mechanical degradation of the material. That means that the 2D C/SiC composites have a **better tensile resistance** in addition to a better oxidation resistance when the oxygen partial pressure in the environment is lowered.

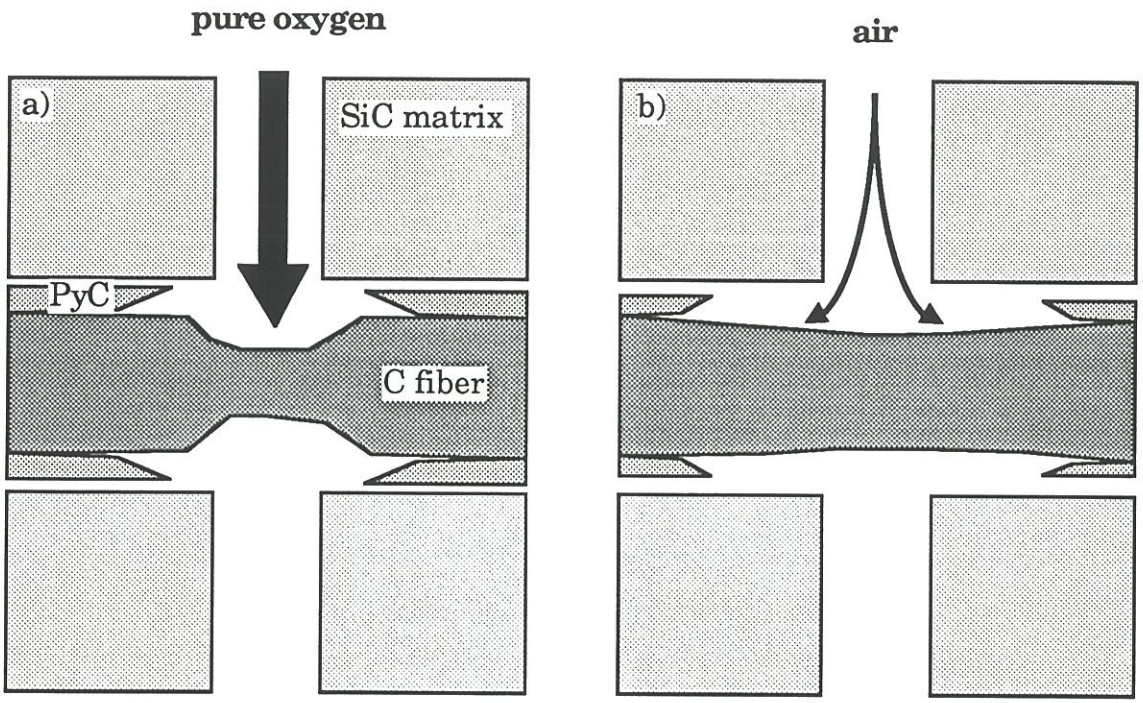

Fig.18: Schematic representation of the differences in the degradation of the carbon phases induced by ageing treatments performed: a) in pure oxygen and b) in dry air.

4.3 - Thermally unstabilized material.

The stress-strain curve of the as-processed (unstabilized) 2D C/SiC composite exhibits a larger domain of matrix microcracking. The transition with the second domain corresponding to the progressive loading of the fibers occurs at a higher stress as-compared to the stabilized composite. This difference in the behavior of the two materials is related to the thermomechanical damage induced by the stabilizing treatment. During this treatment, the CTE mismatch between the carbon fiber and the matrix results in another onset of damage in addition to that resulting from processing. The fiber-matrix bond strength has also been **weakened by the stabilizing treatment**. Consequently, the initial tensile modulus as well as the load-transfer conditions have been lowered by the stabilizing treatment.

Prior to the stabilizing treatment, the microcracks present in the material are thinner (see table 1) and the carbon reactivity is higher [9,10]. The **temperature domains** corresponding to the mechanisms controlling the oxidation kinetics **are shifted to lower temperatures**. Therefore, different behaviors concerning the tensile resistance after ageing treatments are observed. Both the strength and strain to rupture of the as-processed composite aged at 700°C are similar to those of the stabilized composite aged at 900°C (see stipple lines in fig.15). The same comparison can be made between the as-processed composite aged at 900°C and the stabilized composite aged at 1200°C.

When the as-processed 2D C/SiC composites are oxidized at 700°C, the degradation mode is non uniform [9]. The higher carbon reactivity limits the oxygen diffusion into the composite material. The oxidizing attacks remain at the level of the carbon free surfaces (intra and intertow cracks and interfacial debonding). This results in a strength to rupture higher

than for the stabilized composite (fig.15). The oxidation rate of the as-processed composite at 700°C is lower than for the stabilized material. A better conservation of the tensile properties with the duration of the oxidative treatments is consequently observed (fig.17).

The oxidizing attacks of the as-processed composite at 900°C remains superficial. Consequently, the notch effect which takes place under these conditions, is responsible for the decrease of the strength to rupture (fig.15).

At 1400°C, the degradation mode of the reinforcement preferentially takes place parallel to the plies of the composite. This phenomenon is related to the radial expansion of the carbon fibers. As a consequence, the pores formed during oxidation of the as-processed composite at 1400°C will not induce any notch effect, as illustrated in figure 19. Therefore, the strength to rupture of the as-processed composite decreases more slowly after 1400°C ageing treatments than with the stabilized material. This phenomenon is illustrated in figure 17b which shows that the drop of the residual strength as a function of the duration of the ageing treatments for both materials is in contradiction with their respective mass loss.

These results clearly show that the tensile resistance of oxidized composites is reduced when the 1600°C stabilizing treatment is performed. Such a modification can be explained by the **translation of the three temperature domains** associated to the oxidation mechanisms and to the morphological changes induced by the oxidizing treatments.

5 - CONCLUSIONS

Tensile tests performed after ageing 2D C/SiC composites in dry oxygen coupled to morphological observations of fractured specimen have

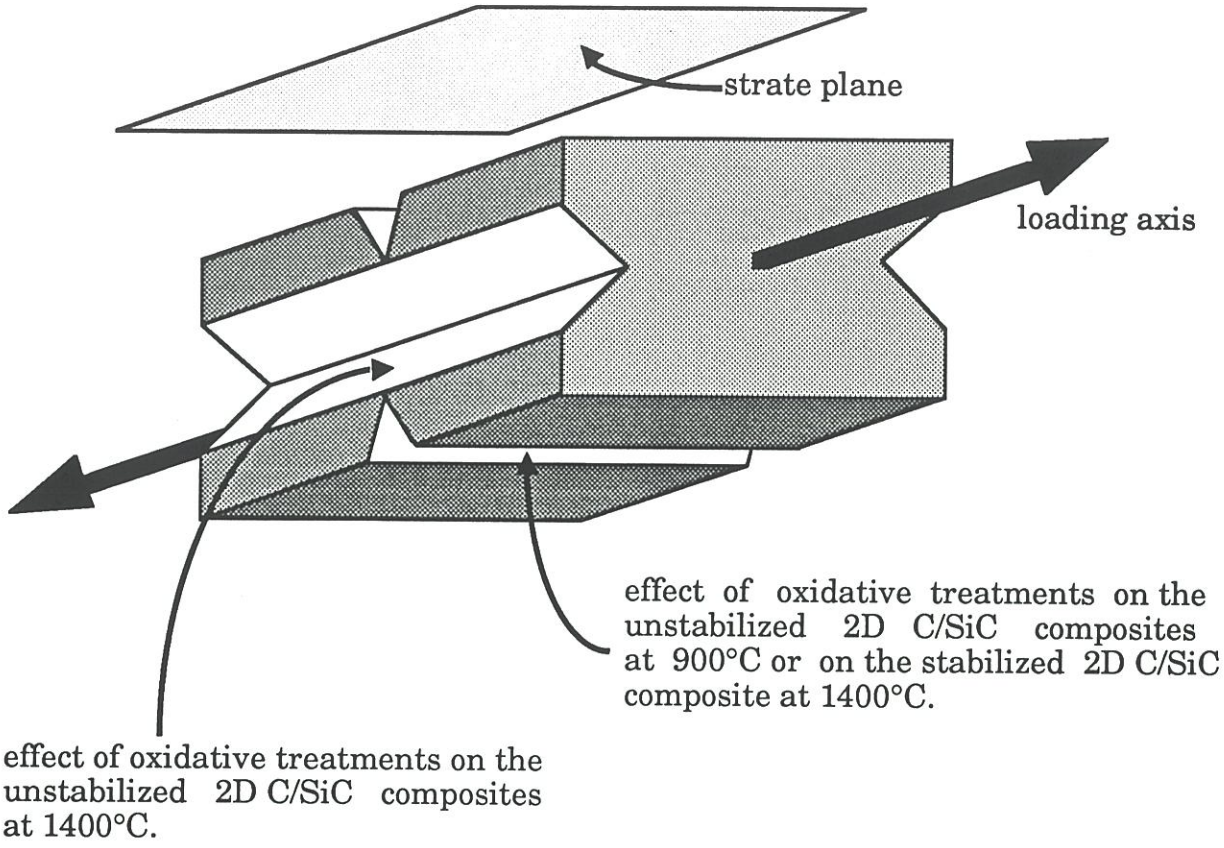

Fig.19: Schematic representation of the localization of the superficial attacks supposed to induce a notch effect on the tensile behavior of the 2D C/SiC composites.

evidenced the main mechanisms responsible for the loss of strength of the materials. These mechanisms have been correlated to three degradation modes of the carbon reinforcement. Uniform degradation during oxidation induces the composite rupture preferentially through a carbon fiber **notch effect**. Non uniform degradation causes the composite rupture by an **overloading** of the carbon plies. Superficial degradation induces premature rupture by a **notch/overloading** effect from the outer fiber tows. The tensile strength of the composites thus decreases with the ageing temperature.

Oxidation under pure oxygen enhances the mechanisms which are responsible for the decrease of the tensile properties. However, when the oxygen content is decreased, a **better preservation of the composite tensile strength** may be observed. The nocth effects (in the fiber and/or in the composite) and the overloading effects thus decrease with the oxygen content.

The stabilizing treatment performed on 2D C/SiC composites after processing leads to a decrease in the tensile properties. This phenomenon may be explained by a **translation of the three temperature domains.**

ACKNOWLEDGEMENTS

This work has been supported by MRT and SEP through a grant given to F.L. The authors acknowledge the assistance that they received from SEP for the CVI-processing of the materials and through valuable discussions. The authors are indebted to B. HUMEZ for performing the tensile tests.

REFERENCES

[1] F. LAMOUROUX, G. CAMUS and J. THEBAULT, "Oxidation resistance and strength after oxidation of a 2D woven carbon fiber silicon carbide matrix composite"; pp 499-504 in *Developments in the science and technology of composite materials*. Edited by A. R. Bunsell, J.F. Jamet and A. Massiah. Elsevier, London, 1992.

[2] D.W. McKEE, "Oxidation behavior and protection of carbon/carbon composites", *Carbon*, 25 [4] 551-557 (1987).

[3] J. R. STRIFE and J. E. SHEEHAN, "Ceramic coatings for carbon-carbon composites", *Ceram. Bull.*, 67 [2] 369-374 (1988).

[4] K. L. LUTHRA, "Oxidation of carbon/carbon composites–A: Theoretical analysis", *Carbon*, 26 [2] 217-224 (1988).

[5] K. PREWO and J. BATT, " The oxidative stability of carbon fibre reinforced glass-matrix composites", *J. Mater. Sci.*, 23, 523-527 (1988).

[6] N. FRETTY and M. BOUSSUGE, "Relationship between high-temperature development of fibre-matrix interfaces and the mechanical behaviour of SiC-SiC composites", *Composites Science and Technology*, 37, 177-189 (1990).

[7] L. FILIPUZZI, G. CAMUS, J. THEBAULT and R.NASLAIN, "Effect of high temperature ageing treatments on the mechanical behaviour of unidirectional SiC/SiC fribrous composites"; pp 283-289 in *Structural Ceramics Processing, Microstructure and Properties*. Edited by J.J. Bentzen, J.B. Bilde-Sorensen, N. Christiansen, A. Horsewell, B. Ralph. RISØ National Laboratory, Roskilde, Denmark, (1990).

[8] - J. THEBAULT, "Fabrication process of a composite material with a refractory reinforcement and a ceramic matrix and structure elaborated with such process", French Patent 2 567 874 A1, July 20, 1984.

[9] F. LAMOUROUX, G. CAMUS, R. NASLAIN and J. THEBAULT, "Kinetics and mechanisms of oxidation of 2D woven C/SiC composites: 1 - experimental approach", (submitted to *J. of Am. Ceram. Soc.*)

[10] F. LAMOUROUX, X. BOURRAT, and R. NASLAIN, "Oxidation phenomena in HR PAN-based carbon fiber bundles bare or infiltrated with pyrocarbon", in *Proceeding of the fifth international Conference on Carbon*, pp. 650-652, Essen, Germany, 1992.

[11] - R. NASLAIN, J.Y. ROSSIGNOL, P. HAGENMULLER, F. CHRISTIN, L. HERAUD and J.J. CHOURRY, "Synthesis properties of new composite materials for high temperature application based on carbon fibers and C-SiC or C-TiC hybrid matrices", Rev. Chimie Minerale, 18, 544-564 (1981).

[12] - W.J. LACKEY and T.L. STARR "Fabrication of fiber-reinforced ceramic composites by chemical vapor infiltration: processing, structure and properties", in *Fiber reinforced ceramic composites* (K.S. Mazdiyasni, ed.), pp. 397-450, Noyes Publications, Park Ridge, USA, 1990.

[13] - J.M. JOUIN, "Cyclic loading behavior of bidirectional silicon carbide matrix composites" (in french), in *Composite materials for high temperature applications* (Ed. R. Naslain, J. Lamalle and J.L. Zulian), pp 169-180, AMAC/CODEMAC, France, Bordeaux, 1990.

CONCLUSIONS GENERALES

CONCLUSIONS GENERALES

Ce travail s'inscrit dans le cadre plus général des recherches conduites au Laboratoire des Composites Thermostructuraux (LCTS) sur les CMCs. Ces matériaux, et plus particulièrement les composites C/SiC, sont destinés à des applications en milieu oxydant à hautes températures. Il apparaît donc essentiel de connaître l'effet de cet environnement sur le comportement du matériau. Ce travail avait pour objectif de déterminer les mécanismes de l'oxydation des composites C/SiC à interphase de pyrocarbone et d'en étudier les effets sur le comportement mécanique.

Dans un premier temps, une relation a été établie entre la microstructure des fibres de carbone T300 et leur comportement à l'oxydation. Par la suite, les mécanismes gouvernant la cinétique d'oxydation, d'une part et l'évolution microstructurale du composite induite par l'oxydation, d'autre part, ont été mis en évidence expérimentalement. La modélisation de ces mécanismes a permis d'étudier les effets des paramètres liés à l'environnement oxydant (température et teneur en oxygène) et ceux liés au matériau (morphologie du revêtement en carbure de silicium, présence d'une sollicitation mécanique). Enfin, la dernière partie de ce travail a consisté à déterminer les conséquences sur le plan mécanique de l'oxydation des composites C/SiC.

Les analyses microstructurales réalisées sur des coupes transversales de fibres de carbone T300 ont mis en évidence une **texture particulièrement hétérogène** comprenant (i) une **zone microporeuse** située à proximité de la surface fibreuse et (ii) **une zone à plus forte densité**, en forme d'anneau, localisée à mi-distance de la surface et du centre de la fibre. De manière

plus générale, la structure de cette fibre est faiblement organisée comparée à celle du carbone pyrolytique. Par ailleurs, un traitement thermique de la fibre à 1600°C sous gaz neutre a pour effet d'améliorer sensiblement son organisation structucturale sans changer pour autant le caractère hétérogène de la texture. Les oxydations ménagées réalisées sur des torons de fibres revêtues de pyrocarbone conduisent à une **dégradation préférentielle** de la zone microporeuse superficielle. La cinétique d'oxydation de la fibres est contrôlée à basse température (T<700°C) par un **régime mixte** de diffusion des espèces gazeuses à travers les pores de la fibre et de réaction du carbone avec l'oxygène. A haute température (T>700°C) la cinétique est gouvernée par la diffusion des espèces gazeuses à travers la couche limite. Le faible degré d'organisation de cette fibre lui confère une **vitesse d'oxydation élevée**. Le traitement thermique à 1600°C sous gaz neutre a pour effet d'abaisser la réactivité de cette fibre dont la cinétique d'oxydation à basse température (T<750°C) est seulement contrôlée par des **mécanismes de réaction**. Cependant, l'oxydation se porte toujours préférentiellement sur la zone microporeuse de la fibre de carbone. Cette microporosité de surface a plusieurs effets sur le comportement mécanique de la fibre en milieu neutre ou oxydant: (i) en environnement neutre, les dimensions relativement importantes de ces défauts superficiels abaissent le niveau de résistance mécanique de la fibre de carbone, et (ii) en environnement oxydant, la taille de ces défauts augmente sous l'effet de l'oxydation ce qui provoque une chute brutale de la résistance mécanique de la fibre.

Les composites C/SiC se caractérisent par le fait qu'ils sont endommagés dès la fin du processus d'élaboration. Cet endommagement résulte de la différence des coefficients de dilatation entre la fibre de carbone et la matrice en carbure de silicium. Cela se traduit par l'apparition de

fissures dans la matrice et de décohésions dans l'interphase de pyrocarbone. Un traitement thermique réalisé à une température supérieure à la température d'élaboration de la matrice (i.e. T>1000°C) a pour effet d'accroître le degré d'endommagement du matériau: les fissures et les décohésions deviennent plus larges et plus nombreuses. Lorsque le composite C/SiC est utilisé en environnement oxydant, les fissures de la matrice constituent les chemins privilégiés de la diffusion de l'oxygène vers les fibres et l'interphase de carbone. La cinétique d'oxydation du composite C/SiC est alors le résultat de la **compétition** entre les **mécanismes des réactions** carbone/oxygène et les **mécanismes de diffusion** des espèces gazeuses à travers la texture du composites (fissures, décohésions et porosité intra et intertorons). Le réseau de fissuration du seal-coat de SiC arbitre cette compétition en limitant, selon la température, la diffusion des espèces gazeuses. La cinétique d'oxydation du composite se résume alors en trois domaines de températures. A basses températures (T<800°C), la cinétique d'oxydation est contrôlée par les mécanismes de **réaction** entre le carbone et l'oxygène, et la dégradation du renfort fibreux se fait de façon **uniforme**. A moyennes températures (800<T<1100°C), la cinétique d'oxydation est gouvernée par la **diffusion** des espèces gazeuses à travers les fissures de la matrice. La dégradation du renfort fibreux **n'est plus uniformément répartie** puisque les strates superficielles sont plus fortement oxydées que les strates centrales. A hautes températures (T>1100°C), la diffusion des espèces gazeuses est fortement **limitée** par l'étroitesse des fissures du seal-coat de SiC. L'oxydation se porte uniquement sur les strates **superficielles** où un front d'oxydation apparaît. Les domaines de température associés à ces **trois modes d'oxydation** peuvent varier en modifiant (i) **la réactivité du substrat** en carbone et (ii) **la taille des fissures** du seal-coat de SiC. Ainsi, lorsque le composite ne subit pas de traitement thermique à 1600°C sous

gaz neutre, une différence de comportement est observée, tant sur le plan de la cinétique d'oxydation que sur le mode de dégradation du renfort fibreux. Un **déplacement des trois domaines de température** correspondant aux divers modes d'oxydation définis précédemment explique une telle différence de comportement.

La modélisation de ces mécanismes a permis de comprendre le processus de l'oxydation des composites C/SiC. Ce modèle a été utilisé pour étudier l'effet de certains paramètres sur l'évolution de la cinétique d'oxydation. Ainsi, une simulation de la perte de masse du composite en environnement oxydant à **faible teneur en oxygène** montre une **amélioration de la résistance à l'oxydation** du composite en ce sens que le processus de cicatrisation des fissures du seal-coat de SiC est moins affaibli par la diminution de la teneur en oxygène que ne le sont les mécanismes gouvernant la cinétique d'oxydation du renfort fibreux. Par ailleurs, l'étude de l'évolution de la cinétique d'oxydation du composite avec l'épaisseur du seal-coat de SiC, montre l'importance de ce paramètre. En effet, bien que la taille des fissures augmente avec l'épaisseur du revêtement, il est observé un **ralentissement de la vitesse d'oxydation** du composite lorsque l'épaisseur du seal-coat augmente. De plus, cet effet est d'autant plus marqué que la température augmente. Enfin, la cinétique d'oxydation du composite C/SiC **sollicité mécaniquement** a été étudiée. Les résultats de cette simulation sont quantitativement peu représentatifs du comportement réel du matériau, puisqu'ils sont sous-tendus par des hypothèses trop simplificatrices. Néanmoins, l'analyse qualitative de l'évolution de la cinétique d'oxydation avec le niveau de chargement montre un **déplacement des domaines de température** correspondant aux différents modes d'oxydation. Ainsi lorsque le niveau de chargement mécanique est élevé (i.e. 200MPa), le

processus de cicatrisation du revêtement SiC n'est plus efficace, et la vitesse d'oxydation augmente alors régulièrement avec la température. Cette évolution de la cinétique d'oxydation doit probablement s'accompagner d'un **changement dans le mode de dégradation du renfort fibreux**. C'est dans ce dernier point que réside l'intérêt du présent modèle, puisqu'à partir de la cinétique d'oxydation simulée, il est possible de déterminer le mécanisme d'oxydation et donc le mode de dégradation du renfort fibreux du composite.

Une corrélation étant établie entre les mécanismes d'oxydation d'une part et les évolutions morphologiques en cours d'oxydation d'autre part, il était nécessaire de déterminer les différents **effets de l'environnement sur le comportement mécanique**. Ainsi, les oxydations à basses températures des composites C/SiC, qui engendrent une dégradation du type uniforme, sont les plus pénalisantes sur le plan de la résistance à la traction après oxydation. En effet, **les fibres sont localement dégradées** au droit des fissures de la matrice, ce qui a pour effet de faire chuter de manière importante la résistance en traction du composite. Les oxydations à moyennes températures engendrent une dégradation non uniforme du renfort fibreux. La rupture du composite est alors induite par **un effet de surcharge** des strates portant réellement la charge. A haute température, la dégradation du renfort fibreux n'étant que superficielle, la rupture est engendrée par **un effet d'entaille** généré par la porosité se développant à la surface. Cependant, la résistance résiduelle du composites après oxydation à hautes températures est mieux préservée que dans le cas d'oxydations à basses et moyennes températures. Ces différents mécanismes de rupture sont associés aux différentes morphologies du composites après oxydation. La validité de cette association a pu être vérifiée en utilisant des composites **non stabilisés** thermiquement. Pour ce

type de matériaux, les **domaines de température** correspondant aux divers mécanismes explicités précédement, sont **déplacés** du fait de la variation de la réactivité du renfort fibreux vis à vis de l'oxygène et de la finesse du réseau de fissuration. Il est alors constaté que les valeurs des résistances résiduelles après oxydation sont toujours en accord avec un mécanisme et un mode particulier d'oxydation. Par ailleurs, il faut noter qu'une **diminution de la teneur en oxygène** a pour effet d'atténuer ces modes d'oxydation, et donc de **préserver les propriétés mécaniques** du composite.

Cette étude a permis d'établir une corrélation entre un **mécanisme** d'oxydation, une **morphologie** et un **mode de rupture** en traction après oxydation des composites C/SiC. La comparaison entre les matériaux stabilisés et non stabilisés a permis de valider les relations ci-dessus. La compréhension des mécanismes d'oxydation de ces composites est due en grande partie au développement d'un modèle capable de simuler la cinétique d'oxydation de ce matériau. Ce travail est le résultat d'une démarche mise au point et expérimentée au LCTS lors de précédentes études sur d'autres CMCs, notamment les composites SiC/SiC.

RESUME:

Le comportement à l'oxydation des composites 2D C/SiC est étudié sur le plan de la cinétique de perte de masse, des modifications microstructurales en cours d'oxydation et de l'évolution des propriétés mécaniques en traction à l'issu des traitements oxydants. Dans un premier temps, une relation est établie entre la microstructure et le comportement à l'oxydation des fibres de carbone revêtues de pyrocarbone dans l'objectif de déterminer la cinétique d'oxydation du renfort fibreux et de localiser les zones les plus sensibles à l'environnement oxydant. Par la suite sont déterminés les mécanismes responsables de la cinétique d'oxydation des composites 2D C/SiC et de leur évolution microstructurale en cours d'oxydation. La connaissance de ces mécanismes a mené à la modélisation de la cinétique d'oxydation du composite. Ce modèle est utilisé pour étudier l'influence des principaux paramètres sur la cinétique d'oxydation du composite, à savoir: la pression de l'environnement oxydant, l'épaisseur du revêtement partiellement protecteur en carbure de silicium et la présence d'une sollicitation mécanique. Enfin, une corrélation est établie entre les modes de dégradation du renfort fibreux et les modifications du comportement en traction induites par l'oxydation des composites 2D C/SiC.

Mots clés: carbone, oxydation, composites C/SiC, cinétique, morphologie.

ABSTRACT:

The oxidation behavior of C/SiC composites has been investigated on the basis of mass loss kinetics, morphological changes induced by oxidation and tensile properties variations. In a first step, the microstructure of the carbon fibers coated with a pyrocarbon has been correlated to the oxidation kinetics of the fibrous reinforcement and its local degradations in oxidizing environment. Then, the mechanisms responsible for the oxidation kinetics of the 2D C/SiC composites as well as their morphological changes induced by oxidation have been determined. The knowledge of these mechanisms has allowed to model the composite oxidation kinetics. This model has been used to investigate the effects of the main parameters on the oxidation kinetics, such as the oxygen pressure, the thickness of the SiC seal-coating (which partly protects the composite) and the mechanical loading. Finally, correlations between the different modes of degradation of the fibrous reinforcement and the residual tensile properties after oxidation of the 2D C/SiC have been established.

Key words: carbon, oxidation, C/SiC composites, kinetics, morphology.

RESUME

Le comportement à l'oxydation des composites 2D C/SiC est étudié sur le plan de la cinétique de perte de masse, des modifications microstructurales en cours d'oxydation et de l'évolution des propriétés mécaniques en traction à l'issu des traitements oxydants. Dans un premier temps, une relation est établie entre la microstructure et le comportement à l'oxydation des fibres de carbone revêtues de pyrocarbone dans l'objectif de déterminer la cinétique d'oxydation du renfort fibreux et de localiser les zones les plus sensibles à l'environnement oxydant. Par la suite sont déterminés les mécanismes responsables de la cinétique d'oxydation des composites 2D C/SiC et de leur évolution microstructurale en cours d'oxydation. La connaissance de ces mécanismes a mené à la modélisation de la cinétique d'oxydation du composite. Ce modèle est utilisé pour étudier l'influence des principaux paramètres sur la cinétique d'oxydation du composite, à savoir: la pression de l'environnement oxydant, l'épaisseur du revêtement partiellement protecteur en carbure de silicium et la présence d'une sollicitation mécanique. Enfin, une corrélation est établie entre les modes de dégradation du renfort fibreux et les modifications du comportement en traction induites par l'oxydation des composites 2D C/SiC.

Mots clés: carbone, oxydation, composites C/SiC, cinétique, morphologie.

ABSTRACT

The oxidation behavior of C/SiC composites has been investigated on the basis of mass loss kinetics, morphological changes induced by oxidation and tensile properties variations. In a first step, the microstructure of the carbon fibers coated with a pyrocarbon has been correlated to the oxidation kinetics of the fibrous reinforcement and its local degradations in oxidizing environment. Then, the mechanisms responsible for the oxidation kinetics of the 2D C/SiC composites as well as their morphological changes induced by oxidation have been determined. The knowledge of these mechanisms has allowed to model the composite oxidation kinetics. This model has been used to investigate the effects of the main parameters on the oxidation kinetics, such as the oxygen pressure, the thickness of the SiC seal-coating (which partly protects the composite) and the mechanical loading. Finally, correlations between the different modes of degradation of the fibrous reinforcement and the residual tensile properties after oxidation of the 2D C/SiC have been established.

Key words: carbon, oxidation, C/SiC composites, kinetics, morphology.